CALIFORNIA INSTITUTE OF TECHNOLOGY

SEDIMENTATION LABORATORY

THE RESUSPENSION OF FLOCCULENT SOLIDS IN SEDIMENTATION BASINS

by
Alfred C. Ingersoll
and
Ronald T. McLaughlin

Final Report
1 October, 1955 through 31 December, 1959

May 1960

A Report on Research Conducted Under
Grants from the
United States Public Health Service -
National Institutes of Health

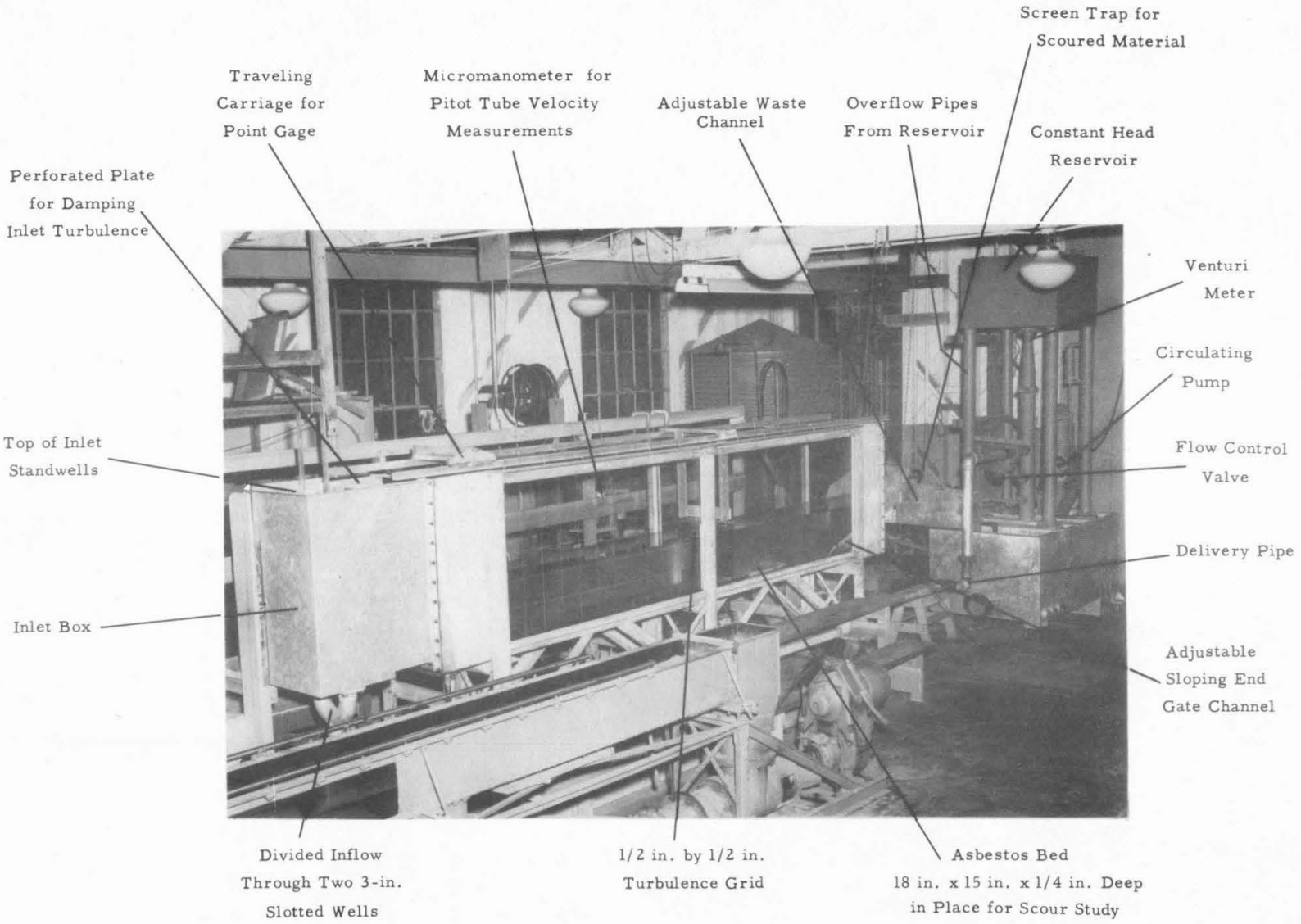

Fig. 1.1 LABORATORY SCOUR FLUME

Final Report

THE RESUSPENSION OF FLOCCULENT SOLIDS IN SEDIMENTATION BASINS

by

Alfred C. Ingersoll, Principal Investigator

and

Ronald T. McLaughlin, Project Engineer

United States Public Health Service - National Institutes of Health

RG-4405 through RG-4405(C3)

1 October, 1955 through 31 December, 1959

California Institute of Technology

20 May 1960

TABLE OF CONTENTS

LIST OF FIGURES

Synopsis of Project Results

The phenomenon of resuspension has been considered to be an important factor in the imperfect behavior of sedimentation basins receiving suspensions containing flocculent solids. Resuspension is the entrainment into the flow of particles that have once settled to the floor of the basin. This investigation has been undertaken to study the resuspension phenomenon and to find ways in which its harmful effects can be reduced.

Resuspension has been found extremely difficult to isolate and define scientifically because many other factors produce the same overall effect upon the settling tank. Furthermore it is practically necessary to identify individual particles in order to know whether a particular one found in suspension in the downstream portion of a settling tank had earlier been settled out and resting on the floor.

Laboratory studies on settling tank behavior were conducted on a glass-walled "scour flume" 1.27 ft wide by 14 ft long with depth adjustable from 0.5 to 2.0 ft (see Fig. 1.1). In order to simulate certain aspects of the behavior of full-scale settling tanks the laboratory flume was fitted with moving flight scrapers similar to those installed in primary sewage settling tanks. For some of the later tests the flume was fitted with 14 probes that made it possible to sample the tank contents at practically any point of five cross sections along the length of the flume.

Most of the studies on the laboratory flume utilized a discrete suspension of gilsonite (s. g. 1.04) particles or a flocculent suspension of ferric chloride and bentonite clay particles. Tests for critical velocity required for entrainment of particles from a smooth bed showed that fine light particles are more easily lifted from the bed than was previously supposed. With scrapers moving upstream, the critical velocity for two sizes of gilsonite tested was found to vary between 10.5 and 14.5 times the particle settling velocity.

Field and laboratory studies on one scheme proposed to improve the performance of settling tanks - a series of transverse sloping baffles installed throughout the main body of a rectangular settling tank - both indicate that baffling a tank is not the answer.

Tests on full-scale settling tanks of a sewage treatment plant showed that conventional measures of settling tank performance are meaningless when the suspension entering the tank is flocculent (as is sewage). Newer measures of performance are proposed, which show promise in evaluating the behavior of settling tanks receiving flocculent suspensions.

Chapter 1

INTRODUCTION

The sedimentation process, while apparently a simple application of mechanics for discrete particles settling in quiescent tubes, becomes one of the most complex and least-understood hydraulic phenomena when it is applied to flocculent suspensions in continuous-flow settling basins. It is complicated by turbulence from inlet and outlet devices and sludge-scraping equipment, by density currents and wind action, and by bed-load movement and scour of previously deposited material. Seldom do basins perform as well as indicated from their design and seldom can the operating results of basins be compared by means of conventional measures of performance.

Previous investigators have made theoretical and empirical studies of overflow rates, detention periods, inlet and outlet arrangements, length/width/depth ratios, and related aspects. No one has come to light, however, who has thoroughly recognized or investigated the significance of resuspension of previously deposited sludge by turbulent eddies, from whatever source. Throughout this project it has been the contention of the investigators that resuspension, that is, the lifting from the bed of particles that have previously settled to the bottom, is a major hindrance to the efficient performance of sedimentation basins. The broad aims of the project were established at the start:

1. To study the resuspension of flocculent settled material from the sludge bed in settling tanks and to formulate laws governing the equilibrium that is established between sedimentation and resuspension.

2. To determine methods by which this resuspension can be minimized, to improve the efficiency of settling tanks.

3. To test these methods in laboratory models and in full-scale settling tanks.

4. To evaluate the current parameters of performance for such basins and to devise laboratory apparatus that will provide better measures of performance.

Except for the "laboratory apparatus" part of the fourth aim, these specific aims were accomplished within the project period. The laboratory tests were carried out principally in a glass-walled flume 1.27 ft wide by 14 ft long, with depth adjustable up to 2 ft, installed in the Sedimentation Laboratory on the Caltech campus (see Fig. 1.1). Studies on full-scale sedimentation basins were carried on in the primary settling tanks of the Los Angeles County Joint Disposal Plant (reported in Chapter 3) and in the basins of the Imperial Desilting Works where the All-American Canal draws its supply from the Colorado River (reported in Chapter 4).

The Resuspension Problem

As far as is known to the authors, the resuspension of settled solids was first observed and recognized as a problem in the Valley Settling Basins of Los Angeles, California. This phenomenon, which is described graphically in Fig. 16 of Ref. 1.1, involves the entrainment or pickup of flocculent solids that have settled to the sludge layer at the bottom of the tank. The immediate cause of resuspension is simply that the mean velocity, which by the nature of the operation of these basins has a wide diurnal variation, increases after a period of low velocity in which the sludge blanket has settled. In the case of the rectangular basins cited, the velocity increases to 4 ft. per min. with no appreciable entrainment, but beyond this the resuspension is such that the concentration of settleable solids in the effluent increases by a factor of 10 or 20 for a 20 % increase in velocity. It is thus said that 4 ft per min is the "critical velocity" which will lift alum floc particles from the bed of the Valley Settling Basins. There are other factors involved. With most kinds of flocculent solid it makes a difference how long the flocculent bed has had a chance to consolidate before the test of increased velocity begins.

Laboratory and Field Observations of Resuspension

A major part of this project has been devoted to the examination of the critical velocity of various solids under various circumstances, including the movement of flight scrapers within the tank. Extensive laboratory tests have been conducted on both granular and flocculent solids. In order to find an extremely light granular sediment the investigators turned to the asphaltic resin, gilsonite, which has a specific gravity of only 1.04. This has made possible the observation by eye and by camera of particles having settling velocities that are low enough to be in the range of settling velocities encountered in the primary tanks of sewage treatment plants.

The flocculent solid tested was made of ferric chloride and bentonite clay. The various sediments tested are described in detail in Chapter 5, while the hydraulic properties of the laboratory flume are discussed in Chapter 6.

Studies on the critical velocity for gilsonite (and some flocculent solids) being lifted from a flat bed prepared in advance of the test are described in Chapter 7.

The outward effect of resuspension is of course the decrease in removal performance of the settling basin. Removal studies conducted on the laboratory flume containing gilsonite, with both the prepared bed and continuous injection, are described in Chapter 8. Removal studies on flocculent suspensions are presented in Chapter 9.

In order to study the behavior of the laboratory flume receiving a flocculent suspension it was desired to sample the contents of the flume at various locations in the cross section downstream from the inlet.

Fourteen holes were made through the glass wall of the flume and fitted with sampling tubes which made possible a rather complete probe of five cross sections. The results of these tests, together with the analyses of the suspensions in a specially constructed quiescent settling column, are presented in Chapter 10.

One of the schemes proposed in Ref. 1.1 was the concept of a baffled settling tank, the main body of the basin being divided by transverse baffles having their upper ends sloping downstream. The baffles were to reach close to the water surface in the tank, but not to intersect it. This idea had been successfully applied to the separation of ore slimes. It was arranged through the Los Angeles County Joint Disposal Plant to install baffles - in one of two identical rectangular settling tanks - something like the ones proposed. The other tank was left unimpaired. The results of tests on both tanks are given in Chapter 3. At the very end of the project similar baffles were installed in the laboratory flume and tested with continuous injection of the ferric chloride-bentonite floc. The results of these tests are described in Chapter 11.

Acknowledgments

A great many people have participated in this project over the past four years. The authors are especially grateful to Mr. Charles E. Brockway, graduate student in civil engineering at Caltech, for his assistance in preparation of the final report. Mr. Brockway was project assistant during the summer and fall of 1959 and was responsible for many of the studies on flocculent suspensions.

Undergraduate students at Caltech who have assisted in the project are listed below, together with their period of service and contributions:

Lyle Hoag	December, 1955	Tests at Joint Disposal Plant
Byron Johnson	"	"
Paul McHorney	December, 1955 - April, 1956	"
Tom Cooper	April, 1956 - September, 1956	Construction of laboratory flume and laboratory tests of suspensions
Gary Dietrich	October, 1956 - May, 1957	Velocity distribution tests in flume
Paul King	" "	"
Jerry Eggleston	" December, 1956	Flume tests
Harold Dessau	" "	Laboratory analyses
Itiel Haissman	January, 1957 - April, 1957	Literature survey
Gene Beisman	January, 1957 - May, 1957	Preparation of suspensions
Robert Hangebrauck	June, 1957 - June 1958	Laboratory work with suspensions

Allan Porush	June, 1957 - April, 1958	Critical velocity tests
Jerry Hansen	" "	"
Malcolm Whitt	October, 1957 - May, 1959	Modifications to flume, and testing
Dale Parkhurst	October, 1958 - May, 1959	Gilsonite tests on flume
Charles Deemer, Jr.	June, 1958 - May, 1959	"
Michael Kane	" "	"
Steven Crow	June, 1959 - December, 1959	Flocculent solid tests on flume
William Ripka	" "	"
Gustav Wassel	August, 1959 - December, 1959	Drawing

Colleagues in the Department of Civil Engineering at Caltech have been helpful in counseling on many points of the research program. In this connection the authors are especially grateful to Professors N. H. Brooks, J. E. McKee, and V. A. Vanoni. Professor Brooks was also co-principal investigator during the first year of the project.

Notation

a = height of sluice-gate opening (Chap. 3)

b = width of sluice-gate opening (Chap. 3)

c_r = suspended solids concentration in raw influent

c_e = suspended solids concentration in effluent

D = diameter of particle

$\mathcal{E}$ = total or integrated efficiency of tank

$\mathcal{E}_o$ = overflow residual efficiency

$\mathcal{E}_{eo}$ = effluent overflow efficiency

f = conventional friction factor for tank

f_r = distribution function for concentration frequency of raw influent

H_m = Hazen number for particle with median settling velocity

f_i = distribution function for concentration frequency of ideal effluent

Q = discharge through tank

r_a = actual removal ratio for given fraction of particle suspension

r_i = ideal removal ratio for given fraction of particle suspension

r_{im} = ideal removal ratio for particle with median settling velocity

$\mathcal{R}_a$ = actual total removal ratio

$\mathcal{R}_i$ = ideal total removal ratio

s = specific gravity of particle

y_1 = upstream depth over sill of sluice gate (set flush with floor) (Chap. 3)

V_c = critical horizontal velocity in tank for start of bed scour

v, w = settling velocity of particle

v_m, w_m = median settling velocity of particle suspension

v_o, w_o = overflow rate for tank, equal to depth divided by detention time

η = elementary efficiency, equal to r_a/r_i

References

1.1 "Fundamental Concepts of Rectangular Settling Tanks," by Alfred C. Ingersoll, Jack E. McKee, and Norman H. Brooks, Trans. ASCE, Vol. 121, p. 1179. (1956)

Chapter 2

THEORETICAL BACKGROUND OF THE RESUSPENSION PROBLEM

The phenomenological approach to the resuspension problem was stated in Chapter 1. The definition of a phenomenon as used in science is "any fact or event of scientific interest susceptible of scientific description and explanation." After four years of study and experimenting in this field there remains much question in the authors' minds about whether the resuspension phenomenon can be scientifically described, and even more about how best or whether it can be scientifically explained. The student of sedimentation is familiar with the terms "scour" and "entrainment" in which particles are lifted from the bed of a stream and are suspended in the main flow, quite likely to be deposited farther downstream in a region of lower velocity. The concept of resuspension involves the entrainment of flocculent particles from the sludge bed at the bottom of a settling tank.

An important part of the resuspension idea is that the particles were at one time suspended in the flow through the tank, but have settled to the bottom. It is not necessary that the particles were in an equilibrium state of suspension. Indeed the usual thing is that the particles are in suspension at the inlet end of a settling tank by virtue of their being thoroughly mixed with the influent liquor. As the suspension passes through the progressively quieter zones of the tank the particles settle out and fall to the bed, making a thick blanket of sludge there which becomes fairly stable against erosion. With an increase in velocity, however, floc particles are torn loose from the bed and become entrained in the flow again. This is one type of resuspension, involving an increase in velocity. It is this type that was observed in the Valley Settling Basins described in Ref. 1.1. It was this unsteady-flow type of resuspension that was studied in the experiments described in Chapter 7.

A second type of resuspension involves no change in the mean velocity, but for some other reason particles are lifted from the bed after they have settled. It is this type of resuspension which is more difficult to describe and elusive to observe. The outward effect of such resuspension is no different from the case in which the particles never did settle to the bottom but were held entrained by excessive turbulence. It is well to point out here that the natural sedimentation process in a stream involves a continuous settling out and resuspension of particles so that the bed is at all times in equilibrium with the streamflow above it. The settling tank is not intended to involve such an equilibrium process, however, as the concentration of particles in suspension presumably decreases from the inlet to the outlet. If particles are lifted into suspension after they have settled to the bottom, therefore, it is a non-equilibrium phenomenon. Such resuspension is difficult to explain if the turbulence in the tank is derived primarily from inlet mixing and should therefore decay in the downstream direction.

It is this constant velocity, non-equilibrium type of resuspension which has been investigated in the gilsonite tests reported in Chapter 8 and in the floc tests of Chapters 9 and 10. Unfortunately it is virtually

impossible to "track" individual particles and learn whether they have in fact settled to the bottom and have been resuspended or, more likely, whether they never settled to the bottom at all, even though the hydraulic conditions were theoretically such that settling should have occurred. The end result in terms of settling performance, an easy thing to measure, is the same in either case.

2.1 Measures of Settling Tank Performance

In order to investigate the phenomenon of resuspension it is necessary to know more about measures of settling tank performance, for otherwise it is not possible to identify a certain type of performance deficiency and learn whether resuspension may be responsible for it. In order to obtain a real measure of the performance of a settling tank it is necessary to compare the removal ratio achieved with that which should be achieved in an "ideal tank." The removal ratio, generally applied to the suspended solids concentration, is conventionally defined as

$$\mathcal{R}_a = \frac{c_r - c_e}{c_r} \qquad (2.1)$$

in which c_r is the raw influent concentration and c_e is that in the effluent.

The "ideal tank" is simulated by the quiescent settling tube, wherein the suspension settles for a time that is in proportion to the detention period in the tank as the depth in the tube is to the depth in the tank. That is, both the tank and the tube operate at the same overflow rate, v_o, which is equal to the discharge divided by the surface area or, what comes to the same thing, the depth divided by the detention time. Actually the settling tubes used in the tests of Chapter 3, shown in Fig. 3.10, were used to determine complete analyses of the suspensions.

As explained in Ref. 1.1, the settling analysis distribution curve of the raw influent suspension, $f_r(v)$, together with the overflow rate makes possible the determination of the ideal removal ratio, r_i, for any fraction, dv, of the suspension. The total ideal removal is now defined

$$\mathcal{R}_i = \int_o^\infty r_i f_r \, dv \qquad (2.2)$$

and a total or integrated efficiency can be defined,

$$\mathcal{E} = \frac{\mathcal{R}_a}{\mathcal{R}_i} \qquad (2.3)$$

This definition is based on the settling mechanics of a suspension of discrete particles and, as will be seen from the results of the tests in Chapter 3, it has little if any meaning when applied to a flocculent type of suspension. Two other measures of performance will be discussed in connection with the results of floc tests.

2.2 Mechanics of Entrainment and Bed-Load Movement

The elementary mechanics of entrainment is reasonably well understood

and explained for the case of granular particles, but there exists almost no literature relating such behavior to that of the flocculent particles such as are to be found in sewage treatment settling tanks. In making a thorough study of the literature it was revealed that previous works, notably that of T. R. Camp (Ref. 2.1, p. 912), were essentially correct in their analyses of the sedimentation phenomenon except for the problem of scour and bed-load movement. Camp derived an expression for the channel velocity required to start motion of particles of size D,

$$V_c = \sqrt{\frac{8}{f}\beta g\,(s-1)\,D} \qquad (2.4)$$

in which s is the specific gravity of the particles, f is the conventional fraction factor for the channel, and β has a value of about 0.04. Here Camp relied on the experimental data of Shields, but it was noted by the authors of Ref. 1.1 that Shields' data applied only to coarse granular particles and not to the fine flocculent material on the upper surface of deposited sludge. Shields' data apply to values of the Bed Reynolds number,

$$R_b = u_* D/\nu \qquad (2.5)$$

of 1.5 and greater, in which $u_* = \sqrt{\tau_o/\rho}$ is the friction velocity, (with bed shear τ_o and density ρ), D is the diameter of particle on the bed, and ν is the kinematic viscosity.

The fine light flocculent material to be found on the bed of a sewage settling tank, however, is of an altogether different character from granular solids, and scour of such flocculent particles commences at values of R_b of only half the abovementioned figure, and less.

Vanoni (2.2) summarizes the forces acting upon a particle in the bed of a channel: its buoyant weight, the lift, and the drag. Both lift and drag forces are proportional to the velocity squared. Vanoni remarks that White has considered the motion of particles both inside the laminar layer and in turbulent flow. After many approximations White arrived at the relation (valid for spherical grains),

$$\tau_c = 0.18\,(\rho_1 - \rho)\,g\,D\tan\theta \qquad (2.6)$$

in which τ_c is the critical shear, $\rho_1 - \rho$ is the differential density, and θ is the angle of repose. This critical condition evidently occurs when approximately 27 % of the bed surface is taking shear. Eq. (2.6) is restricted to conditions well within the laminar range, when $R_b < 3.5$. At incipient turbulence, with $R_b = 3.5$, τ_c is approximately half of the value given by Eq. (2.6) and when $R_b > 3.5$, τ_c drops to one fourth of the value given by Eq. (2.6). These observations confirm the intuitive approach, that the more turbulent flows decrease the amount of bed shear necessary to move particles. White's studies of turbulence (2.3) in a large flume indicated that no more than half the stress variation at the bed originated from disturbance far from the bed.

Some of the most interesting work on very light granular particles has been that of Bagnold (2.4). He adjusted particles and transport fluid so that large grains differed in density from the fluid by only 4 parts in

1,000. Relatively very high shear stresses were attained at the loose-grain bed. Bagnold purports to show that several of the current ideas about the mechanism of grain transport by fluids becomes paradoxical. Fluid turbulence, for example, is certainly not an essential feature (although this observation apparently applies to mean grain concentrations on the order of 35% and above).

Bagnold is much concerned with the mechanical interaction of particles striking against each other. With no turbulence present, therefore, it is still possible for a moving particle to strike a stationary one and to dislodge it and set it in motion in the fluid. Bagnold has not concerned himself with the flocculent type of particle, however, and it is doubtful if the mechanical striking action of particle on particle is so important in the case of flocculent particles as it is for the granular particles.

Many other references could be cited to show refinements in the approaches of White or Shields, leading to slightly different expressions for critical shear or critical velocity. Little or no reference has come to light, however, relating to the behavior of flocculent particles in a bed subject to fluid shear stress. That is why this project was undertaken.

References

2.1 "Sedimentation and the Design of Settling Tanks," by Thomas R. Camp, Trans. ASCE Vol. 111, p. 895 (1946).

2.2 "A Summary of Sediment Transportation Mechanics," by V. A. Vanoni, The Proc. Third Midwestern Conf. on Fluid Mech., Univ. of Minn. (1953).

2.3 "The Equilibrium of Grains on the Bed of a Stream," by C. M. White, Proc. of the Royal Society of London, Series A, No. 958, Vol. 174, pp. 322-338 (Feb. 1940).

2.4 "Some Flume Experiments on Large Grains but Little Denser than the Transporting Fluid, and their Implications," by R. A. Bagnold, Proc. Inst. of Civil Engineers, Part III, Vol. 4, No. 1, pp. 174-205 (April, 1955).

Chapter 3

TESTS ON CONVENTIONAL AND BAFFLED PRIMARY SETTLING TANKS, JOINT DISPOSAL PLANT OF LOS ANGELES COUNTY SANITATION DISTRICTS

In connection with the overall project on the resuspension of flocculent solids in sedimentation basins, it was believed desirable to run performance tests on full-scale settling tanks in order to help identify and define the rather nebulous problem of resuspension. The Los Angeles County Sanitation Districts kindly made the primary tanks of their Joint Disposal Plant available for this purpose and, in addition, modified one of the 300-ft long tanks with sloping baffles to allow study of one possible method of reducing resuspension.

The tests at the Joint Disposal Plant were divided into two principal groups, viz:

(a) in December, 1955, measurements of velocity, settleable and suspended solids were taken throughout the length, width and depth of two tanks in parallel, Tank No. 29 being of standard design and Tank No. 30 being modified with transverse sloping baffles, and

(b) in March and April, 1956, after laboratory apparatus had been developed to determine settling analyses of the influent and effluent suspensions, further tests on one of the four-tank units were conducted to relate actual suspended solids removal rate with that predicted from settling theory and the suspension analyses.

3.1 Tests on Tanks Nos. 29 and 30

Geometry and Arrangement of Tanks

The primary settling tanks of Unit No. 5 (Tanks Nos. 27 to 30) of the Joint Disposal Plant are 300 ft long, 18 ft wide, and operate at a depth of from 8.2 to 9.0 ft or more depending on the depth over the launder weirs, as shown in Fig. 3.1. The influent to each tank is conducted through six 14-in. diameter diffuser ports arranged in pairs so that the jets, entering at right angles to the axis of the tank, oppose one another with the maximum dissipation of kinetic energy.

The effluent is carried over simple sharp-edged weirs to 100-ft long launder troughs on each side of the tank. The sludge scraping mechanism, not shown in Fig. 3.1 except for the location of the sprockets, consists of 3" x 8" redwood flights on two endless chains, moving upstream along the floor of the tank and downstream through the upper half, rising above the water surface at only one point. The flight scrapers move at a rate of 3 ft per min.

The modifications to Tank No. 30 are also shown in Fig. 3.1. The upstream half of the tank was fitted with transverse baffles extending between the side walls, spaced on 4-ft. centers and sloped downstream at 3:1. The baffles in the downstream half of the tank are seen to be

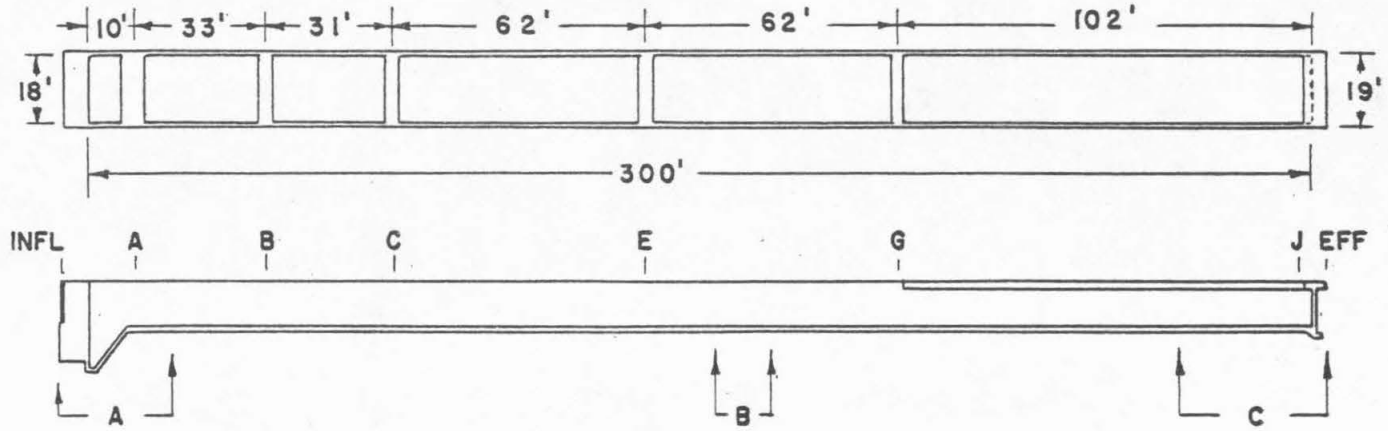

ABOVE DESIGN COMMON TO TANKS 27-30
SCALE 1" = 40'

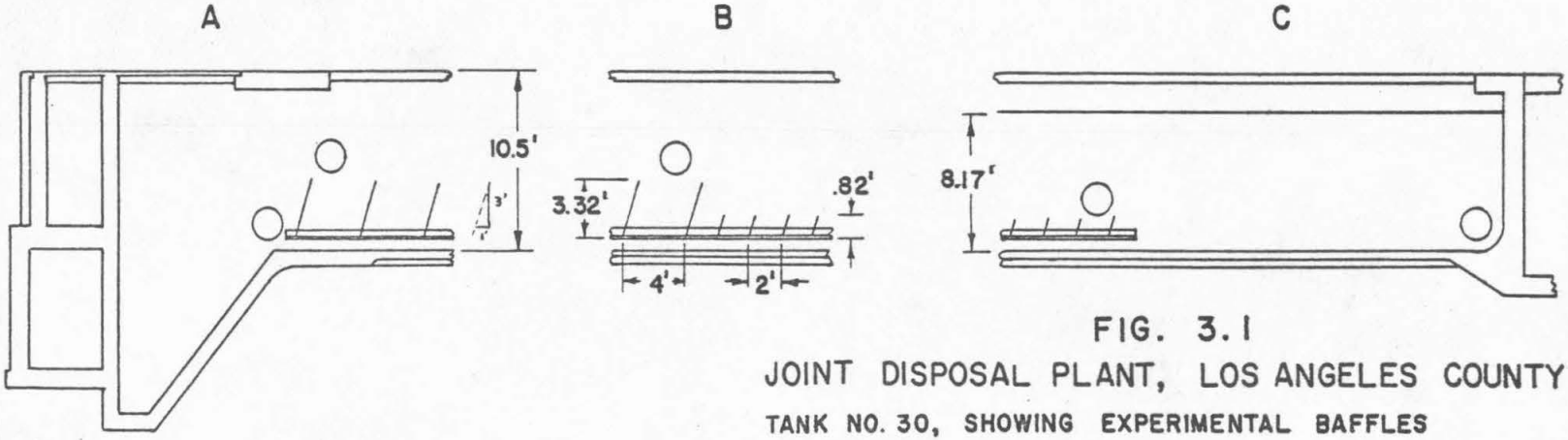

FIG. 3.1
JOINT DISPOSAL PLANT, LOS ANGELES COUNTY
TANK NO. 30, SHOWING EXPERIMENTAL BAFFLES
SCALE 1" = 10'

shorter and more closely spaced, owing to the lower suspension of the returning flights. The baffles were made of corrugated plastic and were set to clear the flight scrapers on the tank floor. In every other way Tank No. 30 was identical to Tank No. 29.

The baffles were installed by the Sanitation Districts following a suggestion appearing in Ref. 1.1. It was hoped that the baffles would prevent eddies near the sludge bed and thereby reduce resuspension of light flocculent material that had settled to the bottom. The upper or non-baffled part of the tank should theoretically operate as well as the full-depth basin, inasmuch as its overflow rate would be the same with or without baffles and, according to basic settling theory, the removal should be primarily a function of the overflow rate.

Measurement of Velocity and Discharge

At the end of each launder trough is a sluice gate, 18 in. x 18 in., operating at times submerged and at other times with a free jet, depending on the water level in the effluent collection channel. These gates provided the best means of measuring the discharge through any one tank. The flow through the entire unit of four tanks was obtained from one of the plant venturi meters, and with simultaneous readings of head and gate opening on all eight sluices it was possible to determine an overall orifice coefficient of $C_d = 0.72$ for the gates. The discharge through any one gate, therefore, was obtained from the formula:

$$Q = \frac{0.72\ ab\ \sqrt{2g(y_1 - a/2)}}{\sqrt{1 - (0.72\ a/y_1)}} \qquad (3.1)$$

wherein Q is the discharge in cfs, a is the height of the gate opening, in ft, b is the width of gate opening, in ft, y_1 is the upstream depth over the sill of the gate (set flush with the floor), in ft. Mean velocities either through the straight tank or the free space above the baffles, were computed from these discharge measurements.

Point velocity measurements were made with a standard Price current meter. Surface velocities were measured approximately by visual observation of the movement of a fluorescein dye patch through the tank.

Measurement of Settleable and Suspended Solids

Samples of sewage were taken from various depths in the tanks with an Eakin spring-loaded sediment sampler. This was so designed that the flow to be sampled was not disturbed hydrodynamically until the spring was released by dropping a messenger down the line suspending the device, and a volume of about one-half liter was trapped in the sampler. Inasmuch as the two tanks receive the same influent suspension, the influent samples were taken from the common distribution channel just upstream from the two tanks, where the velocity was quite high and the influent suspension well mixed by turbulence.

The settleable solids concentrations were determined from field observation after settling one hour in standard Imhoff cones. The suspended

solids determinations were made by bringing the samples in one-pint jars back to the Sanitary Engineering Laboratory at Caltech, where they were analyzed according to standard methods, Ref. 3.1.

Results and Discussion

Representative data from this series of tests are shown in Figs. 3.2 through 3.8. The settleable solids data of Fig. 3.2 show that the concentration at a depth of 3 ft at point A, some 10 ft into the tank, was the same in both tanks. Farther downstream in the tank, however, it is clear that the baffled tank was behaving poorly in comparison to the straight chamber, this being most noticeable at the mid-point E. The lower baffles in the downstream half of Tank No. 30 were evidently beneficial (or at least not harmful), as the effluent settleable solids concentration was about the same as in Tank No. 29.

The suspended solids data of Fig. 3.3 reveal the extent to which the higher velocity flow through the upper part of Tank No. 30 was keeping a uniform concentration (point E) whereas in Tank No. 29 the characteristic profile was developed, with the higher concentrations at the bottom. For this run the removal rate in Tank No. 29 was 66.1%, as compared to 55.6% in Tank No. 30. The advantage of the straight tank in this test is emphasized as one considers that the flow through it was about 8% greater than that through the baffled tank.

On an earlier day a test was run with discharge of about 60% of the amount in the test just described. In this test the suspended solids removal of 63.6% in the baffled tank was distinctly superior to that of 56.0% in the straight tank. In this case also, the tank giving higher removal was also the tank with the higher flow, an anomolous situation. Furthermore, in comparing the two tests on the straight tank alone, a 41% decrease in flow rate resulted in a decrease in removal from 66.1 to 56.0%. This only serves to show that one cannot place too much weight on the results of any single test in an operation of this sort.

The variation in suspended solids with depth and lateral location across the tank is shown in Fig. 3.4 for the tests cited above. Although the variation is small, there does seem to be a consistently higher concentration on the right side of Tank No. 29 at the midsection (Station E) than on the left side. The same is true of Tank No. 30 although less noticeable.

To search for an explanation of lateral variation in concentration one looks for evidences of shortcircuiting. Point measurements of velocity should reveal such a condition if it exists. Accordingly, Figs. 3.5 and 3.6 show simultaneous measurements of local velocity and suspended solids concentration. These measurements were taken on a different day from those of Fig. 3.4 and no significant variation in either velocity or suspended solids is discernible across the tank section. Based on the meager data available, no significance can be attached to the slight variations shown in Fig. 3.4

It should be remarked that the velocities shown in Fig. 3.5 pertain to

(Text continued on page 21)

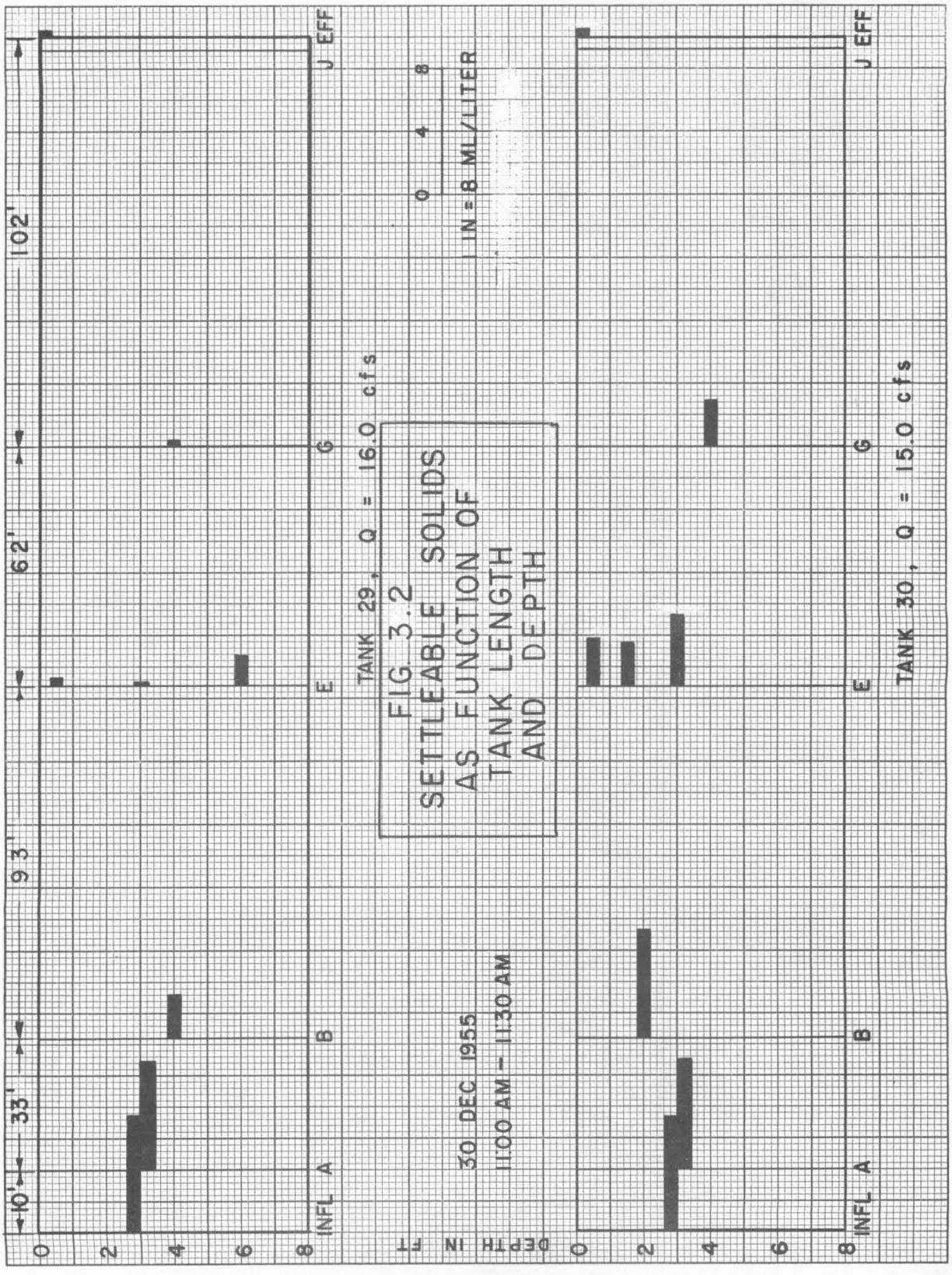

FIG. 3.2
SETTLEABLE SOLIDS
AS FUNCTION OF
TANK LENGTH
AND DEPTH

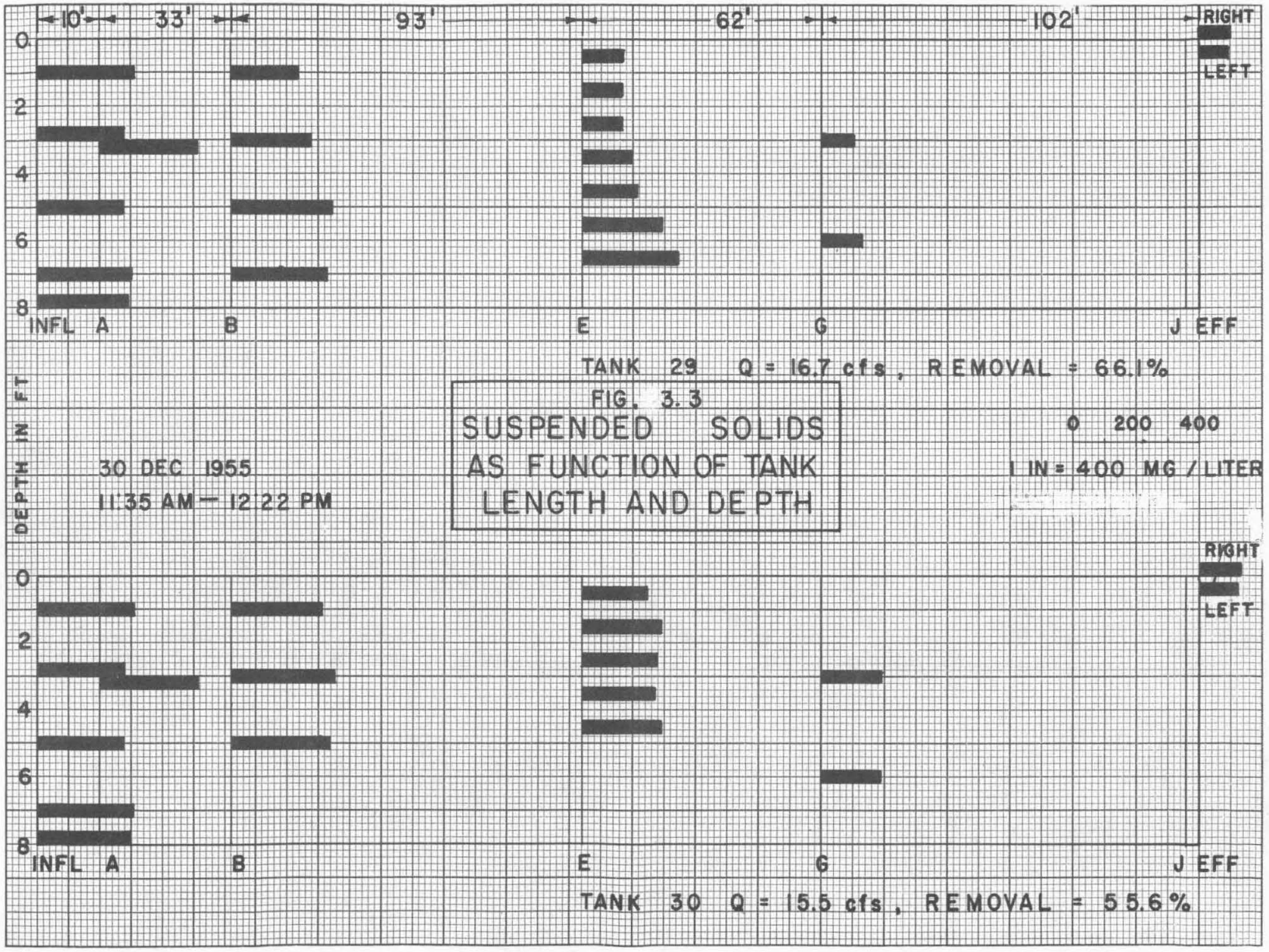
10'
33'
93'
62'
102'
RIGHT
LEFT
0
2
4
6
8
INFL
A
B
E
G
J
EFF
TANK 29 Q = 16.7 cfs, REMOVAL = 66.1%
FIG. 3.3
SUSPENDED SOLIDS AS FUNCTION OF TANK LENGTH AND DEPTH
0 200 400
1 IN = 400 MG / LITER
DEPTH IN FT
30 DEC 1955
11:35 AM — 12:22 PM
TANK 30 Q = 15.5 cfs, REMOVAL = 55.6%

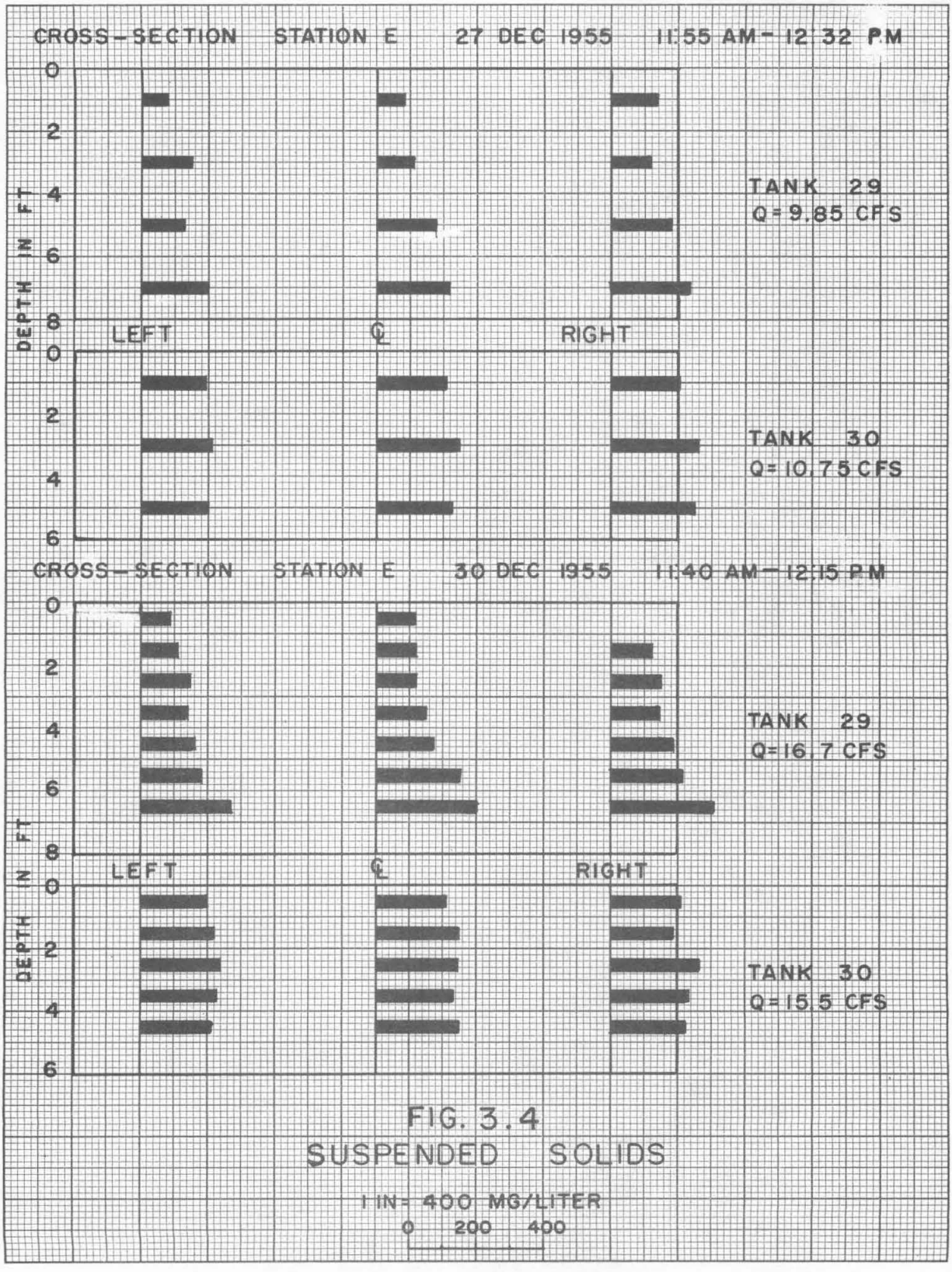

FIG. 3.4
SUSPENDED SOLIDS

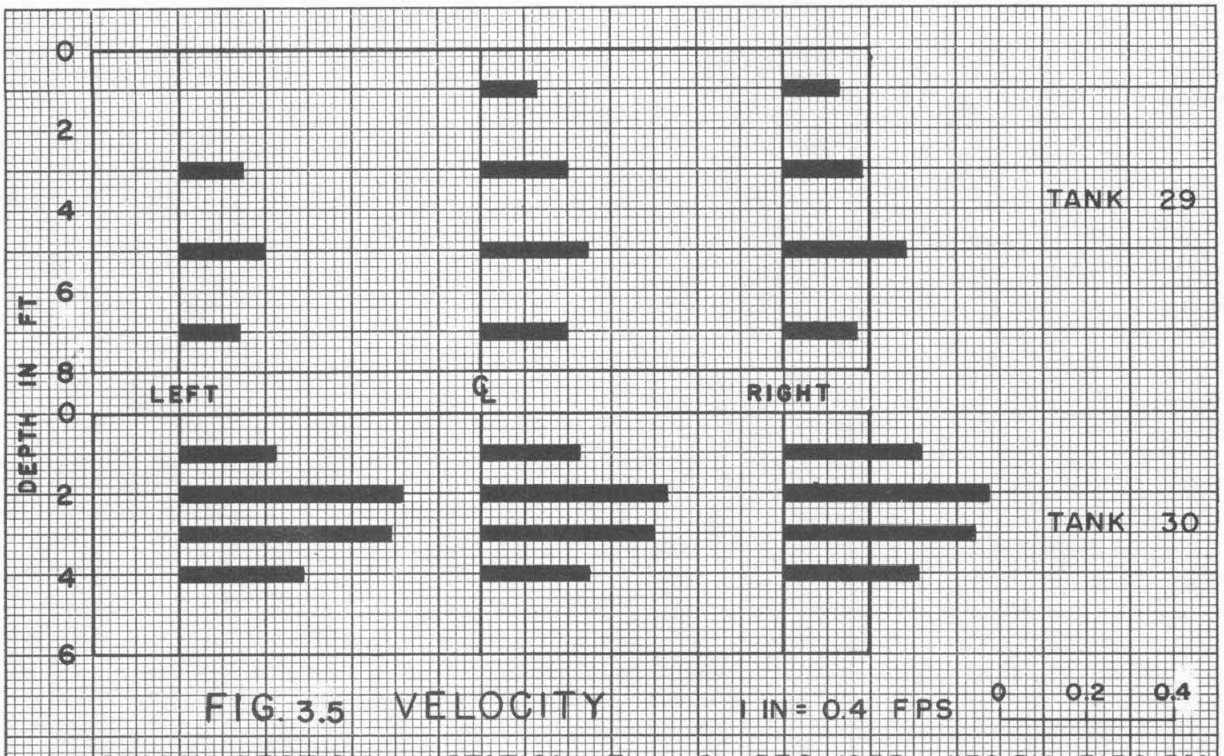

FIG. 3.5 VELOCITY 1 IN = 0.4 FPS

CROSS – SECTION STATION E 21 DEC 1955 1.32 PM – 3.50 PM

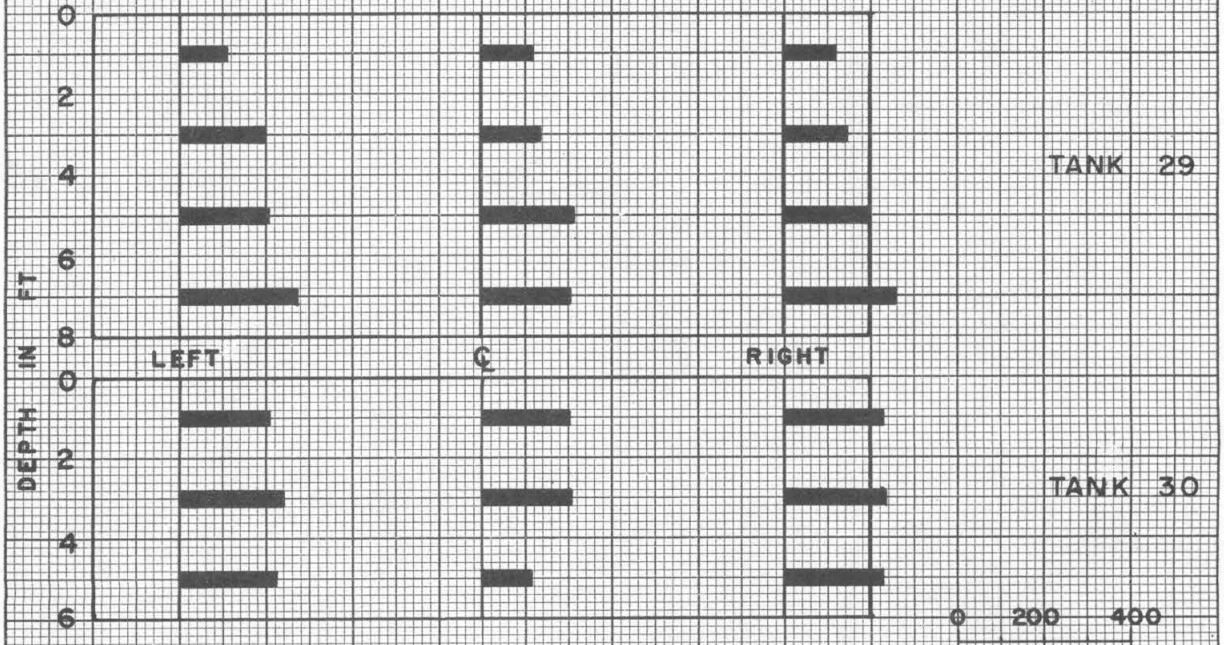

FIG. 3.6 SUSPENDED SOLIDS 1 IN = 400 MG/L

CROSS – SECTION STATION E 21 DEC 1955 11.55 AM – 12.25 PM

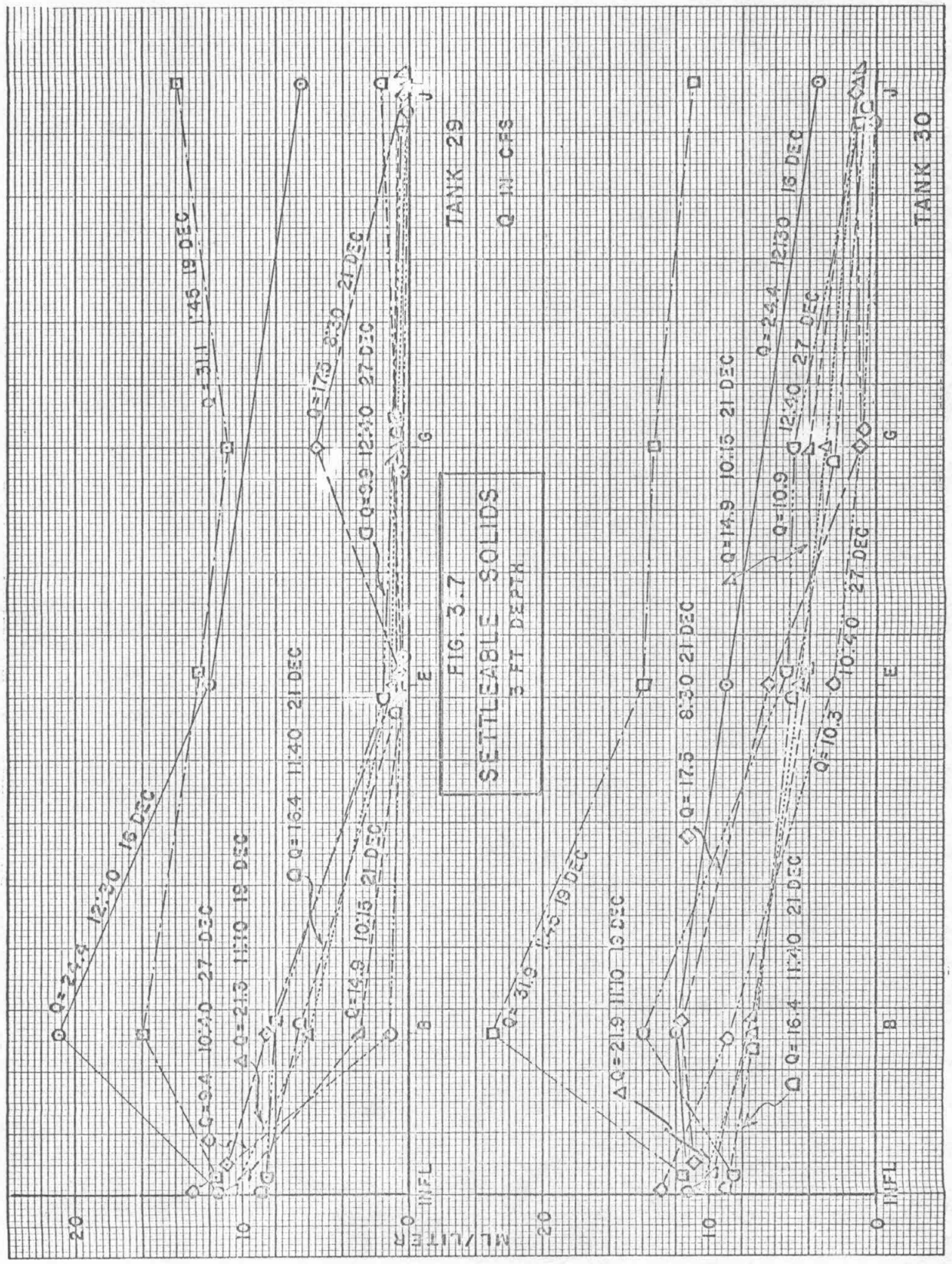
TANK 29
TANK 30
Q IN CFS
MG/LITER
INFL
E
G
J
FIG. 3.7
SETTLEABLE SOLIDS
3 FT DEPTH
Q=24.4 12:30 16 DEC
Q=31.1 1:45 19 DEC
Q=24.4 12:30 16 DEC
Q=21.9 11:10 19 DEC
Q=16.4 11:40 21 DEC
Q=14.8 10:15 21 DEC
Q=10.4 10:40 27 DEC
Q=9.9 12:40 27 DEC
Q=17.5 8:30 21 DEC
Q=31.9 1:30 19 DEC
Q=21.9 11:10 19 DEC
Q=16.4 11:40 21 DEC
Q=14.9 10:15 21 DEC
Q=10.9 12:40 27 DEC
Q=10.3 10:40 27 DEC

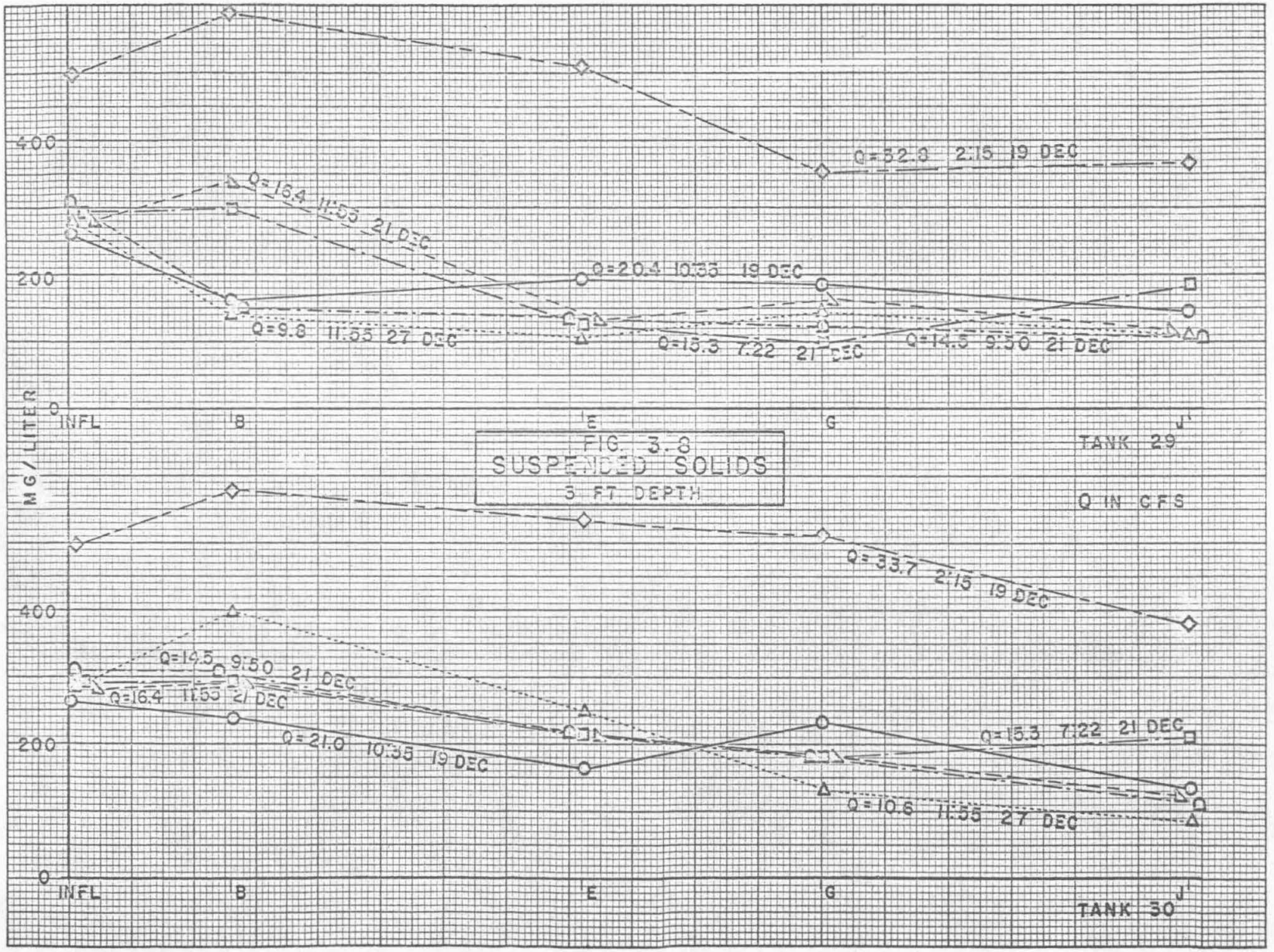

FIG. 3.8
SUSPENDED SOLIDS
3 FT DEPTH

the afternoon peak condition, with the tanks running at considerable overload, and are distinctly above design values, even in Tank No. 29. It is of interest to observe in Fig. 3.5 that the filament of maximum velocity occurred at a depth of about 5 ft in Tank No. 29 and at a depth of 2 ft in Tank No. 30. This location was much affected by the surface conditions, especially wind, prevailing at the time of the test. The higher velocities and resulting turbulence in Tank No. 30 were, of course, responsible for the more uniform concentration of suspended solids with depth in the tank. The difference between this and the more characteristic concentration curve in Tank No. 29 is clearly shown in the lower part of Fig. 3.4.

Summaries of all the data taken in this series of tests are shown in Figs. 3.7 and 3.8. The settleable solids concentrations of Fig. 3.7 show that effective removal was generally accomplished within the first half of Tank No. 29, while the full length of Tank No. 30 was required to bring the effluent to the same condition. The same type of difference between the two tanks is to be observed in the suspended solids data summarized in Fig. 3.8, although the superiority of the straight tank is not so marked as it is for the settleable solids.

Discounting the overloaded conditions of afternoon peak flow, at which neither tank performed well, the unbaffled tank shows a clear advantage over the baffled one, most demonstrably in the settleable solids data for the upstream half of each tank.

Resuspension

It is instructive to compare the two tanks with respect to the settleable solids data of 16 and 19 December at flows of about 24 and 22 cfs, respectively. As is shown in Fig. 3.7, the settleable solids concentrations in Tank No. 29 reveal no consistent difference among flows of 21.3 cfs and less. Let the discharge be increased 15% to 24.4 cfs, however, and the settleable solids are suddenly increased by 200 to 400%. This is taken as a clear indication that resuspension of settleable solids was taking place. The mean horizontal velocity at which resuspension commences in Tank No. 29 was thus about 8.5 ft per min. This checks closely with Mr. T.R. Camp's formula for scour, Eq. (2.4), which yields a value of 7.6 ft per min. for the critical velocity required to scour organic particles of specific gravity, s = 1.2 and diameter, D = 0.06 mm., with conventional values of 0.04 and 0.025 for β and f respectively. On the other hand, if it be compared with the data shown in Fig. 16 of Ref.1.1 the value of 8.5 ft per min. is seen to be just twice the critical value of about 4.25 ft per min. for the alum-dosed sewage in the Valley Settling Basins of Los Angeles.

In the baffled tank the critical velocity and resultant evidence of resuspension did not seem to be so distinctly indicated as in the straight tank. Thus in the lower plots of Fig. 3.7 there appears to be a more gradual increase of settleable solids with discharge, with the largest jump coming between 24.4 and 31.9 cfs. Considering the decreased cross section owing to the baffles, this would represent a "critical velocity" of something like 18 ft. per min. in the upstream half of the tank and 12 ft per min. in the downstream half. Thus the baffles may have some beneficial effects in reducing resuspension, although these appear to be obscured by adverse effects

from other sources such as turbulence caused by eddies around the baffle plates.

Settling Efficiencies

As explained in Eq. (6) and Fig. 3 of Ref.1.1, the settling efficiency, η, for any particle size may be defined as the ratio of actual to ideal removal ratios,

$$\eta = \frac{r_a}{r_i} \qquad (3.2)$$

The difficulty in applying this definition to the tests described here is that there was no method for determining the settling analysis of either influent or effluent, and consequently it was not possible to isolate any fraction of the suspension for efficiency analysis. Four months later, however, in tests reported hereinafter, settling analyses of raw sewage at this same plant were determined and the mean velocity, v_m, was found to be about 0.1 ft. per min. Using this rough value coupled with the measured overflow rate, v_o, it is possible to compute a Hazen number based on the "mean particle,"

$$H_m = \frac{v_m}{v_o} \qquad (3.3)$$

for each run. The total actual removal ratio, $\mathcal{R}_a$, can then be plotted against H_m to yield a graph something like Fig. 3 of Ref. 1.1.

In only four of the runs reported here were the discharge and removal data considered sufficiently accurate to analyze in this way. These four runs are plotted for both tanks in Fig. 3.9. The straight line at 45° represents the ideal removal that would be obtained for a suspension of discrete particles of uniform size having settling velocity equal to v_m of the actual suspension. Inasmuch as the ideal removal for the median particle, r_{im}, is equal to H_m if $H_m < 1$, (true for all runs reported), a kind of pseudo-efficiency can be computed for each run by taking the ratio of $\mathcal{R}_a$ to H_m.

As it happens, two of the runs on each tank lie above the "ideal removal" line and two lie below it. It is not possible to draw any firm conclusion from this plot, but it is safe to say that the runs representing over 100% "efficiency" reveal the effects of flocculation and quite possibly the predominance of particles that settle faster than v_m, while the runs lying below the "ideal" line represent the effects of turbulence, shortcircuiting, resuspension, etc., together with the possible predominance of particles settling slower than v_m. The data are clearly inadequate to support any more definite conclusions, but it is interesting to note that on this plot the baffled tank comes off no worse than the straight tank and, if anything, somewhat better at the higher values of H_m, i.e., at the lower overflow rates or discharges.

Conclusions from Comparison Tests of Baffled and Non-Baffled Tanks

The summary data plotted in Figs. 3.7 and 3.8 show clearly that the baffled tank, No. 30, has on the average a higher concentration of both

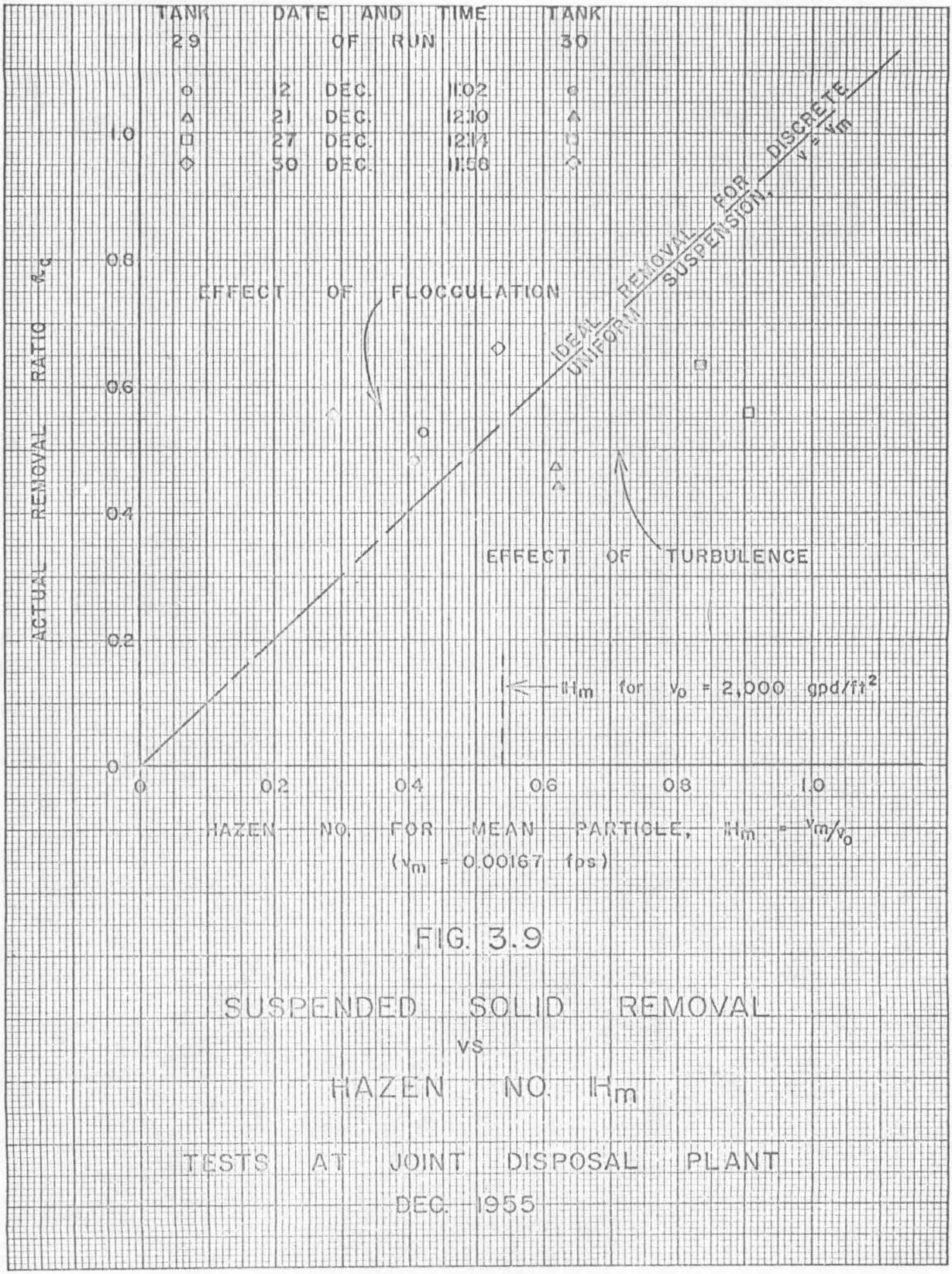

FIG. 3.9

SUSPENDED SOLID REMOVAL

vs

HAZEN NO. H_m

TESTS AT JOINT DISPOSAL PLANT

DEC. 1955

settleable and suspended solids throughout its length than does the straight rectangular tank, No. 29. For this reason the baffles were removed by the Joint Disposal Plant following this series of tests.

The failure of the baffled tank to show any clear advantage in these tests is felt to be due principally to the wide spacing of 4 ft between the higher baffles and 2 ft between the lower ones. This is wide enough for large eddies to form between baffles and prevent particles from settling quietly into the space from the high-velocity flow above. Despite the lack of any support for the baffled tank in Figs. 3.7 and 3.8, there was in plots like Fig. 3.9 enough evidence in favor of the baffles to warrant further investigation of the idea. Three years later it was possible to make tests on the effect of baffles in the laboratory model tank, where conditions could be more readily controlled than in full-scale tests. These are reported in Chapter 8.

3.2 Tests on Unit No. 4

Test Procedure

To test the performance of a sewage settling tank, 2-gal. specimens of influent and effluent suspensions were taken in the morning and analyzed in the laboratory in the afternoon of the same day. Each specimen was stirred in a crock and five 500-ml aliquots were taken with a dipper to determine an average total suspended solids concentration. The remainder of the sample was then poured into one of the settling tubes shown in Fig. 3.10 and mixed for one minute by moving a mixing device up and down the length of the settling tube above the intakes at about one cycle per second. The hand mixer was simply a rod and plunger device, the plunger being 7.8 cm in diameter and containing 4 holes of 1.27 cm diameter so as to occlude 47% of the tube cross-section.

At time zero the mixer was removed and 50-ml samples were drawn from the sampling intake at 16, 32, 64, 128 ..... seconds until the last of the suspension had settled past the intake. These samples were then submitted to the standard suspended solids determination, and the results were plotted on a cumulative frequency curve like that of Fig. 3.11, with the velocity for each point being equal to the distance from the free surface to the sampling intake divided by the sampling time.

It should be remarked here that the temperature in the laboratory settling apparatus was always about 10°C warmer than the sewage in the settling tanks. This effect has been compensated in the curves and computations that follow by adjusting the field data, such as overflow rate, to the laboratory conditions. The adjustment is based on the change in viscosity with temperature and the consequent effect on the settling velocity as obtained from Stokes' law.

Results and Discussion

Of the four tests made on Unit No. 4 in the spring of 1956, only three were subject to analysis. The venturi meter measuring the effluent from the unit at that time was so situated that it was possible for the throat to be non-submerged (a condition which has since been corrected), and consequently the discharge calculations were erroneous for one run in which this

(Text continued on page 30)

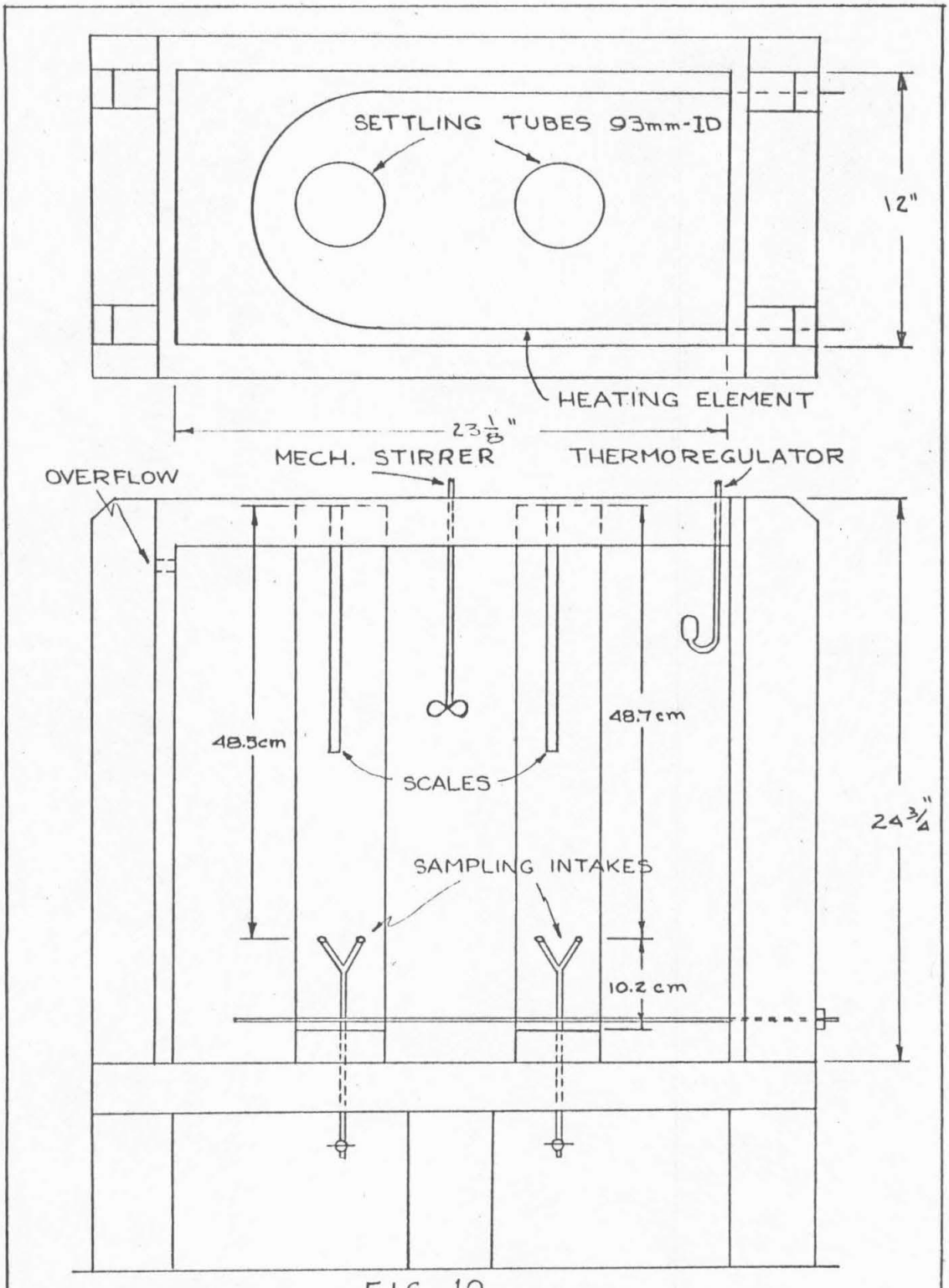

FIG. 10
SETTLING TUBES IN CONSTANT TEMP. WATER BATH

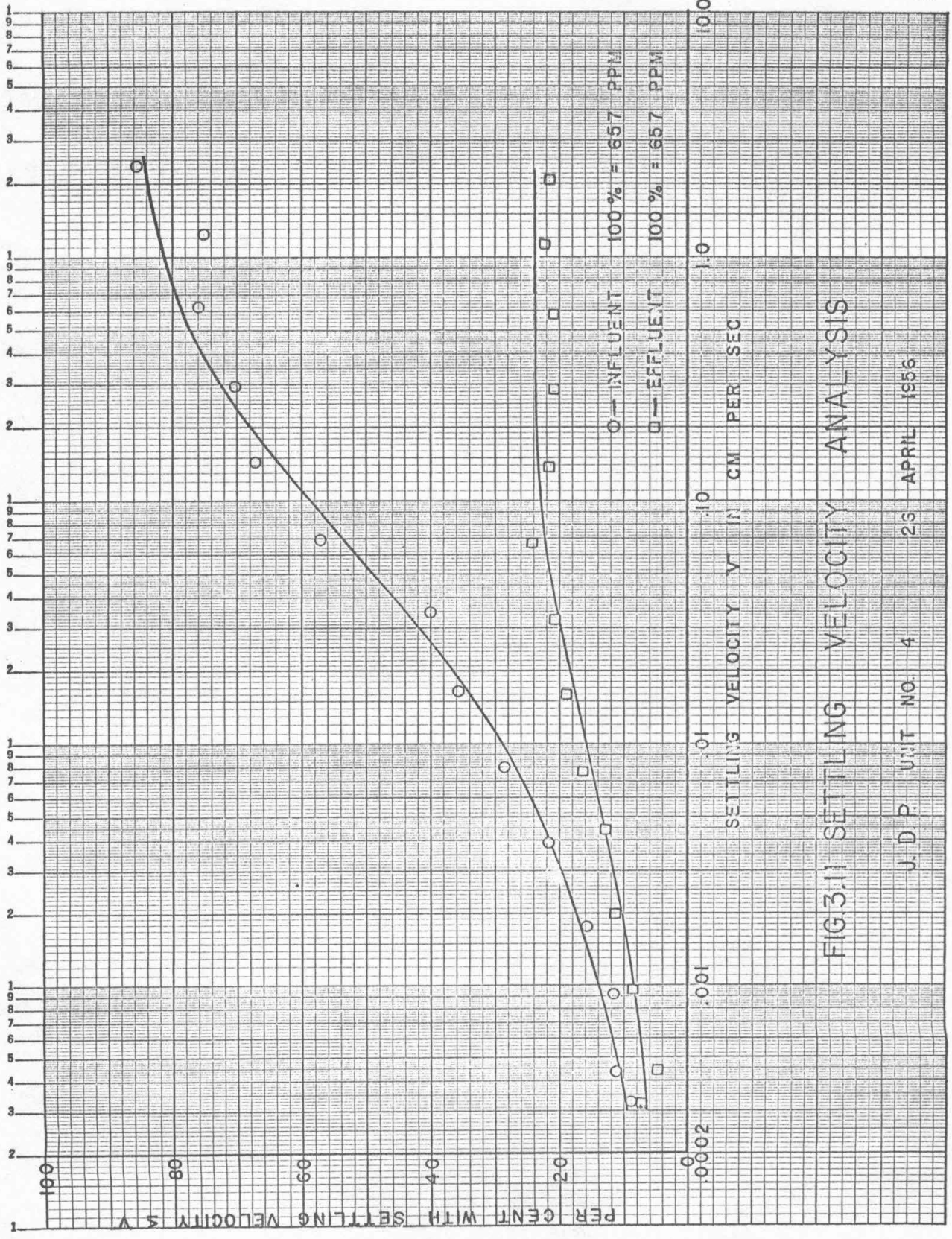

FIG 3.11 SETTLING VELOCITY ANALYSIS

J. D. P. UNIT NO. 4 26 APRIL 1956

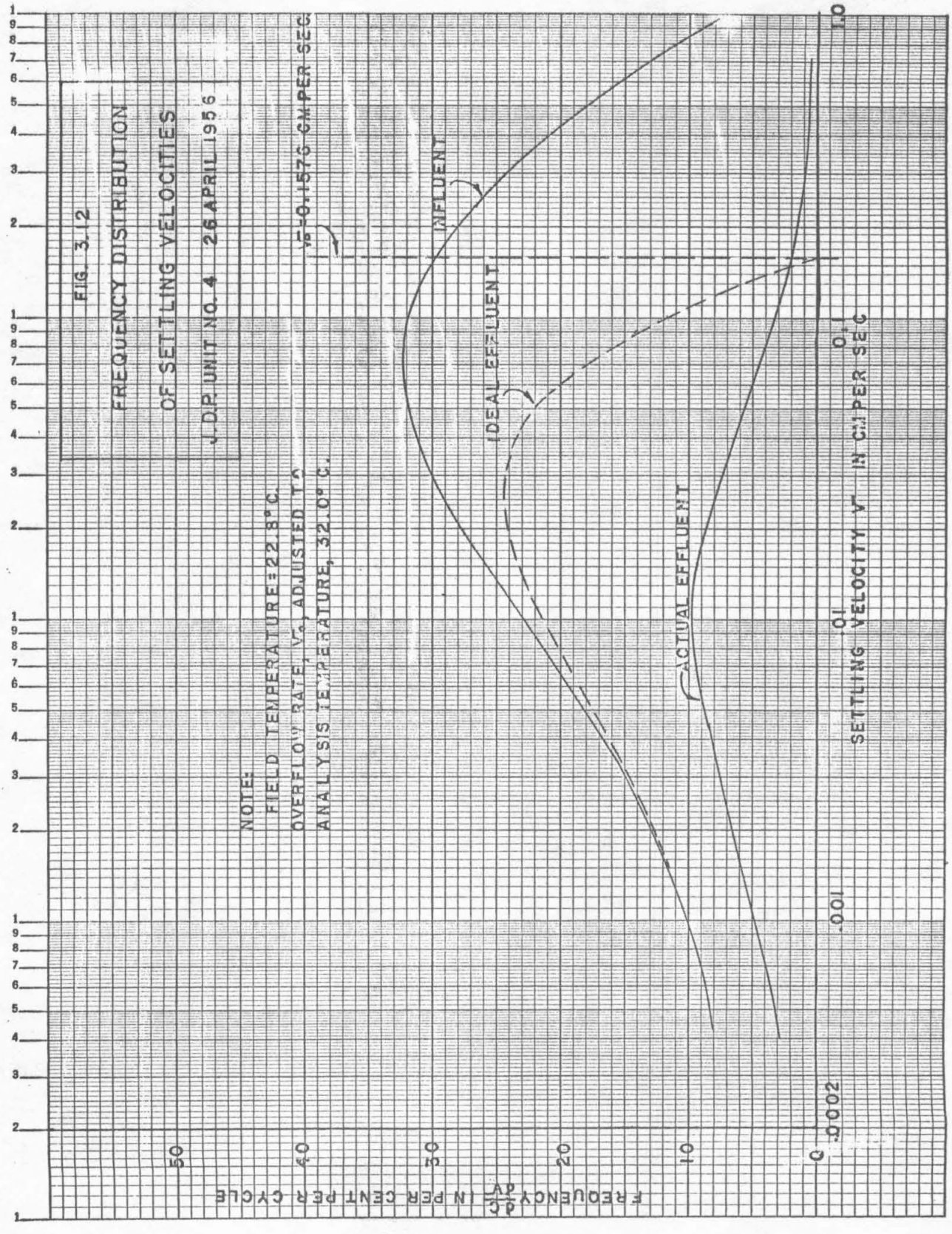
FIG. 3.12
FREQUENCY DISTRIBUTION
OF SETTLING VELOCITIES
I.D.P. UNIT NO. 4 26 APRIL 1956
NOTE:
FIELD TEMPERATURE = 22.8°C.
OVERFLOW RATE, Vo, ADJUSTED TO
ANALYSIS TEMPERATURE, 32.0°C.
Vo = 0.1575 CM. PER SEC.
INFLUENT
IDEAL EFFLUENT
ACTUAL EFFLUENT
FREQUENCY dV/dv IN PER CENT PER CYCLE
SETTLING VELOCITY V IN CM. PER SEC.
50
40
30
20
10
0
.0002
.001
.01
.1
1.0

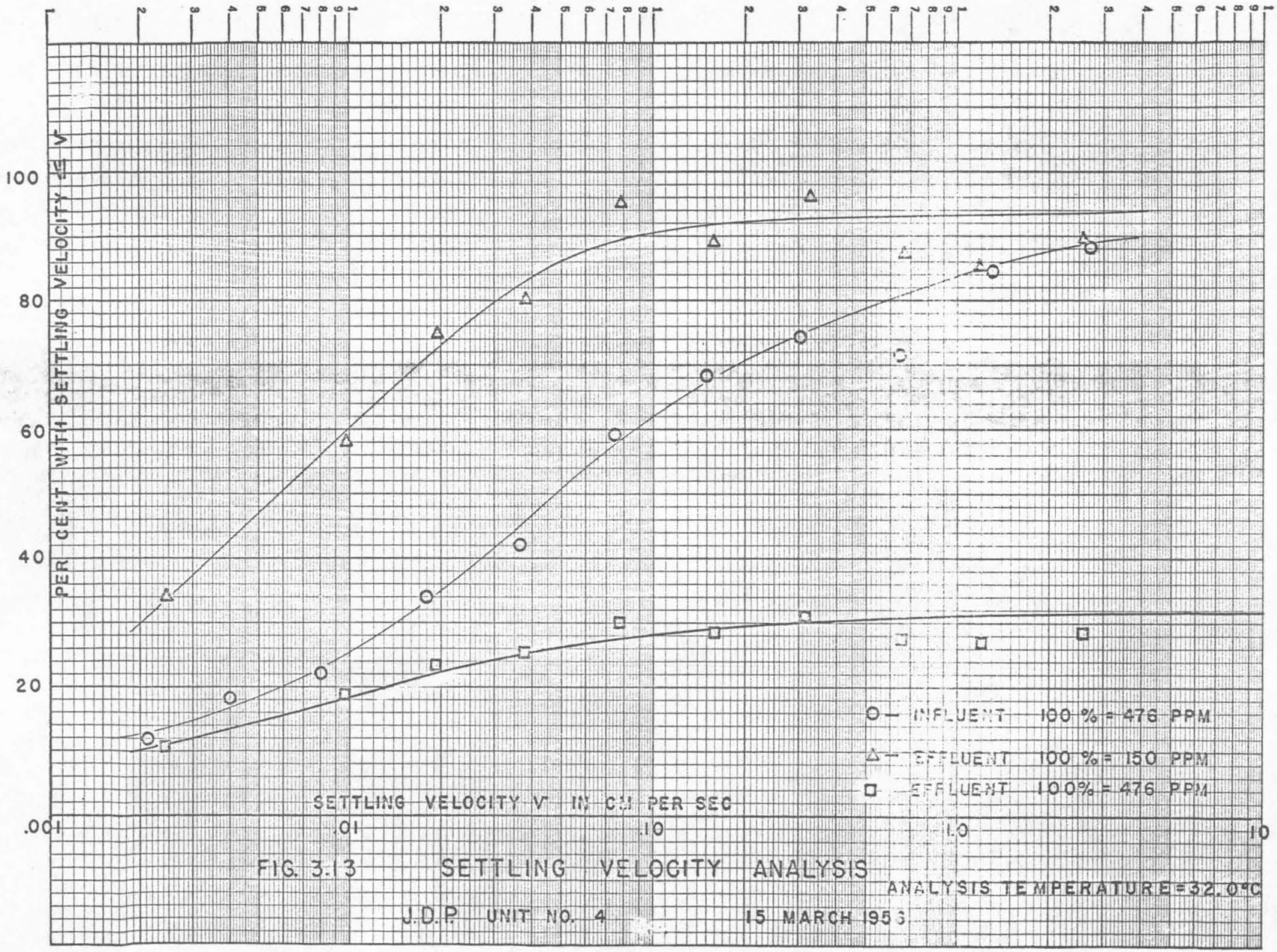

FIG. 3.13 SETTLING VELOCITY ANALYSIS

ANALYSIS TEMPERATURE = 32.0°C

J.D.P. UNIT NO. 4 15 MARCH 1953

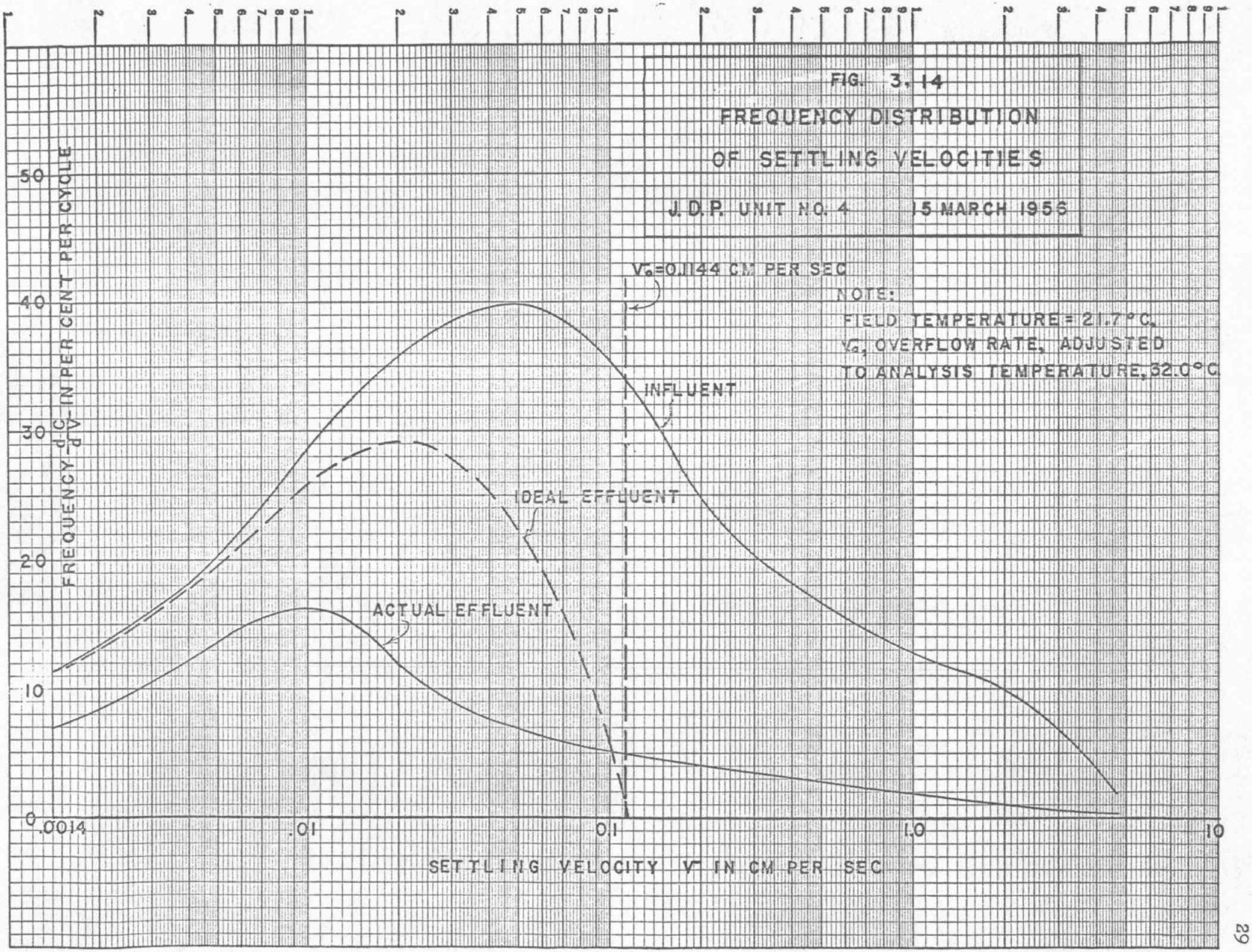
FIG. 3.14
FREQUENCY DISTRIBUTION
OF SETTLING VELOCITIES
J.D.P. UNIT NO. 4 15 MARCH 1956
V_o=0.1144 CM PER SEC
NOTE:
FIELD TEMPERATURE = 21.7°C.
V_o, OVERFLOW RATE, ADJUSTED
TO ANALYSIS TEMPERATURE, 32.0°C.
INFLUENT
IDEAL EFFLUENT
ACTUAL EFFLUENT
FREQUENCY $\frac{dC}{dV}$ IN PER CENT PER CYCLE
50
40
30
20
10
0
.0014
.01
0.1
1.0
10
SETTLING VELOCITY V IN CM PER SEC

condition obtained.

Unit No. 4 of the Joint Disposal Plant has the same capacity as the four tanks of Unit No. 5 described earlier, but there are no longitudinal walls separating the tanks. Presumably, therefore, this unit should be more subject to transverse mixing. The cumulative settling velocity analyses of the influent and effluent suspensions for the run of 26 April is shown in Fig. 3.11. It is interesting to note that even the first sample taken, at 16 seconds which is about as fast as physically possible for the equipment used, already shows a concentration of only 85% of the average influent concentration as determined by the five aliquots taken from the crock. As would be expected, this is not a problem when examining the effluent suspension because the faster settling particles do not appear in the total sample. In fact, three aliquots taken before the effluent suspension was analyzed yielded an average concentration of 157 ppm or about 24% of the raw influent concentration. The plotted data show that this same concentration prevailed more or less, at the beginning of the settling test, even to samples taken as long as 8 minutes after the start of the test.

A more revealing form of these data is given in the frequency distribution curve of Fig. 3.12. Here the first derivative of the concentration is plotted, so that the area under one of the curves represents the total amount of the suspension, in this case 657 ppm for the influent. The dashed line shows the effluent suspension that would be expected in an ideal tank operating at the same overflow rate, as explained in Ref.1.1. For any settling velocity, $v < v_o$, the ideal effluent concentration, f_i, is obtained simply from the relation

$$f_i = f_r\left(1 - \frac{v}{v_o}\right) \qquad (3.4)$$

The effect of flocculation in this unit is clearly shown by comparison of the ideal and actual effluent frequency curves. For a suspension of discrete particles such as sand or silt, it would be theoretically impossible for the actual effluent curve to fall below the ideal effluent curve, as this would represent the particles in the tank falling faster than those in the settling tube.

The definition for a total or integrated efficiency given in Eq. (2.3), when translated to the frequency distribution curves, means that the efficiency is given by the ratio of the total area under the influent curve less the area under the actual effluent curve to the area under the influent less that under the ideal effluent. Should that definition be applied to the flocculent suspension, however, the "efficiency" of this basin would plainly be something on the order of 200%! There is obviously a need for a realistic definition of efficiency of a settling basin handling flocculent suspensions, one that will truly be a characteristic of the basin itself, and upon which one can build a series of comparative tests to determine whether one basin design is superior to another.

The "overflow residual efficiency," discussed in Ref. 1.1 , can be applied with limited significance to tests of flocculent suspensions. The definition of overflow residual efficiency, which is the ratio of the area between

influent and actual effluent curves to the area under the influent curve, all taken to the right of the overflow rate only, avoids the anomolous situation of an efficiency greater than 100%.

Inasmuch as the area under the frequency curves is given by values of the ordinate on the cumulative curves, the overflow residual efficiency for this run can be computed readily from Fig. 3.11. The ordinate to the influent curve at the overflow rate of 0.1576 cm per sec is 65% so that 35% of the suspension should have settled out completely. The effluent curve at this velocity, however, shows an ordinate of 21.7%. Since the total suspended solids concentration in the effluent was 157 ppm or 23.9% of the influent concentration, the area under the effluent curve to the right of v_o would be 23.9 - 21.7 or 2.2% and the overflow residual efficiency would be

$$\mathcal{E}_o = \frac{35 - 2.2}{35} = 93.7\%$$

Another simplified measure of efficiency suggests itself here, one that would be independent of the influent suspension and would therefore be just half as much work as the overflow residual efficiency to determine. For the present it may be termed "effluent overflow efficiency" and it can be defined as the ratio of the area under the effluent curve to the left of v_o to the total area under the effluent curve. In terms of the above numerical values for this run, it would be

$$\mathcal{E}_{eo} = \frac{21.7}{23.9} = 90.9\%$$

Other tests were made on the same unit on 11 April and 15 March, of which the latter yielded the cumulative distribution curves of Fig. 3.13, and the frequency distribution curves of Fig. 3.14. The triangles plotted on Fig. 3.13 not shown on the other cumulative curves, show the sharp difference between influent and effluent suspensions when each is plotted against its own total concentration of 100%. The flat top on the effluent curve, which was observed in Fig. 3.11, is especially clear here. In fact the flat part of the curve appears to begin at just about the overflow rate of 0.1144 cm per sec, as would be expected.

The overflow residual and effluent overflow efficiencies for these three runs may be summarized in the following table:

	Fig. 3.11-3.12 26 April	11 April	Fig. 3.13-3.14 15 March
Influent concentration at v_o,%	65.0	64.0	84.5
Per cent of infl. suspension with $v > v_o$	35.0	36.0	15.5
Effluent concentration at v_o,%	21.7	31.0	31.0
Total effluent concentration,%	23.9	33.6	31.5
Per cent of effl. suspension with $v > v_o$	2.2	2.6	0.5
Infl. less effl. for $v > v_o$	32.8	33.4	15.0
Overflow residual efficiency	93.7	92.8	96.8
Effluent overflow efficiency	90.9	92.3	98.3

On account of the predominant effects of the flocculation it is difficult to say whether either of these efficiency measures has much significance in the case of flocculent suspensions. They are all so nearly 100% that it is difficult to spot the differences. It does appear, however, that the effluent overflow efficiency is about as revealing as the overflow residual efficiency. In effect, it asks the question: "What per cent of the particles in the effluent properly belong there?" In either case, practical usage of such a parameter for sewage treatment plants would require an elutriation meter that could measure the concentration of particles having velocity greater (or less) than the overflow rate without going through a complete suspension analysis. The complete laboratory procedure, as followed here, is probably more than can be expected of the normal sewage plant laboratory and personnel.

Observations

It is significant that the influent suspension in the tank and in the tube commences settling in either case from a previous condition of violent mixing. In the tube, however, this quickly dies away to the true quiescent condition, while in the tank there is a gentle continuous mixing by turbulence that is quite evidently beneficial in the formation of flocs that settle more rapidly than the smaller particles.

This series of tests reveals little if any information on the resuspension problem, but it helps to show the vast difference in the nature of the settling process in a tank handling a flocculent suspension from that in a tank receiving a suspension of discrete particles.

The conventional measure of total or integrated efficiency is shown to be clearly meaningless for the settling tank receiving a flocculent suspension, as the values come to well over 100% in all cases. The overflow residual efficiency, however, continues to have a valid meaning although it is obscured by flocculation. A new performance measure, the effluent overflow efficiency, appears to be about as valid as the overflow residual efficiency and is much simpler to compute. Its ultimate usefulness will depend upon the development of a simple elutriation meter for sewage treatment plant laboratory use.

References

3.1 "Standard Methods for the Examination of Water, Sewage and Industrial Wastes," Tenth Edition, American Public Health Association, Inc., New York, 1955.

Chapter 4

TESTS AT IMPERIAL DESILTING WORKS OF ALL-AMERICAN CANAL

From the tests of the primary settling tanks of the Joint Disposal Plant reported in the last chapter, it was clear that none of the existing or proposed measures of performance was properly applicable to a settling tank receiving a flocculent suspension. It remained to be demonstrated whether these measures would apply to a sedimentation basin receiving a suspension of discrete particles. Although the project was established to study the behavior of flocculent suspensions, it has been recognized from the first that the simpler mechanics of discrete suspensions had to be understood as thoroughly as possible before undertaking the more complex study of flocculent suspensions.

It was conjectured that the silt of the Colorado River would properly represent a suspension of discrete particles. On a single day in May of 1956, accordingly, samples were taken from the influent to and the effluent from Basins Nos. 1 and 3 of the Imperial Desilting Works at the entrance to the All-American Canal on the lower Colorado River. In addition, a sample was taken from the sludge line of Basin No. 1. The sludge gathered by the 24 rotary scrapers in each basin is returned to the river just below the desilting works.

Each basin is divided into two parallel sections, 255 ft. wide by 820 ft. long. The flow progresses across the 255 ft. width, encountering twelve 125 ft. diameter rotary scrapers in each section and spilling over an effluent weir 767 ft. long. At the time of sampling, the flow was calculated (by downstream gaging in the canal and measurement of head on effluent weir) to be 3,920 cfs in Basin No. 1 and 4,480 cfs in Basin No. 2. The sludge return was estimated at 100 cfs from each basin. The water temperature was 20.6°C.

The samples were subjected to settling velocity analyses in exactly the same way as for the sewage tank tests of Chapter 3. The results of the samples taken from Basin No. 3 are shown in the cumulative analysis of Fig. 4.1 and the frequency distribution of Fig. 4.2. The analyses from Basin No. 1 are less regular and are not shown here. Comparison of these curves with Figs. 3.11 and 3.12 demonstrates clearly the difference between the flocculent and non-flocculent removal behaviors. While the flocculent suspension produces an effluent of lower concentration than the "ideal effluent" the non-flocculent suspension yields an effluent concentration which is not only considerably higher than the "ideal effluent" but for much of the distribution, it is apparently even higher than the influent concentration!

For Basin No. 3, the actual removal was from an influent concentration of 62.6 ppm to an effluent of 57.3 ppm, or 8.5%. The ideal removal is obtained from observing that the measured overflow rate, v_o, was 6,910 gpd per sq. ft. or 0.327 cm per sec. Since the laboratory analysis was conducted at 32°C, however, it was necessary to adjust the measured overflow rate (on the basis of Stokes' law and the viscosity of water at the two temperatures) to the higher value of 0.4205 cm per sec. The intersection of this vertical line with the cumulative influent curve of Fig. 4.1 shows that 66% of the particles had settling velocity, v, less than the overflow rate, v_o. The ideal removal

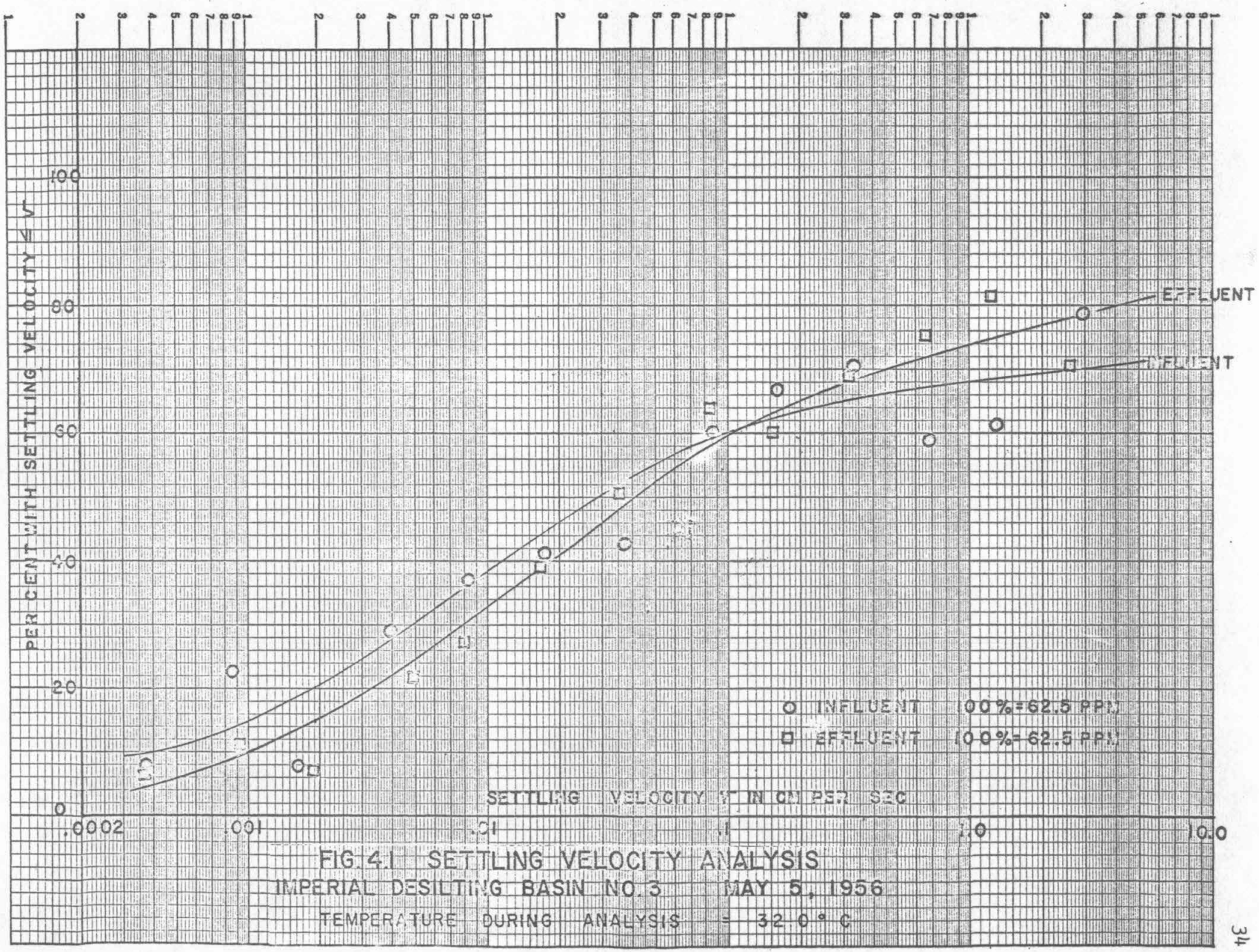

FIG. 4.1 SETTLING VELOCITY ANALYSIS
IMPERIAL DESILTING BASIN NO. 3 MAY 5, 1956
TEMPERATURE DURING ANALYSIS = 32.0° C

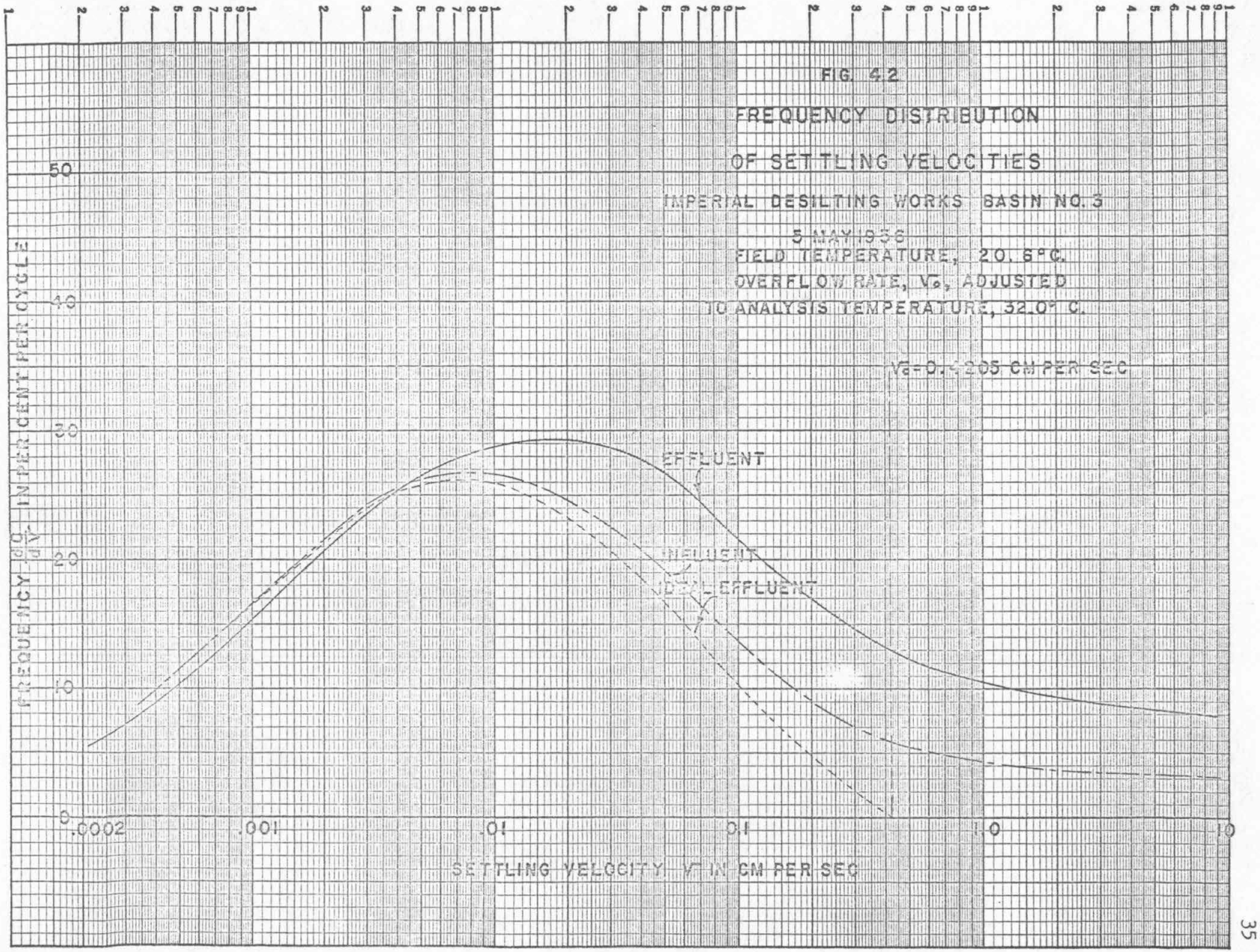
FIG. 4.2
FREQUENCY DISTRIBUTION
OF SETTLING VELOCITIES
IMPERIAL DESILTING WORKS BASIN NO. 3
5 MAY 1958
FIELD TEMPERATURE, 20.6°C.
OVERFLOW RATE, Vo, ADJUSTED
TO ANALYSIS TEMPERATURE, 32.0° C.
Vo=0.1205 CM PER SEC
EFFLUENT
INFLUENT
DESILTEFFLUENT
FREQUENCY (Δp/Δv) IN PER CENT PER CYCLE
50
40
30
20
10
0
.0002
.001
.01
0.1
1.0
10
SETTLING VELOCITY V' IN CM PER SEC

would thus be the 34% of the particles with $v > v_o$, plus the proportion of those with the slower settling rates that should reach the bottom by virtue of having started through the basin at an elevation below the water surface. In Fig. 4.2 this would be given by the area between the influent and ideal effluent curves divided by the area under the influent curve, in each case to the left of the v_o line only. If this ratio may be roughly estimated at 10%, the total ideal removal would be 34 + 10, or 44%. With an actual removal of 8.5%, the "true" or "integrated" efficiency of the basin is seen to be 8.5/44 or about 19%.

It is also instructive to compute the "overflow residual efficiency," defined in Ref. 1.1 as the ratio of percentage removal of particles with settling velocity $v > v_o$ to the total percentage of such particles in the influent suspension. Inasmuch as the effluent curve of Fig. 4.1 crosses the v_o line at about 69.5%, and since the total effluent concentration is 91.5% of the influent, the proportion of the influent suspension that is represented by effluent particles of $v > v_o$ is 91.5 - 69.5 = 22%. The removal of such particles is evidently 34 - 22 = 12% (of the influent) and the overflow residual efficiency is therefore 12/34 or 35%.

Finally we may compute the "effluent overflow efficiency" discussed in Chapter 3. This would be 69.5/91.5 or 76% and it tells us that more than three-quarters of the particles found in the effluent actually "belong" there, i.e., they are too small to have settled through the depth of the tank in the detention time available.

Sludge Balance for Basin No. 1

It will be instructive to compare the computed silt removal in Basin No. 1 with the measured concentration in the sludge return line discharging to the river downstream. This concentration was found to be 206 ppm. With an estimated sludge flow of 100 cfs (could not be measured accurately), this would come to a sludge solids flow of 0.0206 cfs. The solids inflow to the basin was measured from samples to be 0.202 cfs. By this method, then, the net removal was calculated to be 10.4%. Computed on the basis of effluent sampling, however, the removal was found to be 23.8%.

The difference between these two removal figures represents one or more of the following possible conditions: (a) samples not representative, (b) sludge discharge flow approximately 100% greater than estimated, (c) unsteady state condition, i.e., the basin removes twice as much silt from the river as it returns through the sludge discharge. The first two conditions are certainly possible but should not account for the 130% discrepancy, and thus deduction indicates that an unsteady state condition prevails, with the basin capturing a net amount of silt. The confirmation of this reasoning will be found in the photograph of Fig. 4.3, which shows the great quantities of Colorado River sand that have collected in one of the other basins. The basins are shut down periodically and the silt is sluiced out or removed mechanically.

Summarizing the application of the various measures of performance to these few data yield computations of removal and efficiency ranging from 8.5 to 76%. It is not possible to say that one or another method of computing efficiency is fully satisfactory, even for the relatively non-flocculent

suspension of Colorado River water. It is clear, however, that by any standard of performance the desilting basin is far from satisfactory. To what extent resuspension was responsible for this condition was not known from this preliminary test. Other factors entering this picture would include turbulence and shortcircuiting, both of which would prevent the particles from reaching the bottom in the proper numbers. It is believed that the rotary scrapers may cause a good deal of turbulence and resuspension of settled particles from the bed.

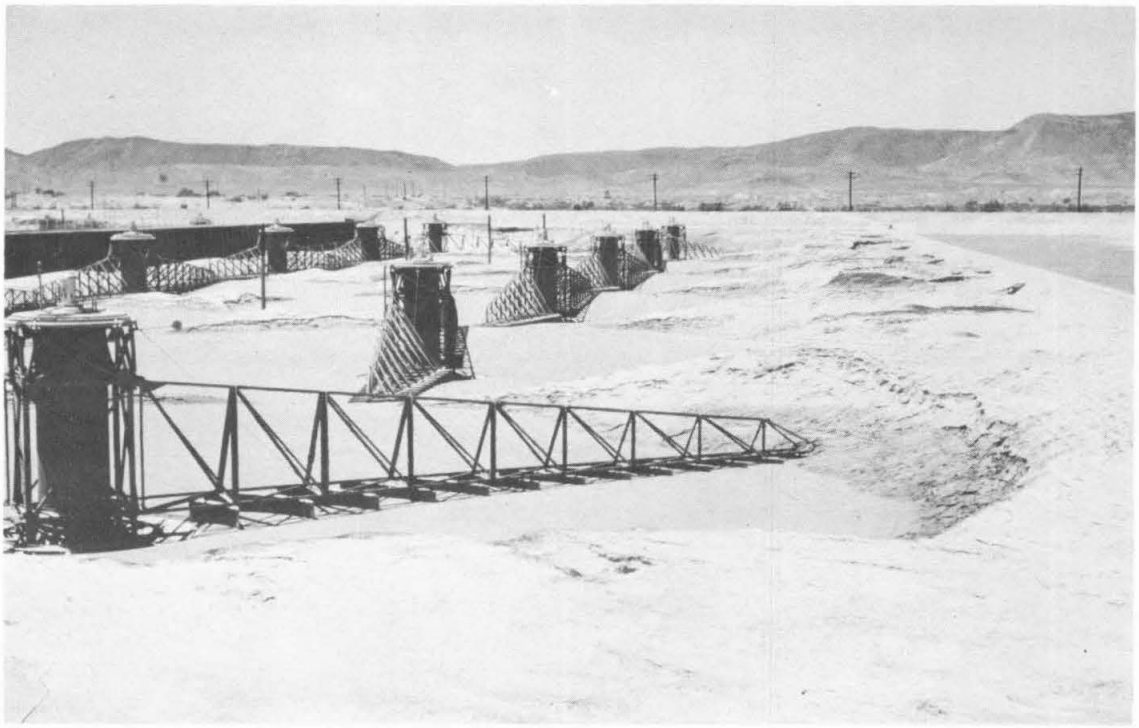

Fig. 4.3

DEPOSIT OF SEDIMENT IN BASIN NO. 2
OF IMPERIAL DESILTING WORKS
(5 May 1956)

Chapter 5

SUSPENSIONS AND SOLIDS FOR LABORATORY STUDIES

In order to carry the study of resuspension from the field tests reported in the two preceding chapters to the laboratory where conditions of flow and turbulence could be carefully controlled, it was necessary to find a suitable suspension for such studies. Raw sewage, while having the practical advantage of being exactly the item under ultimate consideration, has many limitations for laboratory use in which it is desired to make reproducible runs from day to day. It was further decided early in the study that a more thorough understanding of the behavior of non-flocculent suspensions would have to be gained before the flocculent suspensions could be attacked intelligently. One further requirement for a laboratory suspension was that it be amenable to visual and photographic studies. Only in this way would it be possible to analyze the all-important effects of turbulence.

5.1 Desired Characteristics of Laboratory Suspensions

The most important characteristic of a suspension is its settling velocity, or rather its distribution of settling velocities since there exists almost no natural suspension consisting entirely of particles having the same settling velocity. Thus, referring to Figs. 3 and 4 of Appendix A, the settling velocity of Pasadena sewage is seen to vary over a thousandfold range, and even then approximately 30% of the suspension settled too slowly to be measured at all.

The first part of the laboratory study was to check existing theories on scour of particles from a smooth flat bed, the idea being that the mechanics of initial suspension must be well defined before the resuspension problem could be attacked. It was further believed desirable to make the initial studies on suspensions of uniform size or settling velocity so that the observed particle movement could be related to known particle settling velocities. Consequently the search began for a non-flocculent "photogenic" suspension of particles that could be readily classified as to settling velocity, and having velocities falling within the range encountered in raw sewage.

Several materials were selected as possible solids for the bed scour studies. These were tested for some of the following five properties: (a) specific gravity, dry and saturated, (b) ability to be wetted by water and to be dispersed in water, (c) shape and appearance, (d) settling velocity, and (e) intensity of stirring required for resuspension in glass beaker. A brief description of the tests is given in the following paragraphs.

a. Specific gravity. For dry solids, the specific gravity was obtained by the method described in Ref. 5.1, p. 15. If a material such as wood sawdust is to be used for solids in suspension, the particles must be saturated with water, which will act as part of the particle. In order to calculate the effective specific gravity it is necessary to determine the water content of the submerged particle. This determination was attempted by rapidly filtering a suspension of water and saturated particles through a porous stone, then

measuring the water content of the residue on the stone. Auxiliary tests were run to estimate the filtration time necessary to remove superficial water without removing the water in the particles.

b. Wetting and dispersion of particles. Several of the materials had a strong tendency toward flocculation of particles in water and attaching themselves to air bubbles in water. A number of wetting and dispersing agents were tested for their ability to counteract these tendencies.

c. Visual inspection. All materials were examined under the microscope at low magnification to determine the shape of particles, range of size of particles, tendency to be wetted and tendency to flocculate. Color and opacity were observed for photographic purposes.

d. Settling velocity of particle. The distribution of settling velocities in a suspension was obtained by a slightly modified pipette analysis procedure, described in Appendix A, p. 22.

e. Resuspension by stirring in a beaker. A bed of a material to be tested was laid down in the bottom of a liter beaker containing one liter of distilled water. The beaker was placed on a standard laboratory stirring device with the paddle placed just below the water surface. The stirring speed at which the bed material began to be picked up provided a comparison among the various solids as to resuspension, and especially between artificial flocculent suspensions and natural sewage.

The results of the foregoing tests are summarized in Table 5.1 and Fig. 5.1.

f. Angle of repose. One further test was performed on the gilsonite and sand particles only. This was the determination of the angle of repose in both the dry and submerged conditions. The angle of repose is related to the shearing force (in terms of the particle's weight) necessary to produce incipient motion in each particle. It may be expected that the angle of repose should be independent of submergence inasmuch as the forces are all static and all are proportional to the net effect of gravity on the particle. The tests confirmed this hypothesis, showing a mean angle of repose of approximately 39° with less than a degree variation from this value encountered in four sizes of gilsonite, both submerged and dry. There is a slight increase in angle of repose, from 38° to 39.5° with increase in mean particle size from 0.35 to 0.99 mm. This may be expected because the structure of gilsonite tends to make the sharp points more effective in increasing the angle of repose in the larger particles than in the smaller ones.

Although the angle of repose does measure the tendency toward resuspension it is true that if two suspensions of discrete particles had exactly the same static values of angle of repose, but one consisted of heavier particles than the other, then the bed of lighter particles would be the more easily suspended because the available resisting force would be less. This is illustrated in the comparison of gilsonite with the Ottawa "90" sand. The gilsonite has actually a greater angle of repose (39°) than has the sand (33°), but when it is subjected to hydrodynamic forces that are proportional to kinetic quantities rather than to the particle weight it is suspended more easily than is the sand.

FIG. 5.1

SETTLING VELOCITY ANALYSES OF VARIOUS SUSPENSIONS
Gilsonite tested is 20-28 Tyler Mesh, with
Ds = 0.71 mm

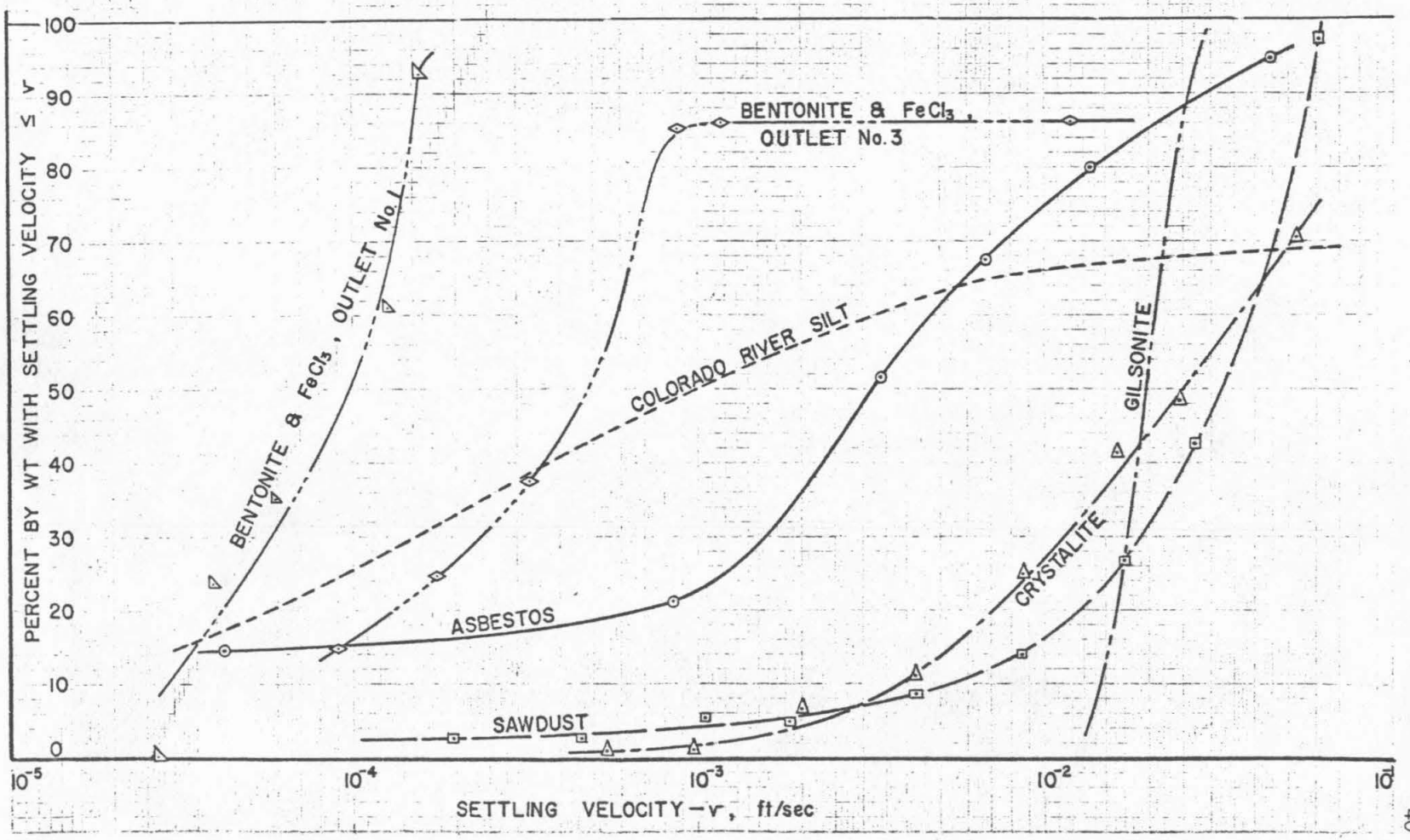

TABLE 5.1

Name of Material	Description	Particle Shape	RPM for Resuspension	Specific Gravity Dry	Specific Gravity Saturated	Mean Settling Velocity	Wetting Agent	Dispersing Agent
Sawdust	Mixture of many woods. Product of circular saw	Irregular	--	1.50	1.12	0.9 to 1.0 cm/sec at 28.5°C	--	--
Crystalite	Compression moulding powder of acrylic resin. Mfg. by Rahm and Haas	Spherical	--	1.24	--	0.3 to 0.8 cm/sec at 28.7°C	x-100 Rohm and Haas Product	Daxad 11 Dewey and Almy Product
Ottawa Sand	Ottawa "90" sand D_g = 0.137 mm (geom. mean diameter) σ_g = 1.38 (geom. std. dev.)	Spherical	--	2.656	--	2.70 cm/sec = 0.0885 fps (Angle of repose, 33.4° dry, 33.5° submerged)	--	--
Gilsonite	Natural asphalt mined by American Gilsonite Co. Crushed and sieved.							
	20-28 Tyler mesh (D_s = 0.71 mm) (arith. mean diam.)	Irregular	13	1.037	--	0.6 cm/sec = 0.0197 fps	Ethyl alcohol	Ethyl alcohol
	28-35 Tyler mesh (D_s = 0.50 mm)	"	--	"	--	0.365 cm/sec = 0.012 fps	"	"
	35-48 Tyler mesh (D_s = 0.35 mm)	"	--	"	--	0.230 cm/sec = 0.00755 fps	"	"
Sewage	Settled solids from domestic sewage resuspended in distilled water	Irregular	9	1.2 est.	--	0.02 cm/sec = 0.00065 fps (See Figs. 3 & 4 of Appendix A)	--	--
Asbestos	Fiber used for mats in Gooch crucible	Light floc	10	2.92	--	0.1 cm/sec at 21.2°C	--	--

TABLE 5.1 (cont.)

Name of Material	Description	Particle Shape	RPM for Resuspension	Specific Gravity Dry	Specific Gravity Saturated	Mean Settling Velocity	Wetting Agent	Dispersing Agent
Tea Leaves	Tea leaves soaked 4 hours, boiled 10 minutes	Irregular	--	1.48	1.04	(not measured)	--	--
Peat Moss	Commercial grade Sphagnum peat moss 14-20 Tyler mesh (D_s = 0.99 mm)	Irregular, stringy		1.57	1.03	1.02 cm/sec = 0.0335 fps	x-100 (vacuum method superior)	--
	35-48 Tyler mesh (D_s = 0.35 mm)			"	"	0.4 cm/sec = 0.0131 fps	"	--
Tobacco	Sir Walter Raleigh smoking tobacco	Irregular		1.633	1.06	(not measured, seen to be too heavy)		
Bentonite $FeCl_3$ Floc	Ferric chloride floc particles 0.5 to 1 mm across largest dimension formed around nuclei of bentonite clay	Light floc	10	--	--	0.013 to 0.02 cm/sec 0.000426 to 0.00065 fps	(see Chap. 9)	

5.2 Selection of Suspensions for Laboratory Studies

From among the materials described in Table 5.1 (and any others available) it was necessary to select one discrete and one flocculent suspension which could be used in the extensive flume studies described in the following chapters. Most materials were ruled out quickly for one reason or another. Among the discrete particles, sawdust was found to settle too rapidly, and it required some 32 hours for complete wetting. The Crystalite spheres were heavy enough so that they had to be extremely small in order to have reasonably slow settling velocities, and this made them hard to collect and photograph. The Ottawa sand was of course still heavier and faster. The gilsonite particles, on the other hand, were light enough in specific gravity to settle very slowly while retaining a shape large enough and black enough to see and photograph well. Thus practically all of the tests on discrete particle suspensions were performed on gilsonite particles in one of three size ranges. These particles were crushed in a roller device and then sieved mechanically. As the particles became worn down in the tests it was necessary to resieve the supply in any one size group to keep eliminating the fines.

As for the flocculent solids, real sewage served as the standard. It was originally hoped that a mechanically flocculent solid could be found that would be completely reproducible as to settling characteristics. The asbestos fiber suspension was the first such to be tried and it did indeed look promising. It was found, however, that a bed of asbestos floc would "set up" with time so that it became extremely stable against resuspension. This introduced another parameter, time, which clouded the resuspension picture, already quite complicated enough.

There followed three hopeful possibilities, tea leaves, peat moss, and tobacco. The best of these was peat moss and it was used in the flume for a number of motion pictures illustrating the behavior of a semi-flocculent suspension. It required great pains in sieving this light stringy material, however, and the settling velocity was still too great for any of the practical sieve fractions.

The best floc for the laboratory studies was made of a bentonite clay suspension with ferric chloride as a coagulant. This was found to behave most closely like a natural sewage floc, including a settling velocity in the same range as sewage itself. This meant that all of the hydraulic parameters of the laboratory work, such as mean velocity, bed Reynolds number, overflow rate and the like, could be the same as for prototype settling tanks, a considerable advantage in evaluating the laboratory tests. Accordingly, the ferric chloride-bentonite floc was perfected and used for all the floc tests of 1959, described in Chapters 9 and 10.

5.3 Characteristics of Floc used in Flume Runs

The floc generated for introduction into the flume (to be described in Chapter 6) was a suspension consisting of approximately 4% bentonite clay slurry at 40 g/l, 1.5% ferric chloride solution at 50 g/l, and 94.5% Pasadena tap water. This resulted in a flocculent suspension with an average concentration of 2.6 g/l. The clay used in the tests was Ibex bentonite clay obtained

from the Kennedy Minerals Company, Los Angeles, California. Analysis of the clay showed the following composition:

Fe_2O_3	1.90%	SiO_2	40.28%
Al_2O_3	16.02%	Moisture at 105 C	6.54%
CaO	10.38%	Ignition loss at 850 C	14.44%
MgO	9.94%	Specific Gravity	2.393
Na_2O and K_2O	0.48%		

The detailed procedure followed in making this floc and utilizing it in the flume tests will be found in Chapter 9.

Multiple pipette analyses were made on suspensions taken from the flume and on suspensions mixed manually to determine the settling characteristics of this floc. A 10-ft lucite settling tube designed by R. T. McLaughlin was used in the analyses (see Fig.10.4). The results of a test performed on floc taken from the flume during a typical run are shown as the two curves farthest to the left in Fig. 5.1. This figure also shows a comparison of settling velocity distributions for a number of other suspensions.

It is difficult to obtain frequency distribution curves of settling velocity for flocculent suspensions since the particles of floc do not remain discrete throughout the settling period. As the initial particles fall, those with higher settling velocities overtake the slower particles and cohere, thereby forming new and larger particles with different characteristics and higher settling velocities.

The effect of progressive flocculation in the settling tube is illustrated by the two bentonite curves of Fig. 5.1. Outlet No. 1 is the upper one and there is little flocculation affecting the samples drawn from it. By the time the particles have settled to the lower outlet, No. 3, however, flocculation has caused the particles to coalesce and fall more rapidly, yielding the distribution curve to the right. This illustrates, of course, the principal limitation on all the floc tests. Since the extent of flocculation was a function of both the motion and the time, it was often difficult to declare for certain just which effect was being demonstrated.

References

5.1 "Soil Testing for Engineers," by T. W. Lambe, John Wiley & Sons, New York (1951).

Chapter 6

HYDRAULICS OF THE 15-IN. FLUME

In order to carry the study of resuspension from the preliminary field tests into the laboratory, it was necessary to devise a tank or flume that would represent the basic features of a full-scale settling tank, of the type that might be found in the primary treatment of sewage, for example. A glass-walled flume, 14 ft long, 3 ft high, and 15-1/4 in. wide was made available from surplus equipment, and this was fitted out for the resuspension study as shown in Figs.1.1 and 6.1.

At the upstream end of the original flume, an inlet box is attached, extending an additional 3 ft. The depth can be varied from approximately 0.2 ft to 2.5 ft by means of an adjustable sloping weir at the effluent end. A circulating (or continuous fresh) water supply system provides a measured discharge through either one of two metering systems up to approximately 0.3 cfs. Water is introduced to the inlet box through two parallel 3-in. standwells, each discharging through a 1/2-in. wide slot extending the full water depth and so oriented that the two-dimensional jet is dissipated against the upstream end of the inlet box before it reverses direction to flow through the flume.

There is a considerable amount of turbulence in the inlet box. This is effectively damped out in passing through a perforated plate baffle, having approximately 19% free area, at the inlet to the flume proper. Point gages are mounted on carriages which roll along a pair of rails at the top of the flume.

The flume as it is shown in Fig. 6.1 contains many features that were not part of the first studies. The first flume bed, for example, consisted of a layer of 3/4-in. dummy floor section, so that a movable bed of any length and any depth up to 3/4 in. could be placed flush with the smooth floor at any point in the flume. These sections, which were originally made of plywood covered with mastic waterproofing, suffered serious deterioration from being submerged continuously and were soon replaced with aluminum floor sections of the same size.

After the first smooth bed scour studies were completed, the flume was fitted out with a model flight scraper system of the endless chain-belt type. Each flight scraper was 3/16-in. thick and 1/2-in. high, extending across the width of the flume. The flights were spaced at approximately 10 in. intervals and the whole system was driven (upstream along the floor) at speeds varying up to 0.036 fps, on the same order of magnitude as the speeds of prototype flight scrapers. The installation of flight scrapers made necessary a sludge hopper at the inlet end of the flume, so that the sludge scraped upstream by the flights could be removed from the flume. This was accomplished on the laboratory flume, with a slot extending across the width of the flume just upstream from the first window. During all scraper runs, the draft through this slot was approximately 0.014 cfs.

Another feature of the flume added after the completion of all of the gilsonite and a part of the floc tests are the 14 side-outlet sampling tubes

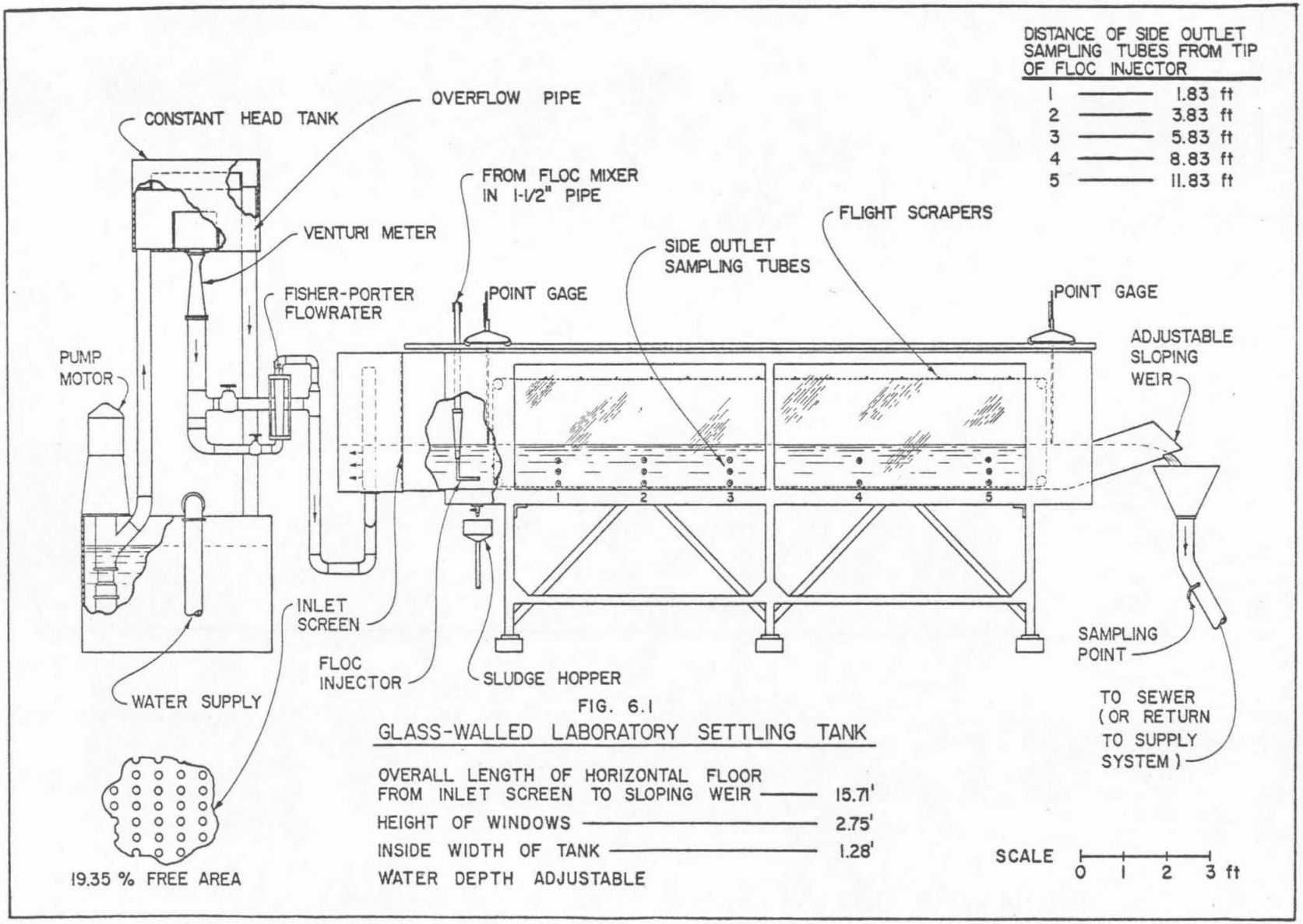

FIG. 6.1

GLASS-WALLED LABORATORY SETTLING TANK

OVERALL LENGTH OF HORIZONTAL FLOOR FROM INLET SCREEN TO SLOPING WEIR —— 15.71'

HEIGHT OF WINDOWS —— 2.75'

INSIDE WIDTH OF TANK —— 1.28'

WATER DEPTH ADJUSTABLE

shown in Fig. 6.1. These tubes are arranged in five stations along the length of the flume. Each station, except No. 4, consists of three of these tubes so that, with sliding in and out and slight rotation of the "L" shaped tubes the entire cross section of the flume can be sampled. Details of this procedure are left for Chapter 10.

Although it was originally contemplated to make quite a series of tests at different depths in this flume, the greater part of the studies on both flocculent and non-flocculent suspensions was conducted at a single setting of the effluent sloping weir, resulting in a still water depth of 1.09 ft. The variation of mean tank velocity with meter reading for the various types of flow meter is shown in Fig. 6.2. These velocities are seen to encompass a range extending to some 12 ft per min, considerably higher than would be encountered in normal settling tank practice. It should be noted that the velocities shown in Fig. 6.2 are uncorrected for the flow removed through the sludge hopper at the inlet end of the flume.

The Reynolds number in the flume as a whole is the best indication of turbulence or susceptibility to the same. The channel Reynolds number (based upon a "diameter" of four times the hydraulic radius) is shown in Fig. 6.3 as a function of the mean velocity for a range of temperatures encountered in laboratory work. It will be noticed that for all velocities in excess of 0.01 fps the Reynolds number is above the critical value of approximately 2,000. Thus the hydraulics of the flume for all of the studies in this report is definitely in the turbulent range.

It is recognized, of course, that the actual extent of turbulence in a settling tank has more to do with the inlet conditions than it has with the channel Reynolds number. To distribute the flow across the inlet to the laboratory flume, a perforated metal screen is placed between the inlet box and the flume proper. This screen has a free area ratio of approximately 19.4% so that, for example, a velocity of 0.124 fps in the flume would result in a maximum velocity through the screen of 0.64 fps. The resulting velocity head would be 0.0064 ft or 0.076 in. Upon one occasion when the flume velocity was in fact this much, the measured head loss across the screen was less than 1/16 in., and this is a good check.

To compare the energy dissipation from inlet turbulence with that resulting from wall friction, a representative friction factor may be selected on the basis of a smooth pipe at a Reynolds number of approximately 2.2×10^4. This would be $f = 0.025$ (Ref. 6.1). For a 14-ft length of channel having hydraulic radius of 0.318 ft and velocity of 0.124 fps, this results in a head loss of 7.1×10^{-5} ft. Thus the loss from inlet turbulence is approximately 70 times that contributed from wall friction.

Because of the great difficulty in measuring such low velocities with ordinary equipment such as pitot tubes, a dye injection system was rigged as shown in Fig. 6.4 to inject small globules of dye into the flow at various points. The progress of these globules was timed with a stopwatch to yield a series of curves showing time vs. distance downstream from the injector. The tangent to such a curve gives the local velocity. One study conducted in this way for a mean velocity of 0.74 fps showed clearly that the velocity

distribution was very uniform, with the velocity at an inch from the wall being within 10% of the mean velocity. This confirms what would be expected from the effect of the distribution screen at the inlet and the relatively high Reynolds number.

References

6.1 "Fluid Mechanics," by R. L. Daugherty and A. C. Ingersoll, Fifth Edition, p. 182, McGraw-Hill Book Co., New York (1954).

FIG. 6.2

MEAN VELOCITY IN FLUME VS. METER READINGS

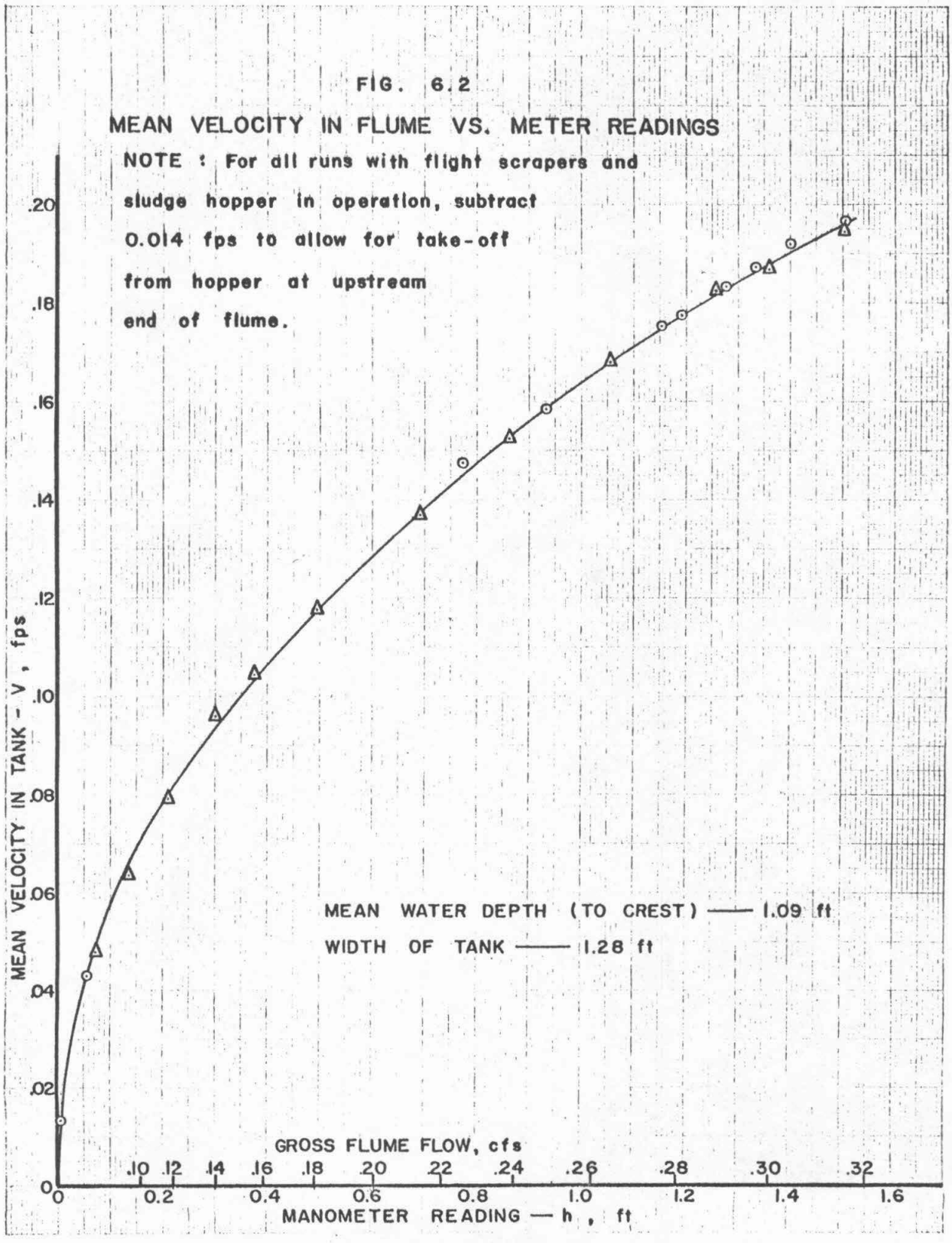

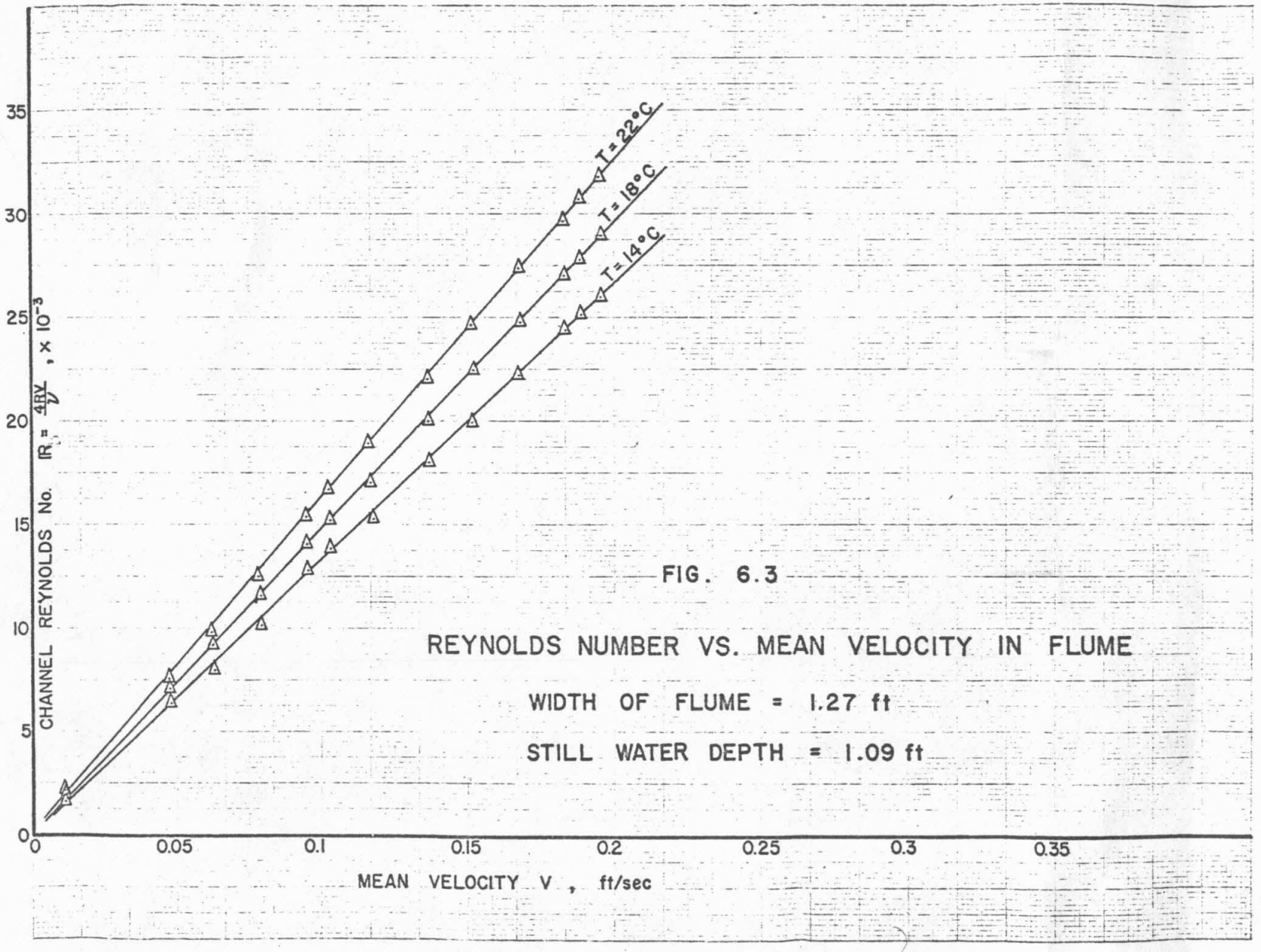

FIG. 6.3

REYNOLDS NUMBER VS. MEAN VELOCITY IN FLUME

WIDTH OF FLUME = 1.27 ft

STILL WATER DEPTH = 1.09 ft

FIG. 6.4

DYE INJECTION SYSTEMS

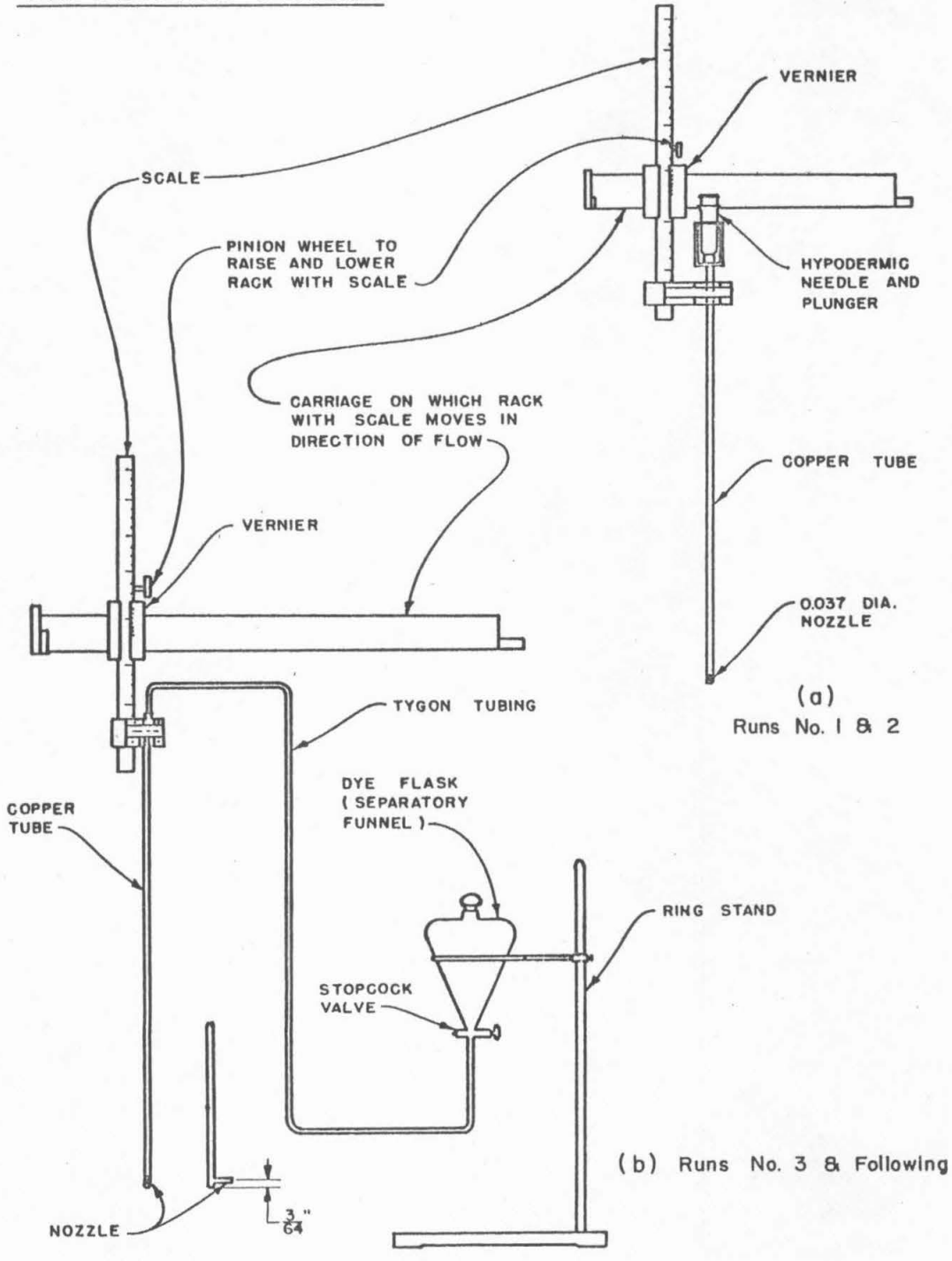

Chapter 7

SCOUR STUDIES - DIRECT MEASUREMENT OF CRITICAL VELOCITY

From the first of this project there had been no clear distinction between "resuspension" and "initial suspension," at least as to the mechanism involved. To put this in the form of a question, "If a particle of sediment lying on the bed of a channel is forced by certain hydraulic conditions to move, can it make any difference what has been the history of that particle before commencement of motion?" If the answer to this question is negative, then one must conclude that initial suspension and resuspension are identical phenomena.

In order to investigate this question it was first considered necessary to gain some primary data on scour of some of the artificial sediments discussed in Chapter 5. The procedure was, in general, to lay a smooth bed (under water) of the particles to be studied. The flow would then be increased gradually until motion of the particles was evident to the eye, and this became a crude determination of the "critical velocity." In some cases the amount of material scoured in a period of time was measured and this provided another parameter of the scour phenomenon. In most cases it was difficult to distinguish between scour in which the particles roll over one another but stay on the bed, and true suspension in which the particles are lifted into the stream.

The scour studies may be divided into two general parts, those in which scour from a recessed bed was induced by artificially generated turbulence, and those in which the natural hydraulic conditions in the flume caused the lifting of particles from the smooth flat bed.

7.1 Scour Tests with Recessed Bed and Turbulence Grid

The tests reported here were all made with a bed 1/4-in. deep, 18-in. long, extending the full width of the flume and located 22 in. upstream from the sloping end of the channel. These tests were also made at about the same water depth (still water depth of 13.1 in. to crest of sloping weir).

In selecting a bed material for the first tests in the scour flume, it was felt that a non-flocculent bed should be studied before attempting the more difficult case of a flocculent bed. It was, moreover, desired to study the lower range of bed Reynolds number, $u_* D/\nu < 1.5$, with a bed of very light particles. The gilsonite particles, of specific gravity 1.04, met this qualification admirably. By choosing a fraction of particles passing No. 20 Tyler sieve and retained on No. 28 ($0.0232 < D < 0.0328$ in.) the bed Reynolds number is held below 3 for channel velocities under 0.20 fps.

The first tests in the unobstructed channel revealed almost no activity of the bed, with the first signs of bed movement coming at a channel velocity, V, of 0.16 fps. The particles rolled very slowly over one another at this velocity, and the activity was not greatly increased when the channel velocity was brought to its maximum for that depth, 0.20 fps.

The purpose of the study is to investigate scour by turbulent eddies. It was, therefore, necessary to introduce upstream from the bed some kind of reproducible and definable turbulence. Fortunately, earlier work in the low turbulence water tunnel of the same laboratory, reported by Vanoni and Brooks, (7.1) offers a clue to the problem. In Figure 14 of reference 7.1, the decay of the vertical component of turbulence is plotted as a function of the relative distance downstream from a rectangular grid constructed of vertical and horizontal dowels, spaced a distance apart equal to their diameters. A fairly straight-line function is observed when the inverse square of the turbulence level, $V^2/\overline{v'^2}$ (in which v' is the velocity fluctuation) is plotted against the ratio of distance downstream to mesh size of grid.

A 1/2-in. dowel grid was installed in the flume a variable distance x_g upstream from the recessed gilsonite bed. A series of scour tests was run at channel velocities of from 0.10 to 0.18 fps, with the grid placed from 1 to 7-1/8 in. upstream from the bed. The results are shown in Fig. 7.1 in which entrainment is plotted against velocity. The length of each run was determined by the appearance of a bare floor scour hole of about 1 sq. in. of area. The weight of material entrained was defined to be the material carried off the bed and placed in any location downstream from the bed, or carried out of the flume in suspension and caught in a screen over the waste channel.

It was observed in all runs that approximately 90% of the particles transported are from the upstream 4 to 6 in. of the bed, and that the configuration of the downstream region of the bed is little changed from the original level condition, either by scour or deposition. It was further observed that the major movement of gilsonite particles is by bed load, the rolling or bouncing of particles along the top of the bed. An estimated 60 to 80% of the total movement, depending on the location of x_g, is carried in this manner. The remainder of the entrainment is truly suspended load as the particles are picked up in the turbulent eddies from the grid. This explains why the upstream end of the bed gets scoured the most, and why the location of the grid is so important. Even the particles entrained by suspension, however, appear largely to settle back to the floor downstream from the bed. From 4 to 30% of the load is carried more than 72 inches downstream as suspended load.

It was found that the age of the bed since the last previous disturbance has a good deal to do with its stability. The critical velocity can be increased some 50% by aging the bed for 16 hours. It must be assumed that the particles consolidate somewhat and settle into a firm position in the aging process. It was also observed that the transport rate decreased as the test continued, i.e., the greatest activity occurs at the very first of a run. This is because of the natural paving process that goes on in any region subject to erosion.

With regard to the flocculent bed materials, only a preliminary observation was made on an asbestos bed. This is the material that behaved most like sewage in the rotating flocculator tests. The trial observation revealed that the age of the flocculent bed is more important than the age of the granular bed. The asbestos bed appeared most unstable as it was being laid down under water, but after two hours it became rather stable and could not be scoured as easily as could the gilsonite.

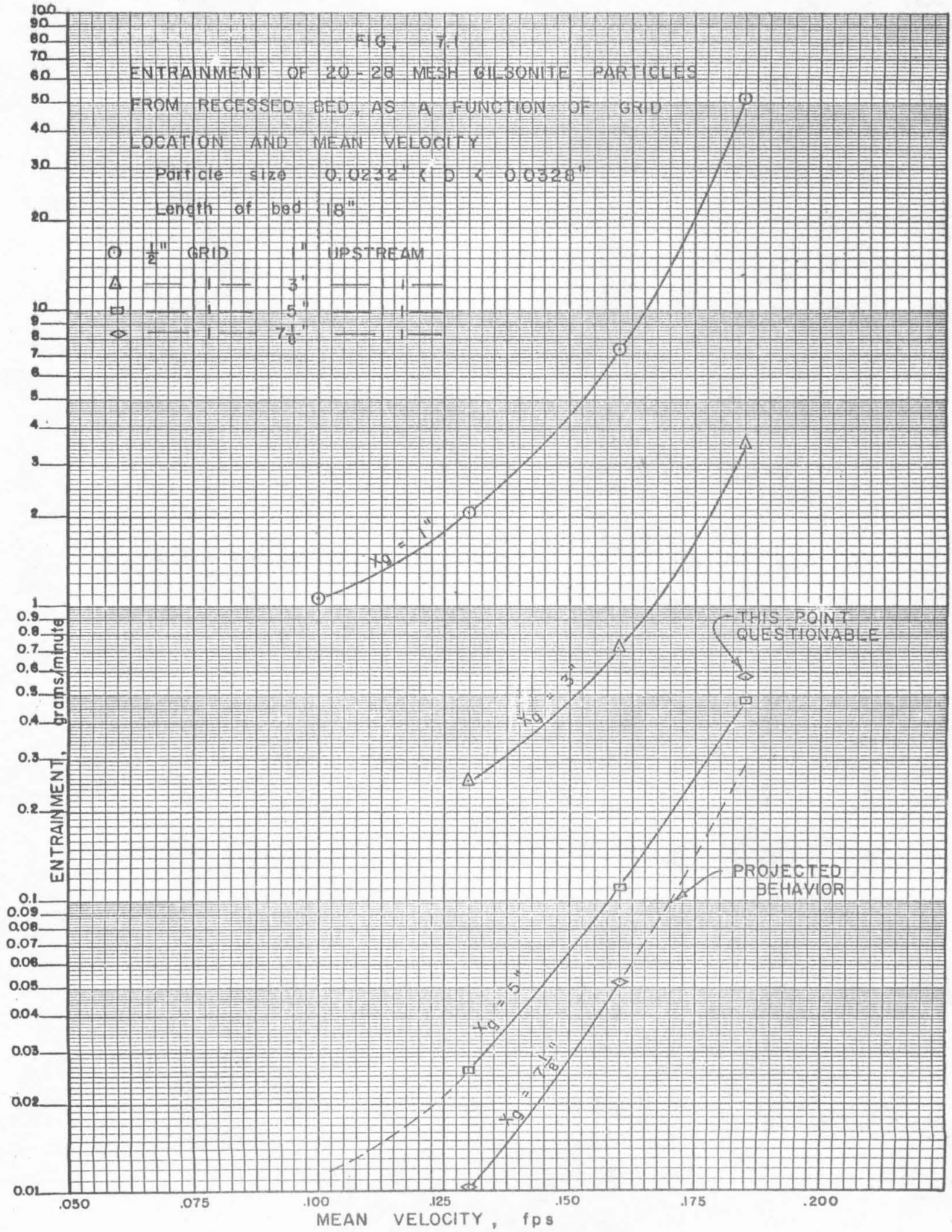
FIG. 7.1
ENTRAINMENT OF 20-28 MESH GILSONITE PARTICLES FROM RECESSED BED, AS A FUNCTION OF GRID LOCATION AND MEAN VELOCITY
Particle size 0.0232" < D < 0.0328"
Length of bed 18"
1/2" GRID 1" UPSTREAM
3" 1"
5" 1"
7 1/8" 1"
X_g = 1"
X_g = 3"
X_g = 5"
X_g = 7 1/8"
THIS POINT QUESTIONABLE
PROJECTED BEHAVIOR
ENTRAINMENT, grams/minute
MEAN VELOCITY, fps
100
90
80
70
60
50
40
30
20
10
9
8
7
6
5
4
3
2
1
0.9
0.8
0.7
0.6
0.5
0.4
0.3
0.2
0.1
0.09
0.08
0.07
0.06
0.05
0.04
0.03
0.02
0.01
.050
.075
.100
.125
.150
.175
.200

7.2 Entrainment of Particles from Bed Shear

Although residual turbulence from inlet conditions has been shown to be the principal source of energy available in the tank for the entrainment of particles from the bed, it is nonetheless desirable to make an appraisal of the entrainment that would occur from bed shear alone. The most useful approach to the evaluation of critical bed shear, that is, the bed shear at which particle movement commences, is that of A. Shields. In Eq. (6), Section 2, of Ref. 7.2, Shields derives an expression for critical bed shear, τ_c, as follows

$$\tau_c = \left(\frac{\gamma}{g}\right)^{1/3}\left[0.1\nu(\gamma_1-\gamma)\right]^{2/3} \qquad (7.1)$$

This expression is stated to be valid for values of bed Reynolds number (u_*D/ν) less than 2. A matter of special interest is that τ_c is not a function of the particle size. Unfortunately, however, Shields' experimental data extend only down to values of R_b on the order of 1.7. It is thus of much interest to check his formula for lower values of R_b, especially in view of the fact that the figures for gilsonite particles run down to approximately half of this value or 0.85.

The difficulty in this procedure is clearly how to obtain an independent evaluation of τ_c against which to check Eq. (7.1). The usual method in the case of long channels is simply to measure the slope for a steady condition of uniform flow at known velocity and discharge. Then the friction velocity, u_* is given by $\sqrt{gRS}$ in which R is the hydraulic radius and S is the measured slope. With shorter more slowly flowing channels such as settling tanks, however, it is virtually impossible to measure such a gradient and one must devise an alternative scheme for arriving at values of τ_c.

One scheme has been suggested by Ingersoll (7.4), derived from the method of Delleur (7.3) in which the bed shear is found to be a function of the ratio of mean velocity to the surface velocity in the channel. This is accomplished through the displacement thickness of the boundary layer, δ_*, in Eq. (1) of Ref. 7.4:

$$\delta_* = R\left(1-\frac{V}{u_1}\right) \qquad (7.2)$$

in which V is the mean velocity and u_1 is the surface velocity. The bed shear stress, τ_o, is computed from Eq. (7) of Ref. 7.3,

$$\tau_o = 0.0225\rho u_1^2 \, m^{1/4}\left(\frac{u_1\delta_*}{\nu}\right)^{-1/4} \qquad (7.3)$$

in which $m = \frac{\delta_*}{\delta} = 1/8$.

From the standpoint of experimental procedure, however, the greatest difficulty lies in determining just when the bed motion physically starts. At very low velocities one or two particles will roll over to readjust themselves in the bed. As the velocity is increased a few particles will begin to roll slowly and continuously over the others or over the smooth bed. This is taken to be the commencement of bed motion even though the vast majority of bed particles haven't budged.

The measurements reported in Table 7.1 below were all taken at a point 8 ft downstream from the inlet to the flume, described in Chapter 6. For comparison purposes, values of τ_o are also computed from the relation $\tau_o = fV^2/8$, where f is determined from the Moody chart for friction factor for pipes, (Ref. 6.1), with Reynolds number equal to $4RV/\nu$ and relative roughness given by the size of gilsonite particles relative to 4R, or 0.0018.

TABLE 7.1

Mean Velocity V fps	Surface Velocity u_1 fps	Displacement Thickness δ^* ft.	Bed Shear by Eq. (7) τ_o psf	Bed Shear by Friction Factor τ_o psf
0.112	0.122	0.0270	0.925×10^{-4}	0.924×10^{-4}
0.116	0.127	0.0272	0.985	0.991
0.122	0.133	0.0258	1.093	1.094
0.128	0.140	0.0268	1.180	1.199

The remarkable agreement between the values of bed shear computed by these two methods is perhaps not surprising inasmuch as each method stems from the application of pipe flow formulas to open channels. The boundary layer approach, however, utilizes the Blasius formula and the concept of the virtual channel, while the friction factor method is based on the Colebrook-White function for flow in rough pipes.

The limited applicability of Shields' analysis to settling tanks is further demonstrated in Fig. 7.2, which shows the bed Reynolds number as a function of particle size and mean velocity in the flume. A constant friction factor of 0.025 has been assumed, together with a constant value of kinematic viscosity of 10^{-5} ft^2/sec, corresponding to a water temperature of 77°F. It will be seen that almost all of the particles studied fall below the lower limit of Shields' range for velocities of 0.10 fps and less, and for #28 mesh and finer the velocity can be as high as 0.15 fps while still yielding Reynolds numbers below Shields' range.

The better part of the summer of 1957 was devoted to an assessment of the critical velocity by direct observation. A great number of tests of different bed materials (principally gilsonite and sand) were made in the 15-in. flume, and many were tested also in the 40 ft long 10 in. flume and the longer 33-in. flume. A number of different bed configurations were investigated, from scattered particles on a smooth hard floor, to a thick bed of particles in a recessed floor.

The object of these runs was to determine the approximate range of critical velocities needed to produce general bed motion, rolling motion, saltation, resuspension etc. of the gilsonite particles on a bare floor. With zero flow going through the flume, a small beaker full of previously wetted gilsonite was dumped onto the surface of the water about 7 ft downstream from the inlet screen and allowed to settle to the bottom. Then a

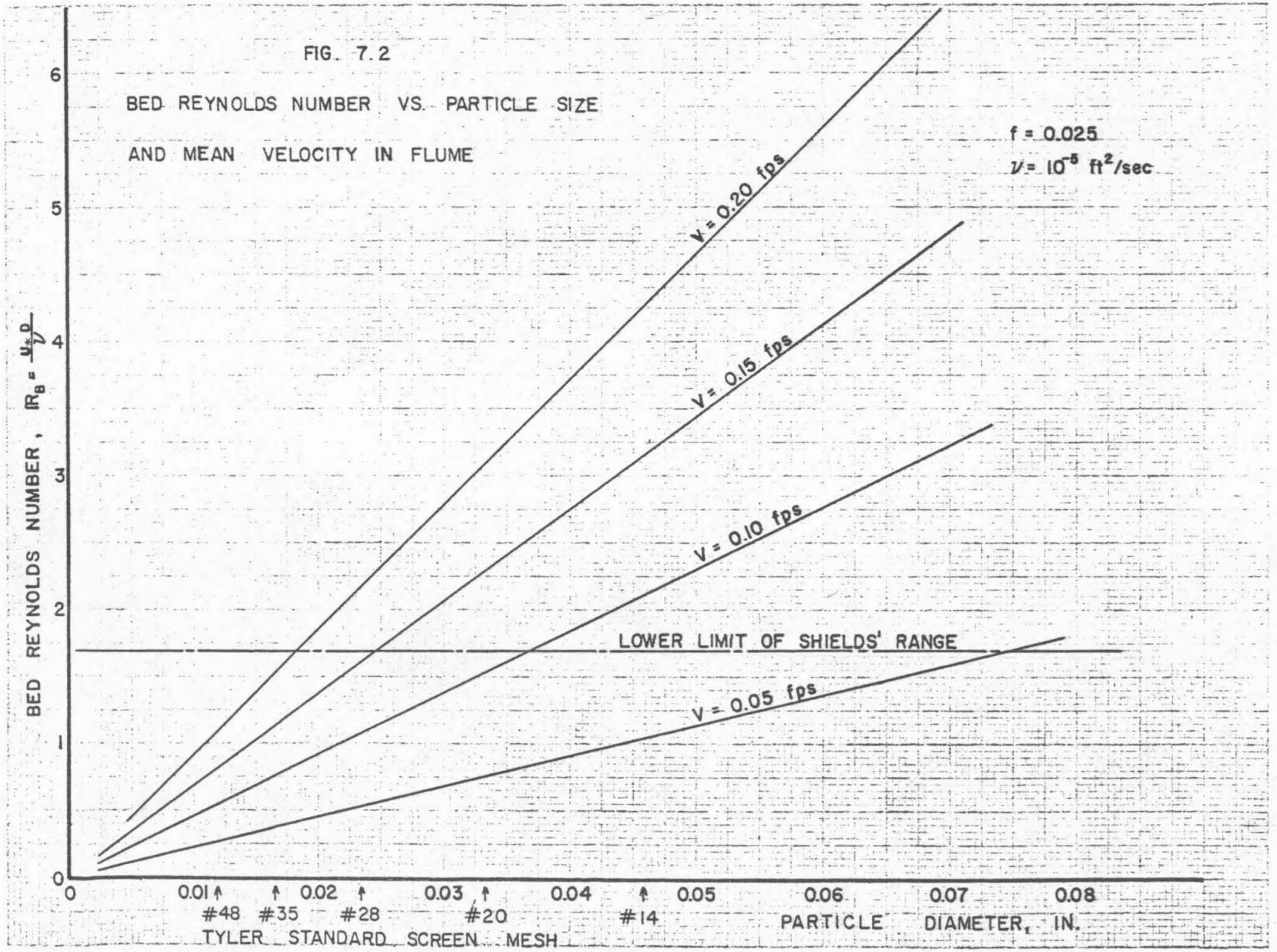
FIG. 7.2
BED REYNOLDS NUMBER VS. PARTICLE SIZE
AND MEAN VELOCITY IN FLUME
f = 0.025
ν = 10⁻⁵ ft²/sec
V = 0.20 fps
V = 0.15 fps
V = 0.10 fps
V = 0.05 fps
LOWER LIMIT OF SHIELDS' RANGE
BED REYNOLDS NUMBER, $R_B = \frac{u_* D}{\nu}$
0
1
2
3
4
5
6
0.01
0.02
0.03
0.04
0.05
0.06
0.07
0.08
#48
#35
#28
#20
#14
TYLER STANDARD SCREEN MESH
PARTICLE DIAMETER, IN.

small flow was allowed to pass through the flume and its effect upon the deposited gilsonite was observed. While small regular increases in the flow were made, the state of bed movement was noted. This observation was continued until the maximum flow of the flume had been reached.

The particles proved to be extremely variable in their susceptibility to entrainment. The velocity at which the very first bed motion could be discerned among a few particles was taken to be the critical velocity. It commonly required a velocity of some four to five times this value before the whole bed could be considered in motion.

The results of all tests for critical velocity (and thereby critical shear through a number of different formulas) are shown in the Shields diagram of Fig. 7.3. It will be noted that almost all of the critical velocity data fall to the left and below the curves proposed by Shields, indicating more susceptibility to entrainment than Shields' work would indicate. The apparent alignment of points in four families sloping upward to the right is not significant and derives only from the fact that the diameter appears in the numerator of the abscissa function, and in the denominator of the ordinate. The fact that so many of the points fall below Shields' curve, however, means either (a) that such light particles are in fact more easily entrained than previously supposed, or (b) that the observed value of "critical velocity" was unrealistically low in most of the observations.

As previously remarked, some tests were made on flocculent suspensions of the type represented by peat moss and finally alum floc. In a recessed smooth bed run the critical velocity for peat moss was measured in one run (on 20 - 28 mesh particles) to be 10% higher than for gilsonite particles of the same size. When a couple of 1/4 x 3/4 in. aluminum bars were inserted across the flume at three points to simulate stationary scrapers, however, the critical velocity for 14 - 20 mesh particles dropped some 25%. An interesting phenomenon was observed in the upstream movement of particles just downstream from the scrapers, that is, the downstream side (or lee) of the scraper bar tended to fill in with a fillet of sediment.

The alum floc was found to be the closest to sewage in its behavior (before the bentonite-ferric chloride floc was formed). Dunes of the material built up between the stationary flights. To quote the laboratory notes, "Some of the floc particles lifted up directly downstream from the flights and don't seem sure about which way they want to go." The critical velocity for the alum floc was found to be approximately 0.09 fps.

References

7.1 "A Study of Turbulence and Diffusion Using Tracers in a Water Tunnel," by V. A. Vanoni and N. H. Brooks, Report No. E-46, Hydrodynamics Lab., California Institute of Technology (1955).

7.2 "Application of Similarity Principles and Imbalance Research to Bed-Load Movements", by A. Shields, Berlin (1936).

7.3 "The Boundary Layer Development in Open Channels," by J. W. Delleur, ASCE, Jour. Eng. Mech. Div., Proc. Paper 1138 (Jan., 1957).

7.4 "Discussion of 'The Boundary Layer Development in Open Channels, '" by A. C. Ingersoll, Proc. ASCE, Jour. Eng. Mech.Div., p. 1520-12 (Jan., 1958).

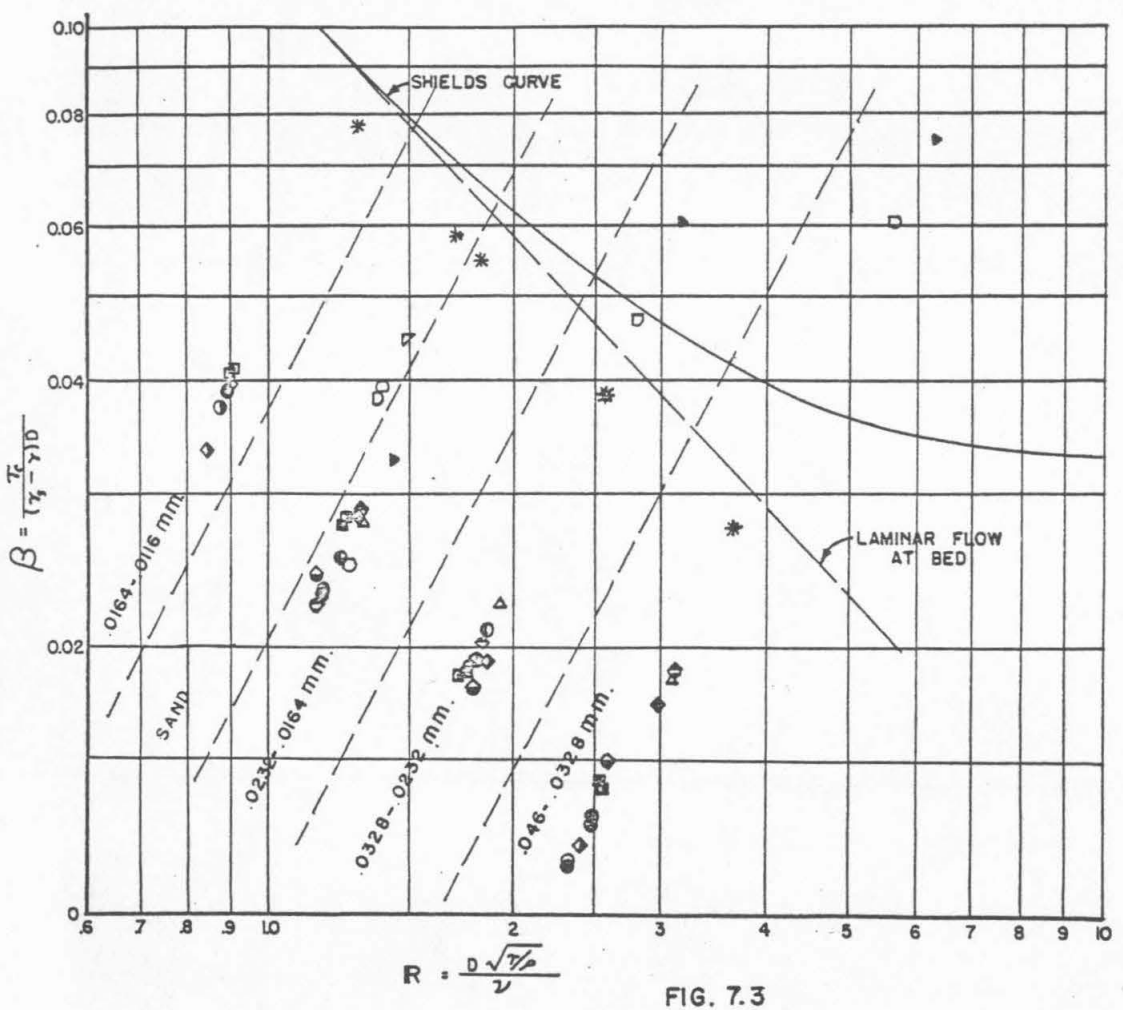

I. τ_c AS PER DELLEUR
A - BARE FLOOR
1. UPSTREAM BED
a. X = 49"
b. X = 73"
c. X = 97"
2. DOWNSTREAM BED
a. X = 73"
b. X = 97"
c. X = 133"
B. - THICK BED
1. SCRAPED
2. UNSCRAPED

II. COMPUTED FROM MEASURED SLOPE AS PER SHIELDS

III. COMPUTED FROM ASSUMED f
A. - 15-1/4" FLUME
1. BARE FLOOR
a. UPSTREAM
b. DOWNSTREAM
2. THICK BED
a. SCRAPED
b. UNSCRAPED
B. - 10-1/2" FLUME

IV. AS PER EQUATION 6 OF SHIELD

V. SAND
A- MEASURED SLOPE
B - ASSUMED f
C - AS PER DELLEUR
D - EQUATION 6 - SHIELD

FIG. 7.3

SHIELDS DIAGRAM

DIMENSIONLESS CRITICAL SHEAR (BEGINNING OF BED LOAD MOVEMENT) AS A FUNCTION OF BED REYNOLDS NUMBER

Chapter 8

CRITICAL VELOCITY AND REMOVAL STUDIES ON GILSONITE

Following the critical velocity measurements by direct observation reported in the preceding chapter, an extensive series of tests was undertaken in which the flat bed of gilsonite was artificially prepared under water in advance of the run. Flow through the flume was then started with as little disturbance as possible while at the same time a set of flight scrapers of the endless chain-belt type was put in motion, scraping the bed toward a hopper at the inlet end of the flume. After a certain time the bed material would be distributed in three places (a) in an effluent catch-screen, (b) in the influent hopper, and (c) remaining on the bed of the flume.

By stopping the flow at intervals and weighing the gilsonite collected on the effluent screen and in the influent hopper it is possible to make a cumulative plot of the disposition of the bed material with time. By sampling the effluent during a continuous run it is also possible to determine the time-variation of the particle flow rate passing out with the effluent (the so-called effluent removal rate). When this operation is repeated for a series of different velocities in the flume and different initial quantities of material on the bed it is possible to see a number of relations. For example if one plots effluent removal rate vs. velocity in the flume it should be possible to extrapolate the curve down to zero removal and determine thereby an indirect measurement of the critical velocity for resuspension. The next two sections of this chapter are devoted to a discussion of the results obtained from some 36 runs in which the foregoing procedures were followed.

8.1. Gilsonite Removal and Residual as Function of Time

Description of Flight Scraper Mechanism: Before treating the results of the removal tests it will be well to say a word about the model flight scraper mechanism that was installed in the flume in order to make the hydraulic conditions of these tests as much as possible like those applying to a full-sized primary settling tank in a sewage treatment plant. This consisted essentially of a model of a commercial type of scraper commonly used for rectangular tanks, constructed on a scale of one inch to the foot. The individual flights are made of brass, 3/16-in. thick by 1/2-in. deep, extending across the width of the flume and spaced at 10 in. intervals. The scraper chain moves at a velocity somewhat slower than the prototype counterpart, which velocity can be varied only by changing the size of gears in the driving train. During all of the tests reported in this chapter the scrapers moved upstream at 0.0357 fps.

Runs Utilizing Effluent Catch Screen for Cumulative Removal: Three sieve fractions of gilsonite were used in the laboratory tests: 20 - 28, 28 - 35, and 35 - 48 Tyler mesh. The characteristics of the particles in these ranges are given in Table 5.1. The largest size particles, 20 - 28, were of course the easiest to observe visually and to photograph, but their relatively high settling velocity, 0.0197 fps, prevented much resuspension activity at the velocities available in the flume. The behavior of this fraction in the

flume with a displacement velocity of 0.151 fps (almost 8 times the settling velocity) is demonstrated in the four pictures of Fig. 8.1. The gilsonite is seen to hug the floor closely and there is no apparent difference between the amount of material in suspension one minute after starting the flow and the scrapers, to that in suspension after three minutes.

The plot of gilsonite removal and residual as functions of time for the foregoing run is shown in Fig. 8.2. Starting with a prepared bed of 2,093 gm (0.129 gm/cm^2) on the floor of the flume, the run continued - with interruptions at 5-min. intervals to measure the cumulative total in the effluent and hopper screens - until less than 5% of the original deposit remained in the flume. The plot shows that the removal rate to the hopper is constant until the amount of sediment in the flume has dropped to about 6% of the original amount in the bed. From this point onward the effluent removal rate dropped essentially to zero and the run was effectively completed.

With the same size of gilsonite particle and approximately the same initial loading on the bed, the displacement velocity was next increased to 0.236 fps or 12 times the median settling velocity. The four pictures of Fig. 8.3 show a greatly increased entrainment activity, with a considerable difference between the photographs taken at 15 and at 90 seconds. The plot of Fig. 8.4 also shows a marked difference from that of Fig. 8.2 in that the proportion of particles being removed from the upstream hopper is greatly decreased. The removal in the effluent is increased many fold. It is interesting to note that the same clock duration of run at the higher velocity has produced a run which is less complete than the slower velocity run as far as the ultimate disposition of the flume load is concerned. This is just opposite to what one would intuitively expect in terms of phenomenon times being related to multiples of the detention period.

The four pictures of Fig. 8.5 show the next smaller size of particle (28 - 35 mesh) subjected to the same displacement velocity as that of Fig. 8.3. The ratio of flume velocity to settling velocity has now increased to 19.7, however, and the entrainment activity is noticeably augmented by this increased ratio. It should be pointed out that the initial floor loading in this run was increased 30% over that of Fig. 8.3, but the major difference is believed to be due to the change in particle size.

The removal of gilsonite in the effluent and in the hopper as a function of time is shown in Fig. 8.6 for a run with smaller particles (35 - 48 mesh) and lower displacement velocity, but with approximately the same ratio of displacement to settling velocity ($V = 20\ w_s$) as that of Fig. 8.5. Comparing Figs. 8.6 and 8.2 it is seen that the rate of particle feed to the hopper in Fig. 8.6 is approximately twice what it is in Fig. 8.2, presumably because the velocity ratios are in the proportion, 20:7.7 or 2.7. This appears to be a good check on the system.

The real difficulty comes in comparing Fig. 8.2 and Fig. 8.6 with Fig. 8.4 which should, with a displacement velocity of $12\ w_s$, lie somewhere between them. In point of fact Fig. 8.4 has a particle flow rate to the hopper which is only about half that of Fig. 8.2, and a rate of removal of particles with the effluent of approximately 10 times that of Fig. 8.2. The curves of Fig. 8.4 yield a removal rate to the hopper which is approximately one quarter

the rate in Fig.8.6. This is supported by considering the ratio of relative velocities, 20 for Fig. 8.6 and 12 for Fig. 8.4. The rate of removal to the effluent is approximately the same in Figs. 8.4 and 8.6.

From this group of runs it may be concluded that in each case the rate of removal to the hopper and to the effluent is maximum at the beginning, carries on a fairly constant rate, and then drops off rapidly as the supply of gilsonite is diminished. The single most important criterion establishing the character of the removal curves is the ratio of displacement velocity to settling velocity. The higher this ratio, in general, the lower will be the rate of removal of particles to the inlet hopper, higher to the effluent. This effect is not, however, uniformly predictable. Unfortunately it was not possible to repeat the runs in question so that this point could be firmly established.

"Critical Velocity" for Removal Tests: When the displacement velocity is increased from the 0.151 fps (20 w_s) of Fig. 8.6 to 0.183 fps, with other conditions remaining the same, a marked change occurs in the proportion of the initial load which is removed in the effluent. In Fig. 8.6 it is seen that the effluent removal is just about 10% of the initial load. With an increase in displacement velocity of only 21%, to 24 w_s, as shown in Fig. 8.7, the effluent removal increases to 45.5% and even at that there still remains 15% of the load still on the bed. It is thus apparent that some kind of "critical velocity barrier" has been crossed and that its value is between 20 and 24 times the settling velocity.

It is also apparent from Fig. 8.7 that the removal rates, either to the effluent or to the hopper, are anything but constant, even for a portion of the run. It appears that the factor of decreasing supply of material on the bed produces the decreasing removal rates directly from the beginning of the run. It is of interest to note that the "rate to effluent" curve approaches the origin apparently asymptotically. Actually the "rate to effluent" curve looks like a curve of concentration decay in an ideal mixing tank. The initial removal rate applicable to such a hypothetical mixing tank would be the floor loading in grams per foot of length times the mean displacement velocity in ft. per min. This would come to 1,550 grams per minute or some 22 times the maximum measured removal rate. This calculation shows that although there may appear to be much mixing and turbulence in the flume for some of the runs made, there is still a lot of leeway before anything like perfect mixing occurs.

Runs Utilizing Effluent Samples for Cumulative Removal: Inasmuch as the catch-screen method involved the cumbersome procedure of shutting down the run every five minutes to remove and weigh the gilsonite caught on the effluent screen, it was desired to accomplish the removal information by effluent sampling if possible. For the first 15 minutes of the run recorded in Fig. 8.6, therefore, one-liter effluent samples were taken at intervals of 30 sec. (at the beginning of each 5-min. interval) and one minute, with the result shown in Fig. 8.8. The discontinuous characteristic of the interrupted run procedure is brought out clearly from this plot. Further, the sampling procedure is well justified, inasmuch as the cumulative effluent removal obtained by plotting the sample concentrations is within 3% of the removal obtained from the collected weight on the effluent screen.

(Text continued on page 72)

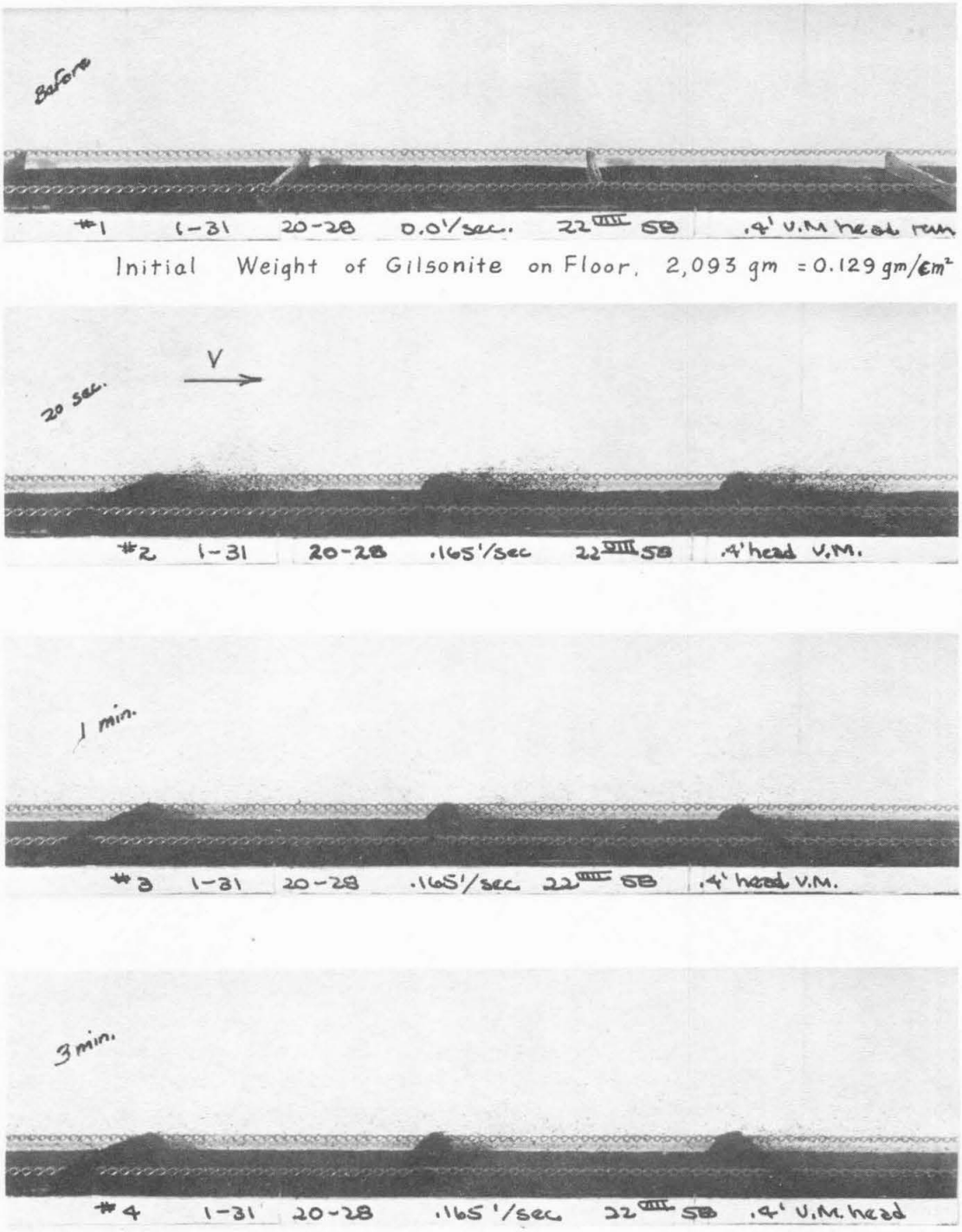

Fig. 8.1

GILSONITE MOVEMENT ON FLOOR

Particle Size	20-28 (D_s = 0.71 mm)
Scraper Velocity	0.0357 ft/sec upstream
Displacement Velocity	V = 0.151 ft/sec = 7.66w_s

Fig. 8.2

GILSONITE REMOVAL
AND RESIDUAL AS FUNCTION
OF TIME

Particle Size 20-28
Scraper Velocity 0.0357 ft/sec upstream
Displacement Velocity V = 0.151 ft/sec $\approx 7.7 w_s$
Run No. 1-31

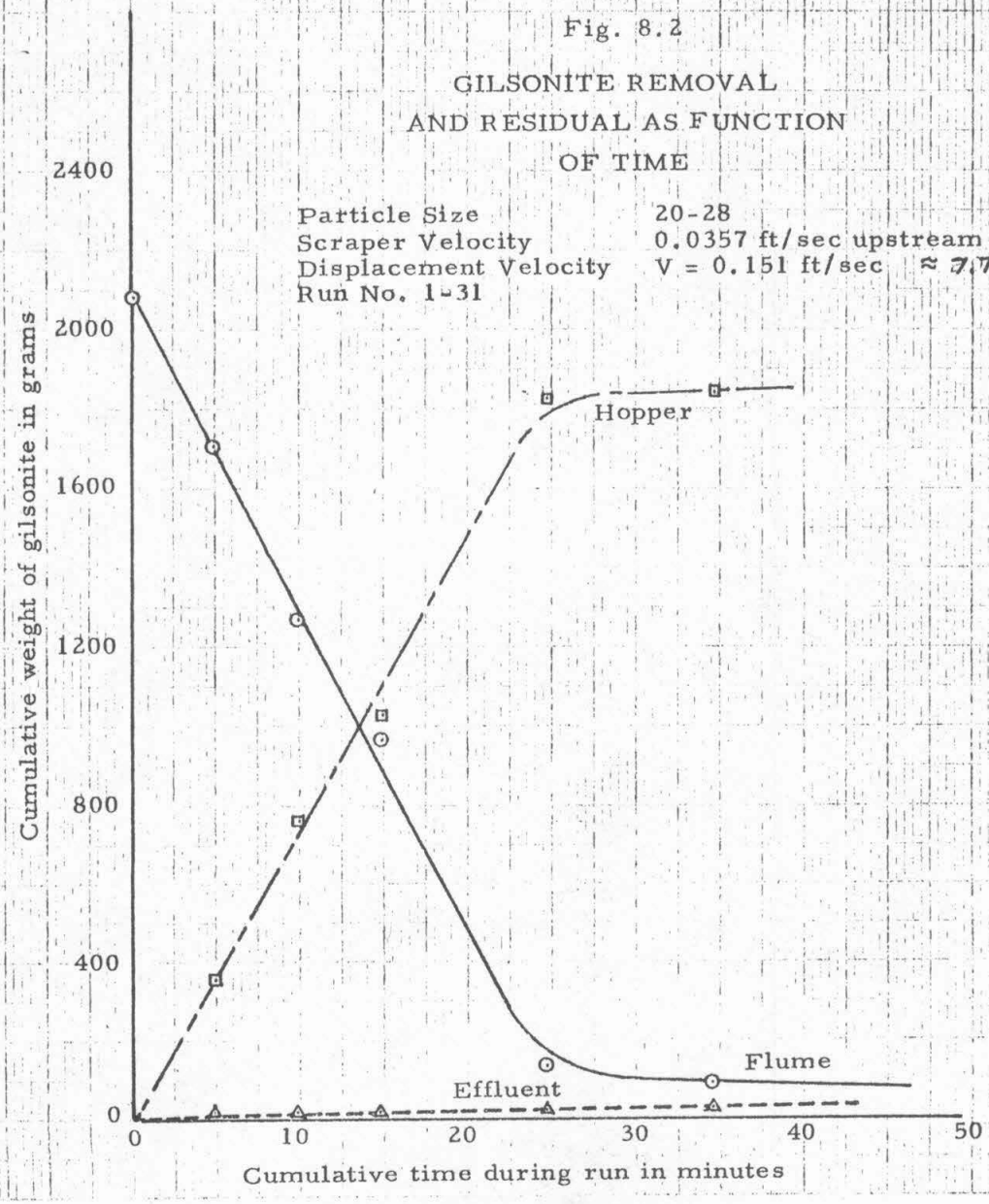

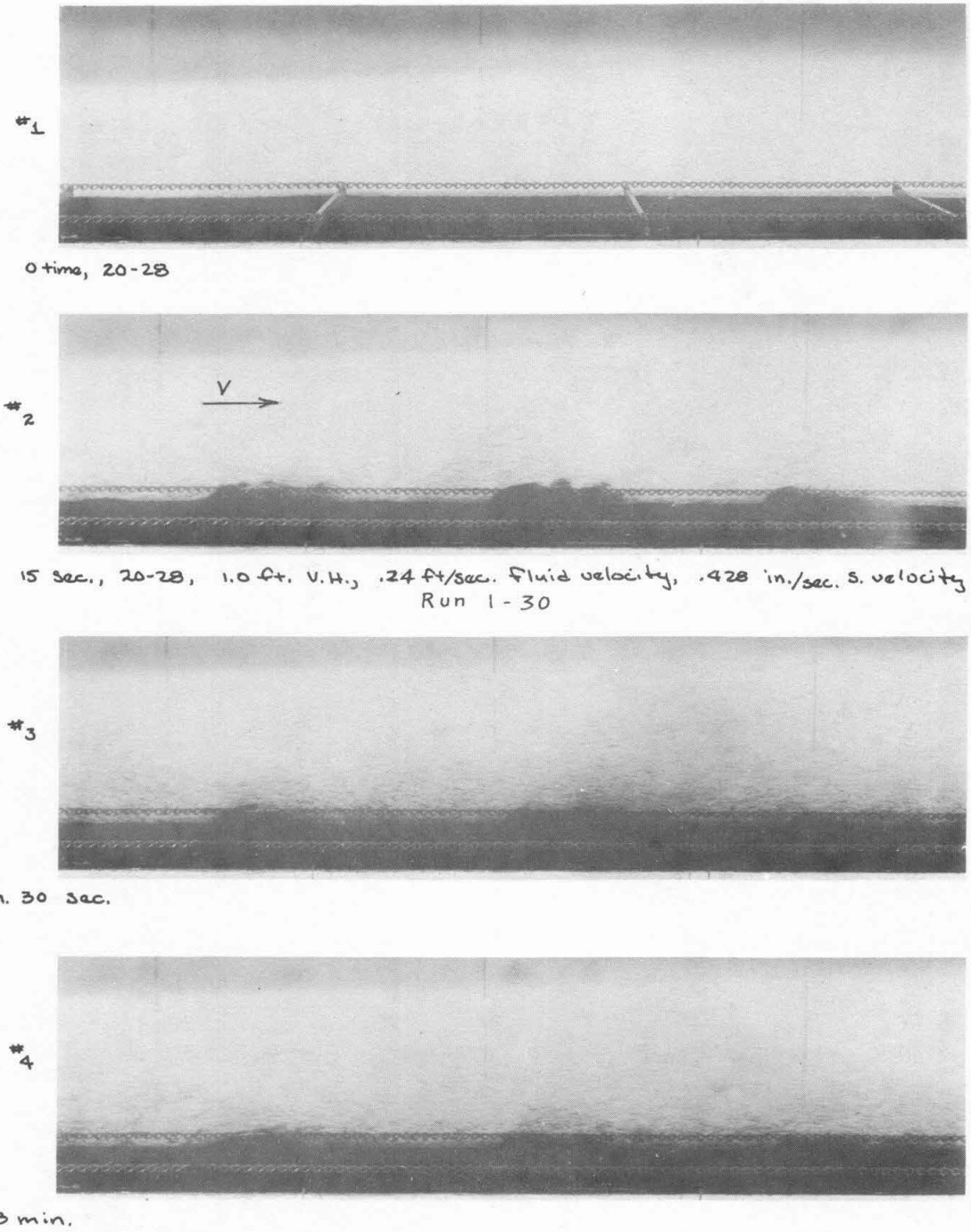

Fig. 8.3

GILSONITE MOVEMENT ON FLOOR

Particle Size	20-28 (D_s = 0.71 mm)
Scraper Velocity	0.0357 ft/sec, upstream
Displacement Velocity	V = 0.236 ft/sec = 12.0 w_s
Initial Weight of Gilsonite on bed = 2156 gm = 0.133 gm/cm^2	

Fig. 8.4

GILSONITE REMOVAL AND RESIDUAL AS FUNCTION OF TIME

Particle Size 20-28
Scraper Velocity 0.0357 ft/sec upstream
Displacement Velocity V = 0.236 ft/sec ≈ 12.0 w_s
Run No. 1-30

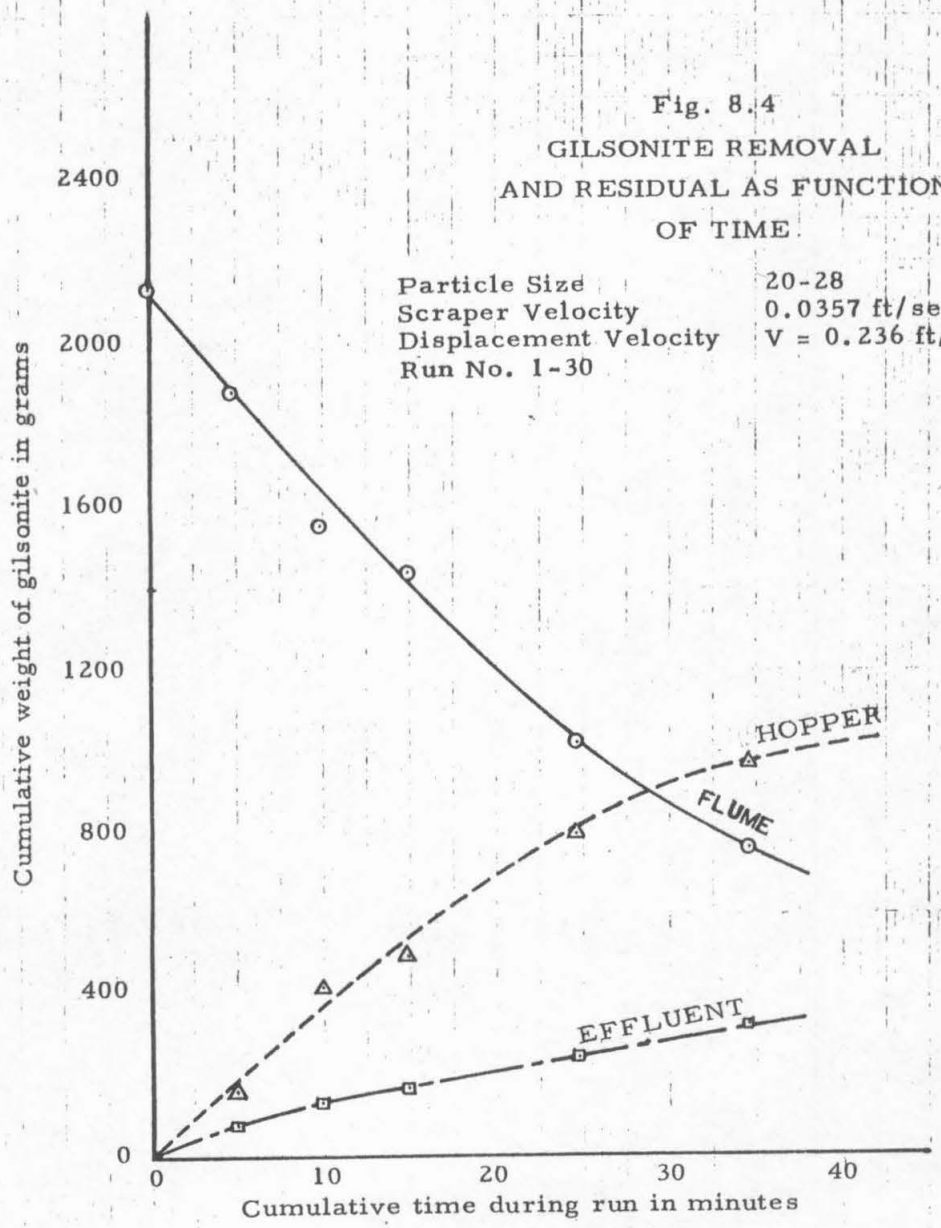

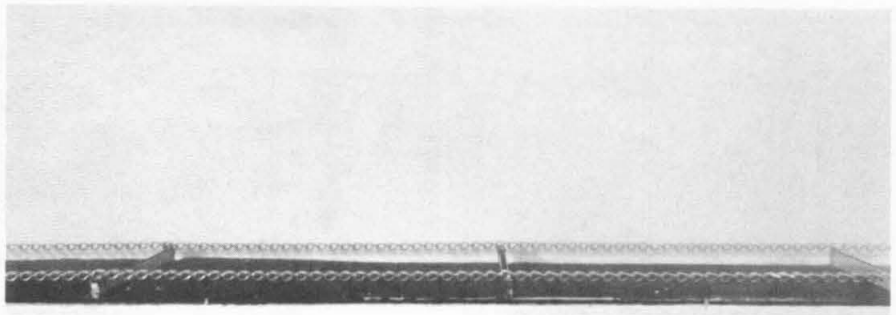

0 time 28-35 1.0 U.M. head, .24 ft/sec. fluid velocity, .428 in./sec S. vel.

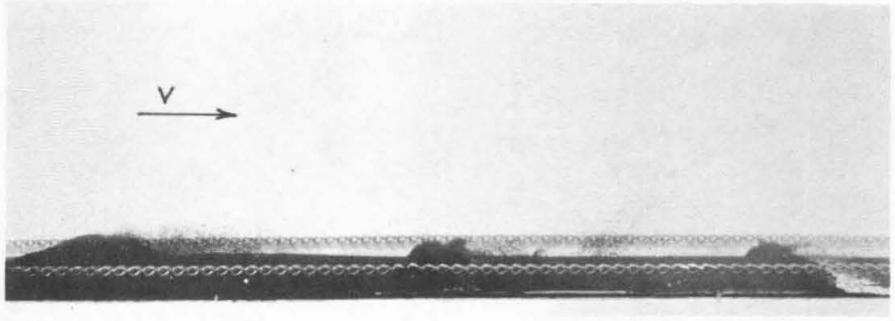

15 sec.

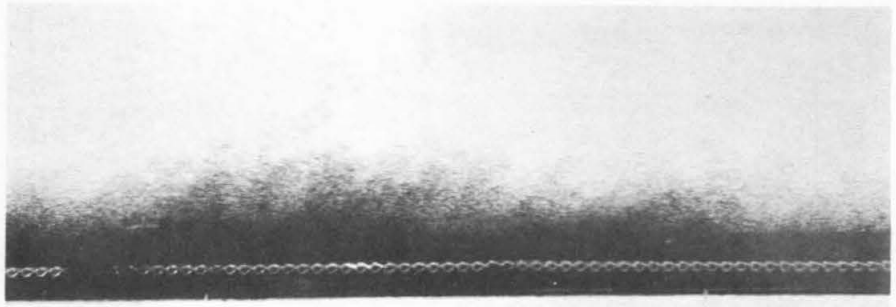

30 sec.

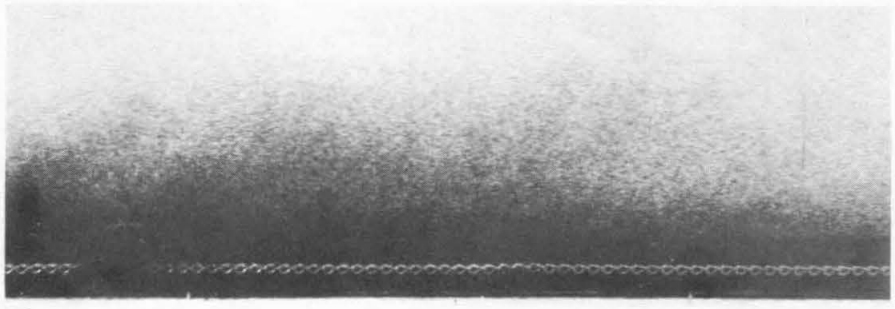

1 min.

Fig. 8.5

GILSONITE MOVEMENT ON FLOOR

Particle Size	28-35 (D_s = 0.50 mm)
Scraper Velocity	0.0357 ft/sec upstream
Displacement Velocity	V = 0.236 ft/sec = 19.7 w_s
Initial Weight of Gilsonite on Floor = 2798 gm = 0.172 gm/cm^2	

Fig. 8.6

GILSONITE REMOVAL
AND RESIDUAL AS FUNCTION
OF TIME

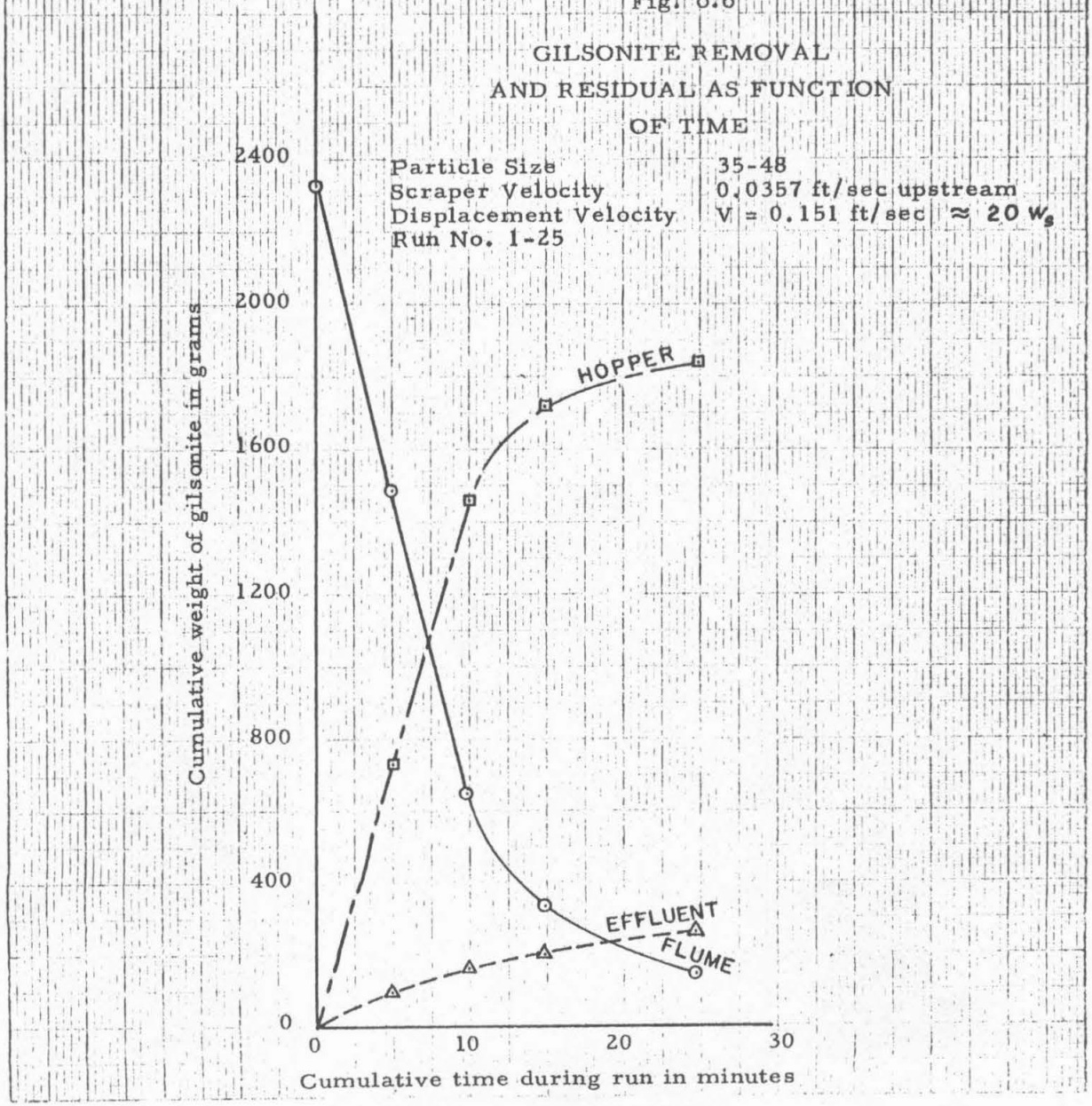

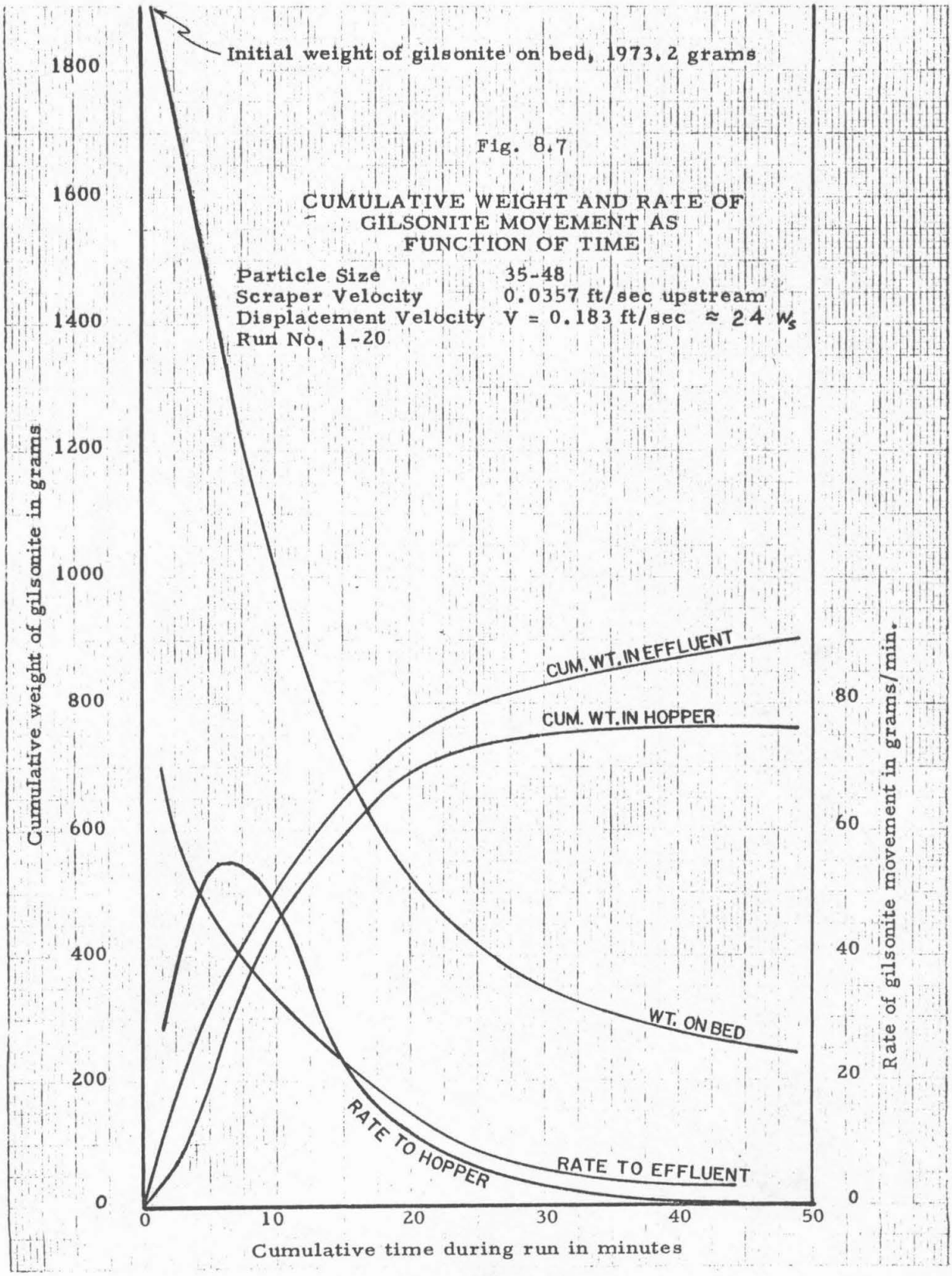

Fig. 8.7

CUMULATIVE WEIGHT AND RATE OF GILSONITE MOVEMENT AS FUNCTION OF TIME

Fig. 8.8

EFFLUENT CONCENTRATION OF GILSONITE VS TIME

Particle Size	35-48
Scraper Velocity	0.0357 ft/sec upstream
Displacement Velocity	V = 0.151 ft/sec $\approx 20\ W_s$
Initial Weight of Gilsonite on Bed	2,342 grams
Run No. 1-25	

Effluent Removal Rates

Time	By Effluent Samples (areas under plotted curves)	By Collected Weight in Effluent Screen
0-5 min	15.96 grams/min avg.	19.00 grams/min avg.
5-10	14.68	13.40
10-15	8.26	7.68
Total Effluent Removal	194.4 grams	200.3 grams

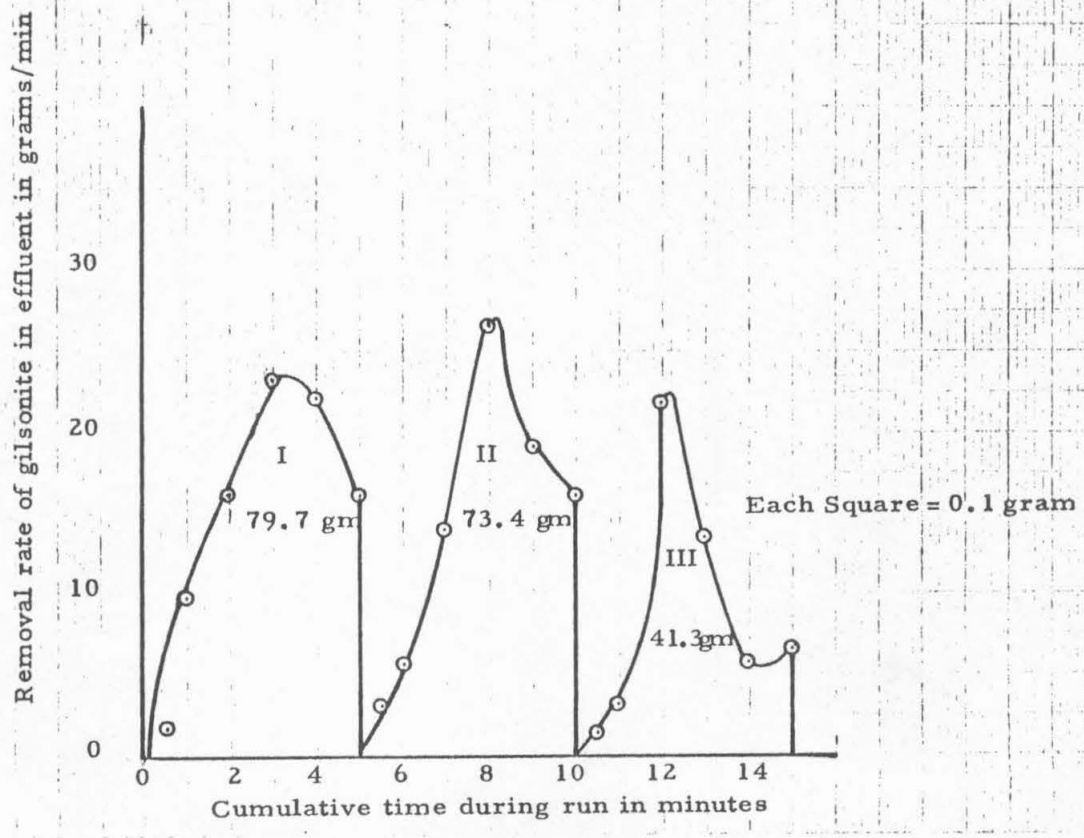

8.2. Effluent Removal vs. Quantity of Gilsonite in Flume

After making the plots of the preceding section one naturally seeks ways in which the data from several runs can be plotted on a single sheet to yield a common variable. One such combination involves the dependent variable, rate of removal of gilsonite in the effluent, vs. the quantity of gilsonite remaining in the flume as the independent variable as shown for three runs in Fig. 8.9. Except for the points of one run which were affected by rising air bubbles, there is good correlation between the points of two other runs despite a disparity of more than 100% in the amount of gilsonite initially on the bed.

The five runs of Fig. 8.10 reveal exactly the same phenomenon, again covering a factor of more than five in the amount of gilsonite on the bed before starting the run proper. In this group of runs, also, there seems to be one which has been affected by rising air bubbles. Also it is seen that the displacement velocity has risen to 24 w_s. Although the scales of the drawings, Figs. 8.9 and 8.10, are not the same it is clear that the increased velocity has caused a continuous rise in effluent removal as a function of quantity of gilsonite in the flume. It is not possible to tell whether a leveling-off stage has been reached in Fig. 8.10, but it appears that this may be occurring at approximately 2,200 grams of gilsonite on the bed. This bears approximately the same ratio to the load at which the leveling-off point occurs in Fig. 8.9 as do the displacement velocities of the two runs (24:15.5 or 1.55).

The velocity was then increased to 30.8 times the settling velocity for a series of three runs on the same particles. The effluent removal rate rises ever more sharply, and there is no sign of a leveling-off point within the range of quantity tested. One run, which started with the largest amount of initial bed loading, displays a steeper slope on the part of the curve showing the falling rate of removal after significant erosion of the bed. (It is well to note here that the progression of time is from right to left in this group of curves). There is no ready explanation for this observation except perhaps the intuitive one that the shallower beds are losing the more easily erodible particles while the deeper beds have worn down to the hard core and the particles remaining on the bed are the more resistant ones. This explanation is supported by observing that the lightest bed of all shows the highest erosion rate over most of its range.

The summary of a dozen runs of this character is shown in Fig. 8.12, utilizing the same coordinates as in the previous plots. The displacement velocity shows clearly here as the primary variable in the effluent removal picture, along with the weight of gilsonite in the flume. From Fig. 8.12 alone, however, it is not possible to ascertain a value for the "critical velocity" at which bed motion commences to take place. If the data of Fig. 8.12 are replotted, however, into the form of Fig. 8.13 it is possible to extrapolate the short distance between small effluent removal and essentially no removal and thus to determine a critical velocity for the commencement of entrainment. If the extrapolation is justified as shown (and this is admittedly a questionable extension of the meager data) it appears that the range of critical velocities for the various amounts of gilsonite in the flume

is not very great, extending from 10.5 w_s to 13.2 w_s. It is interesting to note that this lies directly in the middle of the range of from 9 to 15 times the settling velocity suggested on p. 1193 of Ref. 1.1.

In order that a separate check be made of the critical velocity for entrainment from the floor of the flume with the scrapers in motion, the same runs were repeated with the next larger size of gilsonite, Tyler mesh 28 - 35. The result of three runs is shown in the plot of Fig. 8.14, similar to Fig. 8.12. It is instructive to notice here the distinct crossing of the separate runs as each approaches zero effluent removal, all having started with approximately the same initial bed loading, but with three different displacement velocities. It is clear that the run of lowest velocity continued to yield entrained particles from the bed at values of bed loading of only approximately one quarter of the loading at which the higher velocity runs went to zero removal.

Again, the same data are replotted in Fig. 8.15 to yield a range of values for the critical velocity varying from 13.2 to 14.5 w_s. There is no significance attached to the slightly higher range of values for the coarser sediment. Each of the curves on this plot is, after all, drawn through only three points (one for each run).

8.3. Tests with Continuous Injection of Gilsonite

The unsteady state features of the preceding runs, especially in the ones for which it was necessary to start and stop the run frequently during the test, made it imperative to devise a scheme for continuous injection of the sediment in order to have a steady-state run. This was accomplished by mixing a slurry of gilsonite particles in water, with alcohol as a wetting agent. This slurry was agitated in a small mixing tank and then fed through a single nozzle located at approximately the center of the cross section near the inlet end of the flume. The diffusion of gilsonite from this injection tube is shown in Fig. 8.16 for a particle flow rate of 22.6 grams per min. There does not appear to be great difference between the diffusion pattern at 15 sec. and that shown at 1 min., both for a displacement velocity of 21.8 w_s and a scraper velocity of zero.

When the displacement velocity is reduced to 17.5 w_s, however, a marked difference in the diffusion pattern can be seen, as shown in Fig. 8.17. The injection rate is reduced only slightly from that of Fig. 8.16. The pictures depict the distribution of gilsonite on the floor of the flume after the run had completed its 30 min. duration. The concentration of gilsonite on the floor for each foot of flume length was measured, yielding the plot of Fig. 8.18 which shows a high concentration near the injector, with a steep drop-off upstream to the hopper, and a gradual drop-off downstream. The same data can be plotted cumulatively, yielding the curve of Fig. 8.19, having an average slope of 28.32 gm. per ft.

When the scrapers are put in motion again the floor deposit picture changes radically, as indicated by the pictures of Fig. 8.20 and the cumulative plot of Fig. 8.21. The average deposit on the floor has dropped to 28% of that when the scrapers were turned off, and this for an 11% decrease in displacement velocity (which would normally produce more deposit).

Run No.	Symbol	Wt. on bed after Pre-Run grams	Mean Velocity of Water $ft\ sec^{-1}$	Mean Depth of Water ft
1-18	○	1452	0.119	0.752
1-23	□	3624	0.118	0.760
1-24	△	3359	0.118	0.760

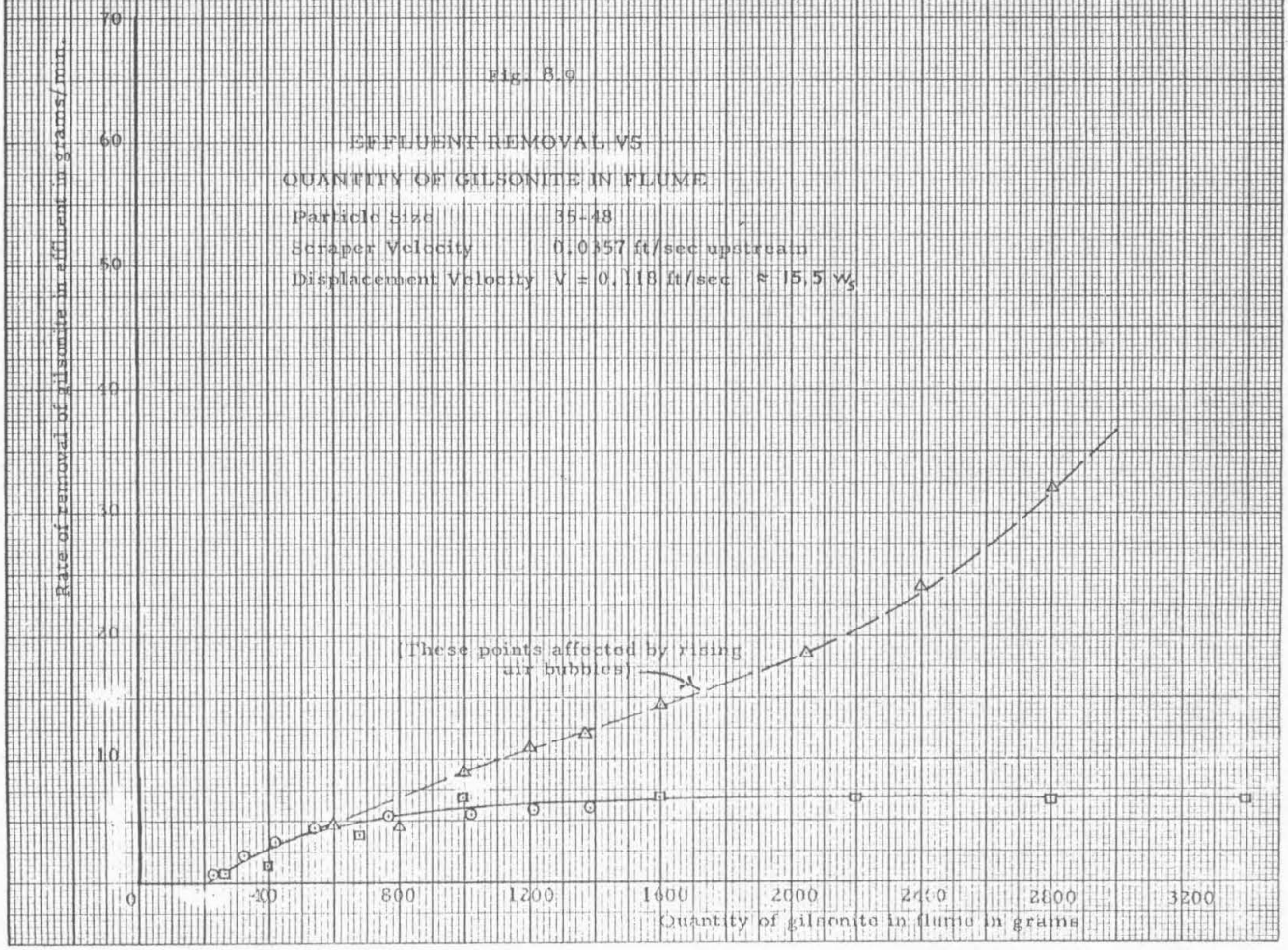

Fig. 8.9

EFFLUENT REMOVAL VS
QUANTITY OF GILSONITE IN FLUME

Particle Size 35-48
Scraper Velocity 0.0357 ft/sec upstream
Displacement Velocity $V = 0.118$ ft/sec $\approx 15.5\ w_s$

Run No.	Symbol	Wt. on Bed after Pre-Run	Mean Velocity of Water	Mean Depth of Water
		grams	ft sec^{-1}	ft
1-17	○	1495	0.184	0.792
1-20	□	1973	0.183	0.797
1-21	△	490	0.184	0.793
1-22	●	992	0.184	0.793
1-27	■	2526.2	0.184	0.790

Fig. 8.10

EFFLUENT REMOVAL VS
QUANTITY OF GILSONITE IN FLUME

Particle Size 35-48
Scraper Velocity 0.0357 ft/sec upstream
Displacement Velocity V = 0.184 ft/sec ≈ 2.4 w_s

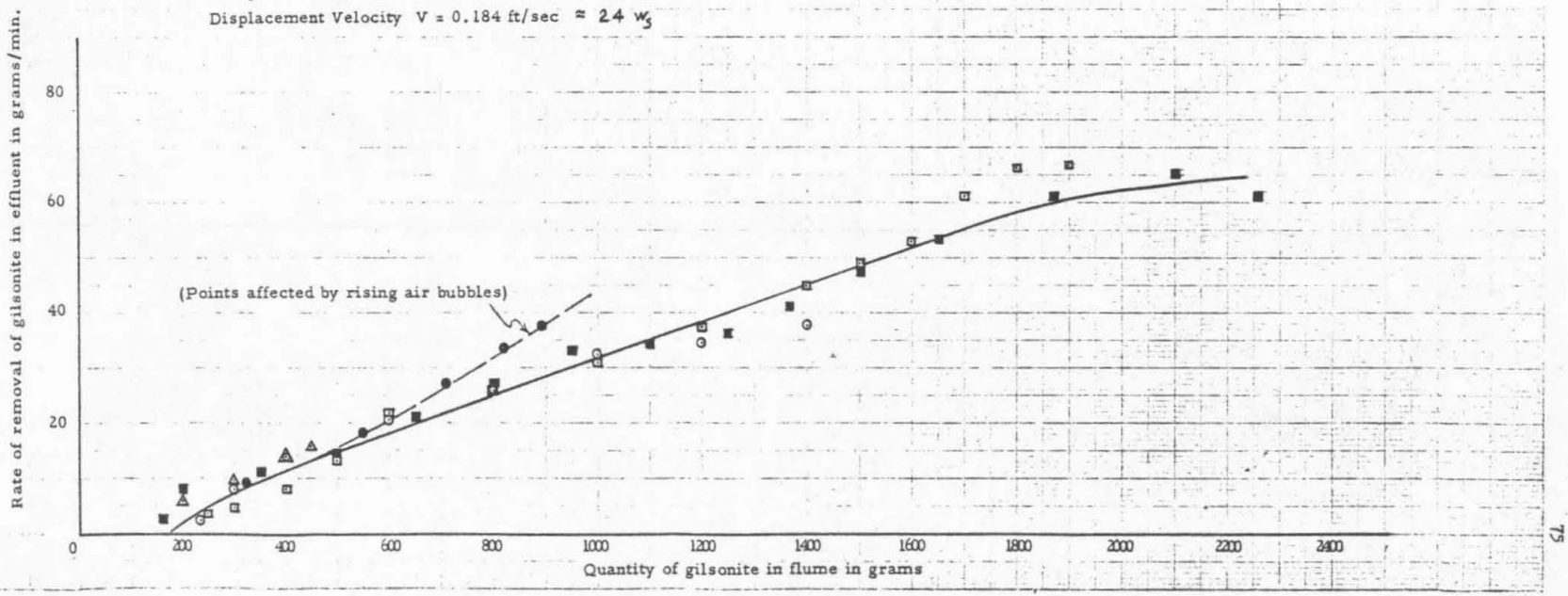

Symbol and Run No.		Wt. on Bed after Pre-Run	Mean Velocity of Water	Mean Depth of Water
		grams	ft. sec^{-1}	ft
1-19	○	1574	0.233	0.818
1-26	□	3301.5	0.235	0.812
1-28	△	2278.4	0.234	0.814

Fig. 8.11

EFFLUENT REMOVAL VS
QUANTITY OF GILSONITE IN FLUME

Particle Size 35-48

Scraper Velocity = 0.0357 ft/sec upstream

Displacement Velocity, V=0.234 ft/sec
≈ 30.8 w_s

Composite Curve

Rate of removal of gilsonite in effluent in grams/min.

260
240
220
200
180
160
140
120
120
100
80
60
40
20
0

400 800 1200 1600 2000 2400

Quantity of gilsonite in flume in grams

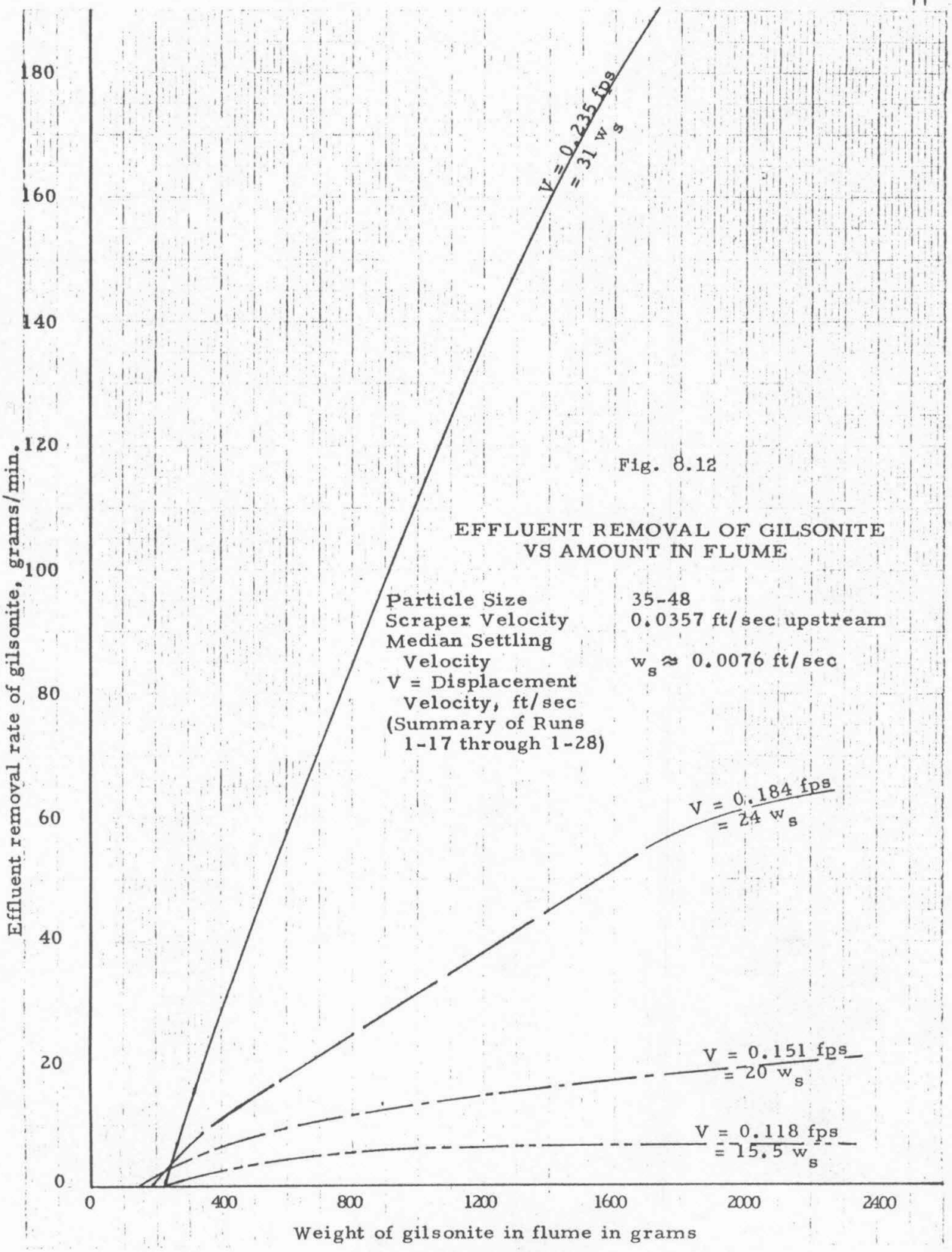

Fig. 8.12

EFFLUENT REMOVAL OF GILSONITE VS AMOUNT IN FLUME

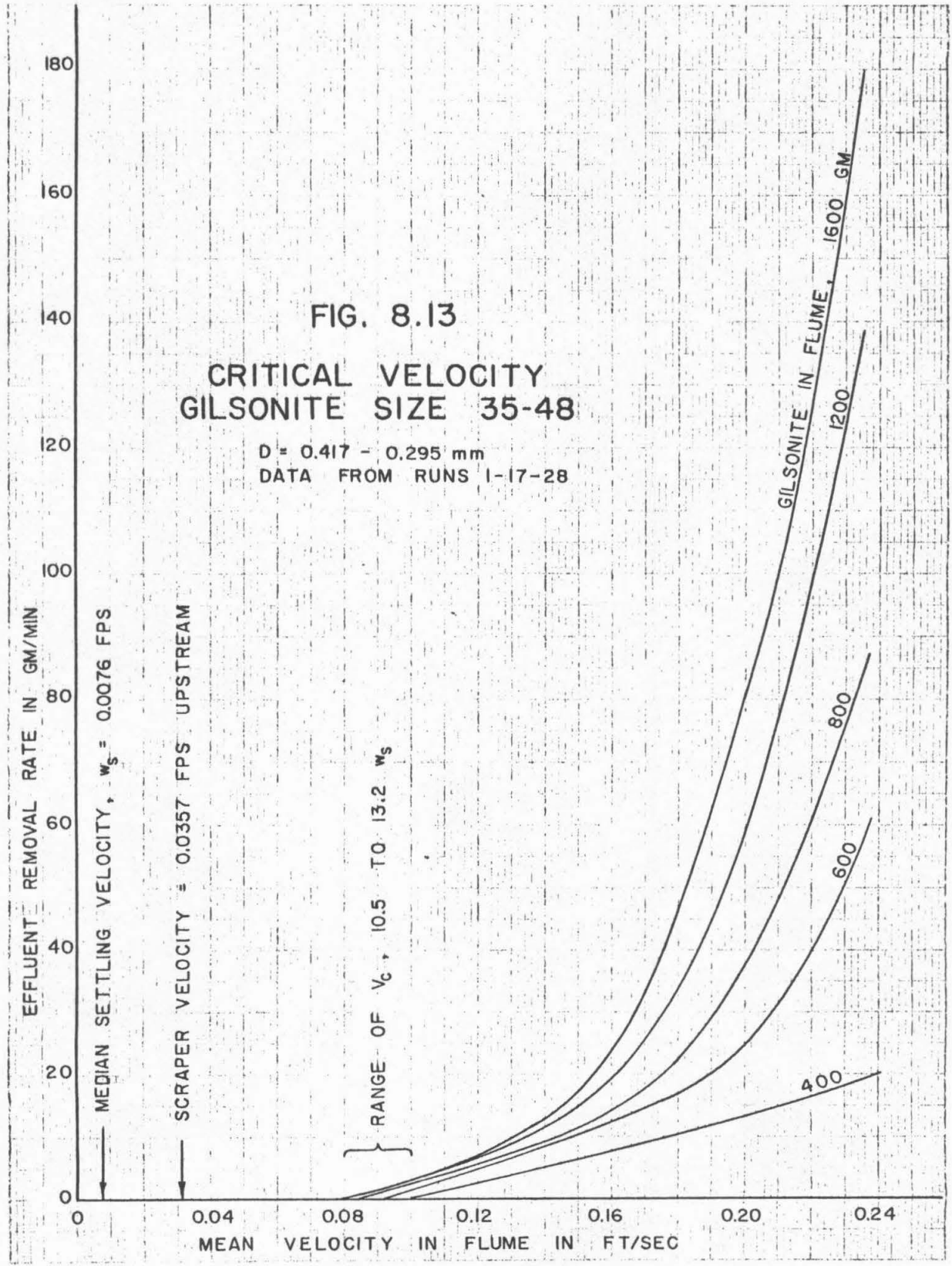
FIG. 8.13
CRITICAL VELOCITY
GILSONITE SIZE 35-48
D = 0.417 - 0.295 mm
DATA FROM RUNS 1-17-28
EFFLUENT REMOVAL RATE IN GM/MIN
MEAN VELOCITY IN FLUME IN FT/SEC
MEDIAN SETTLING VELOCITY, w_s = 0.0076 FPS
SCRAPER VELOCITY = 0.0357 FPS UPSTREAM
RANGE OF V_c, 10.5 TO 13.2 w_s
GILSONITE IN FLUME, 1600 GM
1200
800
600
400
0
20
40
60
80
100
120
140
160
180
0.04
0.08
0.12
0.16
0.20
0.24

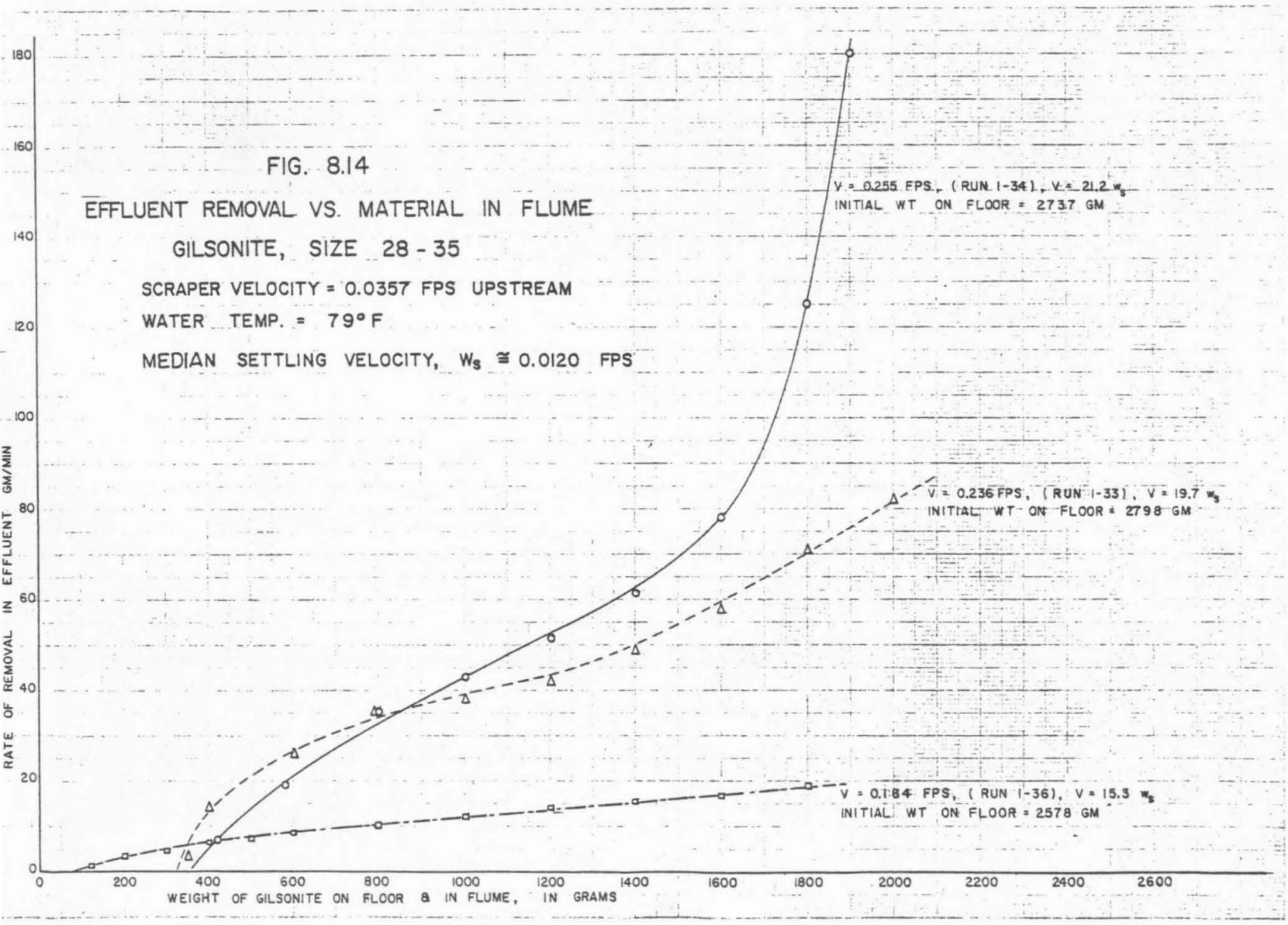
FIG. 8.14
EFFLUENT REMOVAL VS. MATERIAL IN FLUME
GILSONITE, SIZE 28 - 35
SCRAPER VELOCITY = 0.0357 FPS UPSTREAM
WATER TEMP. = 79° F
MEDIAN SETTLING VELOCITY, $W_s \cong 0.0120$ FPS
V = 0.255 FPS, (RUN 1-34), V = 21.2 w_s
INITIAL WT ON FLOOR = 2737 GM
V = 0.236 FPS, (RUN 1-33), V = 19.7 w_s
INITIAL WT ON FLOOR = 2798 GM
V = 0.184 FPS, (RUN 1-36), V = 15.3 w_s
INITIAL WT ON FLOOR = 2578 GM
RATE OF REMOVAL IN EFFLUENT GM/MIN
0
20
40
60
80
100
120
140
160
180
0
200
400
600
800
1000
1200
1400
1600
1800
2000
2200
2400
2600
WEIGHT OF GILSONITE ON FLOOR & IN FLUME, IN GRAMS

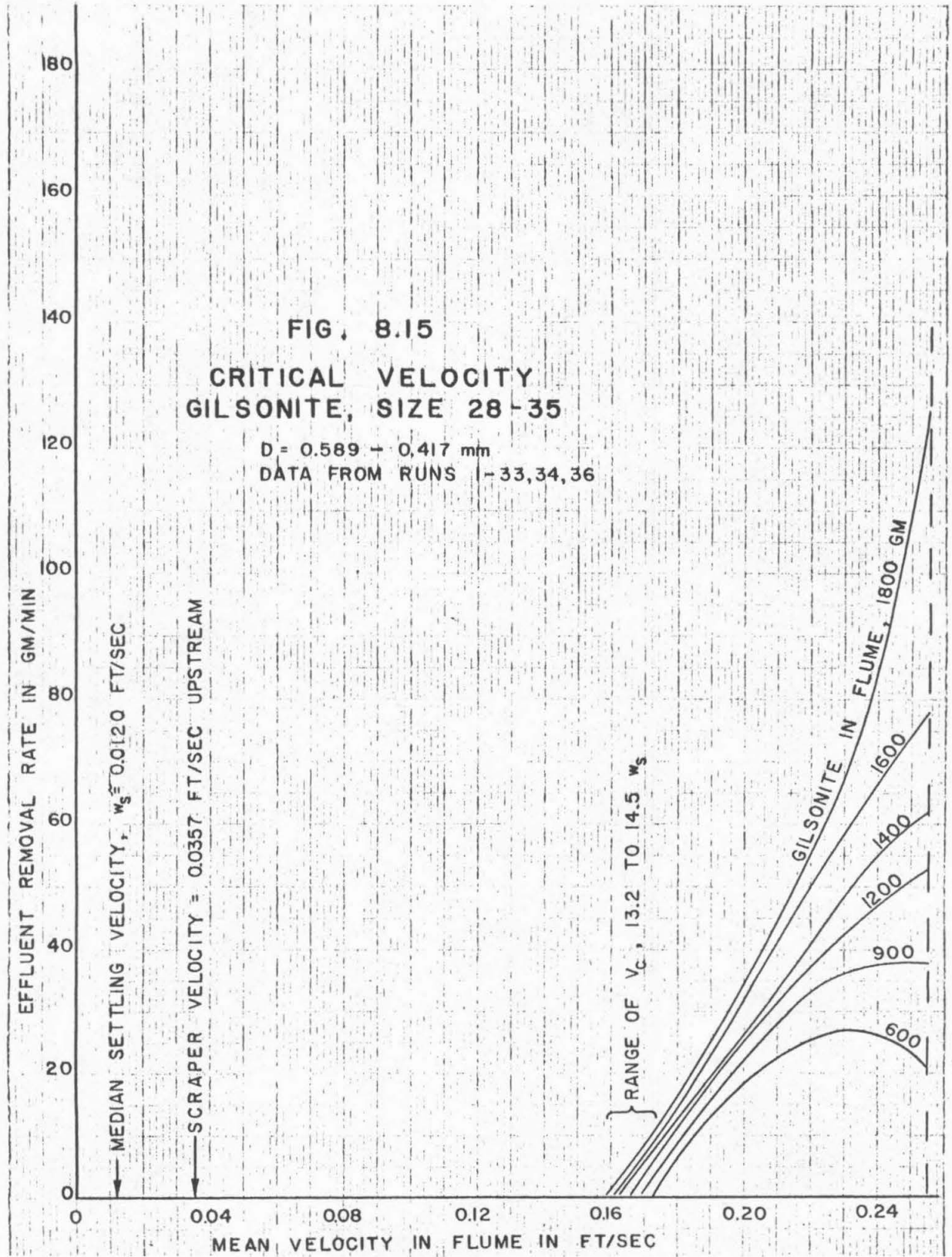
FIG. 8.15
CRITICAL VELOCITY
GILSONITE, SIZE 28-35
D = 0.589 - 0.417 mm
DATA FROM RUNS 1-33,34,36
EFFLUENT REMOVAL RATE IN GM/MIN
MEAN VELOCITY IN FLUME IN FT/SEC
MEDIAN SETTLING VELOCITY, w_s = 0.0120 FT/SEC
SCRAPER VELOCITY = 0.0357 FT/SEC UPSTREAM
RANGE OF V_c, 13.2 TO 14.5 w_s
GILSONITE IN FLUME, 1800 GM
1600
1400
1200
900
600
0
20
40
60
80
100
120
140
160
180
0.04
0.08
0.12
0.16
0.20
0.24

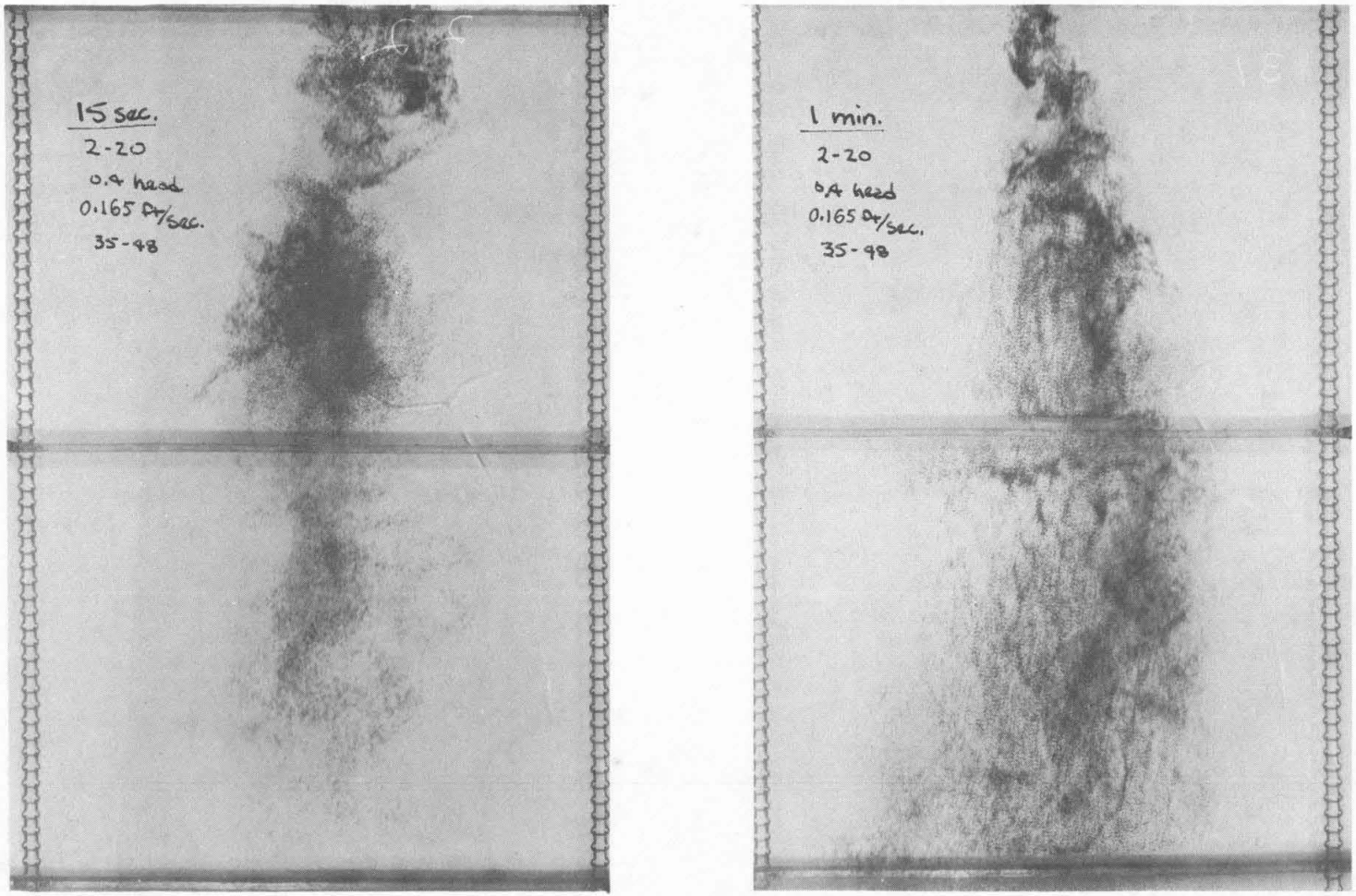

(a) t = 15 seconds

(b) t = 1 minute

] Fig. 8.16

DIFFUSION OF GILSONITE FROM INJECTION TUBE

Particle Size	35-48	Tube Depth	0.308 ft
Scraper Velocity	Zero	Injection Rate	22.6 gm/min
Displacement Velocity	V = 0.165 ft/sec = 21.8 w_s	Distance downstream from tube to center of picture	1.5 ft

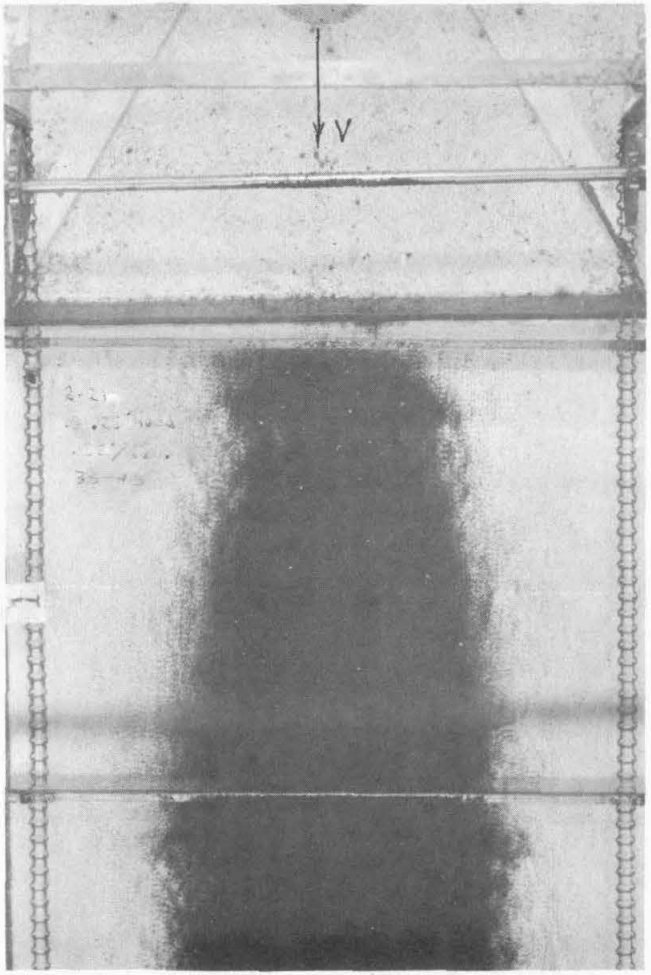

(a) x=1.5 ft (Conc.= 44.9 gm/ft)

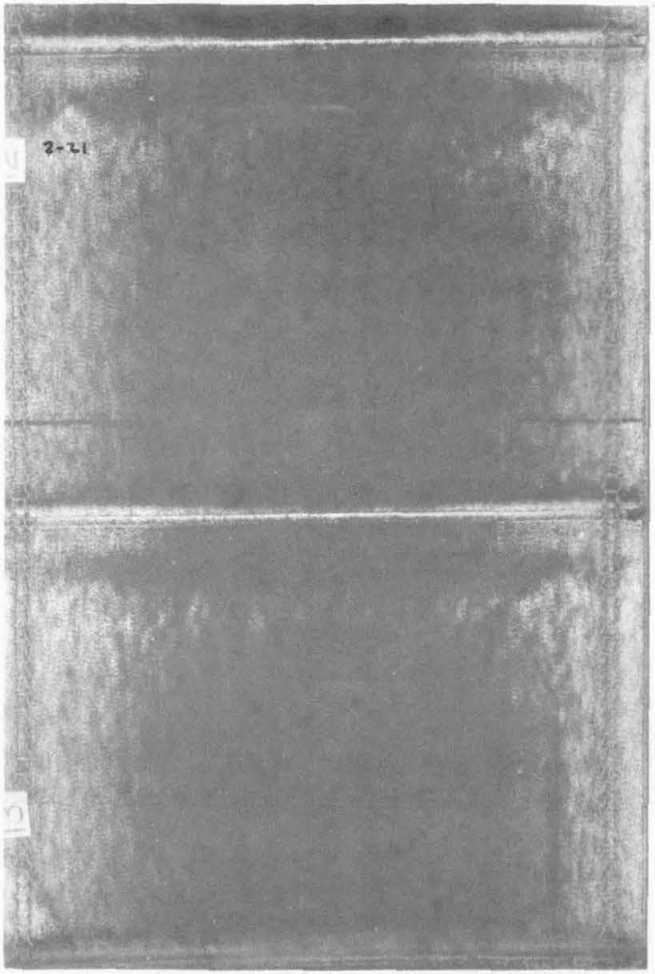

(b) x=10.8 ft (Conc.= 22.2 gm/ft)

Fig. 8.17

DISTRIBUTION OF GILSONITE ON BED FROM CONTINUOUS INJECTION

Particle Size	35-48	Tube Depth	0.308 ft
Scraper Velocity	Zero	Injection Rate	18.21 gm/min
Displacement Velocity	V=0.132 ft/sec = $17.5w_s$	Length of Run	30 min

Fig. 8.18

DISTRIBUTION OF GILSONITE
ON FLUME BED
FROM CONTINUOUS INJECTION

Particle Size	35-48
Scraper Velocity	Zero
Displacement Velocity	V = 0.132 ft/sec = 17.5 w_s
Tube Depth	0.308 ft
Injection Rate	18.21 grams/min
Length of Run	30 min
Run No. 2-21	

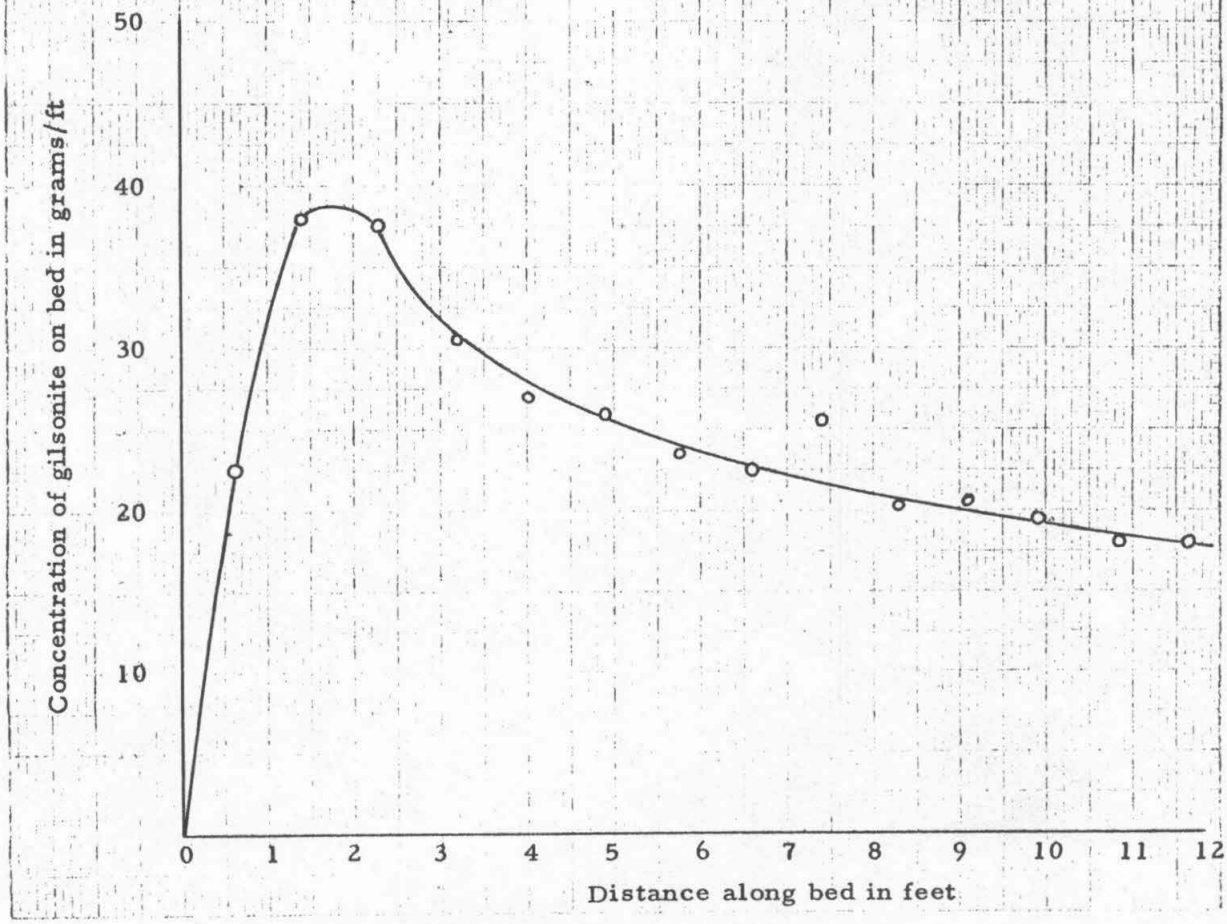

Fig. 8.19

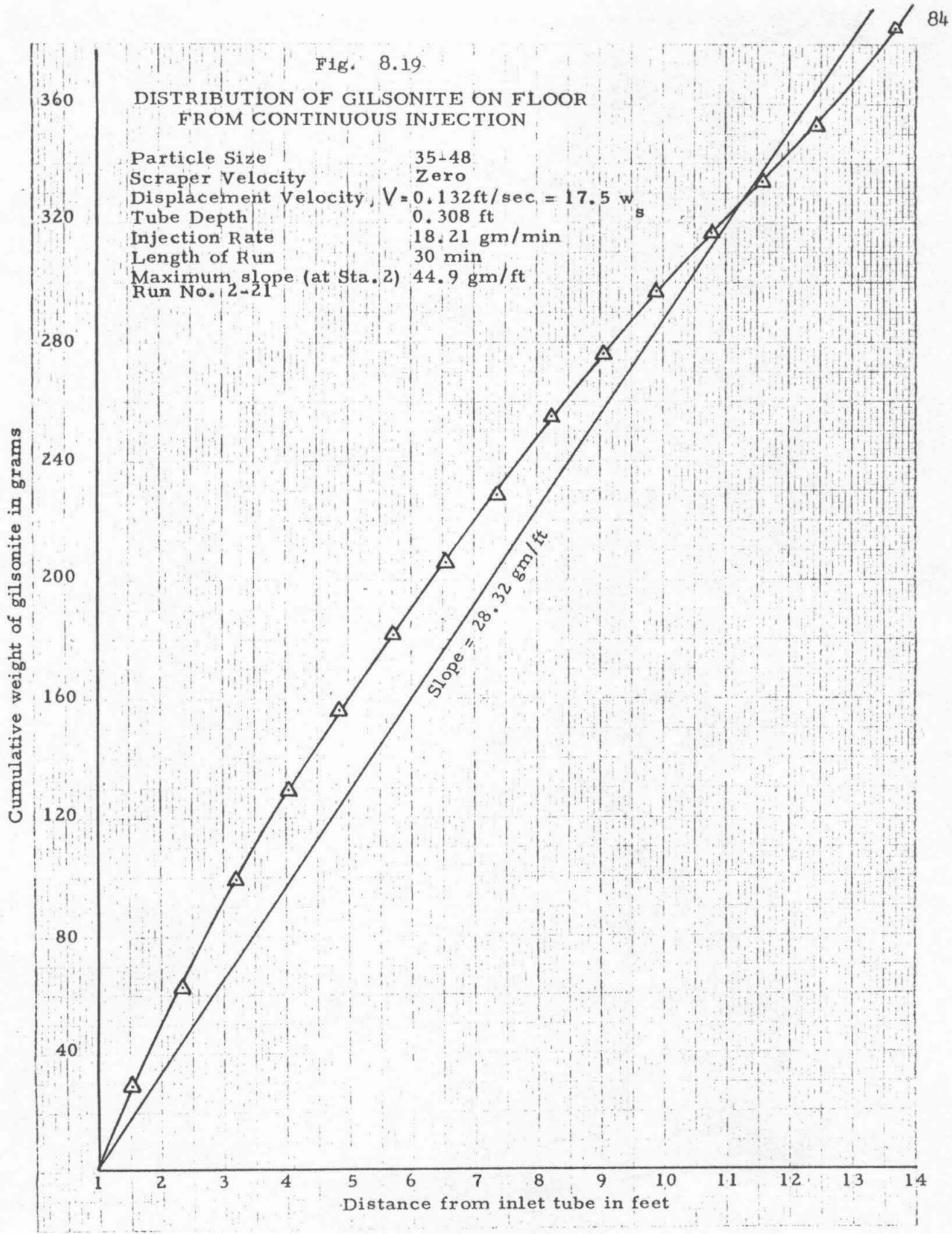
DISTRIBUTION OF GILSONITE ON FLOOR
FROM CONTINUOUS INJECTION
Particle Size 35-48
Scraper Velocity Zero
Displacement Velocity, V = 0.132ft/sec = 17.5 w_s
Tube Depth 0.308 ft
Injection Rate 18.21 gm/min
Length of Run 30 min
Maximum slope (at Sta. 2) 44.9 gm/ft
Run No. 2-21
Slope = 28.32 gm/ft
Cumulative weight of gilsonite in grams
360
320
280
240
200
160
120
80
40
1
2
3
4
5
6
7
8
9
10
11
12
13
14
Distance from inlet tube in feet

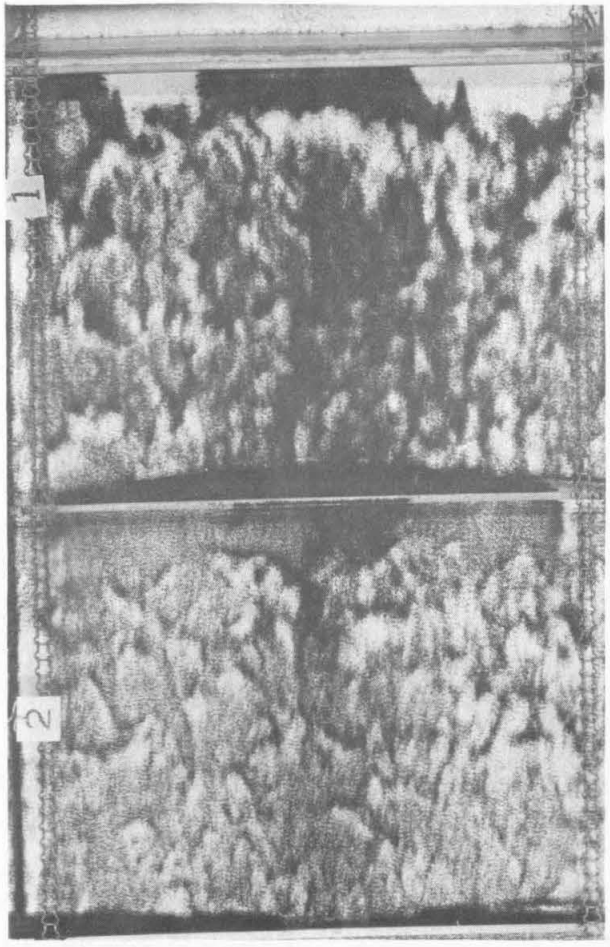

(a) x= 1.5 ft (Conc.= 10 gm/ft

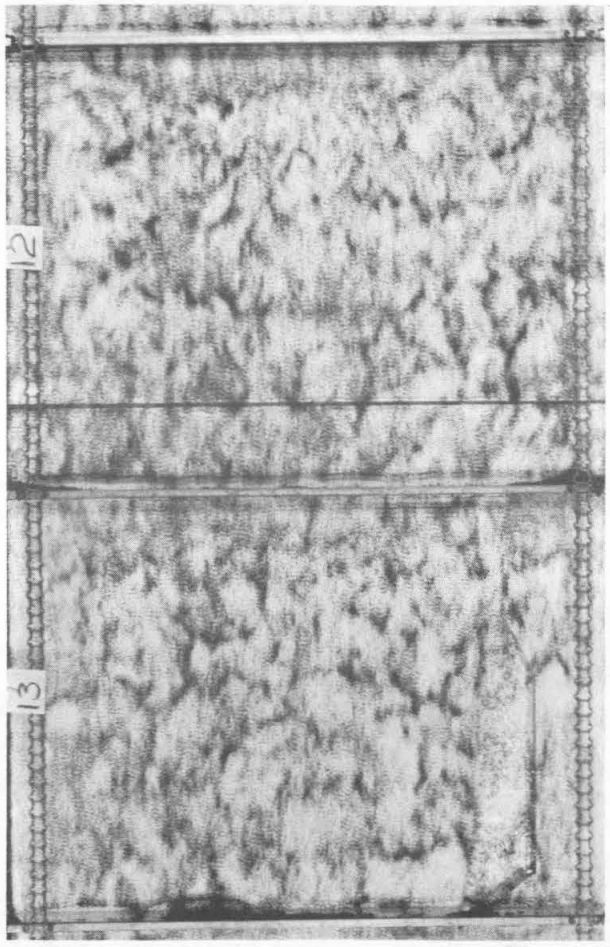

(b) x=10.8 ft (Conc.= 5.0 gm/ft)

F Fig. 8.20

DISTRIBUTION OF GILSONITE ON BED FROM CONTINUOUS INJECTION

Particle Size	35-48	Tube Depth	0.308 ft
Scraper Velocity	0.0357 ft/sec upstream	Injection Rate	18.64 gm/min
Displacement Velocity	V = 0.118 ft/sec=15.6w_s	Length of Run	30 min

Fig. 8.21

CUMULATIVE DISTRIBUTION OF
GILSONITE ON FLUME BED
FROM CONTINUOUS INJECTION

Particle Size	35-48
Scraper Velocity	0.0357 fps upstream
Displacement Velocity	$V = 0.118$ ft/sec $= 15.6 w_s$
Tube Depth	0.308 ft.
Injection Rate	18.64 gm/min
Length of Run	30 min.
Maximum Slope(at 13 ft)	11.0 gms/ft
Run	2-25

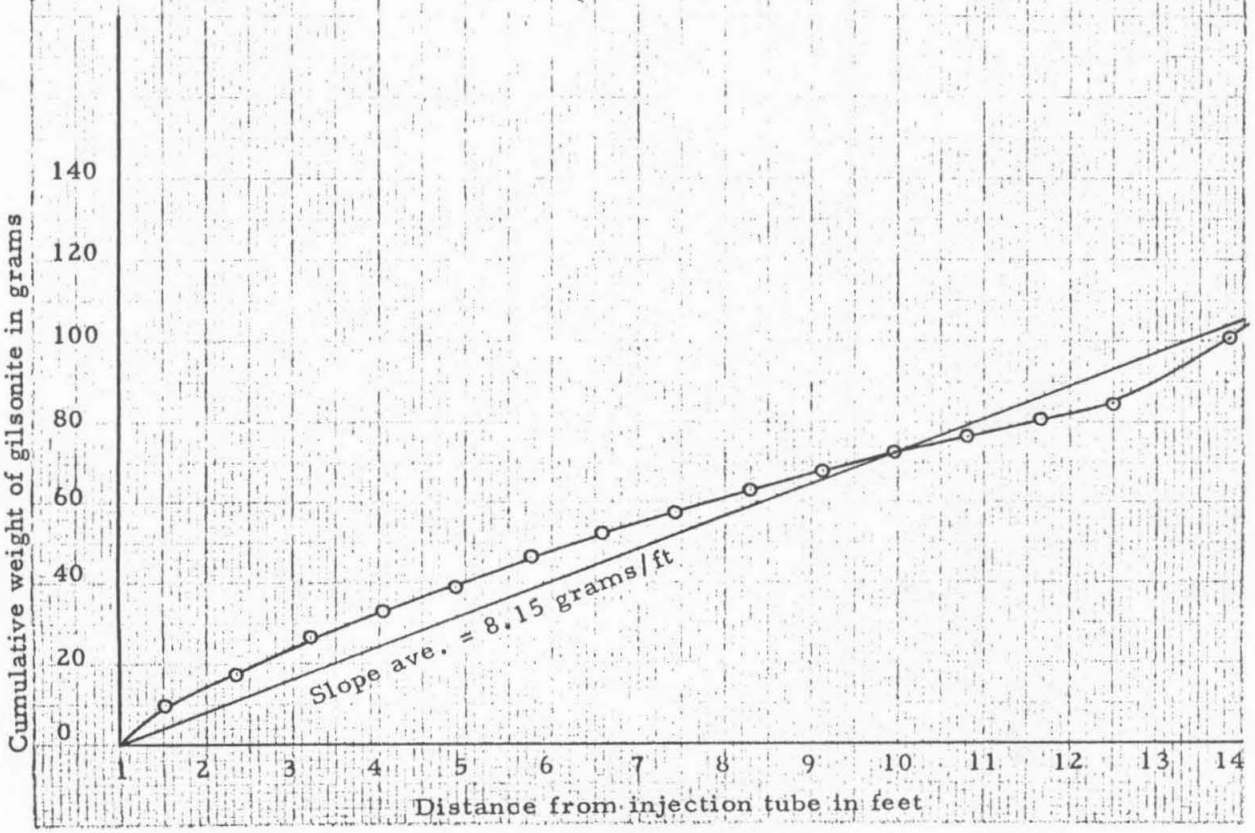

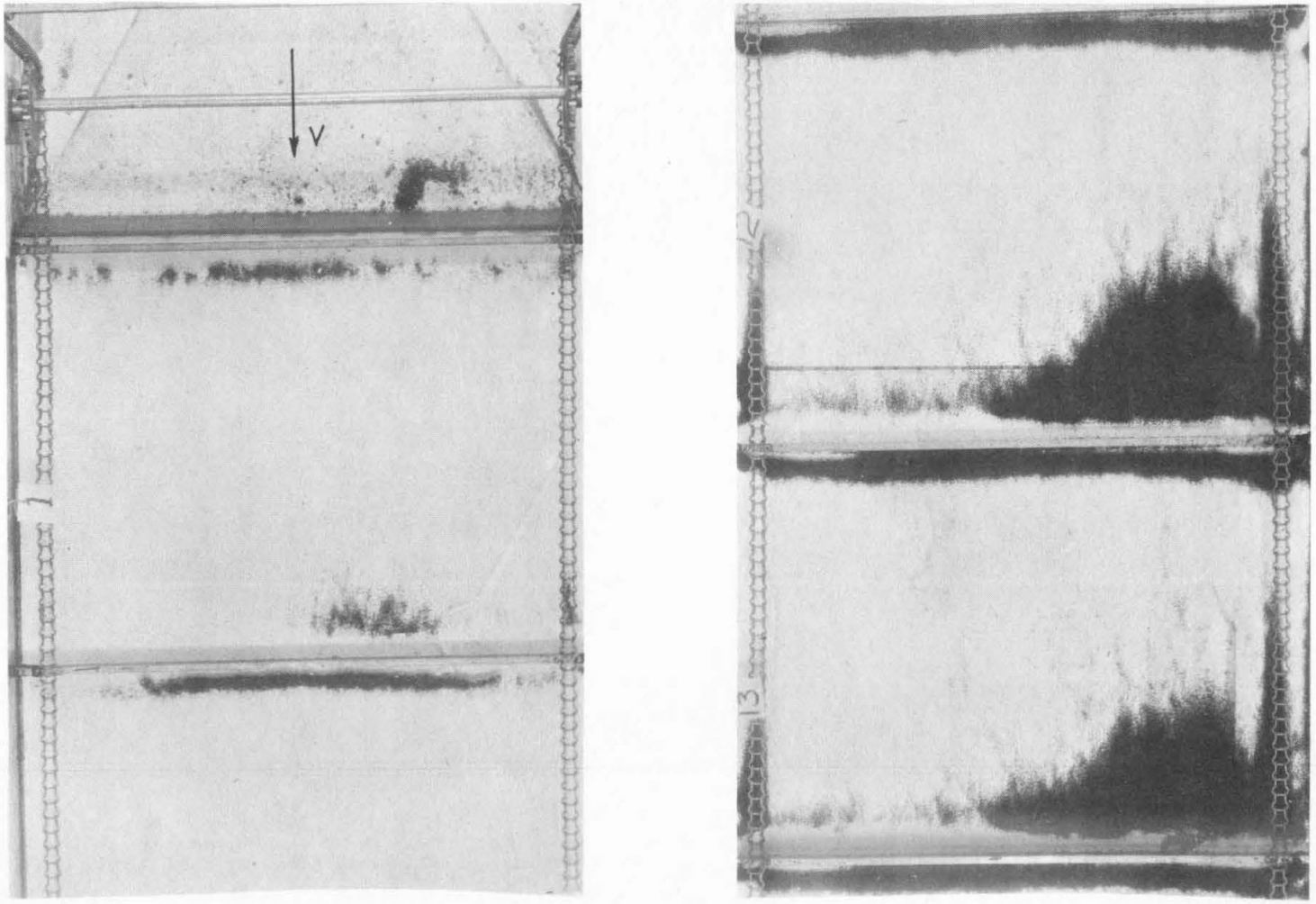

(a) x = 1.5 ft (Conc. = 3.6 gm/ft)

(b) x = 10.8 ft (Conc. = 16.5 gm/ft)

Fig. 8.22
Run No. 2-24
DISTRIBUTION OF GILSONITE ON BED FROM CONTINUOUS INJECTION

Particle Size	35-48	Tube Depth	0.308 ft
Scraper Velocity	Zero	Injection Rate	17.17 gm/min
Displacement Velocity	V=0.249 ft/sec = 33.0w_s	Length of Run	30 min

Fig. 8.23

CUMULATIVE DISTRIBUTION OF GILSONITE ON FLUME BED FROM CONTINUOUS INJECTION

Particle Size	35-48
Scraper Velocity	Zero
Displacement Velocity	V = 0.249 ft/sec = 33.0 w_s
Tube Depth	0.308 ft
Injection Rate	17.17 grams/min
Length of Run	30 min
Maximum Slope (at 13 ft)	16.5 grams/ft
Run No. 2-24	

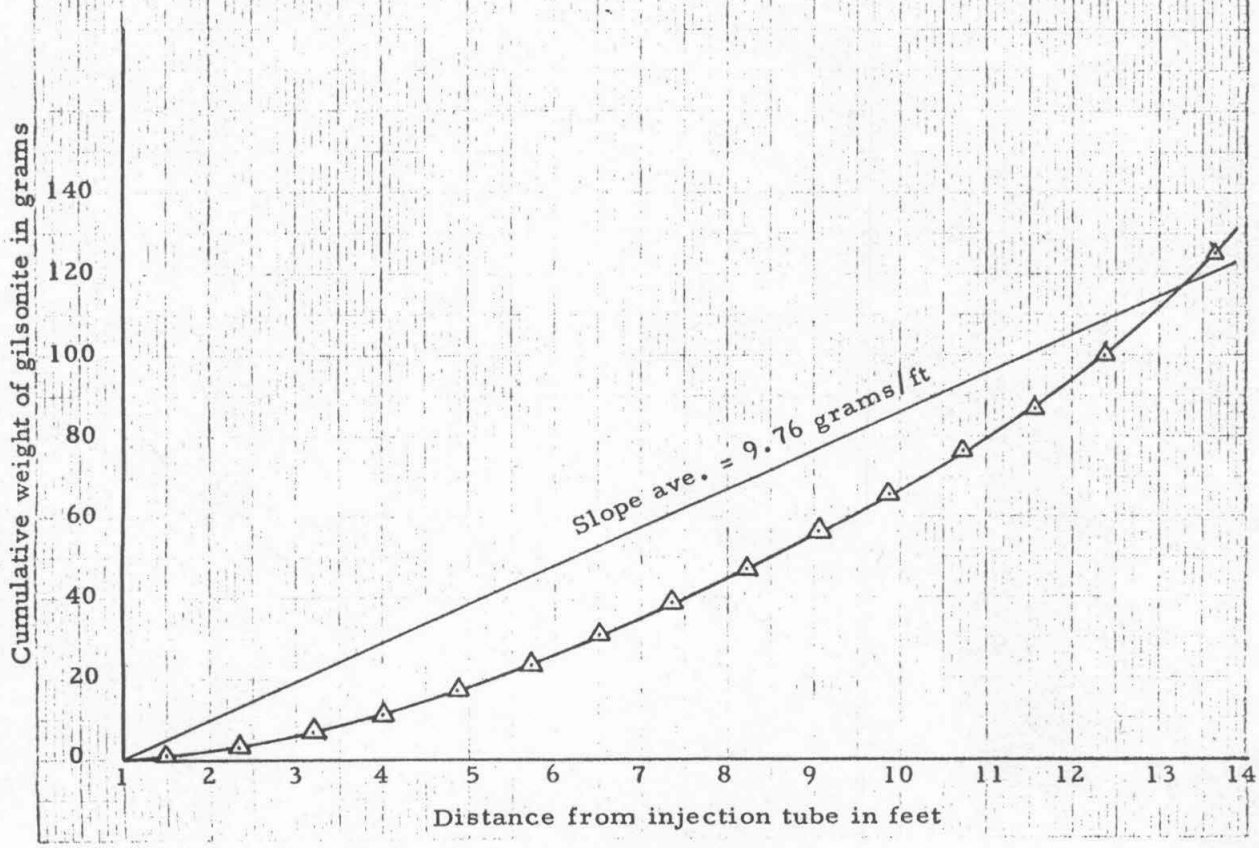

In order to compare further the relative effects of scrapers vs. displacement velocity, the scrapers were now turned off and the flume velocity was increased to a maximum of 0.249 fps or 33.0 w_s. The results are shown in the pictures of Fig. 8.22 and the cumulative plot of Fig. 8.23, which shows the floor deposit to be not greatly different from that of Fig. 8.21 although the displacement velocity has increased by a factor of two. Aside from this the most interesting feature of Fig. 8.23 is the upward concave curve of the cumulative plot, whereas most of the others were concave downward.

8.4. Analysis of Effect of Scrapers

Critical Velocity: The purpose of the tests described in this chapter was to compare theoretical values of critical velocity for entrainment with those observed in the laboratory flume, as summarized in Figs. 8.13 and 8.15. The theoretical values are all related to the roughness of the bed, as in Eq. (12) of Camp's omnibus paper (Ref. 2.1),

$$V_c = \sqrt{\frac{8\beta}{f} g (s - 1) D} \qquad (8.1)$$

in which the value of β is about 0.04, as shown by Camp, while the specific gravity, s, and diameter, D, of the particles may be found in Table 5.1. It remains to evaluate the friction factor, f, for the flume with the scrapers installed.

Inasmuch as direct computation of the friction factor is not practicable for such low velocities, because of the great difficulty in measurement of the head loss in the flume, it becomes necessary to employ empirical relationships devised for similar types of flow. For example, in Chapter 6 the glass-walled flume was compared to a smooth pipe flowing at the same Reynolds number, resulting in a value of f = 0.025. There now follows one plausible scheme for computing theoretically what may be the appropriate value of f for the tank with the scrapers moving slowly upstream.

We shall first determine the energy loss that is occasioned by the drag force exerted upon the scrapers on the floor of the flume. Using the same Reynolds number of 2.2×10^4 employed in Chapter 6 for computing f = 0.025, it is seen from Fig. 6.3 at the middle value of temperature of 18°C that the corresponding displacement velocity is approximately 0.15 fps. This makes the relative velocity between the scraper and the stream 0.15 + 0.0357 = 0.1857 fps.

To find the drag force on each scraper, an appropriate Reynolds number must be found by including the image of the scraper reflected in the floor of the flume so as to present a symmetrical obstruction to the oncoming stream. Thus the stream views an apparent obstruction 1 in. wide whose length extends the full width of the flume. The apparent Reynolds number is then

$$R = \frac{DV}{\nu} = \frac{1}{12} \times \frac{0.1857}{0.0000095} = 1{,}630 \qquad (8.2)$$

From Fig. 13.11 of Ref. 6.1 it is seen that for flow perpendicular to a flat

plate at this value of $\mathcal{R}$, the drag coefficient would be approximately 1.8. This would bring the drag force on each scraper to be

$$F_D = C_D \frac{1}{2} \rho V^2 BL \qquad (8.3)$$

$$= 1.8 \times 0.5 \times 1.94 \times (0.1857)^2 \times (0.5/12) \times 1.27$$

$$= 0.00318 \text{ lb.}$$

The number of scrapers in contact with the floor at any time is 14. Thus the total drag force against the scrapers averages approximately 14 x 0.00318 = 0.0446 lb. To translate this into equivalent head loss, consider the power required to drive the scrapers against this drag force. In this case the velocity will be that of the scraper train. Thus

$$P = F \times V_s = 0.0446 \times 0.0357 = 0.00159 \text{ ft. lb.} \qquad (8.4)$$

The equivalent head loss may be computed by dividing the power requirement for drag force by the weight-flow rate. Thus

$$h_f = \frac{P}{Q\ w} = \frac{0.00159}{0.15 \times 1.27 \times 0.76 \times 62.4} \qquad (8.5)$$

$$= 0.000176 \text{ ft.}$$

in which 0.76 ft. was the average depth of flow, (30% less than the 1.09 ft depth of Fig. 6.3 but the Reynolds number is not materially affected.

The friction factor associated with this loss may be computed from the usual pipe-friction equation, the diameter being replaced by four times the hydraulic radius (R = 0.346 ft for the rectangular section 1.27 ft wide by 0.76 ft deep)

$$h_f = f \frac{L}{D} \frac{V^2}{2g} = f \frac{L}{4R} \frac{V^2}{2g} \qquad (8.6)$$

or,

$$f = \frac{8\ Rg\ h_f}{L\ V^2} = \frac{8 \times 0.346 \times 32.2 \times 0.000176}{14 \times (0.15)^2}$$

$$= 0.0498$$

If this represents only the roughness added by the scrapers, then the total flume roughness is the sum of the scraper roughness plus the resistance factor for the smooth floor (not counting particle roughness here), or 0.025 + 0.0498 = 0.0748, for a displacement velocity of approximately 0.15 fps. Now, returning to Eq. (8.1) a computation for V_c now yields, in cgs units,

$$V_c = \frac{8 \times 0.04}{0.0748} \times 980 \times (1.038 - 0.0997) \times 0.035$$

$$= 2.46 \text{ cm per sec} = 0.0806 \text{ fps}$$

This is seen to be a remarkable check with the range of values from 0.08 to 0.10 fps projected for the critical velocity of these particles (Fig. 8.13).

Bed Reynolds Number: The bed Reynolds number is given in terms of the friction velocity, u_*, and the particle diameter, D:

$$R_b = \frac{u_* D}{\nu} \qquad (8.7)$$

For the above data,

$$u_* = V\sqrt{\frac{f}{8}} = 0.15\sqrt{\frac{0.0748}{8}} = 0.0145 \text{ fps}$$

$$\text{or } R_b = \frac{0.0145 \times 0.035/30.48}{0.0000095} = 1.75$$

Referring to Fig. 7.2, this value of the bed Reynolds number is seen to be just at the lower limit of Shields' range. For lower velocities, R_b falls below the Shields' range. This was the region it was hoped to study extensively in this project, but even with the light gilsonite, the critical velocities for motion fall in (or very close to) the Shields' range. However, as shown in Fig. 7.3, many experiments yielded values of β far below those reported by Shields.

Bed Shear: This is computed readily from the friction velocity,

$$\tau_o = \rho u_*^2 = 1.94\ (0.0145)^2 = 0.000408 \text{ psf}$$

White's Shear: Utilizing C. M. White's expression for critical shear, (Eq. 2.3),

$$\tau_o = 0.18 \times \rho' g\ D \tan\phi$$

in which ϕ is the angle of repose, under water. Many tests were run to evaluate ϕ and the best average value for $\tan\phi$ is 0.78 for all gilsonite sizes. Then

$$\tau_o = 0.18 \times 0.041 \times 980 \times 0.035 \times 0.78 = 0.198 \text{ dyne/cm}^2$$
$$= 0.000412 \text{ psf}$$

which is indeed close to the bed shear computed from the friction velocity just above. It is to be noted that the presence of the scrapers does not affect this calculation.

Delleur's Shear: It is instructive here to compare the foregoing values for bed shear with those based upon entirely different theory. Such a theory is forwarded by J. Delleur (Ref. 7.3). For the size of gilsonite discussed here (#35 - #48 mesh) Delleur's theory yields for the smooth floor condition, $\tau_c = 0.000115$ psf and for the thick bed, $\tau_c = 0.00000962$ psf. Either of these values is only a fraction of the approximate value 0.0004 psf, the bed shear computed using the scrapers, or of that computed using the angle of

repose. No ready explanation is available for this discrepancy. It tends to soften somewhat the support for Delleur's theory forwarded in Chapter 7.

8.5. Conclusions on Scraper Effects

Based upon the many tests reported in this chapter, the following conclusions can be drawn:

A. Gilsonite bed prepared in advance

1. Effluent removal of gilsonite varies with the displacement velocity and also with the amount of gilsonite remaining in the flume. The higher the velocity, or the greater is the amount in the flume, the greater will be the effluent removal.

2. It is possible to extrapolate the data for effluent removal vs. velocity and concentration in flume, and to state that for the two sizes tested (28 - 35 and 35 - 48) the critical velocity for initial movement along the bed against the upstream movement of the scrapers was from 10.5 to 14.5 times the settling velocity of the particle.

3. The presence of the scrapers in the flume, moving upstream at 0.0357 fps, constitutes a sufficient obstruction that the effective friction factor of the flume itself is increased from 0.025 to 0.075. In computing the bed shear by various computational methods, good conformity was obtained between a method in which the scrapers were treated as added roughness and the method of White, involving the angle of repose of the sediment under water. The method of Delleur did not yield values that could be checked with those from other methods.

B. Continuous injection of gilsonite

1. The gilsonite tends to distribute itself along the bed with a peak concentration at about 2 ft from the inlet, then falling off slowly to the effluent end.

2. It is possible to double the displacement velocity if the scrapers are stopped from their upward motion of 0.0357 fps, and to achieve approximately the same deposition of gilsonite on the floor of the flume.

Chapter 9

BEHAVIOR OF FLOCCULENT SUSPENSIONS IN FLUME

Following the tests on suspensions of discrete particles reported in the preceding chapters, the laboratory flume was fitted with the necessary apparatus to generate the ferric chloride-bentonite floc described in Chapter 5, and to introduce it into the inlet end of the flume. The final 14 months of the project were devoted almost exclusively to investigations of the behavior of this floc in the flume and in settling tubes specially constructed for such study. The settling tube and related studies are described in Chapter 10, while the behavior of the floc in the flume fitted with transverse baffles is discussed in Chapter 11.

9.1 Material and Apparatus for Floc Generation and Injection

The equipment used for the generation of the floc described in Section 5.3 is shown in the schematic diagram of Fig. 9.1. The slurry mixing device (1) was a six-liter brass container with a 12-bladed propeller oscillating at 288 cycles per min. The bentonite clay slurry was fed from the mixer through a 32-in. length of 1/4-in. tygon tubing to the flash mixer (2). A constant water flow to the flash mixer was maintained by a double-walled lucite cylinder (3) that utilized the inside cylinder as an overflow weir. Ferric chloride solution was fed from a 4-liter jar (4) through a Fischer and Porter Flowrater tube (5) to the flash mixer.

The slurry, water and ferric chloride solution were blended in the flash mixer and then siphoned into the floc mixing jar (6) where the floc was continuously agitated before being siphoned into the flume. The floc mixing (or "turbulence") jar (6) was a 12-1/2 in.diameter glass cylinder 25 in. high. Agitation was accomplished by an oscillating lattice structure which obstructed 19% of the cross section (in 8 horizontal grids). This lattice oscillated vertically in simple harmonic motion, of 5/8-in. amplitude, thus producing essentially the same degree of mixing over the total volume. The speed of the driving motor was variable, but for all floc studies in the flume the frequency was constant at 47 cycles per minute.

The floc generation equipment is shown mounted on the side of the flume in Fig. 9.2. This system produced a stable floc which could be adjusted to any concentration needed. Fig. 9.3 shows the variation in slurry feed rate with time. It can be seen that the feed rate decreased as the slurry head dropped in the mixer. This variation in slurry flow rate did not affect the concentration of floc in the large mixing jar. This can be seen in Fig. 9.4 which shows the floc concentration vs. time. It was necessary that this floc be stable and of nearly the same concentration on each run in a series in order to compare the results properly.

Floc was injected into the flume immediately downstream from the inlet screen through five 3/8-in. lucite tubes (see Figs. 6.1 and 9.5). The injectors were installed parallel to and 3 in. above the flume bottom and pointed downstream. As the floc settles to the floor of the flume it is moved upstream by the scrapers as shown in Fig. 9.6. Some of the floc can

(Text continued on page 98)

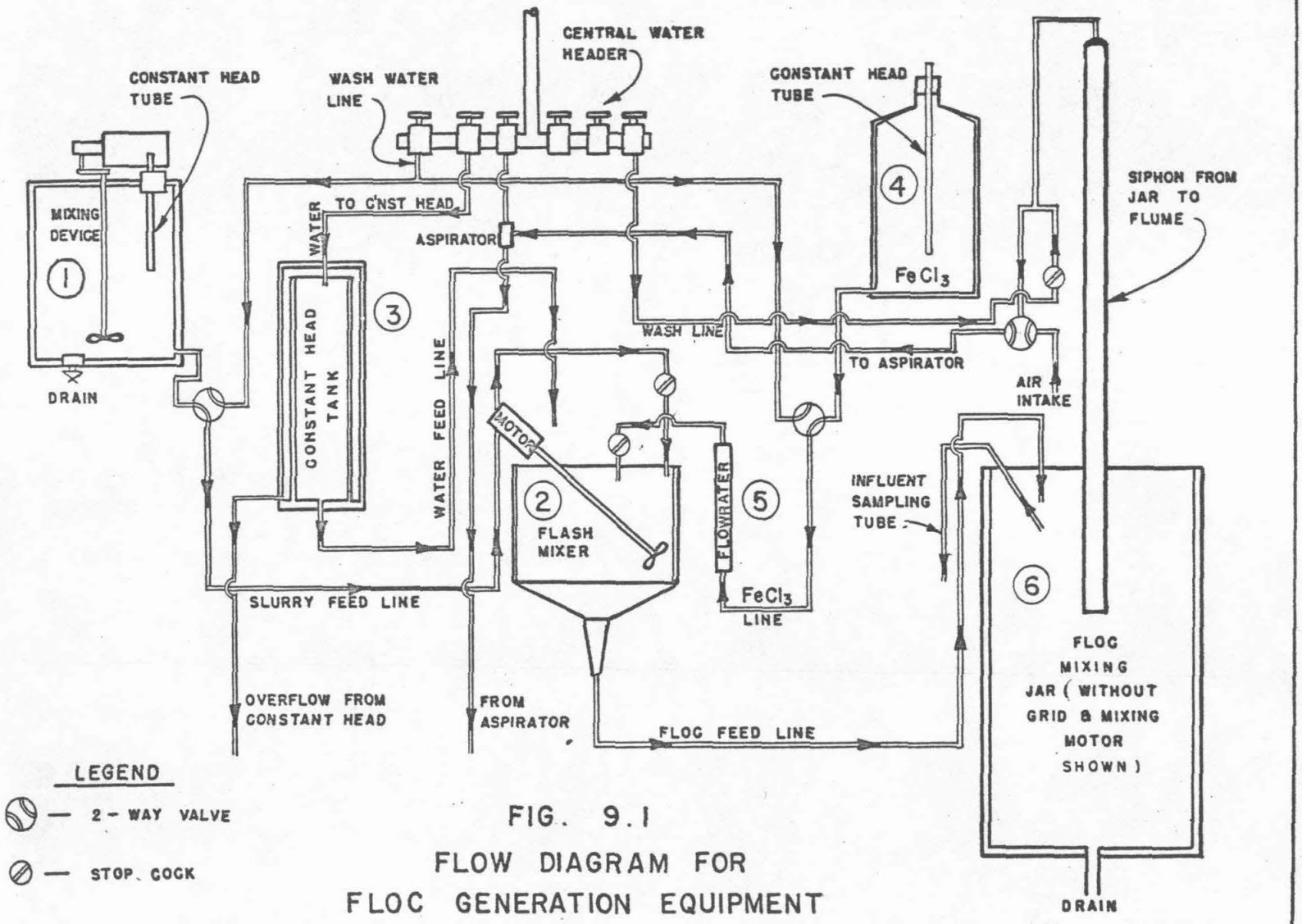

FIG. 9.1

FLOW DIAGRAM FOR

FLOC GENERATION EQUIPMENT

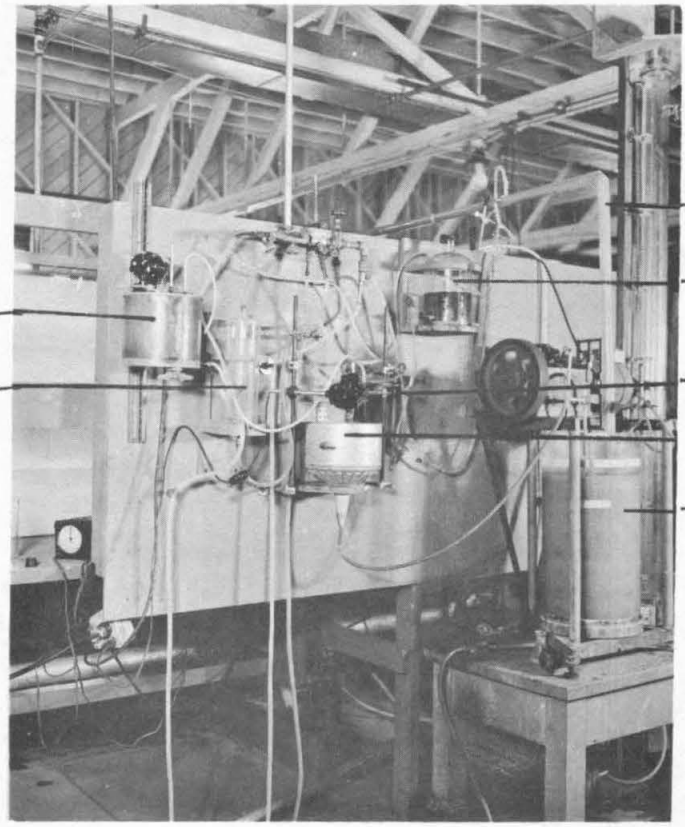

Fig. 9.2

FLOC GENERATION APPARATUS

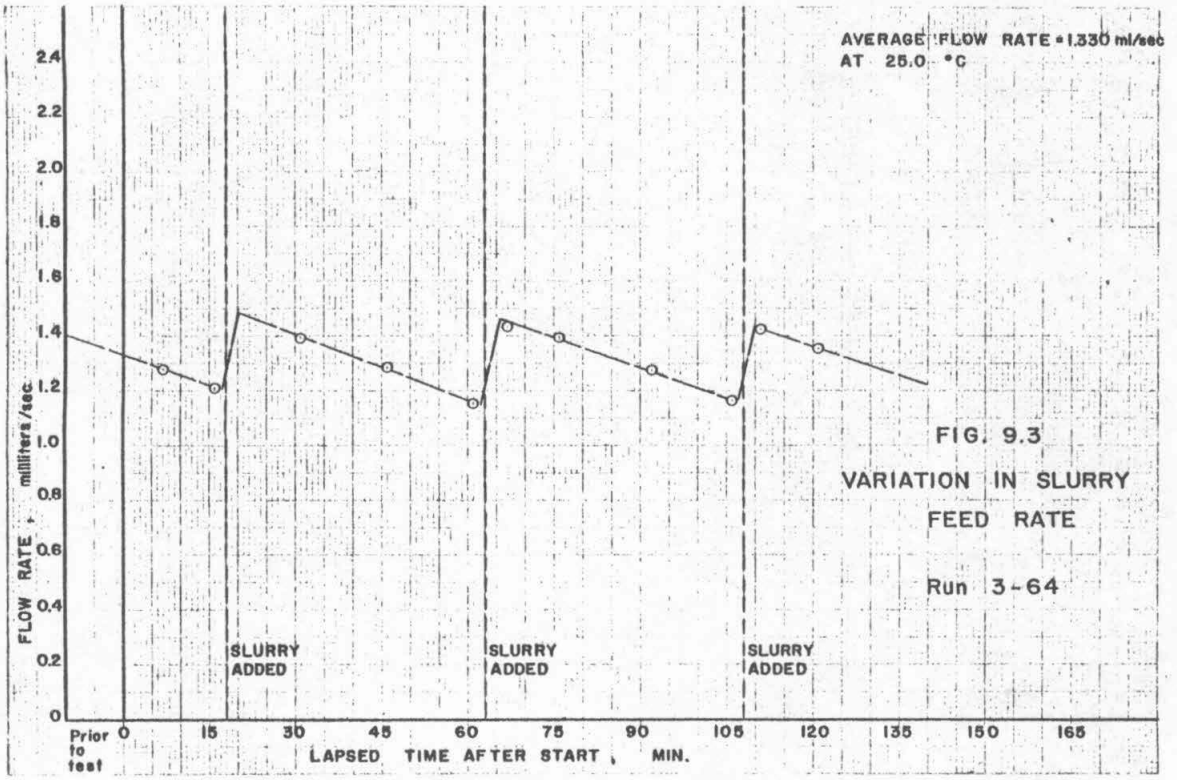

FIG. 9.3
VARIATION IN SLURRY FEED RATE
Run 3-64

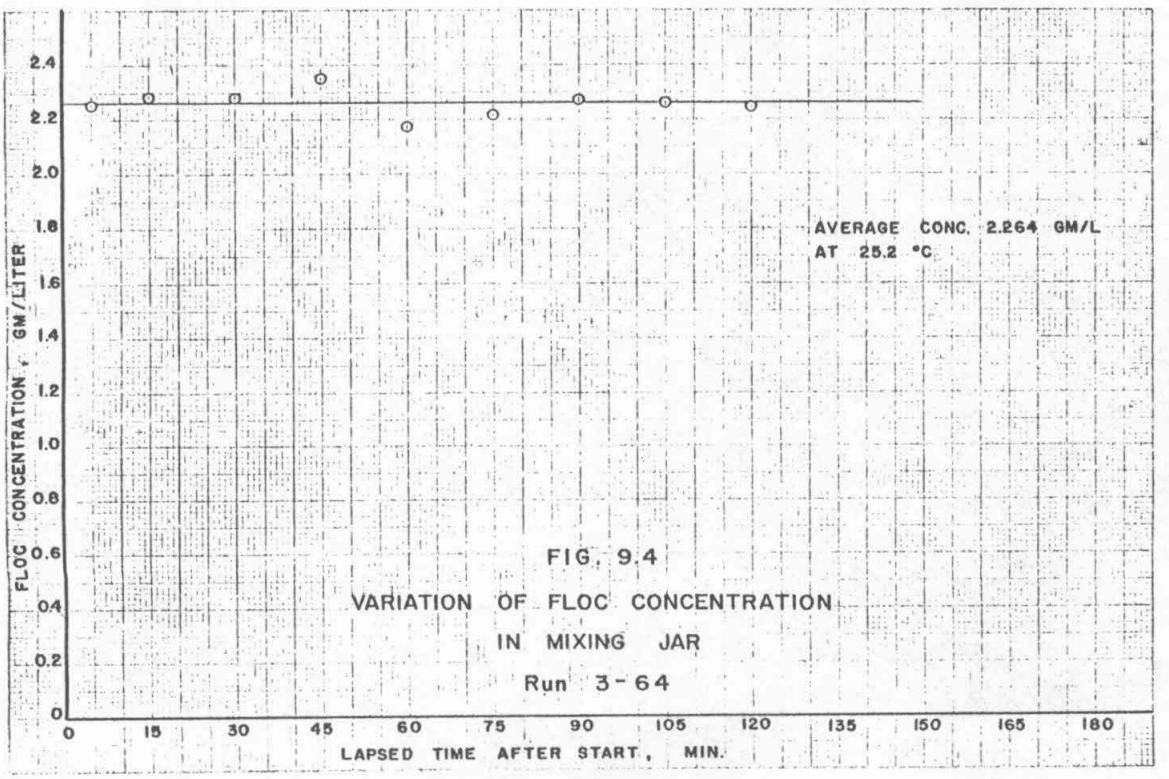

FIG. 9.4
VARIATION OF FLOC CONCENTRATION IN MIXING JAR
Run 3-64

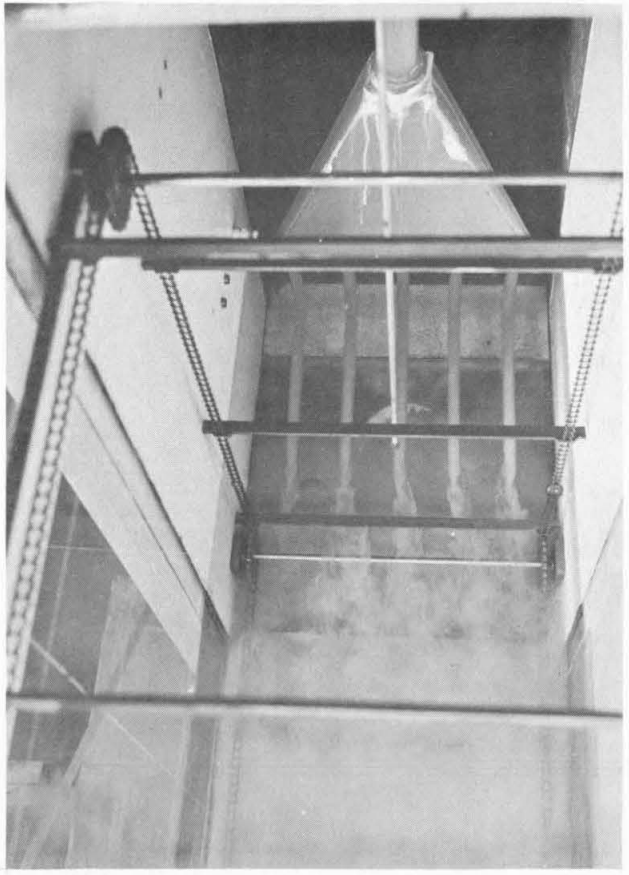

Fig. 9.5

FLUME FLOC INJECTORS
(top view)

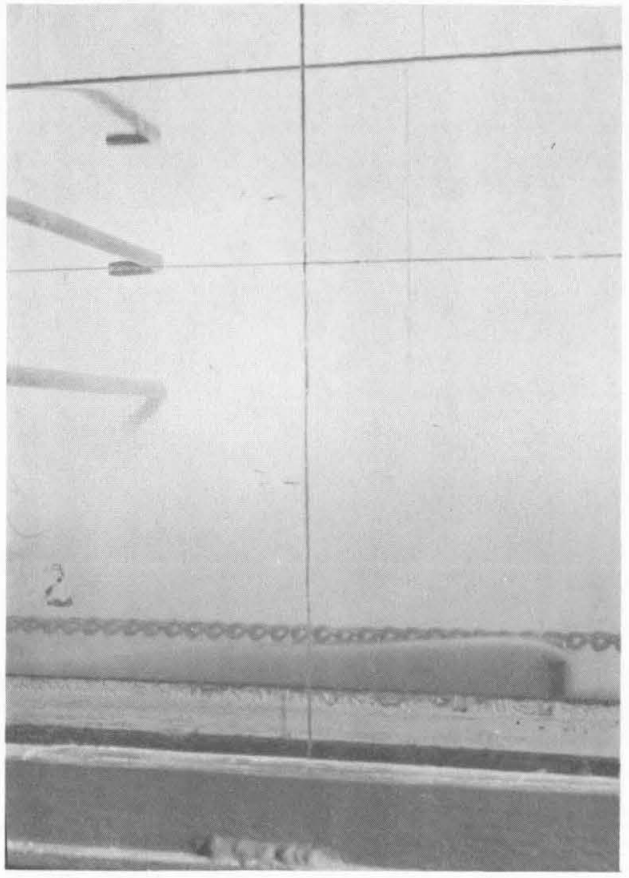

Fig. 9.6

BED CONFIGURATION WITH SCRAPERS
(flow direction to right,
scrapers move to left)

be seen spilling from the crest of the mound over the scraper to the downstream side.

9.2 Procedure for Making Floc Run in Flume

Preparation of slurry: The bentonite clay was prepared by an elutriation process which removed the larger particles from the suspension. The procedure was as follows: First, 50 grams of dry clay was mixed with 500 ml of water in a blender for one minute. After mixing, the suspension was poured into a 500 ml graduate and allowed to stand quietly for 6 minutes. All but 50 ml of the suspension was siphoned into an 18 liter bottle, thereby removing the larger particles which had settled out from the suspension. When the bottle was full, three 50-ml samples were taken and the concentration was determined by evaporation and weighing of the residue. This concentrated slurry was then diluted to 40 g/l and 1 g/l of sodium bicarbonate was added to control the pH of the floc.

Generation of floc: The slurry tank was filled with slurry at 40 g/l and the motor started. The valves leading from the slurry tank to the flash mixer were opened and flushed if necessary. Water flow into the constant head device was regulated so that only a small flow occurred over the inner cylinder and the water valve to the flash mixer was opened. The $FeCl_3$ stopcock was opened and the flow adjusted until the flow-meter indicated approximately 0.3 ml/sec.

The flash mixer was allowed to fill and the mixer motor was started. When the flash mixer hopper was sufficiently full, the siphon was started into the floc mixing jar and the floc agitator started.

The floc jar was allowed to fill while the flume was being prepared for the run (requiring approximately 40 min). During this time, spot checks were taken on the slurry flow rate, water flow rate and $FeCl_3$ flow rate. These checks were made by hand, using 25-and 50-ml graduated cylinders and a time clock. Spot checks were taken every 20 minutes throughout the run on the water flow rate and slurry rate and at 45-min intervals on the $FeCl_3$.

Procedure during run: The water flow in the flume was adjusted to the desired amount by use of the Flowrater or the venturi meter (see Fig. 6.1) depending on the quantity of flow. Flow into the sludge hopper was adjusted to 50 ml/sec. When the level of floc in the mixing jar reached a level slightly higher than the level of the water in the flume, the large siphon from the floc jar to the flume was started by using an aspirator. Time was measured from the point when floc first entered the flume.

During the run, spot checks were taken on the water flow rate and the slurry flow rate at 20 min intervals. Samples of 50-ml size were taken from the floc mixing jar at approximately the same intervals to determine the concentration. Samples of approximately 250 ml were taken from the effluent at 5-to 10-min intervals throughout the run. The slurry supply was filled every 40 min. The water depth at both ends of the flume was measured with a point gage mounted on rails above the flume.

Procedure following run: The volumes of all samples taken during the run were recorded and each sample was filtered through a numbered Gooch crucible (prepared according to Ref. 3.1) using a vacuum of 25 in. of Mercury.

The crucibles were allowed to dry in an oven at 105°C for at least two hours after which they were placed in a glass desiccator until cool. All crucibles were weighed on a beam balance with a sensitivity of 0.1 mg.

9.3 Calculation Procedure

Example: Flume Run No. 3-64

Slurry flow rate = 1.330 ml/sec
(avg of 11 spot measurements)

Water flow rate = 21.81 ml/sec
(avg of 7 spot measurements)

$FeCl_3$ flow rate = 0.296 ml/sec
(from Flowrater)

Average floc flow rate 23.43 ml/sec = 0.02343 ml/sec

Mean influent floc concentration = 2.264 g/l = 2264 mg/l
(avg of 9 samples)

Particle feed rate = (2264) (.0243) = 53.2 mg/sec

Metered flume water flow = .0637 cfs
(Fischer-Porter meter at 40% max)
= (.0637) (28.32) = 1.803 l/sec

Sludge hopper flow rate = 0.0489 l/sec
(avg of 11 spot measurements)

NET FLUME FLOW = 1.803 + .023 - .049 = 1.778 l/sec
= 0.063 ft^3/sec

Water depth upstream = 0.738 ft
(point gage measurement)

Water depth downstream = 0.741 ft

Average water depth = 0.7395 ft

Flume width = 1.28 ft

Mean flume velocity = $\frac{0.063}{(1.28)(.7395)}$ = 0.0669 fps

Effluent floc concentration = 8.88 mg/l
(avg of 24 samples)

Effluent particle rate = (8.88)(1.78) = 15.82 mg/sec

Particles removed = 53.2 - 15.82 = 37.38 mg/sec

Per cent removal = $\frac{37.38}{53.2}$ = 70.3 %

(Text continued on page 105)

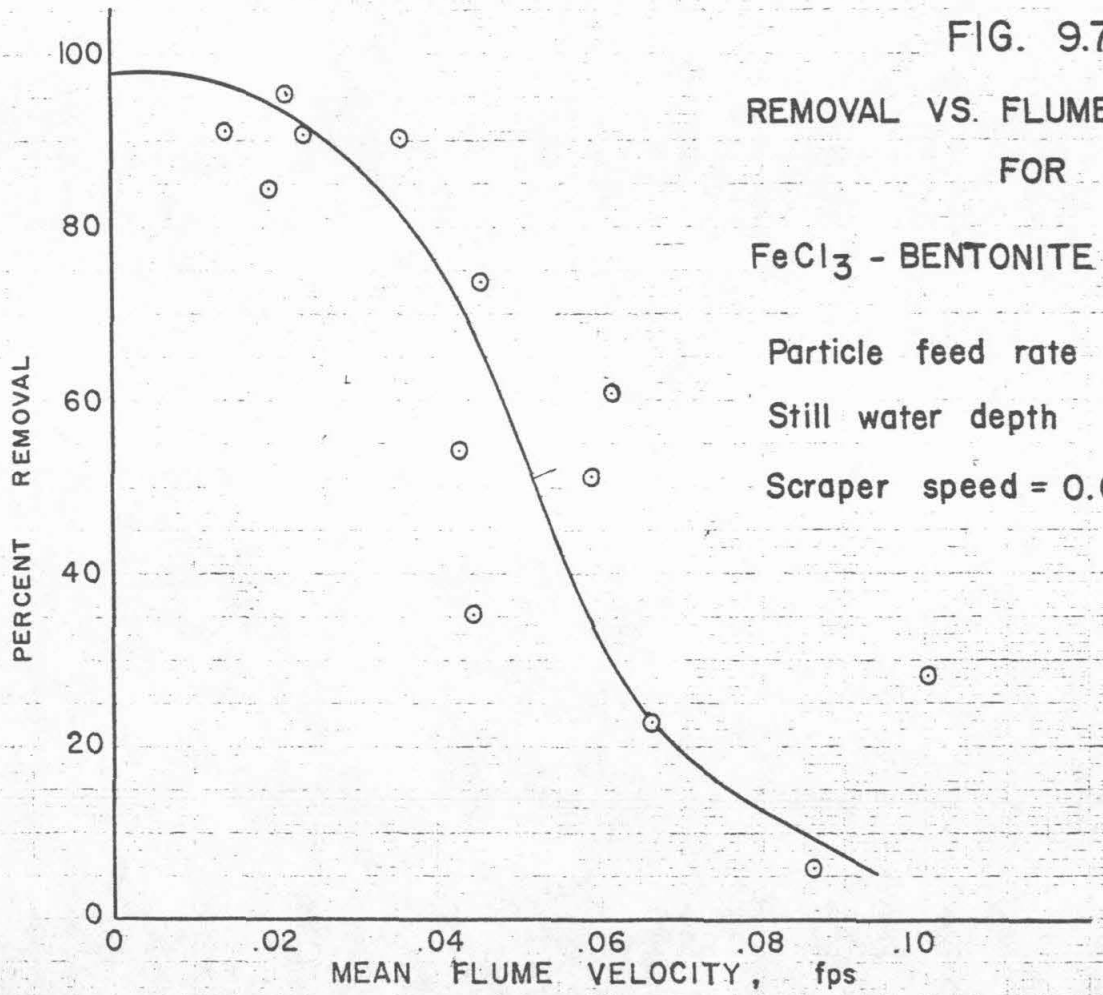

FIG. 9.7

REMOVAL VS. FLUME VELOCITY

FOR

$FeCl_3$ - BENTONITE FLOC RUNS

Particle feed rate ≈ 55 mg/sec

Still water depth ≈ 0.69 ft

Scraper speed = 0.0356 fps upstream

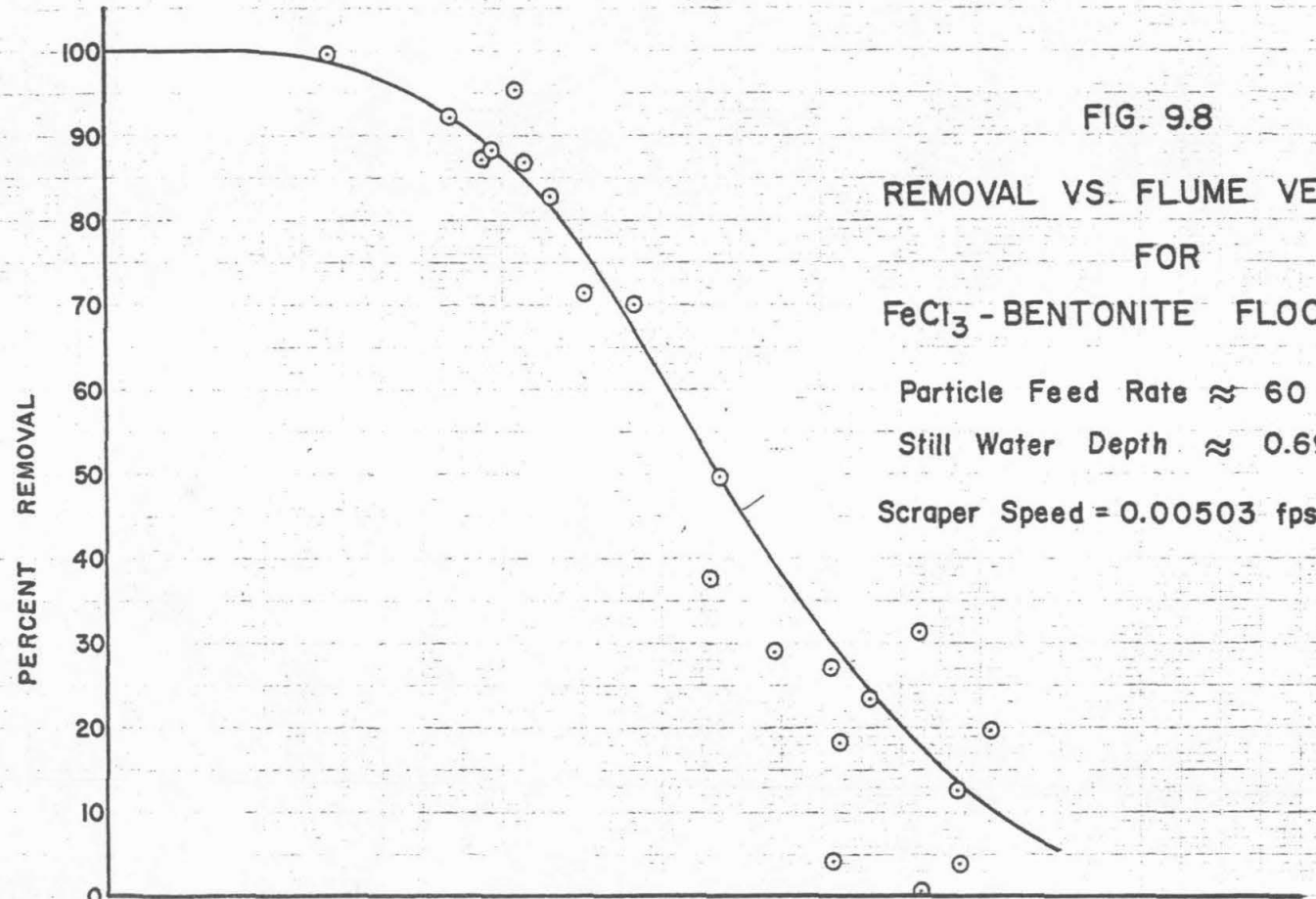

FIG. 9.8

REMOVAL VS. FLUME VELOCITY FOR $FeCl_3$ - BENTONITE FLOC RUNS

Particle Feed Rate ≈ 60 mg/sec

Still Water Depth ≈ 0.69 ft

Scraper Speed = 0.00503 fps upstream

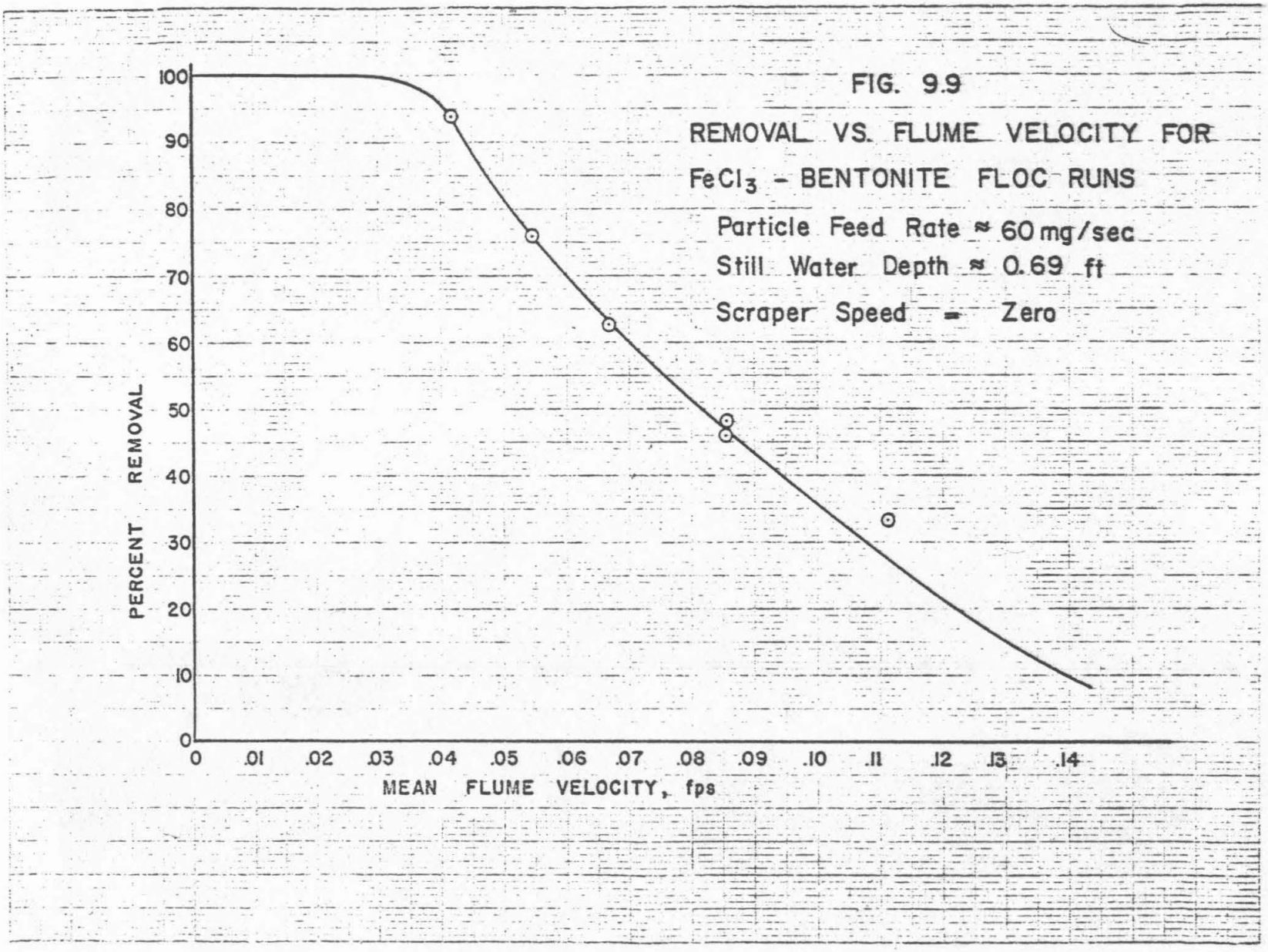
FIG. 9.9
REMOVAL VS. FLUME VELOCITY FOR
FeCl3 - BENTONITE FLOC RUNS
Particle Feed Rate ≈ 60 mg/sec
Still Water Depth ≈ 0.69 ft
Scraper Speed = Zero
PERCENT REMOVAL
100
90
80
70
60
50
40
30
20
10
0
0
.01
.02
.03
.04
.05
.06
.07
.08
.09
.10
.11
.12
.13
.14
MEAN FLUME VELOCITY, fps

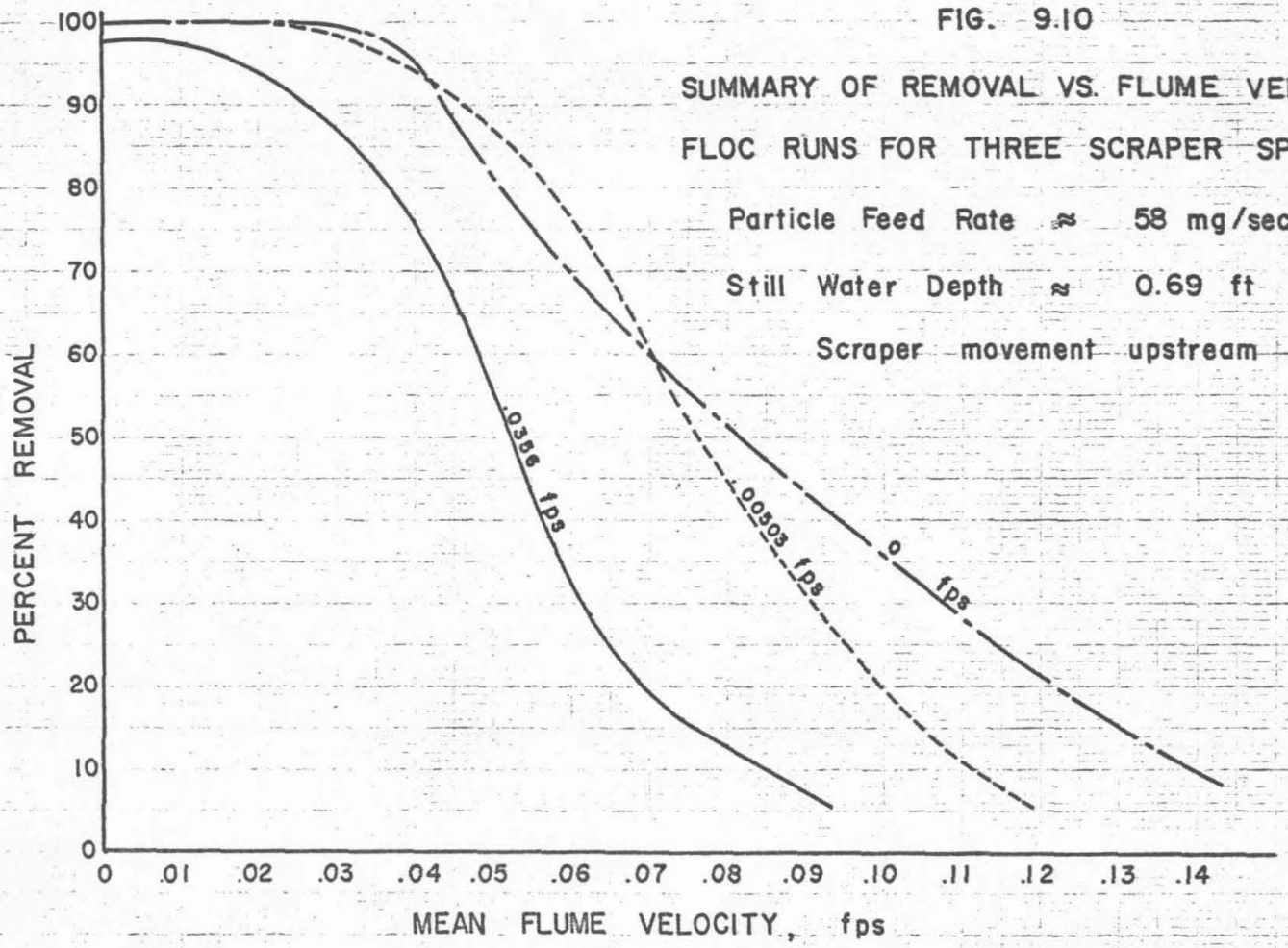

FIG. 9.10

SUMMARY OF REMOVAL VS. FLUME VELOCITY

FLOC RUNS FOR THREE SCRAPER SPEEDS

Particle Feed Rate ≈ 58 mg/sec

Still Water Depth ≈ 0.69 ft

Scraper movement upstream

9.4 Results of Flume Runs with Bentonite Clay Floc

A total of 58 flume runs was performed for the purpose of studying the settling behavior of flocculent suspensions at various flume velocities and scraper speeds. Prior to these runs, some 30 preliminary tests were made to perfect the procedure and produce large, stable floc. Three series were run with scraper speeds of .0356, .00503, and 0 fps.

The variation of per cent removal with net flume velocity for a scraper speed of .0356 fps is shown in Fig. 9.7. Figures 9.8 and 9.9 show the per cent removal vs. net flume flow for scraper speeds of .00503 and 0 ft/sec respectively. The effect of scraper speed on removal is shown in Fig. 9.10 for the three scraper speeds studied.

9.5 Discussion

The random scattering of points can be partly explained by examining the method of floc introduction and the effluent sampling procedure. The floc was introduced into the flow downstream from the inlet screen and therefore was not uniformly distributed throughout the cross section.* This lack of dispersion caused the floc to travel through the flume in "clouds." As each of the clouds reached the effluent sampling outlet the concentration was increased above the average. If the majority of samples happened to be taken as one of these clouds passed the outlet, the average concentration would be too high with a resulting decrease in the removal ratio. Many other variables affect the results, including floc stability, floc size and water temperature.

In order to justify the plotting position of the curves through the widely scattered test points, a least squares analysis was made of the points in Fig. 9.7. It resulted in a curve position nearly the same as that drawn by eye.

It can be seen from the curves of Figures 9.7 to 9.9 that there is a narrow range of velocities for any scraper speed at which the removal ratio starts to drop off sharply with increase in velocity. It is believed that at this point resuspension of the settled floc starts to take place. Observations in the flume showed that at higher velocities, small eddies formed at the crest of the scraper load and floc particles seemed to be swept away from the bed (see Fig. 9.6). The extent of this phenomenon, however, was not easily observed throughout the cross section of the flume because of the heavy concentration of floc at the bed.

A plot of removal vs. flume velocity for zero scraper speed is shown in Fig. 9.9. The scrapers were not removed from the flume. For this case, the removal at a given velocity (for flume velocities above .07 fps)

*It was believed that if the floc were introduced upstream from the inlet screen it would be badly broken up in passing through the screen. In later tests (see Chapter 11) it was considered more important to secure the uniform distribution and the floc was introduced upstream (with some consequent breaking up of particles).

was greater than that which occurred with the scrapers running. This was expected since the turbulence on the bed was decreased. The slope of this curve is smaller than the slope of the curves for the scrapers running. This may possibly be explained by the fact that for zero scraper speed, the bed becomes flat after the spaces between the scrapers are filled whereas when the scrapers are running, the bed is never flat but has undulations in it as the scrapers travel up the flume. With the bed flat, the roughness would be a function of the particle size but with the scrapers running, the roughness would depend on the bed configuration.

The effect of scraper speed on the removal ratio is shown in Fig. 9.10. These curves show that at a given velocity, the removal was 30 to 40% higher for a scraper speed of .00503 fps than for a scraper speed of .0356 fps. This was expected since increased scraper speed causes increased turbulence at the crest of the scraper load and therefore more resuspension. Of course other factors such as bed shear and particle size affect the resuspension rate. Particle size is particularly important in flocculent suspensions. For a discrete suspension the average particle size on the bed decreases in the downstream direction; but for a flocculent suspension, the particle size may stay nearly constant or increase in the downstream direction. This occurs because flocculation increases with time and opportunity for contact. Therefore the rate of growth of particles could increase in such a manner as to make the average particle size on the bed constant throughout the length of the tank.

Chapter 10

SETTLING TUBE AND CONCENTRATION PROBE STUDIES

During the tests to determine the effect of velocity and scraper speed on removal, an attempt was made to determine the actual frequency distribution of settling velocities for the floc used in the flume and the concentration distribution of the floc. To do this it was necessary to design and install concentration probes at various levels throughout the length of the flume. These probes were used to obtain samples from the flume on which settling analyses were performed using the method described by McLaughlin (see Appendix A, p. 24).

10.1 Description of Equipment

Fourteen concentration probes were designed and installed in the glass walls of the flume (see Fig. 10.1). Each probe assembly consisted of a 17-in. tube of 3/8-in. diameter copper tubing and a threaded brass fitting with rubber seals. The fitting was designed to be nearly flush with the inside wall of the flume to minimize disturbance to the flow. An O-ring seal was used between the copper tube and the barrel of the fitting to prevent leakage and provide friction to hold the tube in any desired position. Each fitting was designed with threads in the outside portion of the barrel so that a plug could be inserted when the probe was removed. The end of each tube was bent 1-1/2 in. upstream and the outside wall of the tube was beveled at the end to minimize turbulence. Probes were installed on 3-in. vertical spacing at five cross sections. Since the probe could be rotated so that the end would sweep through a 3-in. vertical distance, the concentration at any depth could be determined.

The settling tube used was a 3-3/4 in. diameter lucite tube 10 ft long with sampling outlets spaced at 1-ft intervals throughout the length (see Figs. 10.2 and 10.4). The sampling outlets were 1/4 in. inside diameter copper tubing with the end terminating at the center of the settling tube (see Fig. 10.3).

10.2 Procedure

In order to determine the amount of removal that had occurred at any section throughout the length of the flume, it was necessary to find the concentration profile at that section. To do this samples were taken from the concentration probes at 3 or 4 cross sections in the flume. At each section 250-ml samples were taken at 3 or 4 levels throughout the depth of flow. No samples were taken below a depth 1-1/2 in. above the flume floor because the level of the sludge bed sometimes reached this height. Inasmuch as the concentration at any level was not constant across the section, the sampling probes were moved continuously so as to traverse the flume in order to obtain an average lateral concentration. All samples were filtered through Gooch crucibles, dried, weighed and the resulting concentration profile was plotted for each section.

For settling velocity analyses of the flume suspension samples were taken from various points in the cross section through the probes. Two methods were used to transfer the suspension from the flume to the settling tube. The first procedure used was simply to transfer the suspension into a clean glass jar and pour it into the tube. This proved unsatisfactory because the floc was completely broken up when the suspension was poured from the top of the 10-ft tube. In the other method, which proved more satisfactory, the suspension was drawn from the flume into the tube by creating a vacuum in the top of the tube. By regulating the aspirator, the amount of vacuum and therefore the rate of flow of the suspension could be controlled. After the tube was full the suspension was mixed either manually by stirring or by allowing bubbles to rise under vacuum from the bottom outlet. The latter method proved more satisfactory but still caused a considerable amount of the floc to break. Settling analyses of control suspensions (made by diluting floc from the turbulence jar with water) were also performed for comparison with the flume suspension.

The settling analysis procedure and calculations are outlined in Appendix A, p. 24.

10.3 Results

A nine-point lateral concentration profile of a typical run is shown in Fig. 10.5. The profile was taken at a depth of 4-1/2 in. above the flume floor at a distance of 46 in. from the floc injectors. The velocity during the run was .084 fps which resulted in a relatively low removal of 28.7%.

The concentration distribution shown in Fig. 10.6 is for a flume velocity of .056 fps with a resulting removal of 82.6%. Each series of 3 bars represents the concentration at the depth of the center bar at 3 points across the section. The top bar represents the concentration at a distance 6 in. to the left of the centerline, the middle bar at the centerline, and the bottom bar at a distance 6 in. to the right, all at the same depth.

A concentration profile for a high velocity run is shown in Fig. 10.7. For this run the flume velocity was .092 fps with a removal of 3.6%.

A plot of concentration vs. height above the flume floor for 3 sections downstream from the floc injectors is shown in Fig. 10.8 for a run similar to those of Figs. 10.6 and 10.7 with a velocity equal to .076 fps. Sections 1, 3 and 5 are respectively 1 ft 10 in, 5 ft 10 in. and 11 ft 10 in. downstream from the floc injectors. The particle flow rate is calculated from the area under the curve which is above a height of 1-1/2 in. assuming a uniform velocity distribution across the section.

A summary of the concentration probe studies is shown in Fig. 10.9. This figure shows the variation in particle flow rate with distance downstream from injectors as a function of the velocity in the flume.

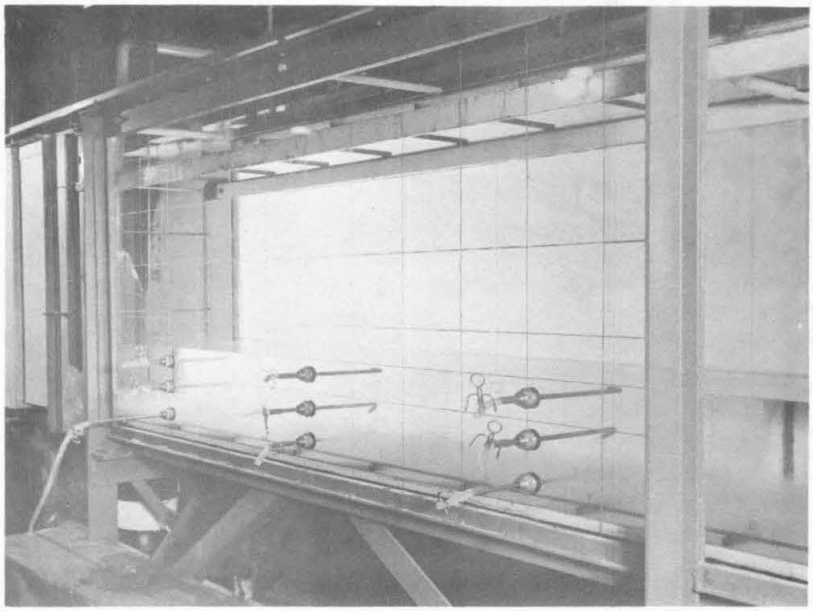

Fig. 10.1
FLUME WITH CONCENTRATION PROBES

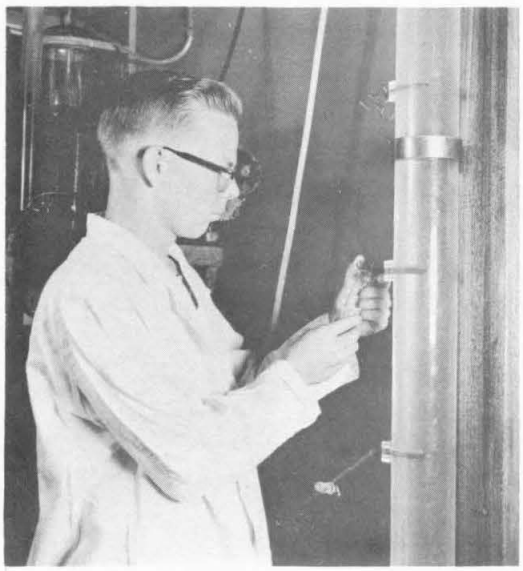

Fig. 10.2
SAMPLING FROM SETTLING TUBE OUTLET

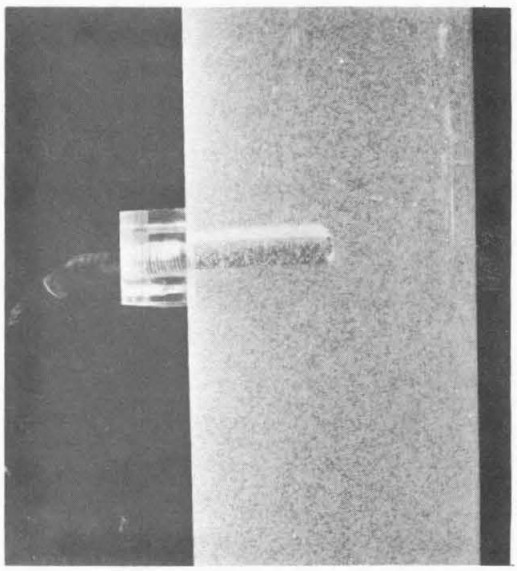

Fig. 10.3
FLOCCULATION IN SETTLING TUBE
1-1/2 hours after filling
(Note deposit on sampling outlet tube).

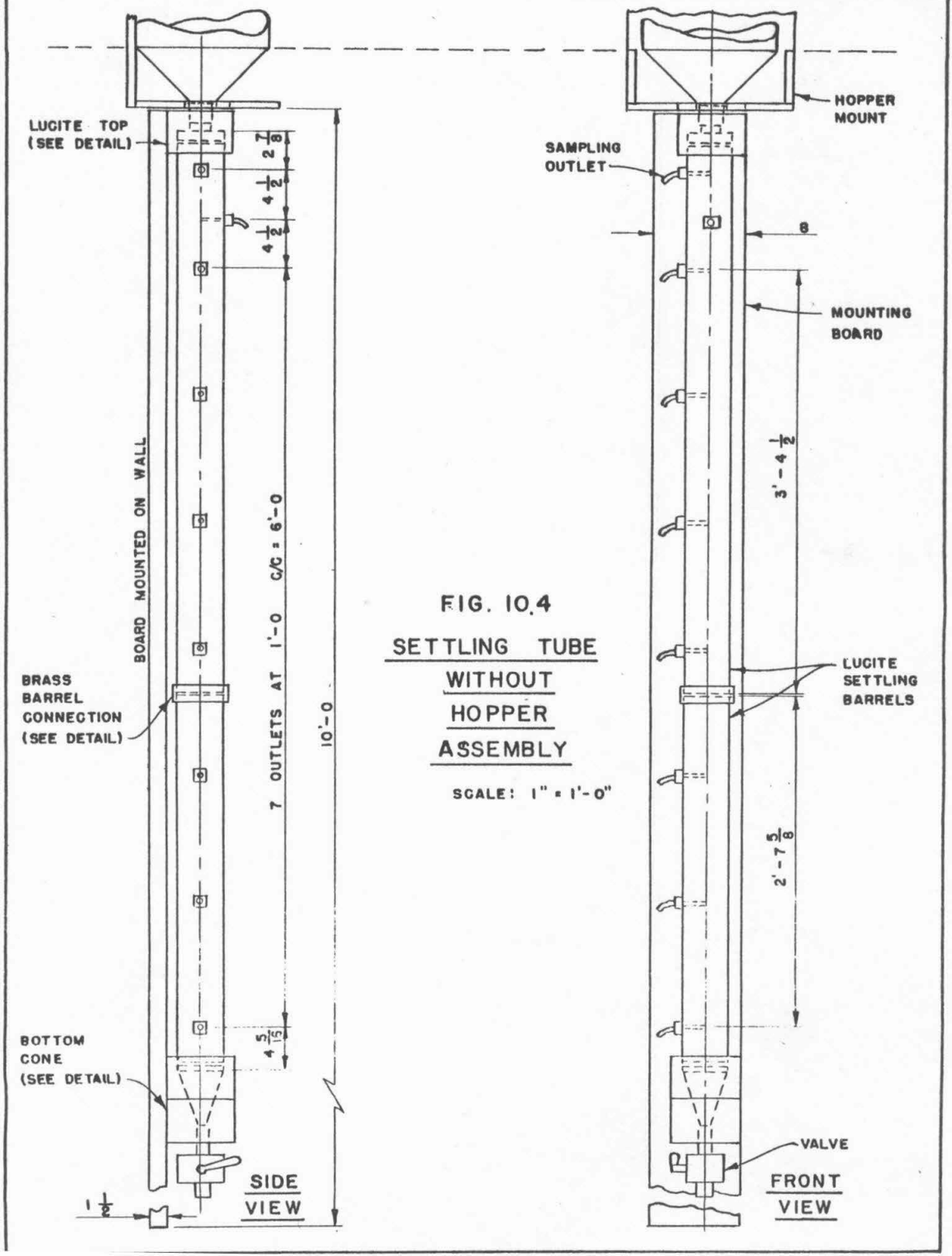

FIG. 10.4

SETTLING TUBE WITHOUT HOPPER ASSEMBLY

SCALE: 1" = 1'-0"

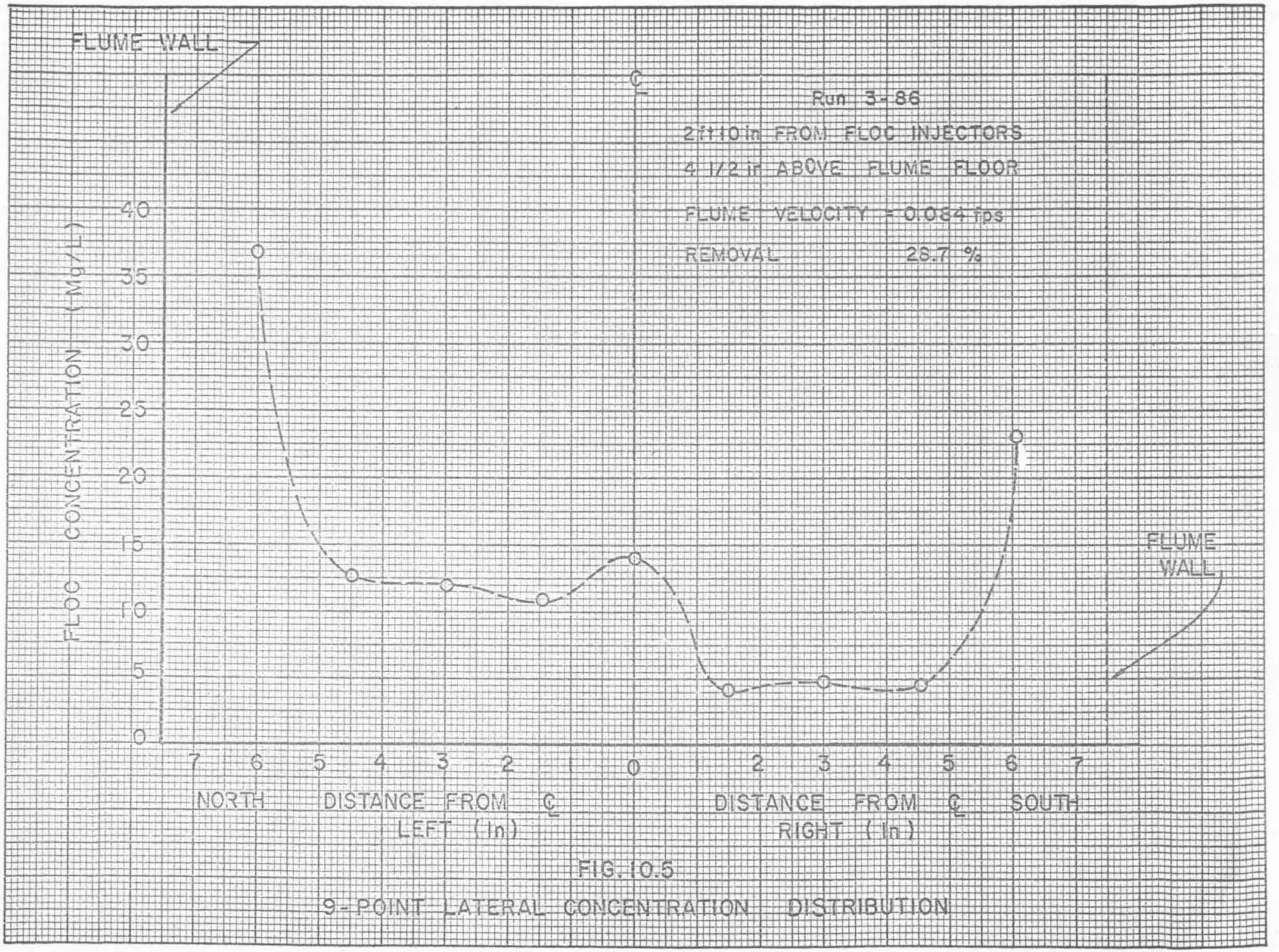

FIG. 10.5

9-POINT LATERAL CONCENTRATION DISTRIBUTION

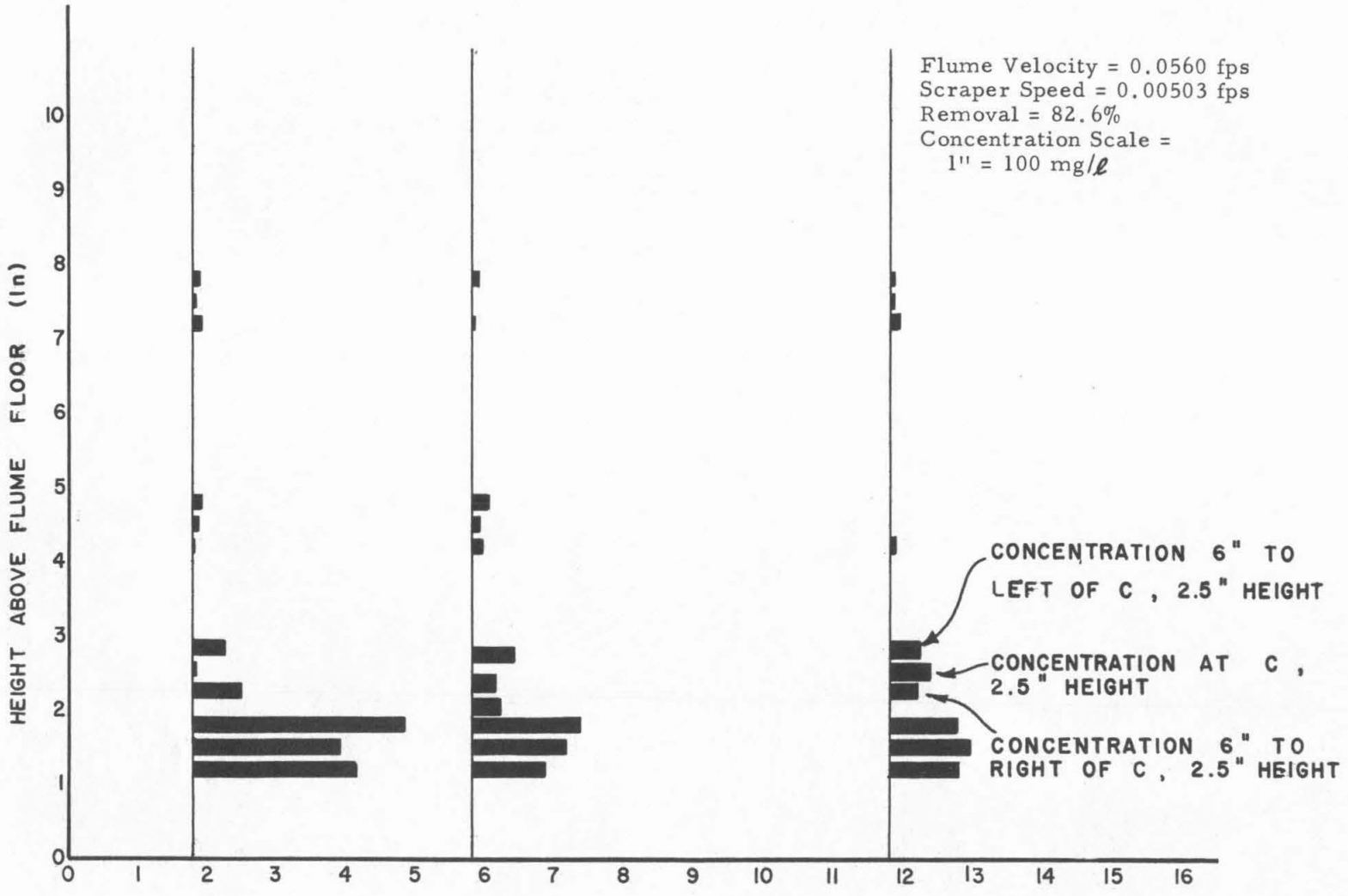

FIG. 10.6

CONCENTRATION PROFILE, Run 3-85

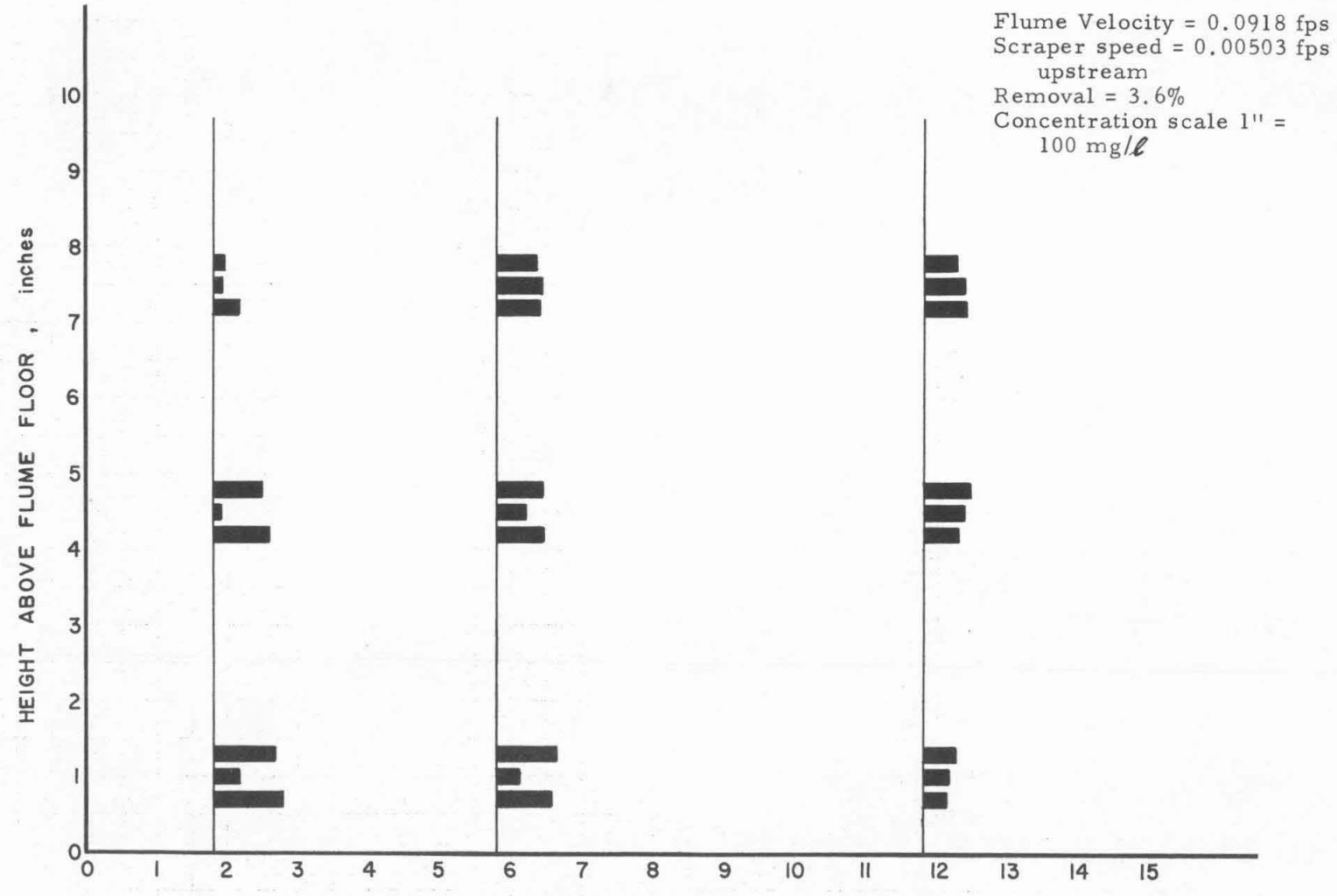

FIG. 10.7

CONCENTRATION PROFILE , Run 3 - 83

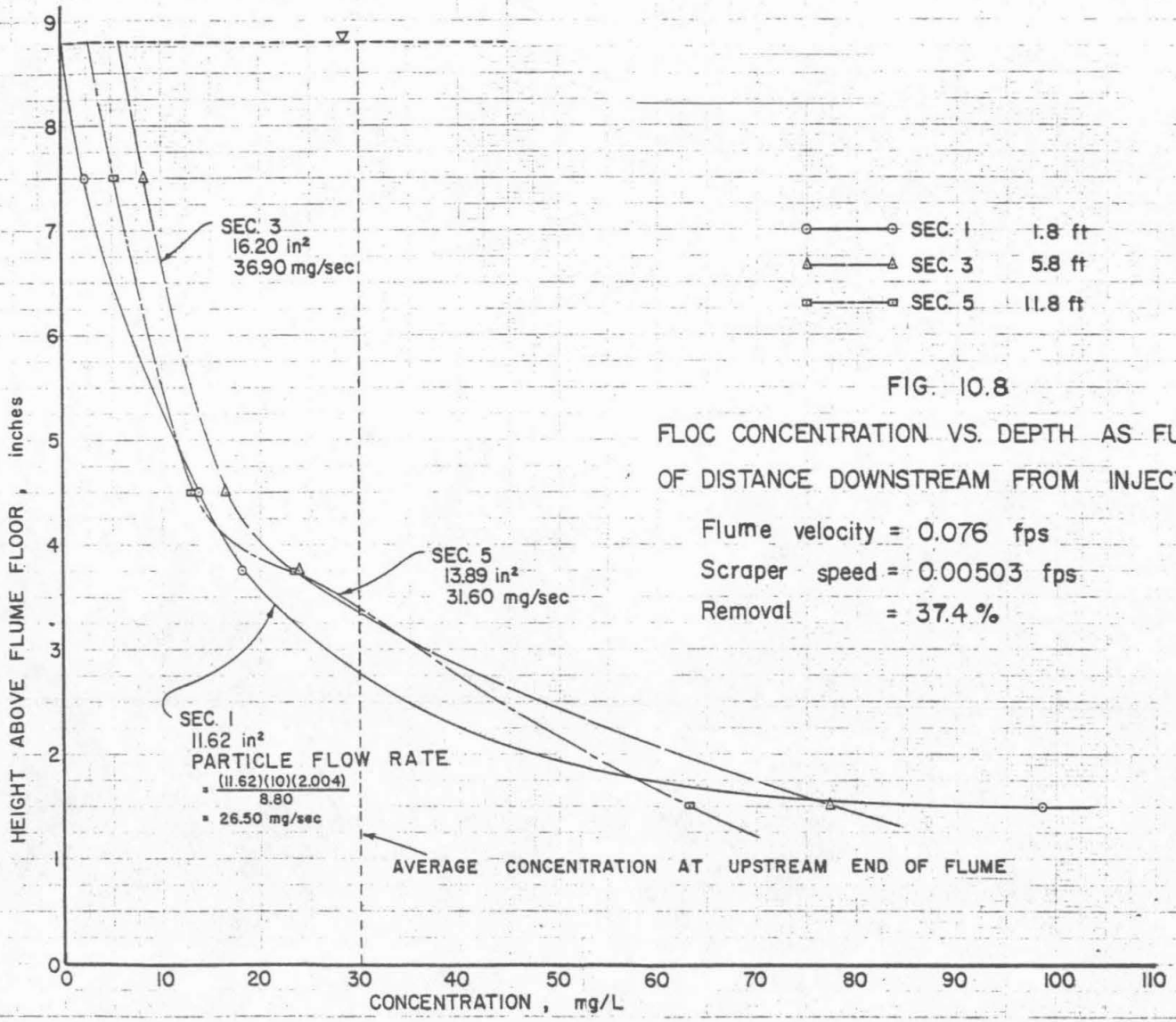

FIG. 10.8

FLOC CONCENTRATION VS. DEPTH AS FUNCTION OF DISTANCE DOWNSTREAM FROM INJECTOR

Flume velocity = 0.076 fps
Scraper speed = 0.00503 fps
Removal = 37.4 %

FIG. 10.9

SUMMARY OF VARIATION IN PARTICLE FLOW RATE WITH DISTANCE FROM INJECTOR AS FUNCTION OF VELOCITY

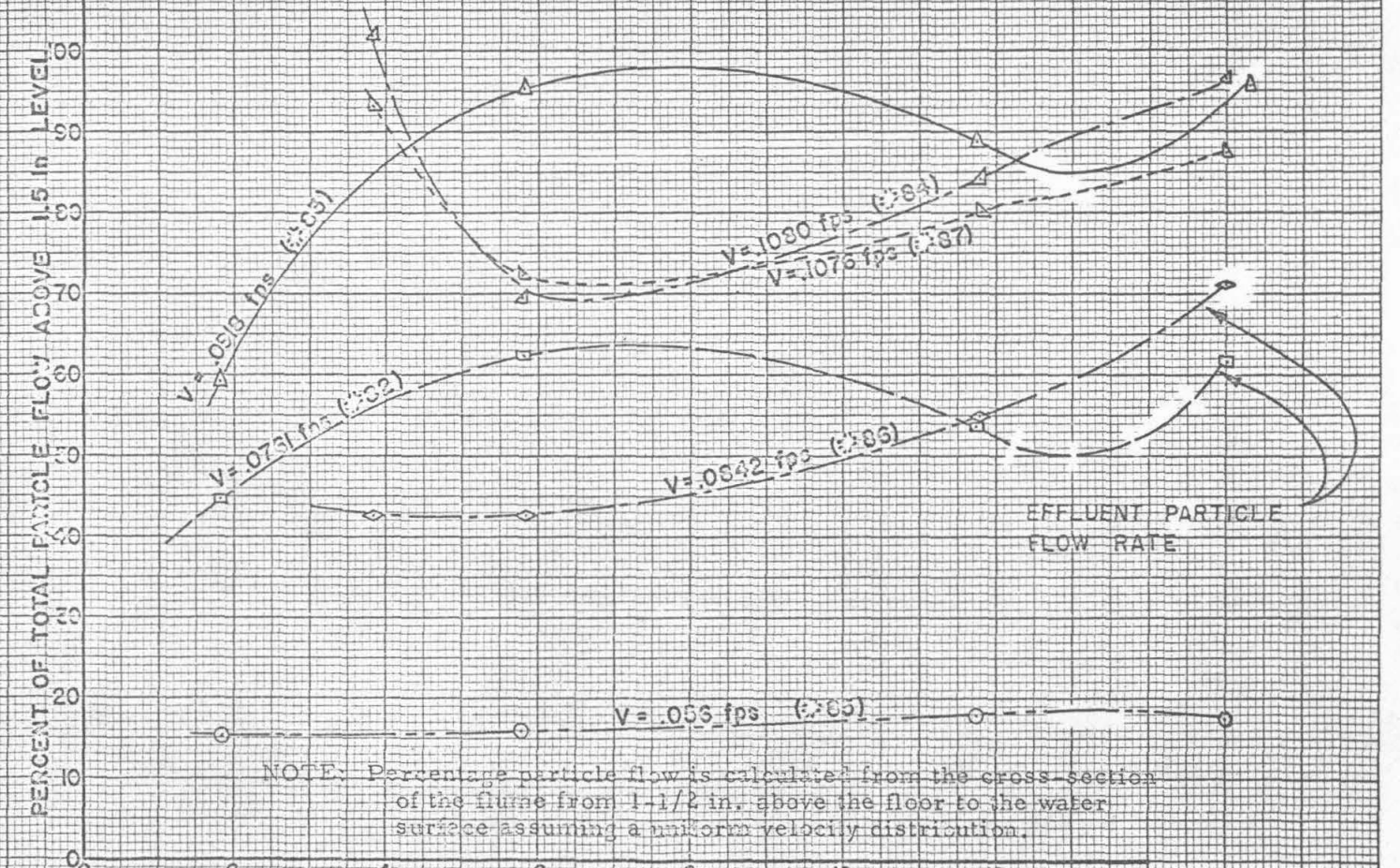

NOTE: Percentage particle flow is calculated from the cross-section of the flume from 1-1/2 in. above the floor to the water surface assuming a uniform velocity distribution.

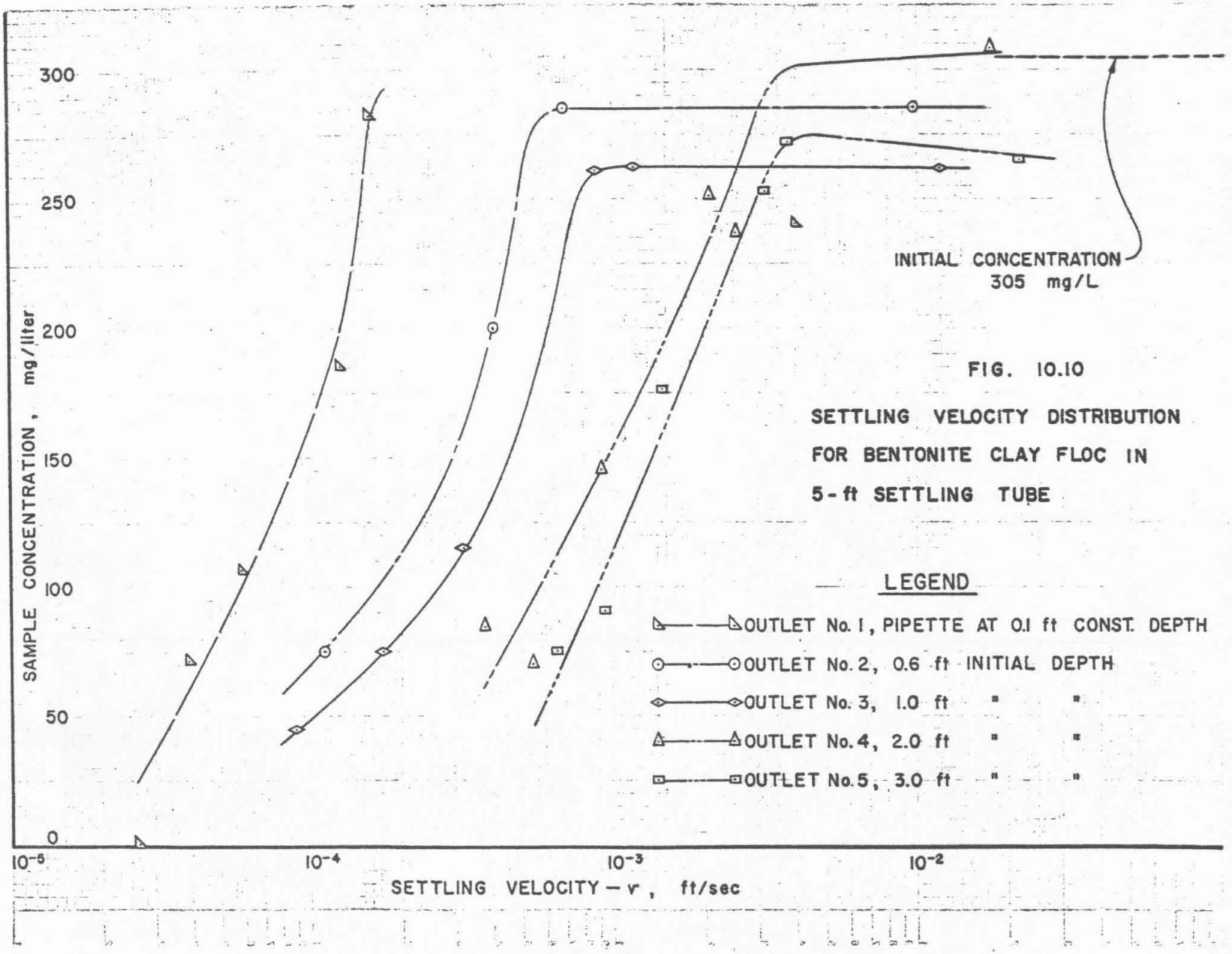

FIG. 10.10

SETTLING VELOCITY DISTRIBUTION FOR BENTONITE CLAY FLOC IN 5-ft SETTLING TUBE

Fig. 10.11

SETTLING VELOCITY ANALYSIS OF FERRIC CHLORIDE BENTONITE CLAY SUSPENSIONS USED IN FLUME

Composite sample was drawn from probe 22 in. downstream from floc injector and 1-1/2 in. above floor.

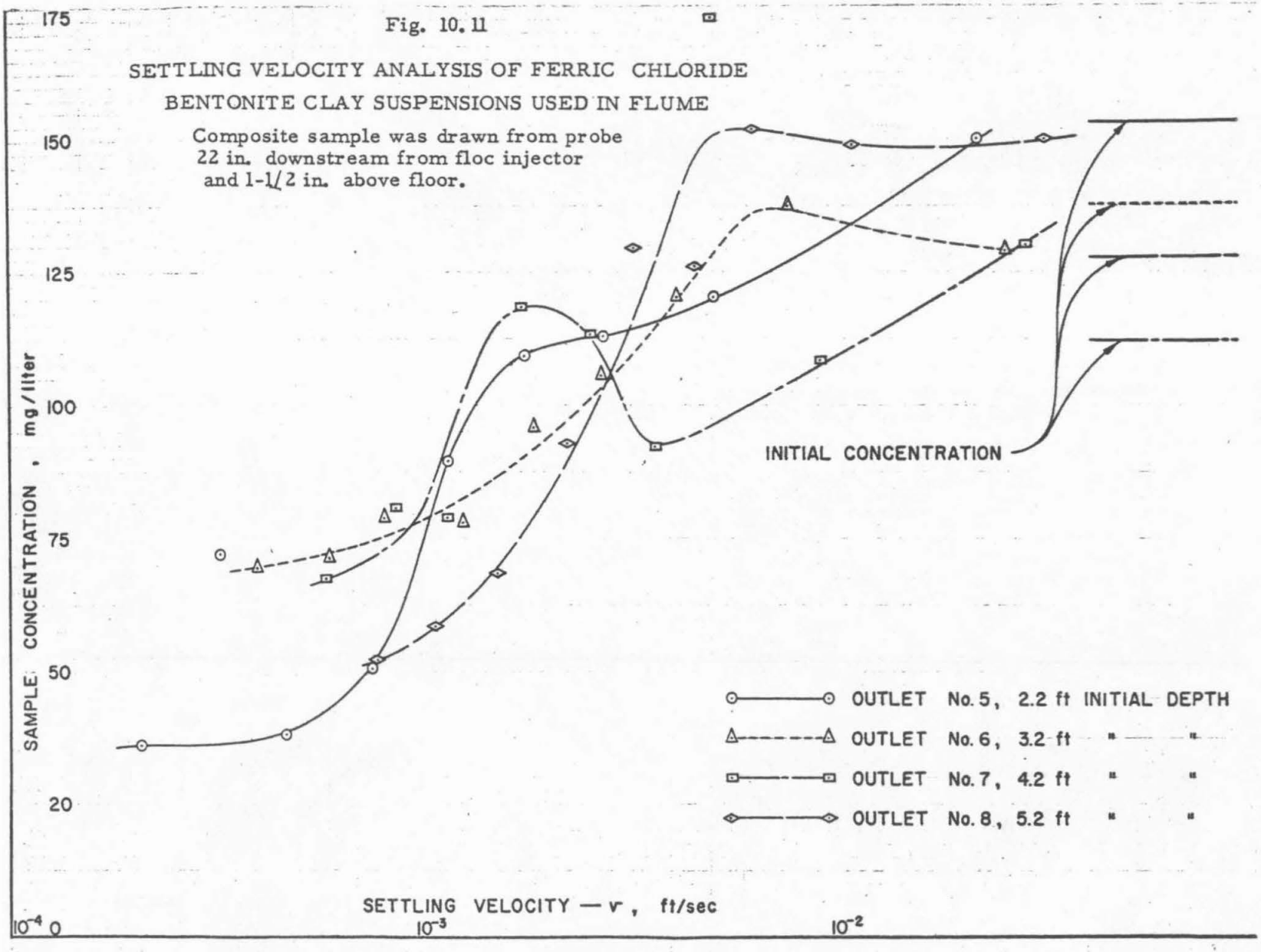

The results of a settling analysis on a suspension consisting of a mixture of floc and Pasadena tap water is shown in Fig. 10.10. The floc had a concentration of approximately 3.2 g/l and was mixed with water in a ratio of 1:31 giving a suspension concentration of approximately 300mg/l.

A settling velocity distribution for a suspension taken from the flume during a typical run is shown in Fig. 10.11. The settling tube was filled using a vacuum as described in Section 10.3 and was allowed to stand 2 hr. before the test was started. Figure 10.2 shows the sampling procedure and the extent of flocculation in the settling tube immediately after filling and Fig. 10.3 shows the extent of flocculation 1-1/2 hr. after filling.

10.4 Discussion

The lateral concentration profile shown in Fig. 10.5 is typical of the profiles obtained in most of the tests. Examination of the plot shows that the concentration near the walls of the flume is much larger than that across the center of the section. A possible explanation for this may be found in the high draft into the tube that occurred during sampling. Because of the extremely low flume velocities that occurred, it was impossible to adjust the velocity in the sampling intake to that in the flume. It was also observed that in most runs, the amount of deposition on the flume floor was greater near the walls than in the center (probably owing to the higher velocity near the center). It is therefore possible that because of the high draft some of the particles that had settled near the wall were drawn into the sample. These results leave much to be desired and further investigation of this subject is necessary before any certain explanations can be made.

The longitudinal concentration profiles shown in Figs. 10.6 and 10.7 show the effect of increased velocity on the concentration at various depths in the flume. It can be seen that for a velocity of .056 fps (Fig. 10.6) the concentration near the water surface is almost negligible compared to the concentration near the bed whereas for a velocity of .092 fps the concentration is nearly constant throughout the depth of the section. This indicates that for high velocities the turbulence and resuspension is sufficient to keep the particles dispersed throughout the section. It should be noted that the floc was injected at a depth 3 in. above the flume floor and in order to have a large concentration near the surface as in the high velocity run, the floc would have to be carried upward by turbulence and diffusion. For the low velocity run it is seen that the majority of the particles have settled in the first 1 ft 10 in. of the flume.

It can also be seen in Figs. 10.6 and 10.7 that for most cases the middle bar of each series of 3 bars is shorter than the other two, indicating a lower concentration at the center of the flume. This corroborates the results of the lateral concentration profile shown in Fig. 10.5.

The concentration profiles shown in Fig. 10.8 are for a relatively fast run (.076 fps). It should be noted that although the sections 1 and 3 are progressively farther downstream from the inlet, the particle flow rate through each section does not decrease as would be expected. The particle flow rate is seen to have decreased between sections 3 and 5 as expected. It is reasonable to assume that the first section (1 ft 10 in. from the floc injectors) would be low since the floc was injected 3 in. above the flume floor and had not dispersed at the time it reached section one. This was observed in the flume in that at this velocity, the floc remained relatively low in the flume until it reached the scrapers where it began to rise and disperse throughout the section.

Inasmuch as the particle flow rate was calculated only for the area of the section above 1-1/2 in. from the floor, any particles flowing downstream below this level would not be included. In Fig. 10.8 it is seen that the concentration at section 1 at a depth of 1-1/2 in. is increasing with depth at a much faster rate than is the concentration at either section 3 or section 5. If the particle flow rate were calculated using the area for the section above 1 in. or 3/4 in. from the flume floor, the rate for section 1 would be considerably increased and a satisfactory distribution which decreased with distance from the injectors would probably result. Also, as pointed out in section 9.5 the floc traveled down the flume in clouds and it is unlikely that the samples taken at any section were truly representative of the time average concentration at that section.

The distribution of particle flow rate throughout the flume for 6 runs at different velocities can be seen in Fig. 10.9. Again, some of the discrepancies must be attributed to the floc clouds which traveled down the flume. For instance, Run 86 (.0842 fps) shows a large increase in particle flow rate from the center of the flume to the end of the working section. Run 82 (.076 fps) and Run 83 (.0918 fps) show a decrease over the same interval even though the velocities are near that of Run 86. It is seen that the particle flow rate distributions for runs of high velocity are radically different from those of the other runs. Two runs of nearly the same velocity show nearly identical results indicating that experimental error is probably not the cause of the different shape of the curves.

A possible explanation for the shape of the distribution curves for different velocities can be shown with the aid of Fig. 10.12.

Fig. 10.12 Particle Distribution in Flume

Consider a steady state condition in which a removal of 30% is obtained. In this case 70% of the incoming particles are being removed from the flume in the effluent and 30% are being discharged through the sludge hopper. For the steady condition there must be a net flow of 70% of the incoming particles at any section downstream from the hopper. The scraper load varies as the scraper moves upstream depending on the velocity and the rate of resuspension.

In Fig. 10.12 the scraper load is shown as the bottom portion of the distribution curves for each section and represents the amount of particles moving upstream. The upper portion of the curves represents the per cent of particles still suspended in the flow and moving downstream. Assume that the scraper load increases by 10% at each section as it progresses upstream from the effluent end of the flume. For this case the suspended material would have to increase by 10% at each section in order to maintain a net flow of 70%.

Starting at the end of the flume at section 8, we know that we have 70% of the total particle flow moving out the effluent. At section 7 the scraper load has increased to 10% and therefore the particles in suspension must have increased by 10% to 80%. This same condition holds for sections 6, 5, 4 and 3 in which the scraper load increases by 10% at each section and therefore the particles in suspension above the load must increase by 10% in order to have a net flow of 70% downstream. It has been observed that the turbulence in the flow near the inlet is considerably greater than that in the remainder of the flume and that resuspension from the scraper crests is greatest near the inlet. At section 2, where the scraper load has reached 50%, the turbulence caused by the inlet conditions becomes effective and the scraper load may start to decrease from 50% to perhaps 40%. The same thing could occur between sections 2 and 1 where the scraper loses another 10% with a resulting flow into the hopper of 30% which constitutes the net removal.

Thus it can be seen that it is possible for the per cent of total particle flow in suspension to become greater than 100% at some section in the flume. This may be an explanation for the rise in the particle flow curves at the center sections as shown in Fig. 10.9. Since the turbulence decays more slowly with increase in velocity, the section of maximum particle flow would be expected to move farther downstream with increase in flume velocity. This is not observed in Fig. 10.9, however, where an increase in velocity caused a marked decrease in the particle flow rate at the center section. For Runs 82 and 83 the increase at the center sections is as expected. Run 85 is a low velocity run in which inlet turbulence was not significant and therefore the particle flow rate shows no increase in the center sections.

It should be noted that for all the runs the curves have a positive slope from the section 12 ft from the injectors to the effluent outlet. This can be explained by the fact that the particle flow rate is calculated for the section above a height of d = 1-1/2 in. (see Fig. 10.12) and any particles flowing downstream past a section below this level would not be included. The effluent particle flow rate was calculated on the basis of total removal and is not subject to this error. Thus for section 8 of Fig. 10.12 there must be 70% flowing downstream past the section but perhaps only 50% would be included in the calculation of flow rate if the reference level were sufficiently high.

A change in the reference level to 1 in. or perhaps 3/4 in. above the flume floor would change the shape of the curves in Fig. 10.12 considerably. The particle flow at the upstream sections would be increased as would the particle flow at sections just upstream from the effluent outlet. This would in a sense flatten out the curves to a more reasonable shape.

The settling velocity distribution shown in Fig. 10.10 is typical of most of the tests run on laboratory prepared flocculent suspensions. It can be seen that after the first 3 or 4 measurements (i.e. at the top of the plot) the curves show that the settling velocity increases with depth for any given concentration. This shows the effect of flocculation on the particle size and therefore on the settling velocity. For example, at a concentration of 50 mg/l the settling velocity at a depth of 0.1 ft below the surface is 3.5×10^{5} fps while at a depth of 3.0 ft the settling velocity is 5.7×10^{4} fps.

For a well behaved velocity distribution for a flocculent suspension, the curves for each outlet should not cross. That is, for any concentration, the settling velocity at any depth should be lower than the settling velocity at any greater depth. For a discrete suspension, however, the curves for any depth should coincide since the particle size does not change with depth (see T. R. Camp, Ref. 2, Fig. 6). The fact that the curves cross for the test shown in Fig. 10.10 can be attributed to mixing procedures and unsteady conditions in the tube. At the end of the mixing period it is possible that some of the floc was broken up at different sections of the tube which would result in an erratic settling velocity distribution for the early measurements.

It is difficult if not impossible to determine reasons for the erratic results of settling velocity analyses run on suspensions taken from the flume. A typical example as shown in Fig. 10.11 reveals very little about the settling properties of the suspension. Although there are some anomalies in the tests run on laboratory prepared suspensions, these are greatly compounded and magnified in runs on floc taken from the flume. Figure 10.12 shows no consistent relation between the relative settling velocities at different depths nor does it give any idea of the effect of flocculation on settling behavior. It should be pointed out also that the results shown in Fig. 10.11 are for one of the better tests and results obtained for other tests were considerably less informative. It seems clear that between the mixing jar and the settling tube, that is, in getting the floc into the flume and the sample out of it, the floc particles are badly broken up and disturbed so that their settling behavior is adversely affected. Unfortunately it is not possible to tell whether the floc is broken up more by entering the flume through the injector tubes or by leaving it through the sampling tubes.

Chapter 11

FLUME STUDIES WITH MULTIPLE INCLINED BAFFLES

From the time of the tests on the baffled and straight tanks at the Los Angeles County Joint Disposal Plant in 1956, it was planned to try out baffles on the laboratory tank. It was believed that the poor results on the full-scale tank may have been due principally to the wide spacing between baffles and to the fact that they did not extend sufficiently close to the surface of the flow. At the very end of the project, therefore, time and materials were found to construct a set of baffles in the laboratory flume. The following sections describe the baffled flume and the studies conducted upon it.

11.1 Description of Equipment

The baffles used were constructed according to a suggested design by Ingersoll, McKee and Brooks (see Ref. 1.1) and installed on a 3 to 1 slope away from the feed end at 2 in. intervals throughout the 12-ft working section of the flume (see Fig. 11.1). The tops of the baffles were 8-1/2 in. above the flume floor and the water level was maintained at approximately 6 in. above the baffles by adjusting the sloping outlet weir (see Fig. 6.1). The bottom of the baffles was 3/4 in. above the floor of the flume to allow the scrapers to move. The baffle material was .020 in. polished aluminum.

The same floc and the same procedure as described in Chapter 9 were used for this study. For these tests, however, the floc was introduced upstream from the inlet screen rather than downstream as in previous runs studies. When the floc was injected downstream from the inlet screen as in previous tests on the unbaffled flume, it was found that none of the floc would flow over the first baffle (see Fig. 11.1). This occurred because the velocity in the approach section had to be very low in order to obtain a reasonable velocity over the baffles and the floc was settling before it reached the baffles. When, in order to correct this condition, the floc was injected upstream from the inlet screen and the water level raised, the turbulence dispersed the floc throughout the section (see Fig. 11.2). It was found, however, that at high velocities the floc was broken up to a large extent when passing through the screen.

11.2 Results and Discussion

The comparative performance of the flume with and without baffles is shown in Fig. 11.3. This figure gives the comparison based on net flume flow and on the velocity in the free depth.

These curves show that the per cent removal is not increased by the addition of baffles, and in fact it is substantially decreased for higher flow rates. For flows less than about 0.8 l/sec the performance of the flume with and without baffles is not changed appreciably. The fact that the curves shown are based on relatively few tests prevents explicit observations in this range of flows. For higher flows, however, the

removal performance of the baffled tank drops considerably faster than that of the unbaffled tank. This can be attributed to two factors. First, with increased flow and therefore increased velocity, the formation of eddies on the crests of the baffles is greatly enhanced. These eddies prevent the floc from settling into the quiescent zone below the crest of the baffles and therefore a lower removal results. Second, increased velocity resulted in the breaking up of the floc as it passed through the inlet screen, which decreased the particle size and therefore lowered the removal. If the latter consideration is predominant, the lower removal of the baffled flume at high flow rates cannot be attributed to poor performance of the baffles.

It can be seen that for a given velocity, either above the baffles or in the full depth without baffles, the removal in the baffled tank is considerably greater than that in the unbaffled tank. This indicates that the effect of the quiescent zone created by the baffles is quite helpful in increasing the removal. A comparison of removal based on velocity, however, is not practical. To achieve the same velocity in the baffled and unbaffled tank, the flow rate in the baffled tank would have to be half as large as that in the unbaffled tank of the same depth.

The results of these tests agree quite well with those obtained from tests on baffled settling tanks of the Los Angeles Joint Disposal Plant (see Sec. 3.1) where it was found that the baffled tank would require twice the length of the straight rectangular tank to achieve the same removal. It should be pointed out that the tests made at the Los Angeles Joint Disposal Plant and in the laboratory are for particular baffle designs and cannot be considered indicative of the performance of any type of baffles used. Further investigation of baffles with different spacing, slope and height should be made before they can be ruled out as a means of increasing the efficiency of settling tanks.

These results do not agree with those obtained by Mr. Hayden using ore slimes in which he found that performance was increased 40% by the use of baffles. Ore slimes as used by Hayden consisted of 2% by weight of granular sand, silt, and colloids in mechanical suspension in water. By comparison, the suspension used in the flume studies consisted of approximately .003% by weight of bentonite clay floc. The settling velocities of the particles in the suspension used by Hayden based on unhindered settling were below .032 fps whereas in the flume suspension the average settling velocity was approximately .003 fps (see Fig. 10.10). It is probable that with particles with such large settling velocities as compared to those in the flocculent suspension, the turbulence caused by the eddies forming on the crest of the baffles does not affect the settling to any large extent. It has been observed in the flume that with flocculent suspensions, the particles are lifted from the quiescent spaces by the eddies in much the same way as the particles are resuspended from the bed in an unbaffled tank with scrapers. It may well be that with further studies, a design can be found which will minimize the effect of the eddies and possibly increase the removal of baffled tanks over straight rectangular tanks.

Although the results obtained to this point on baffles are not encouraging, there are possible avenues for further research. One approach

which has been suggested is to curve the tops of the baffles downstream in order to minimize the opportunity for flow separation and eddy formation.

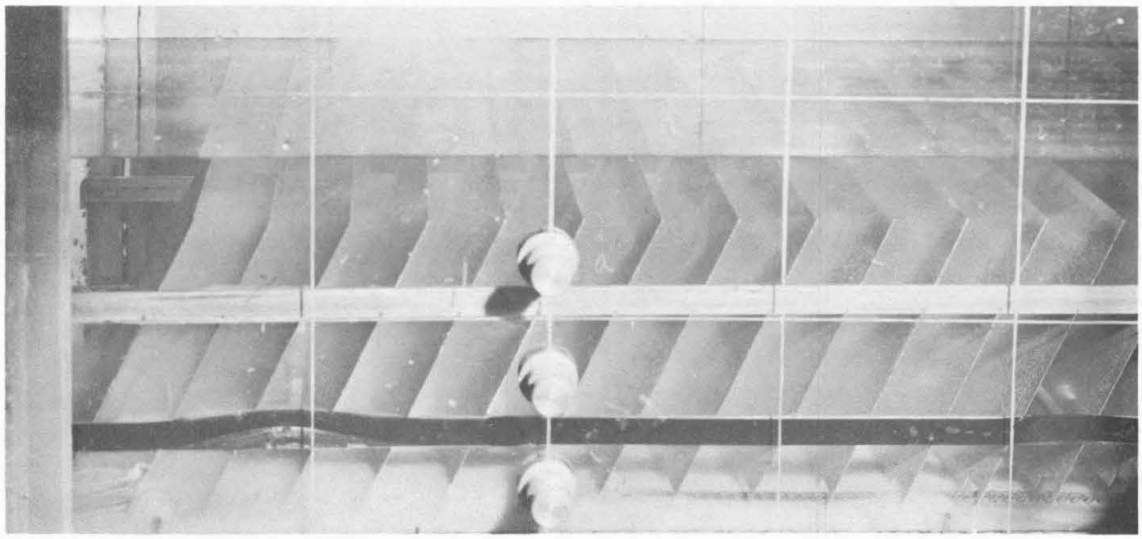

Fig. 11.1

BAFFLED FLUME
(floc injected downstream from inlet screen)

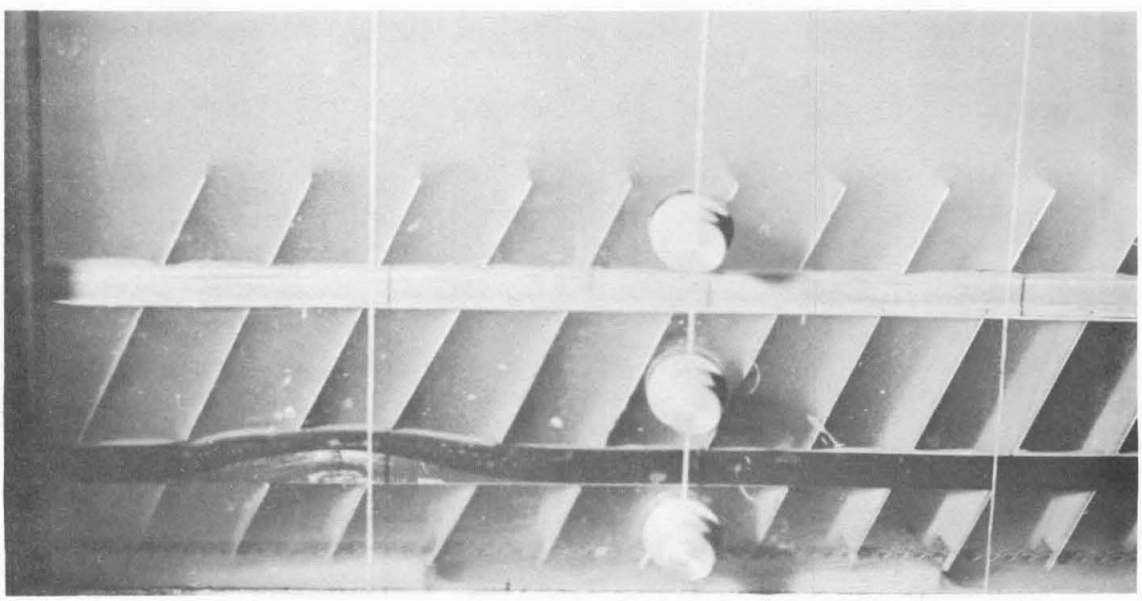

Fig. 11.2

BAFFLED FLUME
(floc injected upstream from inlet screen)

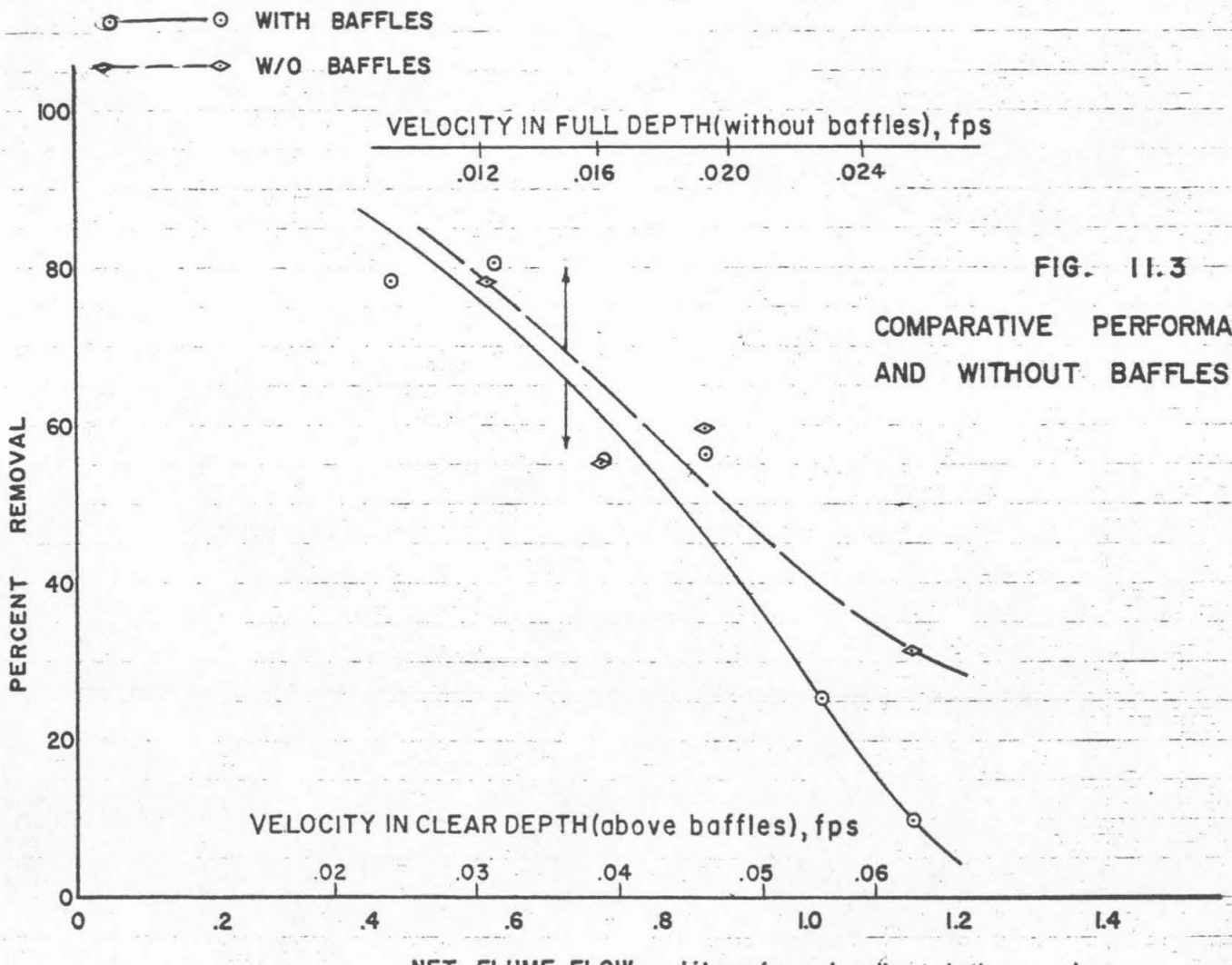

FIG. 11.3

COMPARATIVE PERFORMANCE WITH AND WITHOUT BAFFLES

Chapter 12

SUMMARY AND CONCLUSIONS

This four-year project on the resuspension of flocculent solids in sedimentation basins has resulted in a few concrete results, many speculations, and a few frustrations. Scientifically, the most important results are embodied in the fundamental studies on the settling properties of suspensions, reported in Appendix A. Here the junior author has demonstrated that a multiple-depth pipette analysis can be used to study the effect of hindrance, flocculation, and turbulence on settling, and can be used to calculate expected removal whenever the settling in a flowing suspension can be approximated by settling in a quiescent or turbulent settling tube.

The conclusions to be drawn from the remaining parts of the investigation, conducted on prototype settling basins and on the laboratory test flume, may be summarized as follows:

1. From the tests run on parallel primary settling tanks at the Los Angeles County Joint Disposal Plant - one standard and one modified with sloping baffles - the baffled tank was shown to have a higher average concentration of both settleable and suspended solids throughout its length than had the straight rectangular tank. This failure of the baffled tank to perform as well as the straight tank, not to say to surpass it, was believed to be due principally to the wide spaces between the baffles, in which eddies could form and prevent particles from settling quietly.

2. The performance tests in Unit No. 4 of the Joint Disposal Plant demonstrated that the conventional measure of total or integrated efficiency is meaningless for the settling tank receiving a flocculent suspension, as the values came to well over 100% in all cases. Newer measures of performance, the overflow residual efficiency and the effluent overflow efficiency, show much promise in evaluating the behavior of settling basins receiving flocculent suspensions.

3. Preliminary tests on Basins Nos. 1 and 3 of the Imperial Desilting Works at the entrance to the All-American Canal on the lower Colorado River indicated that the performance of the basins was far from satisfactory. In fact, for much of the distribution of the suspension, the concentration in the effluent was higher than that in the influent, while the overall removal for one basin was but 8.5%.

4. The most satisfactory suspension of discrete or non-flocculent particles for laboratory experiments in settling was found to be gilsonite (specific gravity 1.04), crushed manually and screened mechanically into sieve fractions varying from 0.0116 to 0.0328 inches in particle size. The most satisfactory flocculent suspension was an artificial floc made of ferric chloride in a bentonite clay suspension.

5. Tests for critical velocity required for entrainment of particles from a smooth bed showed that fine light particles are more easily lifted from the bed than was previously supposed by Shields and other workers in this field.

6. Tests in the laboratory flume fitted with scrapers showed that with a gilsonite bed prepared in advance, the concentration of gilsonite in the effluent varied positively with the displacement velocity and also with the amount of gilsonite remaining in the flume.

7. For two sizes of gilsonite tested it was found that the critical velocity for initial movement along the bed against the upstream movement of the scrapers was from 10.5 to 14.5 times the settling velocity of the particle.

8. Utilizing continuous injection of gilsonite into the flume, it was found possible by stopping the movement of the scrapers to double the displacement velocity and hold to the same deposition of gilsonite on the floor.

9. While for a discrete suspension the average particle size (resulting from continuous injection) on the bed ordinarily decreases in the downstream direction, it was found that for a flocculent suspension the particle size may stay nearly constant or increase in the downstream direction, owing to the increased time and opportunity for contact.

10. As the mean velocity was increased in the laboratory flume receiving a flocculent suspension, the percentage removal remained constant up to a point and then dropped sharply, indicating the commencement of resuspension. This critical velocity was directly affected by the movement of the scrapers. The slower the scraper movement the higher would be the critical velocity. Likewise, with continuing increase in velocity, the removal for the higher scraper speeds dropped more rapidly than it did for the lower (including zero) speeds.

11. Measurements of floc concentration within the flume revealed a concentration near the walls which was two or three times the concentration near the center. Further, the average influent concentration was found to exist at heights between 2.8 and 3.3 in. (about one third the depth) above the flume floor for three sections covering the length of the flume. Above this height the concentration was lower, while below it was higher.

12. While the settling analyses of bentonite-clay floc samples drawn from the mixing jar exhibited surprisingly regular characteristics, analyses of similar samples drawn from the flume showed very erratic characteristics, probably owing to the disturbance and breaking of the floc entering the flume or leaving it through the sampling tubes.

13. With the application of sloping baffles to the laboratory flume it was found that for a given velocity in the clear water depth (either above the baffles or in the full depth without baffles) the removal in the baffled tank was considerably greater than that in the unbaffled tank. Based on corresponding overflow rates (flow divided by surface area), however, the baffled tank was no match for the unbaffled one of the same total depth, since the velocity above the baffles was necessarily increased by the reduction in cross section caused by the baffles. Thus, the laboratory tests agreed well with those made on the full-size tanks at the Joint Disposal Plant referred to in Item No. 1 above.

It may be remarked finally that although it may appear that the experiments reported in Chapters 7 through 11 were conducted on a "model settling tank", they cannot be considered as true model settling studies for several reasons. Inasmuch as both gilsonite and ferric chloride floc are close to sewage in settling velocity, the laboratory flume studies correspond to the second case cited in Conclusion No. 6 of Appendix A, wherein the prototype suspension settles in the model. The settling properties of the suspension are studied separately and they are considered in using the model results to predict prototype results. Furthermore, some of the physical features of the laboratory flume are not related to any common settling tank. The inlet and outlet arrangements, for example, do not represent a practical design for a full-scale tank. The experiments must therefore be considered purely as laboratory studies of resuspension, and not as model studies. It is hoped, however, that the results of these studies will indeed be useful in the design of settling tanks.

Journal of the
HYDRAULICS DIVISION
Proceedings of the American Society of Civil Engineers

THE SETTLING PROPERTIES OF SUSPENSIONS

Ronald T. McLaughlin, Jr.,[1] A. M. ASCE

ABSTRACT

This paper contains the results of an analytical and experimental investigation of the settling properties of suspensions of particles in fluid. The use of these properties in predicting the sedimentation of the particles is outlined.

1. INTRODUCTION

In many engineering problems it is necessary to deal with a flowing fluid in which particles are suspended. The engineer commonly encounters such problems in river channels, in water and sewage clarification, in reservoirs and in the delta regions of rivers. One of the tasks associated with these problems is to determine how much material will settle out of suspension and where that material will settle.

The factors that affect the settling of suspended particles can be divided into two groups. Those of the first group can be called the conditions of flow. They are the temperature and pressure in the suspension, the velocity distribution of the flow, and the nature of the turbulence of flow. The factors of the second group can be called the settling properties of the suspension.

The term "settling properties of a suspension" refers to how the particles behave in a given set of conditions of flow. Thus, for some specified temperature, pressure, fluid velocity and turbulence, the particles of a suspension will settle, flocculate or be diffused in some manner. The manner will vary from suspension to suspension, and must be determined experimentally for each.

Hence, the problem of determining how material will settle out of a flowing suspension can be divided into two parts. First the flow conditions must be

Note: Discussion open until May 1, 1960. To extend the closing date one month, a written request must be filed with the Executive Secretary, ASCE. Paper 2311 is part of the copyrighted Journal of the Hydraulics Division, Proceedings of the American Society of Civil Engineers, Vol. 85, No. HY 12, December, 1959.

1. Research Fellow in Eng., California Inst. of Technology, Pasadena, Calif.

measured, and second, the settling properties of the suspension must be measured. Neither of these two is an easy task, and considerable research and development is necessary before either will be done satisfactorily.

This paper deals only with the settling properties of a suspension and their use in calculating the removal of the particles. Section 2 contains a general discussion of the problem of calculating the removal. This discussion points out how the settling properties are to be used and indicates the type of experimental information needed. The experimental determination of settling properties is discussed in Section 3. Some results already obtained are presented, and the experiments yet to be developed are outlined. In Section 4, this research is related to more practical engineering problems.

2. Calculating the Removal of Suspended Particles

a. The Problem

It was stated above that one of the tasks of the engineer is to determine in advance how the particles will settle out of a given flowing suspension. To be specific, consider a suspension of particles in water which is flowing in an open channel. The fluid velocity and turbulence level are low enough for the particles to settle to the bottom of the channel. The problem is to calculate the amount of settled material as a function of distance along the channel.

Such a calculation involves the solution of some form of continuity equation expressing the conservation of suspended matter at any point in the suspension. In order to derive the equation it is first necessary to consider the factors affecting the concentration of particles at a point. The first of these factors is the settling of the particles.

b. Settling of the Suspended Particles

The term "settling velocity of a suspended particle" refers to the velocity that the particle would have if it were settling in perfectly still fluid. A suspension may contain particles of many settling velocities and the distribution of these settling velocities is an important settling property of the suspension. In calculations related to settling it is just as reasonable to characterize particles by these settling velocities as by their size, shape, and density. For, it is the settling velocity that indicates how soon the particle is going to be removed from suspension by settling to the bottom.

Let w represent settling velocity and let it be positive downward. The velocities of the particles in a suspension will range from zero to the velocity of the fastest particle. For numerical calculations and theoretical discussions it is convenient to divide the range of values of w into a number of increments Δw. Then w_1 can refer to a class of settling velocities between the values 0 and Δw, and w_2 to those velocities between Δw and $2\Delta w$. In general, w_i will indicate velocities between the values $(i - 1)\Delta w$ and $i\Delta w$. The particles with velocity w_i will be called i-particles.

The concentration of i-particles at any point in the suspension will be called f_i, the units of which are mass per unit volume of suspension. This concentration can vary from point to point and from time to time. Letting x, y, and z represent coordinates which locate a point, and t represent time, the concentration will be a function, $f_i\,(x,y,z,t)$. The term f_i indicates that f is a function which varies as i varies. Hence, f is the frequency function for the

settling velocities at point x,y,z. In this paper it will be called the settling velocity distribution at x,y,z.

At any point in the suspension, the flux of i-particles due to settling will be given by

$$w_i f_i (x, y, z, t)$$

This is the rate at which i-particles pass through a unit horizontal area at point x,y,z, and time t. The rate at which all particles pass through this area is

$$\sum_{i=1}^{\infty} w_i f_i (x, y, z, t)$$

By definition, this total flux is simply the product of the local instantaneous mean settling velocity, $\overline{w}(x,y,z,t)$, and the local instantaneous particle concentration, $\phi(x,y,z,t)$. That is,

$$\overline{w}(x, y, z, t)\ \phi\ (x, y, z, t) = \sum_{i=1}^{\infty} w_i f_i (x, y, z, t) \qquad (1)$$

where

$$\phi\ (x, y, z, t) = \sum_{i=1}^{\infty} f_i \qquad (2)$$

Hence, the product $\overline{w}\phi$ describes the motion of particles due to settling.

c. Movement of Particle Due to Fluid Motion

At any point in the suspension, the particles also have a motion due to fluid flow at the point. If the flow is without turbulence, this motion is simply the resultant fluid velocity. Let this resultant be represented by the vector $\underline{U}(x,y,z,t)$. It will have x,y, and z-components of U(x,y,z,t), V(x,y,z,t) and $\overline{W}(x,y,z,t)$ respectively.

When the flow of a suspension is turbulent, the motion of the particles is usually considered in two parts. First, the particles are considered as being carried along by the temporal mean fluid velocity, also called $\underline{U}(x,y,z,t)$. Superimposed on this motion is the diffusion of particles by the turbulent fluctuations of fluid velocity. The decision as to what is the main flow and what is turbulence will depend upon the flow pattern for each individual case.

In order to deal with the particle motion caused by turbulence, it is common to define a coefficient of diffusion. Let e_{ik} be the coefficient for i-particles and x direction. Then the flux of i-particles through a unit area normal to the x direction can be given as

$$-e_{ik} \frac{\partial f_i}{\partial x}$$

Since there may also be an e_{iy} and e_{yz}, the coefficient will be called e_i when no specific direction is implied.

The coefficient e_i should not be confused with the coefficient for diffusion or transfer of momentum between neighboring elements of fluid. For the sake

of differentiation the latter will be called e_m. A reasonable assumption, often made, is that e_i is equal to e_m. For a detailed discussion of this point, the reader is referred to the experimental and analytical work of Vanoni[1] and Ismail.[2] Their work indicates that e_i not only differs e_m, but that the manner in which it differs varies with i. For coarse sand (w_i large) in flowing water, e_i was smaller than e_m while for fine sand (w_i small) e_i was larger. Nevertheless, the order of magnitude of the difference was such that it may be reasonable to assume that $e_i = e_m$ in engineering calculations. With this assumption there is no need for the subscript i and the diffusion coefficient for particles can be called e with an appropriate subscript when specific directions are mentioned.

Vanoni also found that e appears to vary with the particle concentration, ϕ. As yet, there is so little information on this variation that it cannot be considered in the calculation of removal. However, it must be an important effect when ϕ is large. It is hoped that future research will yield quantitative information about the effect of ϕ on e. In this paper, the effect is ignored.

d. Equation of Continuity

The motion of particles due to settling, mean temporal fluid velocity and turbulent diffusion produces a flux of particles in one or all of the x,y, and z-directions. The resultant flux can be represented by the vector. In order to describe the vector let $\underline{i}$, $\underline{j}$ and $\underline{k}$ be unit vectors in the x,y and z-direction respectively and let z be positive in the direction of positive w.

Consider first the flux of i-particle. The resultant is represented by the vector, $\underline{a}_i$, where

$$\underline{a}_i\,(x, y, z, t) = \underline{k}\, w_i\, f_i + \underline{U}\, f_i - \underline{i}\, e_{ix} \frac{\partial f_i}{\partial x} - \underline{j}\, e_{iy} \frac{\partial f_i}{\partial y} - \underline{k}\, e_{iz} \frac{\partial f_i}{\partial z}$$

The conservation of i-particles at x,y,z,t dictates that the divergence of vector $\underline{a}$ plus the time rate of change of f_i minus any source flow of i-particles is zero. Hence,

$$\nabla \cdot \underline{a} + \frac{\partial f_i}{\partial t} - P_i\,(x, y, z, t) = 0 \qquad (3)$$

where

$$\nabla = \underline{i}\, \frac{\partial}{\partial x} + \underline{j}\, \frac{\partial}{\partial y} + \underline{k}\, \frac{\partial}{\partial z} \qquad (4)$$

The term, P_i, in Eq. (3) represents a distributed source of i-particles of x, y,z. This term accounts for the effects of hindered settling and flocculation. If a particle of class w_i becomes attached to another in the process of flocculation it will generally experience a change in settling velocity. Hence, it disappears from class w_i and appears in another class. Similarly a particle may have one settling velocity when the local concentration has a certain value; when the local concentration changes, hindered settling may change the velocity to w_i. It follows that P_i must represent the rate at which particles acquire settling velocity w_i less the rate at which i-particles acquire other velocities. The units of P_i are mass per unit time per unit volume.

For an incompressible fluid the expansion of Eq. (3) becomes

$$\frac{\partial f_i}{\partial t} + \frac{\partial (w_i f_i)}{\partial z} + U \frac{\partial f_i}{\partial z} + V \frac{\partial f_i}{\partial y} + W \frac{\partial f_i}{\partial z} - \frac{\partial}{\partial x}\left(e_{ix} \frac{\partial f_i}{\partial x}\right)$$

$$- \frac{\partial}{\partial y}\left(e_{iy} \frac{\partial f_i}{\partial y}\right) - \frac{\partial}{\partial z}\left(e_{iz} \frac{\partial f_i}{\partial z}\right) - P_i = 0 \qquad (5)$$

Except for the last term this equation is similar to that expressed by Dobbins,[3] McNown,[4] Van Driest,[5] and others.

There is an Eq. (5) for each value of i. By summing these equations and introducing Eqs. (1) and (2) into the sum, the continuity equation for total concentration becomes

$$\frac{\partial \phi}{\partial t} + \frac{\partial (\overline{w}\, \phi)}{\partial z} + U \frac{\partial \phi}{\partial x} + V \frac{\partial \phi}{\partial y} + W \frac{\partial \phi}{\partial z} - \frac{\partial}{\partial x}\left(\sum_i e_{ix} \frac{\partial f_i}{\partial x}\right)$$

$$- \frac{\partial}{\partial y}\left(\sum_i e_{iy} \frac{\partial f_i}{\partial y}\right) - \frac{\partial}{\partial z}\left(\sum_i e_{iz} \frac{\partial f_i}{\partial z}\right) - \sum_i P_i = 0 \qquad (6)$$

Since flocculation and hindered settling produce no mass,

$$\sum_i P_i = 0 \qquad (7)$$

Substituting Eq. (7) into (6) and assuming that e_i is the same for all i gives the following equation:

$$\frac{\partial \phi}{\partial t} + U \frac{\partial \phi}{\partial x} + V \frac{\partial \phi}{\partial y} + W \frac{\partial \phi}{\partial z} + \frac{\partial}{\partial z}(\overline{w}\, \phi) - \frac{\partial}{\partial x}\left(e_x \frac{\partial \phi}{\partial x}\right)$$

$$- \frac{\partial}{\partial y}\left(e_y \frac{\partial \phi}{\partial y}\right) - \frac{\partial}{\partial z}\left(e_z \frac{\partial \phi}{\partial z}\right) = 0 \qquad (8)$$

The effects of flocculation and hindered settling do not appear explicitly in Eq. (8). These effects do appear implicitly, however, because they cause changes in $\overline{w}$. Eq. (8) cannot be solved without information on how $\overline{w}$ will change with particle concentration, flocculation, differential settling, and diffusion. This information will be obtained from studies of the settling properties of the suspension. In short, the settling properties of the suspension occur implicitly in Eq. (8) in the term $\overline{w}$.

e. Initial and Boundary Conditions

The solution of Eq. (8) requires a knowledge of initial conditions or boundary conditions or both. It becomes necessary, therefore, to think about specific physical situations. For present purposes, consider the section of open channel shown in Fig. 1. The distance along the channel is called x and is taken as positive in the direction of flow. The distance down from the free surface of the suspension is called z and is positive downward. The y-direction is normal to x and z in such a way as to produce a right-handed xyz system.

For this channel, the initial condition is the settling velocity distribution in the plane x = 0. Hence, it is necessary to take a sample of suspension from a point at x = 0 and obtain the settling velocity distribution of the sample by experimental analysis. If the distribution is not constant over the channel cross-section, samples must be taken from several points in the section and each

sample must be analyzed. The result will be a spatial distribution of settling velocity distribution at x = 0, and this result is the initial condition for settling in the channel.

The boundary conditions occur at the top surface of the suspension and at the bottom of the channel. At the top, the condition is the rate at which particles cross the surface. Usually no particles pass through this surface. But, in a density current along the bottom of a reservoir or settling tank, material may be settling out of relatively still water above into the current below.

At the bottom of the channel, the boundary condition depends on the behavior of the particles which have already settled to the bottom. If particles which once settled to the bottom of the channel are picked up into the flow, the process is called entrainment or resuspension. Let the rate at which particles are picked up per unit area of bed be E. The boundary condition can then be stated as

$$E = -\left(e_z \frac{\partial \phi}{\partial z}\right)_{\text{at bed}} \tag{9}$$

This equation is of the form used by Dobbins[3] to describe pickup of uniform particles in a turbulence jar. Dobbins verified this equation experimentally for E = constant and E = 0.

Theoretical work by Lane and Kalinske[6] shows that E will depend upon the settling velocities of the settled particles, the roughness of the bed and the pattern of turbulence near the bed. Thus for a given flow and bed conditions, E will depend on the properties of the suspension.

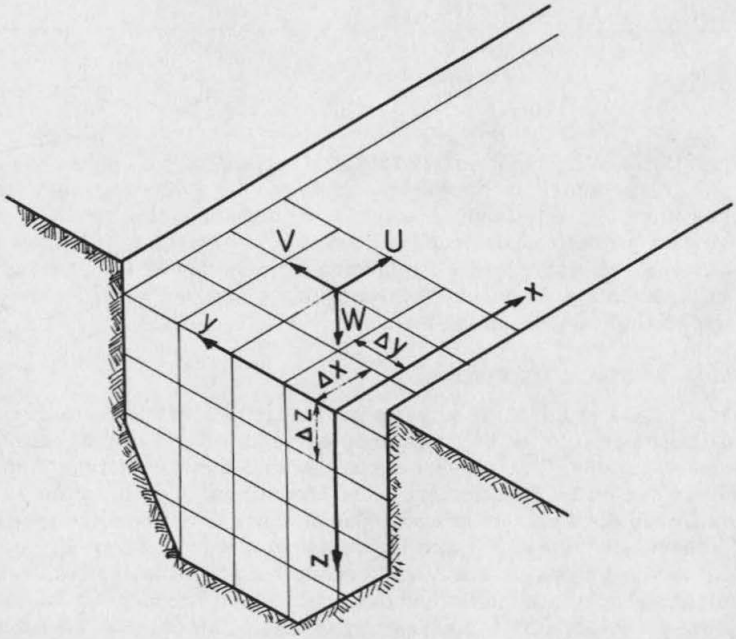

Fig. 1. Suspension flowing in open channel.

The resuspension of particles must be studied experimentally for each suspension. During the study, the flow conditions should be varied and resuspension measured. The end result should give the resuspension rates as a function of flow conditions for the suspension being studied. Experiments of this sort are currently in progress at the California Institute of Technology. It appears that a great deal of research is still to be done before the results can be used in calculating removal.

f. Solution of the Continuity Equation

Except for a few simple cases it is necessary to solve the equation of continuity by some numerical method. For this purpose, Eq. (8) is written in the form

$$\frac{\partial \phi}{\partial t} + \left(U - \frac{\partial e_x}{\partial x}\right)\frac{\partial \phi}{\partial x} + \left(V - \frac{\partial e_y}{\partial y}\right) + \left(W - \frac{\partial e_z}{\partial z}\right)\frac{\partial \phi}{\partial z}$$

$$+ \frac{\partial(\bar{w}\,\phi)}{\partial z} - e_x \frac{\partial^2 \phi}{\partial y^2} - e_y \frac{\partial^2 \phi}{\partial y^2} - e_z \frac{\partial^2 \phi}{\partial z^2} = 0 \qquad (10)$$

In Eq. (10), U, V, W, e_x, e_y and e_z are all determined by measurements. In general, they will be functions of x, y, z. However, if turbulence is affected by particle concentration, the e's will also be a function of ϕ. In such a case the relationship between e and ϕ will have to be determined experimentally.

Eq. (10) is in a form easily reduced to finite-difference form. For this purpose, the space occupied by the suspension is divided into rectangular parallelpipeds as shown at the upstream end of the channel in Fig. 1. Each parallelepiped has the dimensions Δx, Δy and Δz as shown. The corners of the parallelepipeds form a lattice of points where the value of ϕ is to be found.

The subscript ℓ will indicate that a point in the lattice has an x-coordinate of $\ell \Delta x$, while subscripts m and n indicate coordinate $m\Delta y$ and $n\Delta z$ in the y- and z-directions respectively. Using this notation, Eq. (10) can be written in the following form, for steady state settling.

$$\left(U - \frac{\partial e_x}{\partial x}\right)_{\ell, m, n} \frac{\phi_{\ell+1, m, n} - \phi_{\ell, m, n}}{\Delta x}$$

$$+ \left(V - \frac{\partial e_y}{dy}\right)_{\ell, m, n} \frac{\phi_{\ell, m+1, n} - \phi_{\ell, m, n}}{\Delta y}$$

$$+ \left(W - \frac{\partial e_z}{\partial z}\right)_{\ell, m, n} \frac{\phi_{\ell, m, n+1} - \phi_{\ell, m, n}}{\Delta z}$$

$$+ \frac{(\bar{w}\,\phi)_{\ell, m, n+1} - (\bar{w}\,\phi)_{\ell, m, n}}{\Delta z}$$

$$-(e_y)_{\ell,m,n} \frac{\phi_{\ell+1,m,n} - 2\phi_{\ell,m,n} + \phi_{\ell-1,m,n}}{\Delta x^2}$$

$$-(e_y)_{\ell,m,n} \frac{\phi_{\ell,m+1,n} - 2\phi_{\ell,m,n} + \phi_{\ell,m-1,n}}{\Delta y^2}$$

$$-(e_z)_{\ell,m,n} \frac{\phi_{\ell,m,n+1} - 2\phi_{\ell,m,n} + \phi_{\ell,m,n-1}}{\Delta z^2} = 0 \qquad (11)$$

To use Eq. (11) it is necessary to know ϕ and $\overline{w}$ at all points in the plane $x = r = 0$. This knowledge constitutes the initial condition. Any resuspension of particles between the planes $x = 0$ and $x = \Delta x$ constitutes the boundary condition and must also be known. With these known quantities, it is possible to calculate ϕ at all points in the plane $x = \Delta x$ or $r = 1$.

In order to repeat the process, it is necessary to know $\overline{w}\phi$ at points in the plane $r = 1$. Hence, the fundamental part of this calculation is to determine how $\overline{w}\phi$ changes between the plane $r = 0$ and $r = 1$, or, in general, between any two planes, r and $r + 1$. This change in $\overline{w}\phi$ will depend on the settling properties of the suspension.

Once the ϕ is calculated over cross sections at various values of r it is a simple matter to compute the rate at which particles are removed in any distance, $r\Delta x$. Thus the problem stated in part (a) above can be solved.

The procedure outlined here requires more information than is usually available to the engineer. Its main value, at present, is in showing specifically what research and development are necessary for complete calculations. Methods of measuring fluid velocity and turbulent diffusion must be improved, methods of measuring resuspension must be developed, and methods studying the settling properties of a suspension must be expanded.

Furthermore, the finite-difference calculation shows that information about the settling properties of a suspension must be obtained in a very specific form. This information must relate changes in the local mean settling velocity $\overline{w}(x,y,z)$ to particle settling, particle concentration, flocculation, hinderance, turbulence and any other conditions prevailing in the immediate neighborhood of the point x,y,z. A program of research was initiated for the purpose of obtaining this kind of information about suspensions. The progress made to date is reported in Section 3.

Due to the problems involved in calculating removal, it is natural to think of studying settling in hydraulic scale models. However, the model study may be misleading unless the similarity of settling is considered. Such similarity is discussed next.

g. Scale Models and Similarity in Sedimentation

The relationship between settling in the model and the prototype is best obtained by reducing Eq. (8) to dimensionless form. All velocities in the equation can be given in terms of a characteristic velocity U_o and dimensionless velocities U*, V* and W*. The result is

$$U = U^* U_o, \quad V = V^* V_o, \quad W = W^* W_o, \quad w_i = w_i^* U_o$$

Similarly, distance can be written in terms of a characteristic length x_o, and diffusion coefficients can be written in terms of a characteristic coefficient, e_o, as follows:

$$y = y^* y_o, \quad y = y^* y_o, \quad z = z^* z_o$$

$$e_x = e_x^* e_o, \quad e_y = e_y^* e_o, \quad e_z = e_z e_o$$

A dimensionless concentration can also be written in terms of a characteristic value, ϕ_o.

$$\phi^* = \frac{\phi}{\phi_o}$$

Dimensionless time can be written in terms of characteristic length and velocity.

Substituting these dimensionless quantities in Eq. (8) gives

$$\frac{\partial \phi^*}{\partial t^*} + U^* \frac{\partial \phi^*}{\partial x^*} + V^* \frac{\partial \phi^*}{dy^*} + W^* \frac{\partial \phi^*}{dz^*} + \frac{\partial (\bar{w}^* \phi^*)}{dz^*}$$

$$+ \frac{e_o}{U_o x_o} \frac{\partial}{\partial y^*} (e_x^* \frac{\partial \phi^*}{\partial x^*}) + \frac{\partial}{\partial y^*} (e_y^* \frac{\partial \phi^*}{\partial y^*}) + \frac{\partial}{\partial z^*} (e_z^* \frac{\partial \phi^*}{\partial z^*}) = 0 \tag{12}$$

There are three kinds of similarity involved in Eq. (12). The first two are geometric and kinemetric. Because of them the quantity $\frac{e_o}{U_o x_o}$ will be the same dimensionless constant in model and prototype. Furthermore, the value of $\bar{w}/U_o$ at a point in the model must be equal to that at a corresponding point to the prototype. Hence geometric and kinematic similarity demands that the settling velocities in the suspension be scaled in the same ratio as the fluid velocities.

The third type of similarity concerns the changes in settling velocities. Suppose that in the prototype, the mean settling velocity changes by an amount $\Delta\bar{w}$ in some distance Δx. For similarity $\bar{w}$ must change in the model such that the dimensionless rate of change is the same for both model and prototype. Denoting scale model quantities by s and prototype quantities by p it follows that

$$\frac{(\frac{\Delta \bar{w}}{U_o})_s}{(\frac{\Delta x}{x_o})_s} = \frac{(\frac{\Delta \bar{w}}{U_o})_p}{(\frac{\Delta x}{x_o})_p}$$

or

$$\frac{(\frac{\Delta \bar{w}}{\Delta x})_s}{(\frac{\Delta \bar{w}}{\Delta x})_p} = (\frac{U_o}{x_o})_s \; (\frac{x_o}{U_o})_p \tag{13}$$

If, like most open channel models the model was designed according to the Froude model law, Eq. (13) becomes

$$\frac{\left(\frac{\Delta \bar{w}}{\Delta x}\right)_s}{\left(\frac{\Delta \bar{w}}{\Delta x}\right)_p} = \left[\frac{(x_o)_s}{(x_o)_p}\right]^{-1/2} \tag{14}$$

The flocculation may be related to turbulent mixing which is scaled according to Froude's law as follows

$$\frac{(e_o)_s}{(e_o)_p} = \frac{(U_o x_o)_s}{(U_o x_o)_p} = \left[\frac{(x_o)_s}{(x_o)_p}\right]^{3/2} \tag{15}$$

Consequently the ratio of the effect of flocculation is equal to the negative half power of the length ratio while the ratio of a mechanism contributing to flocculation is equal to the three-halves power of the scale ratio.

Eqs. (14) and (15) show that the response of the suspension to flow conditions cannot be the same in model and prototype. It follows that a suspension with "scaled" settling properties must be used in the model. Usually, however, the same suspension must be used in model and prototype. In this situation there are two approaches to using models.

The first approach is to use the model to predict only the flow in the prototype; separate experiments are performed to study the settling properties of the suspension. The measured settling properties are then used to calculate the removal that will occur in the predicted flow. This method is suited to the study of such problems as silt deposition in reservoirs, sedimentation at the mouths of rivers, and the diffusion and sedimentation of sewage on other wastes in bays and estuaries.

In the second approach the settling is studied in the scale model. The model results are then "scaled up" to predict prototype results. In order to perform this scale-up, it is necessary to develop a scale equation giving the removal in the prototype as a function of removal in the model. From the foregoing analysis it is obvious that such an equation should be based as much on the properties of the suspension as on the model laws. Therefore separate experiments on the settling properties should be conducted in conjunction with the model tests. This second approach is frequently used in pilot plant studies of settling tanks.

3. Research on Quiescient Settling

a. Purpose and Scope

The purpose of the research described in this section was to develop methods for determining the settling properties of an individual suspension. More specifically, the objective was to measure the settling velocity distribution of a suspension, the local mean settling velocity at various points in the

suspension, and the factors affecting the local mean velocity. Most of the work was confined to quiescent settling.

The approach was both experimental and theoretical. The experiments consisted of allowing a suspension to settle quiescently in a vertical tube. During the settling, small samples were withdrawn from various locations in the tube, and these were analyzed for suspended-solids concentration. To supplement the experiments, theoretical analyses were made of the quiescent settling of discrete particles in a settling tube, the kinetics of flocculation during quiescent settling, and the analyses of data from the experiments.

b. Settling Velocity Distributions

The purpose of the first phase of the research was to measure the settling velocity distribution of many varied suspensions. The pipette analysis[7] was used for the measurement. A portion of a suspension was shaken and allowed to settle in a vertical glass tube. During settling, samples were withdrawn from a known distance below the top surface of the suspension by means of a broken-tip pipette or small glass tube.

The results of some of the experiments are shown in Figs. 2, 3 and 4. The ordinate represents the ratio of the particle concentration in the sample to the average concentration of the portion at the beginning of settling, while the abscissa indicates that the sample was taken at depth z below the surface at time t after the beginning of settling.

Under the following conditions, a curve from these figures represents a cumulative frequency distribution of settling velocities.

(1) At the beginning of settling the particles of each class of settling velocities were uniformly distributed throughout the suspension.
(2) No flocculation, turbulence, or hindered settling occurred during the experiment. In this case, the settling velocity distribution is the major settling property of the suspension and is often sufficient for calculating removal. Dobbins[3] and Camp[13,16] have calculated the removal for

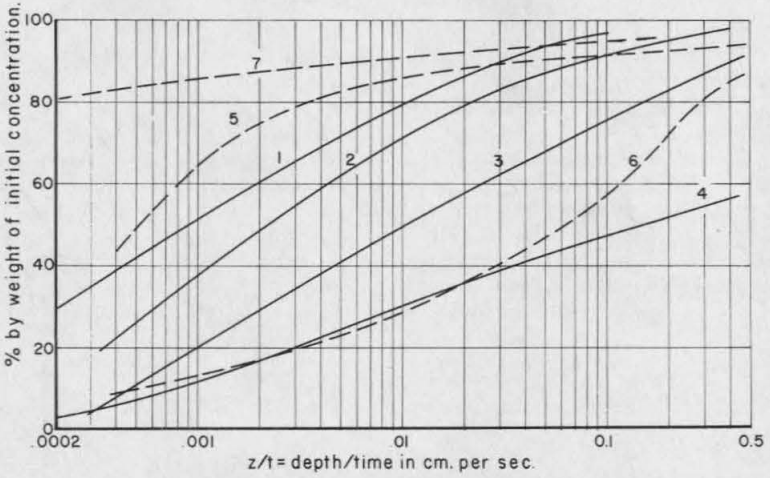

Fig. 2 Comparison of pipette analyses (see table I)

certain cases of particles settling without flocculation or hindered settling.

Fig. 2 shows the results of pipette analyses performed on primary effluent from two large sewage treatment plants, primary and secondary effluent from a third, and various mixtures of effluent with digested sludge and sea water with digested sludge. The analyses were made by the writer in connection with studies of the marine disposal of sewage and sludge in the vicinity of Los Angeles, California.(8) These were made in an apparatus which maintained the temperature of the suspension at 31.5° C. The average depth of sampling was about 40 cms for each analysis.

Even though the pipette analysis takes no account of flocculation or hindered settling, the curves of Fig. 2 indicate large differences between the settling properties of the various suspensions. For example, curves 1, 2 and 3 all represent primary effluents from sewage treatment plants. However, the approximate median settling velocities of suspensions 1 and 3 differ by a factor of 10.

Pipette analyses were also performed on raw Pasadena sewage obtained from a trunk sewer of the Los Angeles County Sanitation Districts. This

TABLE 1

Sources of the Suspensions Represented in Figure 2

Curve	Source	Initial Concentration (equal to Susp. Solids)
1	Primary effluent from the treatment plants of the Orange County (California) Sanitation District	893 mg/l
2	Primary effluent from the Hyperion Sewage Treatment Plant (City of Los Angeles).	212 mg/l
3	Primary effluent from the Joint Disposal Plant of the Los Angeles County Sanitation Districts	314 mg/l
4	Primary effluent plus 1% by volume of digested sludge from the Joint Disposal Plant, LACSD	527 mg/l
5	Primary effluent, plus elutriation effluent from Hyperion Sewage Treatment Plant	289 mg/l
6	One part digested sludge from Hyperion Sewage Treatment Plant plus 19 parts sea water	32,200 mg/l
7	Secondary effluent from Hyperion Sewage Treatment Plant	33 mg/l

sewer serves most of Pasadena, San Marino, South Pasadena, and parts of contiguous communities, with a total sewered population of about 200,000. The samples obtained from the sewer were gross samples; they were taken in the morning and tested in the afternoon of the same day. Before the experiment, the gross sample was poured into a large ceramic crock. When a smaller portion was required for testing, the gross sample was stirred, and while stirring continued, the smaller portion was taken.

A five-gallon gross sample was obtained on each of several days, and a portion was taken from each for pipette analysis. General information about the analyses is given in Table 2 and the results are plotted in Fig. 3. These curves show a variation in settling properties of the sewage from one run to the next. For some engineering purposes, it would be desirable to represent the data from all four runs by a single curve. The median settling velocity for such a curve would be about 0.02 cm. per sec., and the median velocities for the individual curves differ from this value by a factor of 1.5 or less. This deviation is small compared to the differences between median velocities in Fig. 2. Hence, for the purpose of comparing Pasadena sewage with the suspensions of Fig. 2, all four runs could be represented by a single curve.

From the curves of Figs. 2 and 3, two conclusions can be drawn. First, suspension which may be considered as similar can have significantly different settling properties. Second, even for a suspension as heterogeneous as sewage, the difference between runs for a single suspension can be small compared to the difference between suspensions.

Table 2

Pipette Analyses of Pasadena Sewage

Settling tube - 1 liter graduate

Volume used - 1 liter

Temperature control - none

Size of samples withdrawn - 25 ml.

Method of withdrawing samples - 25 ml. broken tip pipette lowered into suspension by hand for each sample.

Depth of samples - 22 cm. below surface of sewage.

Date	Gross Sample Obtained	Pipette Analysis Began	Initial Concentration	Temp. During Test
Thur. Oct. 21/54	8:30 am	2:35 pm	304 mg./ℓ	
Thur. Oct. 28/54	8:45 am	11:40 am	320	22-27°C.
Mon. Nov. 15/54	9:00 am	1:45 pm	374	21-23.5°C
Mon. Nov. 22/54	9:00 am	1:00 pm	380	23-30°C

Part of the difference between the curves of Fig. 3 may be due to sampling error. Whenever a portion is withdrawn from a heterogeneous suspension such as raw sewage, the properties of the portion may not be the average properties of the suspension. To test this error, tests were made on two portions from a single gross sample. By means of two identical glass settling tubes placed in a single constant-temperature water bath, two similar portions of sewage from a single gross sample were subjected to identical pipette analyses. The portions were approximately four liters in volume.

The experiment was rerun for a second gross sample, and the results of both runs were plotted on the graph shown in Fig. 4. The difference between curves for one run is nearly as large as the difference between curves shown in Fig. 3. Hence, some of the variation in the latter curves is due to sampling errors.

Sampling errors can be reduced by increasing the volume of the portion used in the suspension. The portions used in these pipette analyses varied between 1 and 4 liters, and they appear to be too small. Hence larger samples are recommended for suspensions of considerable heterogeneity.

c. Factors Affecting $\overline{w}$

Unless the particles of a suspension settle without flocculation or hindered settling, the pipette analysis gives only a rough indication of the settling properties of a suspension. In a more general situation it is necessary to use an experiment that will show how flocculation and hindered settling affect the settling velocities of the particles.

In hindered settling the concentration of suspended particles is high enough for the presence of one particle to affect the settling of its neighbors. In flocculation, on the other hand, a faster particle overtakes a slower one and becomes attached to it. The two settle henceforth as a unit with a velocity usually different from the original velocity of either particle. These two effects cannot be separated in an experiment. If they occur simultaneously the result is a single change in $\overline{w}$. However, in order to find out precisely how

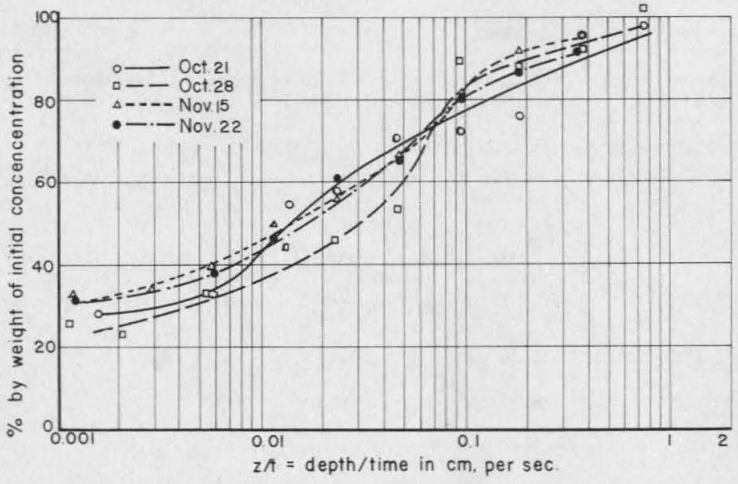

Fig. 3. Pipette analyses of Pasadena sewage (See Table 2).

they produce the changes in $\overline{w}$ it is convenient to think of them separately.

The hindered settling of uniform particles without flocculation has been studied theoretically and experimentally by McNown and Lin[9] and Steinhour,[10] among others. The former found that the individual settling velocity of a particle depends upon the volume concentration of the particles and upon the Reynolds number of the particle. Steinhour, on the other hand, produced a formula giving velocity as a function of volume concentration alone. This formula was based on experiments where particles were settling in the stokes range.

Both of these investigators considered cases where the particle concentration was uniform throughout the settling tube. Kynch[11] went further and made a theoretical analysis of uniform particles in a tube where the concentration varied with depth. By assuming that the individual particle velocity depended solely on the concentration in the neighborhood of the particle, he obtained results which agree with experimental observations on the subsidence of thick slurries.

On the basis of these studies it was concluded that the ratio of the settling velocity at concentration ϕ to velocity at $\phi = 0$ depends primarily on ϕ, with particle velocity as a secondary factor. Hence, in a suspension with particles of many velocities, a change in ϕ will cause the velocity of each particle to change by the same ratio. However, the magnitude of the change in velocity will equal the product of the ratio and the particle velocity. Thus, the magnitude will increase with particle velocity.

It follows, that for a given change in ϕ the mean settling velocity will change by an amount depending upon the distribution of settling velocities at the time of the change. This distribution can probably be characterized by the mean settling velocity and the standard deviation, σ, of the velocities. Therefore, changes in $\overline{w}$ will be a function of $\overline{w}$ itself, σ and the volume concentration of particles.

For flocculation no theories existed which were suitable for this research. The previous theories were all confined to predicting the rate of interparticle contacts, while ignoring the effect on settling velocities. Furthermore, they

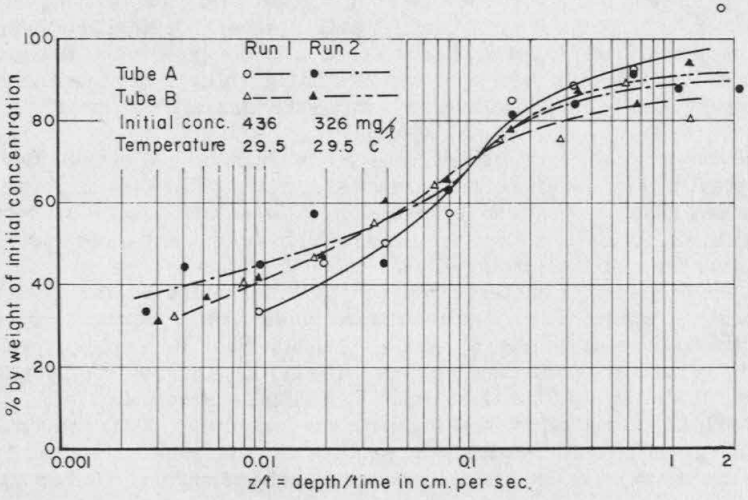

Fig. 4. Duplicate pipette analysis Pasadena sewage.

dealt with suspensions having velocities of only a few classes. Therefore, the kinetics of flocculation during quiescent settling was studied theoretically[12] for the purpose of discovering how flocculation produces changes in $\overline{w}$. Because of the number of unknowns the theory could not be completed, but it was carried far enough to show that the change in $\overline{w}$ at a point depends on the following properties of the suspension at the same point.

(1) The volume concentration of particles.
(2) The mean settling velocity of particles.
(3) The standard deviation of the settling velocities of the particles.
(4) The fraction of inter-particle contacts that result in the union of the particles.

Item (4) is simply a means of accounting for the surface chemistry of the particles.

The value of $\overline{w}$ at a point will also change in free settling. That is, in the absence of flocculation and hindered settling it is easily shown[12] that

$$\frac{\partial(\overline{w}\,\phi)}{\partial t} + \frac{\partial}{\partial z}\left(\sigma^2 \phi + \overline{w}^2 \phi\right) = 0 \qquad (16)$$

Thus, the change in $\overline{w}$ depends on $\overline{w}$ itself and on the standard deviation of settling velocities.

It appears, therefore, that the first three of the items listed above in connection with flocculation are also the most important items in connection with free and hindered settling. Consequently, an experimental study of quiescent settling should involve the determination of at least $\overline{w}$, σ, and concentration by volume. The determination of the first of these, $\overline{w}$, is described in part (d) which follows.

d. Measurement of $\overline{w}$

Since a measurement of $\overline{w}$ has not been reported in the literature, some time was spent in devising a method. Finally, it was decided to use an experiment based on a suggestion by Camp.[13] The suspension was allowed to settle quiescently in a vertical tube as in a pipette analysis. During the settling a series of samples were taken at each of several depths, and these samples were analyzed for particle concentration. This experiment was given the name multiple-depth pipette analysis or, simply multiple-depth analysis. Some very simple equations will show how such an analysis can be used to measure $\overline{w}$.

For the purpose of discussion, consider the hypothetical settling tube shown on the left in Fig. 5. All horizontal cross-sections of the tube are of unit area, and at any time, the particle concentration, ϕ, over any such cross-section is constant. Hence, ϕ is a function of z, the depth below the top of the suspension, and t, the time after beginning of settling.

At the beginning of the test (t = 0) pipette samples are withdrawn simultaneously at many depths. The results are plotted as the curve, t = 0, in the diagram on the right of Fig. 5. At $t = T_1$, another set of samples is withdrawn, and the results are plotted as the curve, $t = T_1$. The curves, $t = T_2$ and $t = T_3$ represent similar operations at times T_2 and T_3, respectively.

Physically speaking, each of these curves is a profile of the concentration at some given instant. When all the profiles from an analysis are put on one diagram, it can be called the concentration profile diagram. Mathematically

speaking, this diagram is a plot of $\phi(z,t)$ as a function of z with t as a parameter. At any stage in the discussion, it is possible to give the diagram a physical or mathematical interpretation, depending on which is more illuminating.

The concentration profile diagram is used in conjunction with the continuity equation for the calculation of $\overline{w}(z,t)$. First, it is noted that for the settling tube, Eq. (8) is reduced to the following:

$$\frac{\partial \phi}{\partial t} + \frac{\partial(\overline{w}\phi)}{\partial z} = 0 \qquad (17)$$

Integrating this equation with respect to z gives

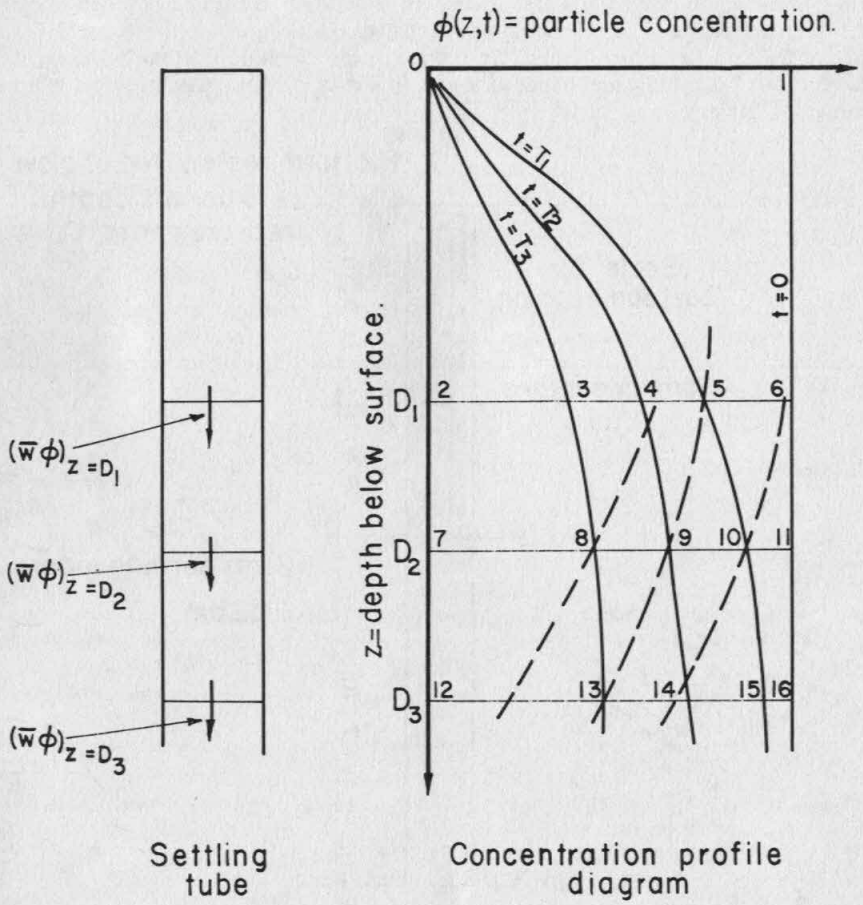

Fig. 5. Analysis of data from multiple-depth pipette analysis.

$$(\overline{w}\,\phi)_{z=D} = -\int_0^D \frac{\partial \phi}{\partial t}\,dz$$

$$= -\frac{\partial}{\partial t}\int_0^D \phi\,dz \qquad (18)$$

Eq. (18) shows how $\overline{w}$ can be calculated. A value of D is selected; for example, consider D_1 in Fig. 5. The areas 025, 024, and 023 are calculated and the values are plotted against t. If this is done for a sufficient number of profiles, the result will be a smooth curve giving the area under the ϕ profile above D_1 as a function of time. The slope of the curve is precisely the right hand side of Eq. (18), and hence is equal to $\overline{w}\phi$ at $z = D_1$. The process can be repeated for any value of D.

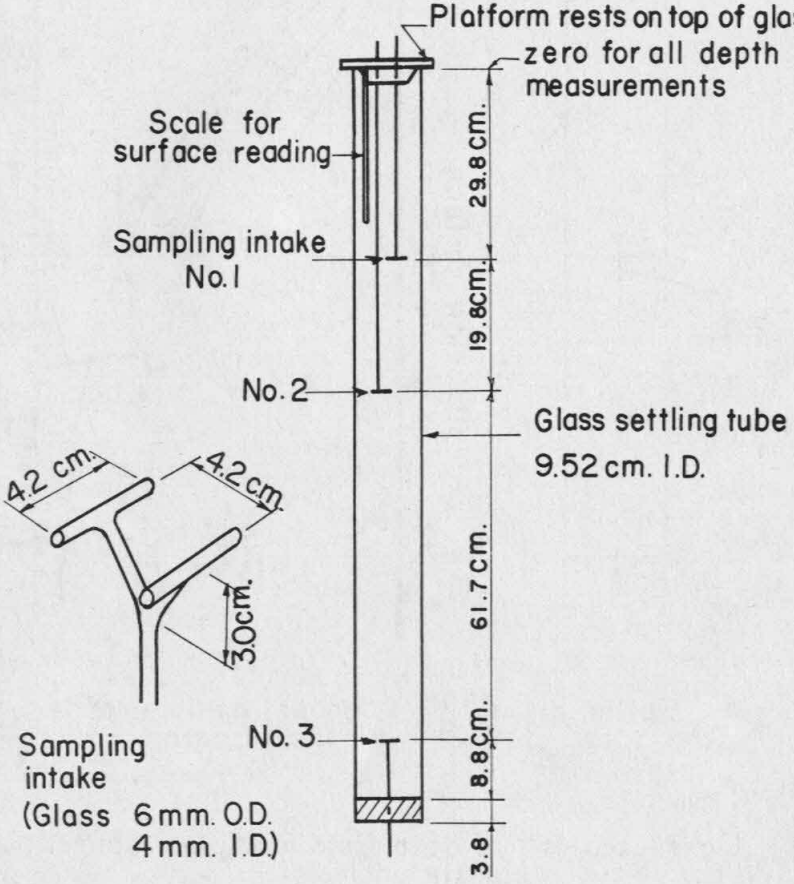

Fig. 6. Multiple-depth settling tube.

In order to test the feasibility of this approach to measuring $\overline{w}$, a pilot experiment was performed using the apparatus shown in Fig. 6. Sampling intakes, or pipettes, were located at three depths as shown. Samples could be drawn through the top two by means of a vacuum and through the bottom one by means of gravity flow.

The suspension to be tested was thoroughly mixed in a separate container and then poured quickly into the tube. Since the upper two intakes are attached to a platform which rests freely on the tube, these intakes could be put in place immediately after pouring. After they were in place, the elevation of the top surface was read on the scale shown and the withdrawing of samples began.

The surface elevation was read again after the withdrawal of each sample. With these readings it was possible to allow for the lowering of the surface in estimating the distance settled by particles. The estimated distance was used as z for each sample. Time, t, was measured from the end of pouring.

Table 3

Multiple-Depth Analysis of a Suspension of Clay and Alum in Water

Time After Start of Settling	Intake	Depth of Intake z	z/t	Volume of Sample	Temp. of Sample	Weight of Particles in Sample	% of Initial Conc.
sec.	No.	cm	cm/sec	ml.	°C	mg	
0					29.5*		
60	2	42.6	0.71	28		17.7	99
90	3	104.3	1.2	27		17.3	104
120	1	21.7	0.18	32 1/2		20.3	99
180	3	103.2	0.57	33		21.6	104
245	2	39.7	0.16	28		18.1	103
300	1	18.4	0.062	37		23.6	102
360	3	101.4	0.28	31 1/2		20.0	101
480	1	17.1	0.036	28		16.7	95
600	2	37.5	0.063	31 1/2	30.3	21.4	108
720	3	99.2	0.14	32	30.3	22.9	114
960	1	15.2	0.016	22		8.1	59
1200	2	35.6	0.030	25		11.2	71
1440	3	97.3	0.068	36		12.9	59
1920	1	13.2	0.069	27		7.7	45
2400	2	33.7	0.014	31		9.0	46
2880	3	95.4	0.033	29	31.5	7.2	40
3840	1	11.1	0.0029	31	32.0	5.1	26
4860	2	31.6	0.0065	32	32.3	5.0	25
5760	3	93.3	0.016	27	32.8	4.6	27
7740	1	8.9	0.0012	31	33.4	2.7	14
10100	2	29.4	0.0029	40	34.0	4.1	16
14100	3	91.1	0.0065	26	34.8	1.2	7

* Measured in mixer

Initial Concentration = 655 mg/l

Alum Concentration = 25 mg./l

This apparatus was used for the multiple depth analysis of a suspension of bentonite clay in Pasadena tap water and alum. ($Al_2(SO_4)_3 \cdot 18\ H_2O$). The initial concentration of clay was 655 mg. per liter, while that of alum was 25 mg. per liter. The results of the experiment are given in Table 3 and plotted in the concentration profile diagram of Fig. 7. Since samples were taken at only three depths some intermediate plotting and interpolation were necessary to produce the profiles.

Once the profiles were obtained, the mean settling velocity $\overline{w}(z,t)$ was calculated in the manner described above. Values for three values of z are given in Fig. 8. It is possible to calculate the order of magnitude of

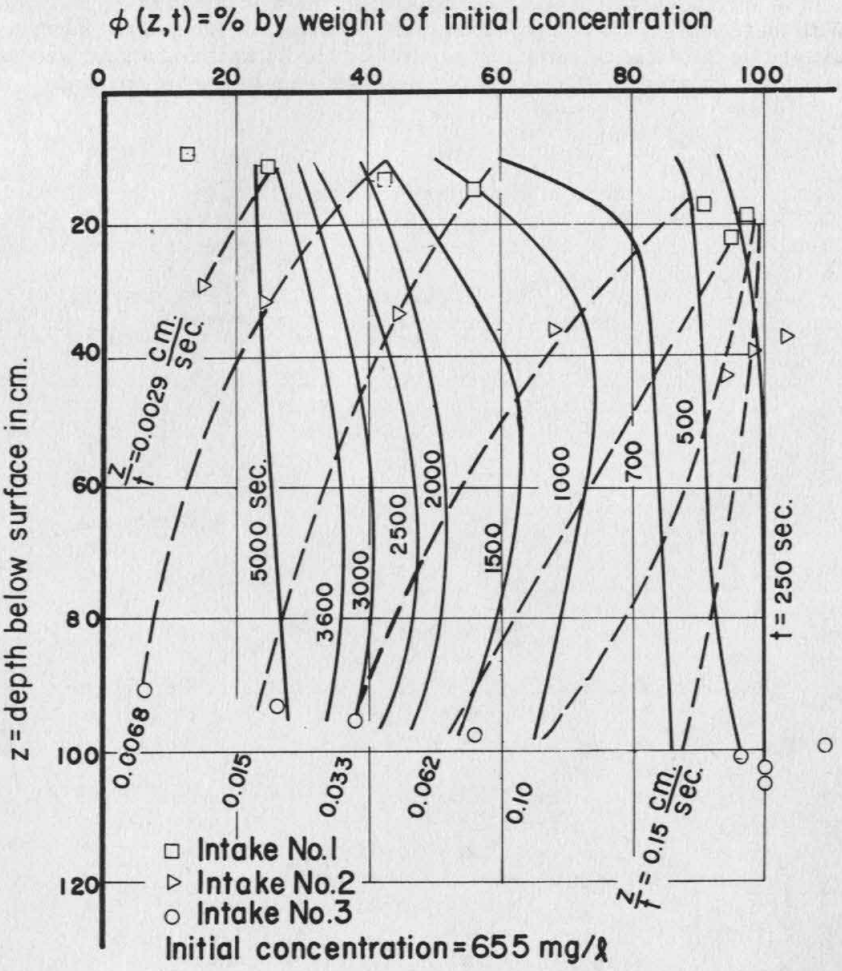

Fig. 7. Concentration profile diagram, Bentonite clay and alum in water.

flocculation effects on local settling. At a depth of 90 cm. the mean settling velocity increases from 0.021 cm. per second at t = 200 seconds to 0.037 at t = 500 seconds. This change represents an increase of 75 per cent and an average rate of increase of 0.000053 cm. per sec. per sec. Furthermore, the change in concentration during the same time was only 3 per cent. The effect of particles settling out of suspension must have been small. Therefore, the rate of change is primarily due to flocculation.

It is possible to tell directly that flocculation is causing the particles to speed up by looking at the dashed lines constant z/t in Fig. 7. The physical significance of these lines is best explained in the following manner. An observer starts at the surface of the suspension at t = 0 and descends through the suspension at a constant velocity. The concentration that he observes at various depths is given by a line of z/t equal to the velocity.

It can be shown[12] that when neither hindered settling nor flocculation occur, these lines are straight and parallel to the z-axis. If hindered settling slows the particles down more than flocculation speeds them up, the lines slope away from the z-axis as depth increases. If the converse is true, the lines slope toward the z-axis so depth increases. For Fig. 7, then, it is seen that flocculation is the predominant effect.

The maximum mean settling velocity for z = 90 cm. occurs at 700 seconds. Its value of 0.056 cm. per second is 2.8 times the mean settling velocity at t = 200 seconds. The average rate of change between t = 200 seconds and t = 700 seconds was 0.00007 cm. per sec. per sec.

A maximum value of $\overline{w}$ occurs at all depths in the settling tube. After this value, the mean settling velocity decreases. Particles are settling out of suspension, and the loss of faster particles offsets the effect of flocculation.

While this work was being done, Fitch[14] presented the results of a multiple-depth experiment on a suspension of whiting ($CaCO_3$) and ferrisul [$Fe_2(SO_4)_3 \cdot 9H_2O$)] in water. The concentration of $CaCO_3$ was 400 parts per million (ppm), while the concentration of ferrisul was 15 ppm. This suspension

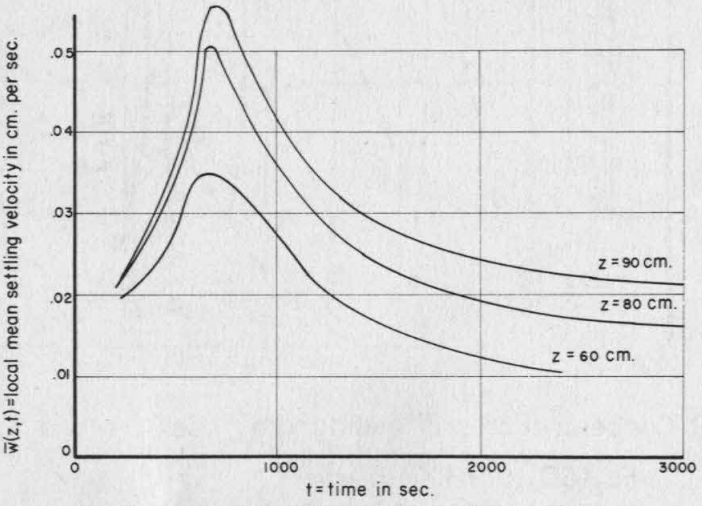

Fig. 8. Local mean settling velocity as a function of time. Bentonite clay and alum in water.

was allowed to settle in a tube seven feet deep and 5-1/2 inches in internal diameter. During the settling, samples were taken at seven depths by means of veterinary hypodermic needles which passed through the walls of the tube. For temperature control, the outside of the tube was covered with insulation one inch thick.

Fitch's results are presented as a concentration profile diagram in Fig. 9. The solid curves are concentration profiles or lines of constant time t, and

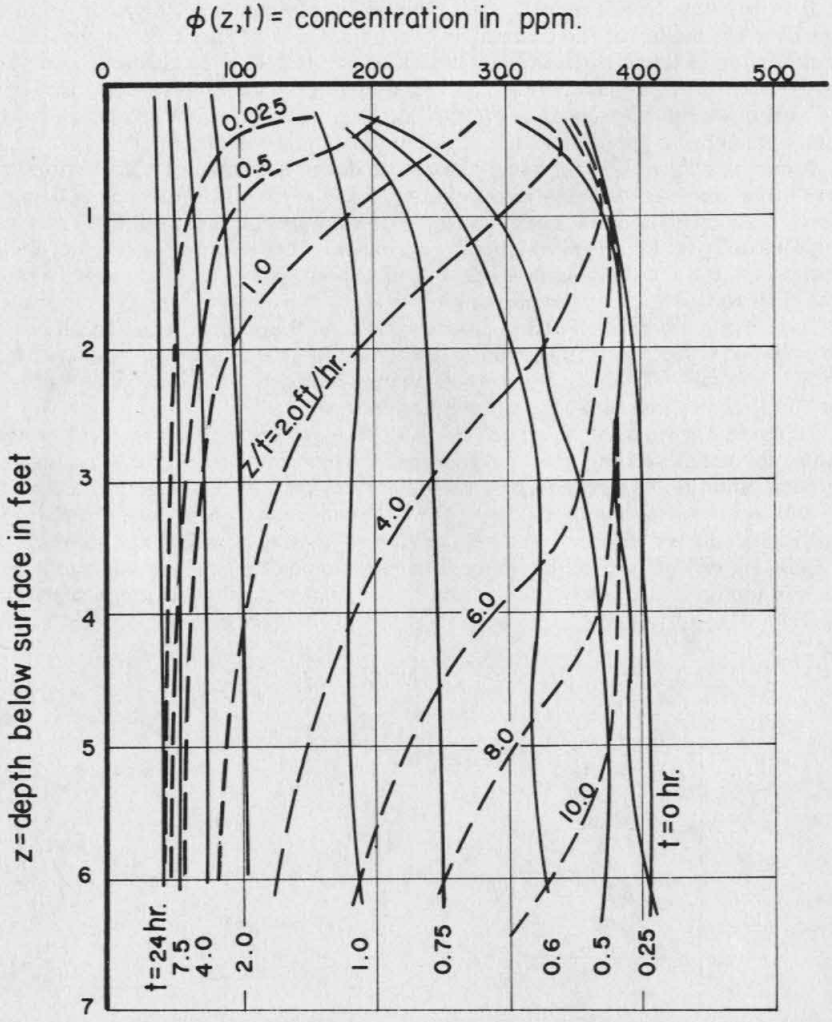

Fig. 9. Concentration profile diagram, $CaCO_3$ and $Fe_2(SO_4)_3 \cdot 9H_2O$ in water (Based on data by Fitch)

the dashed curves are curves of constant z/t. For $t > 0.25$ hours and $z > 2$ feet, the constant z/t lines slope toward the z-axis, showing the effect of flocculation.

Following the method described above, the local mean settling velocity was calculated. The mean velocities for z = 3 feet and z = 6 feet are shown in Fig. 10. At z = 6 feet, the mean settling velocity increased from 0.013 cm. per sec. at t = 0.25 hours to 0.035 cm. per sec. at t = 0.5 hours. The average rate of change during this time was 0.000025 cm. per sec. per sec. At t = 0.5 hours, the concentration at z = 6 feet is 94 per cent of the initial concentration. Consequently, up to this time the change in $\overline{w}$ is caused primarily by flocculation.

It is interesting to compare the change in $\overline{w}$ for whiting and ferrisul with the change for clay and alum. The comparison is valid only for those stages of settling for which the concentration has not decreased significantly. For whiting and ferrisul, the rate of change during this stage of settling was 0.000025 cm. per sec. per sec. For clay and alum, the corresponding rate of change was 0.000053 cm. per sec. per sec. The values differ by a factor of two.

One important practical conclusion can be drawn from these determinations of $\overline{w}$. That is that the effect of flocculation increases with depth from the surface. This is shown by the curves for $\overline{w}$ in Figs. 8 and 10. If the settling tube in either case had been deeper, the peak values of $\overline{w}$ would probably have increased with depth until a limiting value was reached.

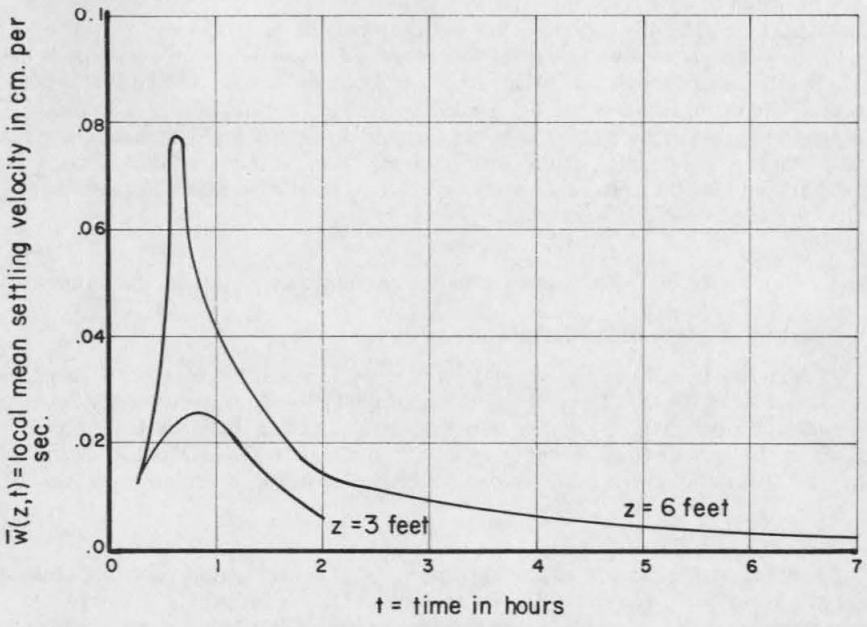

Fig. 10. Local mean settling velocity as a function of time (based on data by Fitch).

e. Proposals for Future Work

The next logical step in this work is to design an experiment in which it is possible to measure $\overline{w}$, σ, and particle concentration. For such an experiment, it is desirable to have a tube about ten feet deep with 7 or 8 sampling intakes. The sampling intakes should enter through the walls of the tube so as to cause a minimum obstruction to settling particles. The tube should be housed in a water jacket for temperature control, but both jacket and tube should have windows for visual observations.

The cross-sectional area of this tube should be at least equal to that of a circle twelve inches in diameter. Because of this large area, the samples withdrawn during settling can be as large as 500 ml. Then each sample can be allowed to settle in a 500 ml. graduate for a simple pipette analysis.

Five or six 25 ml. samples from each 500 ml. graduate should be enough to give a settling velocity distribution for each 500 ml. sample. From this distribution it is possible to calculate the mean and standard deviation of the settling velocities for each sample. Of course, flocculation may occur in the graduate, but the effect is small compared to that in the tube.

The same 500 ml. samples can be used for a determination of ϕ and the concentration by volume. From the former the concentration profile can be drawn. The values of $\overline{w}$ can then be calculated as shown above and checked against the value obtained from the simple pipette analysis.

Before this more elaborate multiple depth-analysis could be performed, the experiments on settling analysis were discontinued, and, as yet, no provision has been made for their continuance. It is hoped that someone will find the problem of sufficient interest to continue the work. If so, it will be economical to modify the tube to allow for the study of turbulence.

It is a simple matter to extend the proposed multiple-depth analysis to include effects of turbulence. Rouse[15] and Dobbins[3] have shown that a uniform field of turbulence can be created by placing a vibrating grid in the settling tube. Furthermore, Dobbins devised a method for controlling the rate of particle resuspension at the bottom of the tube. If these additions are incorporated into the apparatus proposed above, it will be possible to study flocculation in a turbulent fluid.

4. The Multiple-Depth Analysis in Approximate Calculations of Removal

a. Short-Cut Methods in Calculating Removal

There are times when the flow in a channel is such that $V = W = 0$ and U is independent of depth. Then, the settling of particles is similar to settling in a vertical tube which is moving at a velocity U in the x-direction. The profiles in the tube at time, t, corresponds to profiles in the channel at distance x. It follows that these profiles can be used directly to calculate removal.

b. "Ideal" Settling Tanks

Part (a) of Fig. 11 shows the settling zone of a rectangular settling tank of length L, width B, and depth D. By making certain simplifying assumptions about such a basin, Camp[13] devised the concept of an "ideal tank". Using the nomenclature of Section 2, these assumptions can be stated as follows:

$$U(x,y,z) = \text{constant}$$
$$V(x,y,z) = W(x,y,z) = 0$$

$e_x(x,y,z) = e_y(x,y,z) = e_z(x,y,z) = 0$
$f_i(o,y,z)$ = constant for each value of i

No resuspension at the bottom of the tank

Although these assumptions are sufficient to describe the tank, Camp also assumed that all particles in the tank settle without flocculation or hindrance. Since this last assumption is unnecessary, in this paper the term ideal tank will refer only to the assumptions about the tank. In place of the assumption

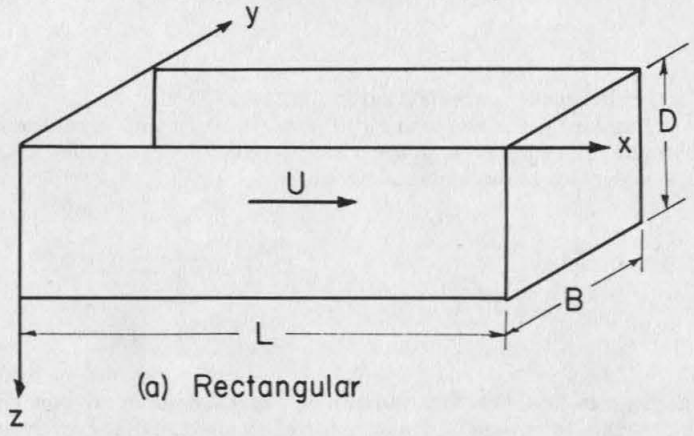

(a) Rectangular

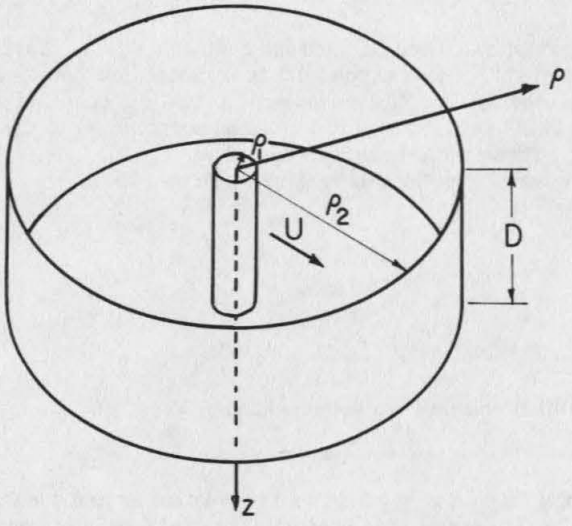

(b) Radial flow

Fig. 11. Settling zones of ideal tanks.

about the settling, the results of a multiple-depth analysis can be used. This approach is based on the fact that in an ideal tank settling is identical to that in a vertical tube, and concentration profiles at distance x in the tank correspond to profiles at time t in the tube. If the concentration profiles from the tube are used, the removal in the ideal tank will be given by

$$R(x) = B\,U \int_0^D \left[\phi\,(z, o) - \phi(z, t)\right] dz \tag{19}$$

where

$$t = \frac{x}{U}$$

and $\phi\,(z,t)$ represents concentration in the tube.

In settling tanks, the removal ratio, r(x), is more important than the removal itself. The former is defined as the fraction of particles entering the tank that settle out in distance x. Hence,

$$r(x) = \frac{R(x)}{\int_0^D \phi(z, o)\, dz} = \frac{\int_0^D \left[\phi(z, 0) - \phi(z, t)\right] dz}{\int_0^D \phi(z, 0)\, dz} \tag{20}$$

The integrals in Eqs. (19) and (20) can be represented on the concentration profile diagram by areas. Consider, for example, the diagram shown in Fig. 5. For a tank of depth D_1, and a distance of UT_1, the removal is represented by area 0561 while the removal ratio is represented by

$$r(x) = \frac{\text{area } 0561}{\text{area } 0261}$$

A similar approach can be used for radial flow tank. Part (b) of Fig. 11 shows what might be considered an "ideal radial flow tank". Fluid enters the tank through the surface of a cylinder of radius ρ_1, centered along the vertical axis of the tank. It then flows radially and horizontally to the cylindrical walls of the tank. These walls have a radius of ρ_2.

The flow conditions for this tank are assumed to be

$$U = \frac{b}{\rho} \qquad (b = \text{a constant})$$

$$V = W = 0$$

$$e_x = e_y = e_z = 0$$

The initial conditions are assumed to be

$$f_i = \text{constant at } \rho = \rho_1 \text{ for each value of i,}$$

while the bottom boundary condition is the same as that for Camp's ideal tank.

Settling in this radial tank is identical to settling in a vertical tube. Concentration profiles at radius ρ in the tank correspond to profiles at time

$$t = \frac{\rho^2 - \rho_1^2}{2b} \tag{21}$$

in the tube. It follows that removal in the tank in radial distance, ρ, is given by

$$R(\rho) = 2\pi \rho_1 \int_0^D U(\rho_1)\, \phi(\rho_1, z)\, dz - 2\pi\rho \int_0^D U(\rho)\, \phi(\rho, z)\, dz$$

$$= 2\pi b \int_0^D \left[\phi(z, o) - \phi(z, t)\right] dz \qquad (22)$$

where t is given by Eq. (21). Eq. (22) shows that removal in the radial tank is represented by an area on the concentration profile diagram just as it is for the rectangular tank.

It is suggested that the combination of assuming an ideal tank and performing a multiple-depth analysis on the suspension will give a first approximation to the behavior of the tank. This approximation will often be better than making an elaborate study of the hydraulics of the tank while ignoring the properties of the suspension.

c. Ideal Tanks with Turbulence

For a better approximation to a rectangular or cylindrical basin, it is possible to add turbulence to the ideal tank. If the turbulent diffusion is assumed to be

$$e_x = e_y = 0$$

$$e_z = \text{constant},$$

the settling in the tank will be equivalent to settling in a tube into which uniform turbulence is introduced.

Dobbins[3] and Camp[16] have assumed this sort of tank in a study of the effect of turbulence in retarding settling. Camp assumed that the particles settled without flocculation or hindrance. However, this assumption is unnecessary, since it is a simple matter to put the actual suspension in a settling tube as deep as the tank and introduce turbulence by means of a vibrating grid.

The combination of assuming an ideal tank and performing a turbulent multiple-depth analysis on the suspension is suggested as a second approximation to the behavior in a rectangular basin. For better approximations, it is necessary to obtain enough information for the step calculation outlined in Section 2.

d. Overflow Rate and Detention Time in Ideal Tanks

In the technical literature, one finds a great deal of discussion about whether a settling tank should be designed on the basis of overflow rate or detention time. The discussion about the merits of these two approaches is inconclusive, because it disregards the properties of the suspension. It will now be demonstrated that whether overflow rate or detention time should be used depends upon the nature of the suspension. Indeed, for a single tank, the removal ratio may be closely related to overflow rate for one suspension, to detention time for a second, and to neither for a third.

The detention is simply the average time that an element of fluid remains in the tank. Let it be called T. For the rectangular ideal tank,

$$T = \frac{L}{U} \tag{23}$$

while for the radial,

$$T = \frac{\rho_2^2 - \rho_1^2}{2b} \tag{24}$$

Overflow rate, on the other hand, is obtained by dividing the volume rate of flow through the tank by the horizontal area of the tank. Let it be w_o. For the rectangular basin,

$$w_o = \frac{UBD}{LB} = \frac{D}{T} \tag{25}$$

while for the radial,

$$w_o = \frac{2\pi \rho_2 \frac{b}{\rho_2} D}{\pi(\rho_2^2 - \rho_1^2)} = \frac{D}{T} \tag{26}$$

Eqs. (25) and (26) show that for constant flow rate and overflow rate, detention time varies with depth. Thus, if the effectiveness of the tank is to depend on overflow rate, r(x) will not vary with D as long as D/T is constant. Conversely, if the effectiveness depends on detention time, r(x) will not vary with D as long as T is constant.

To study the problem experimentally, a multiple-depth analysis is performed on the suspension concerned. The settling tube for this analysis should be as deep as the deepest possible tank to be considered. The results from the analysis are plotted on a concentration profile diagram as shown in Fig. 5.

In this figure, let D_1, D_2 and D_3 represent the depths of three tanks to be considered. The detention times for these tanks are T_1, T_2 and T_3, respectively. The tanks all have the same overflow rate. Therefore,

$$\frac{D_1}{T_1} = \frac{D_2}{T_2} = \frac{D_3}{T_3}$$

and the dashed line 5, 9, 13 is a line of constant z/t. The other dashed lines are also lines of constant z/t.

If the removal ratio is to depend on overflow rate alone, then

$$\frac{\text{area } 0561}{\text{area } 0261} = \frac{\text{area } 0, 9, 11, 1}{\text{area } 0, 7, 11, 1} = \frac{\text{area } 0, 13, 16, 1}{\text{area } 0, 12, 16, 1} \tag{27}$$

Furthermore, this type of relationship must hold for any overflow rate, i.e., for any dashed curve of constant z/t. It can be shown[12] that Eq. (27) will hold for arbitrary overflow rate if and only if the lines of constant z/t are straight and parallel to the z-axis.

If, on the other hand, removal ratio depends only on detention time, an equation of the form

$$\frac{\text{area } 0, 5, 6, 1}{\text{area } 0, 2, 6, 1} = \frac{\text{area } 0, 10, 11, 1}{\text{area } 0, 7, 11, 1} = \frac{\text{area } 0, 15, 16, 1}{\text{area } 0, 12, 16, 1} \tag{28}$$

must hold for each profile. Eq. (28) will hold if and only if the profiles are all straight lines parallel to the z-axis.

It follows that for quiescent settling in ideal tanks the problem of overflow rate and detention time is determined by the pattern of the profile diagram. This pattern, in turn, is determined by the settling properties of the suspension.

As an example of a suspension for which detention time is more important, consider the data obtained by Fitch and plotted in Fig. 9 above. The profiles are almost straight and vertical. Thus, for any tank up to six feet in depth, the removal is affected more by detention time than by overflow rate. Calculations by Fitch substantiate this conclusion.

With only these curves at hand, one might ask the following question. What will be the situation when this suspension settles in a rectangular tank ten feet deep? To answer this question, it is necessary to try to sketch in the lines of constant z/t between the depths of six and ten feet and draw the profiles from these. After a few trials, it becomes evident that the profiles are not likely to change their shape drastically. Hence, removal will still depend primarily on detention time.

e. Detention Time and Overflow Ratio—General

The data by Fitch shows that when flocculation occurs in an ideal tank the removal ratio can be more closely related to detention time. Furthermore, in reference (12) it is shown that flocculation has a tendency to cause the vertical straight profiles which indicate the dependence on detention time.

The reason is quite simple. When particles settle without flocculation, the concentration at a given time will normally increase with depth. Hence, the profile slopes away from the z-axis. With flocculation, however, the faster particles settling through the slower ones gather up the slower ones and drag them out of suspension. This tends to cause the concentration at any given time to decrease with depth. The combined result can cause the concentration to be independent of depth, i.e., a straight profile parallel to the z-axis.

However, Camp[13] has shown that when the particles settle without flocculation or hindered settling, removal depends on overflow rate alone. Between the suspensions discussed by Camp and those discussed by Fitch are suspensions for which both overflow rate and detention time are significant. The diagram of Fig. 7 represents an example of this last situation.

When turbulence during settling is to be considered, the studies of overflow rate and detention time should be based on results from turbulent settling analysis. As yet, the available experimental results of this type are too meager to permit any conclusions.

f. Sediment Deposition in Canals

In the design of canals, it is necessary to consider minimum velocities for non-silting. If the latter cannot be maintained, it is desirable to know where in the canal the silt will be deposited. Some useful information about this problem can be obtained from a turbulent multiple-depth analysis.

This analysis should be performed in a tube as deep as the canal. Inside the tube, the level and vertical distribution of turbulence should be as close as possible to that in the canal. The vertical distribution of turbulence can be obtained by varying the grid spacing and bar size along the vibrating grid. The turbulence level can be obtained by adjusting the frequency of the vibrations.

The tube can be used to find out what velocity is necessary for keeping the particles in suspension. By letting the suspension settle in the tube with various grid frequencies, it will be possible to decide upon the turbulence level that keeps deposition to a reasonably small amount. The velocity in the canal which produces the turbulence is the necessary velocity in the canal.

For each grid frequency, the test should be run for a considerable time. After only a short time in the tube, the particles of a suspension may be reasonably well suspended at a given level of turbulence. However, if flocculation occurs, the particles may increase the settling velocities and begin to settle out. This process may not be evident for thirty minutes or an hour.

If a minimum velocity cannot be maintained in the canal, the results of the analysis will show the pattern of silt deposition. For if the flow in the canal is fairly uniform, profiles at distance x in the canal correspond to profiles in the tube. Removal is calculated in the manner described for the ideal tank.

When the level of turbulence in the canal is sufficiently low, the results of a quiescent multiple-depth analysis may give some information about deposition. Fig. 12 represents the results of a quiescent analysis of bentonite clay

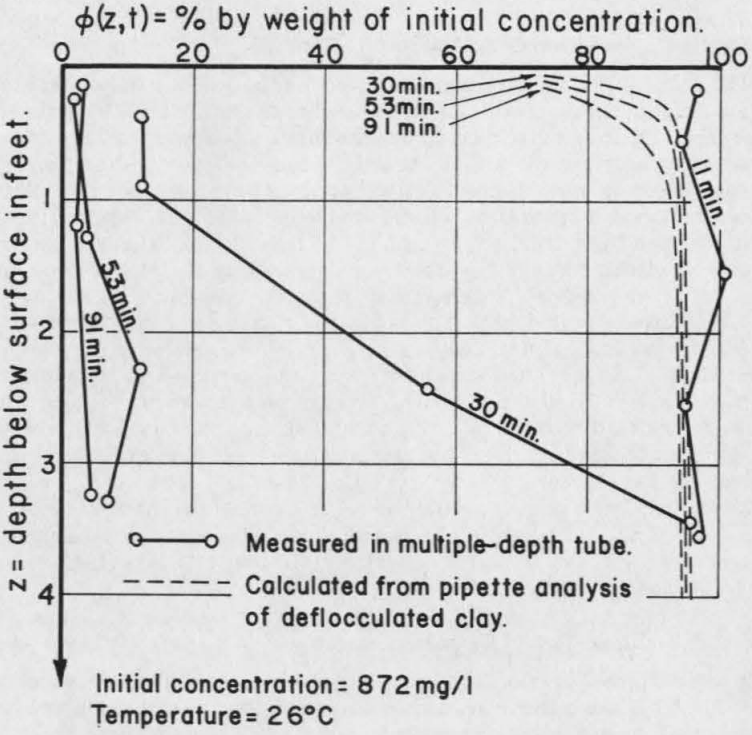

Fig. 12. Concentration profiles for bentonite clay in Pasadena tap water.

in Pasadena tap water. The analysis was performed in a lucite tube with an internal diameter of 3-3/4 inches and a depth of 4 feet. Thus the settling might correspond, roughly, to settling during tranquil flow in an irrigation canal 4 feet deep.

In preparing the suspension, the clay was blended thoroughly with 0.5 liters of water. This blended mixture was then shaken with enough water to bring the final clay concentration to 872 mg per liter. After two minutes of vigorous shaking the suspension was poured into the tube. This mixing might be similar to that which the suspension would receive in passing through a diversions works into the canal.

During the settling, samples were taken at four depths. The concentrations of these samples were used to plot the profiles shown as solid lines in Fig. 12. For the purpose of comparison, the settling velocity distribution of the original clay particles was obtained by means of a pipette analysis of a suspension of clay and deflocculating agent in distilled water. From the settling distribution, the dotted profiles of Fig. 12 were determined. These profile show how the particles would settle without flocculation.

On the basis of the dotted profiles, one would expect that the clay would be carried in suspension indefinitely. Therefore it would pass through the canal. In fact, however, most of the clay would have settled to the bottom of the canal in one hour.

5. CONCLUSIONS

The principal conclusions based on the research are as follows:

(1) In order to predict the settling of particles in a flowing suspension, it is necessary to know the properties of the flow and the settling properties of the individual suspension. In general, it is best to determine both by direct measurement. If a choice must be made, it will often be better to determine the properties of the flow by calculation or reasonable assumption, and to measure the properties of the suspension.

(2) In the initial stages of studying a suspension, it is profitable to obtain a settling velocity distribution by means of a pipette analysis or comparable experiment. When flocculation and hindered settling are negligible this distribution can be used in an estimate of removal; when they are not, the results of the analysis are still useful in comparing suspensions.

(3) A multiple-depth pipette analysis can be used to study the effect of hindrance, flocculation, and turbulence on the settling. For quiescent settling, the analysis should include measurements of the mean settling velocity, the standard deviation of settling velocities and the particle concentration at various depths and times. For turbulent settling the analysis should include these three measurements plus any additional measurements related to the turbulence.

(4) Whenever the settling in the flowing suspension can be approximated by settling in a quiescent or turbulent settling tube, the concentration profiles from a multiple-depth analysis can be used to calculate removal.

(5) When a suspension flows through a settling tank, the removal of particles may depend upon detention time, overflow rate, or both. Whether one or the other is more important depends primarily upon the settling properties of the suspension. For quiescent settling in ideal tanks, a

multiple-depth settling analysis will indicate the relative importance of overflow rate and detention time.

(6) Settling in a hydraulic model will not be similar to settling in the prototype unless a suspension with scaled settling properties is used in the model. When this is not possible, two approaches are available. In one, the model is used to predict the properties of the flow, and separate experiments are used to measure the properties of the suspensions. These properties are used to calculate what the removal will be in the predicted prototype flow. In the other approach, the prototype suspension settles in the model. The settling properties of the suspension are studied separately and these properties are considered in using the model results to predict prototype results.

ACKNOWLEDGMENTS

This paper is based on a thesis[12] submitted to the California Institute of Technology in 1958 in partial fulfillment of the requirements for the Ph.D. degree. The writer is grateful to Professor Jack E. McKee for his supervision and generous assistance during the course of the research.

The experimental work was carried out with the aid of research grant (RG-4405) from the Division of Research Grants, National Institutes of Health, Public Health Service.

REFERENCES

1. Vanoni, Vito A., "Transportation of Suspended Sediment by Water," Trans. Am. Soc. Civ. Engrs., vol. 111, 1946, pp. 67-102.
2. Ismail, Hassan M., "Turbulent Transfer Mechanism and Suspended Sediment in Closed Channels," Trans. Am. Soc. Civ. Engrs., vol. 117, 1952, pp. 409-434.
3. Dobbins, William E., "Effect of Turbulence on Sedimentation," Trans. Am. Soc. Civ. Engrs., vol. 103, 1944, pp. 629-678.
4. McNown, John S., Discussion to "Effect on Turbulence on Sedimentation," Trans. Am. Soc. Civ. Engrs., vol. 103, 1944, pp. 657-660.
5. Van Driest, E. R., Discussion to "Effect of Turbulence on Sedimentation," Trans. Am. Soc. Civ. Engrs. vol. 103, 1944, pp. 674-676.
6. Lane, E. W. and Kalinske, A. A., "The Relation of Suspended to Bed Material in Rivers," Trans. A. G. U., vol. 20, 1939, pp. 637-641.
7. Krumbein, W. C. and Pettijohn, F. J., Manual of Sedimentary Petrography, Appleton-Century, New York, 1938.
8. Brooks, Normal H., "Predictions of Sedimentation and Dilution of Digested Sludge in Santa Monica Bay," Report to Hyperion Engineers, August 7, 1956.

   Brooks, Norman H., "Settling Analysis of Sewage Effluents," Memorandum to Hyperion Engineers, July 5, 1956. See also

   Hyperion Engineers, Ocean Outfall Design, Los Angeles, California, October 1957.

9. McNown, J. S. and Lin, P., "Sediment Concentration and Fall Velocity," Proc. 2nd Midwestern Conference on Fluid Mechanics, Ohio State Univ. 1952, pp. 401-411.

10. Steinour, H. H., "Rate of Sedimentation," Industrial and Engineering Chemistry, vol. 36, no. 7, 1944, pp. 618-624.

11. Kynch, G. J., "A Theory of Sedimentation," Trans. Faraday Soc., vol. 48, 1952, pp. 166-176.

12. McLaughlin, Ronald T., "On the Mechanics of Sedimentation in Artificial Basins," Ph.D. Thesis, Calif. Inst. of Tech., Pasadena, California, 1958.

13. Camp, Thomas R., "Sedimentation and the Design of Settling Tanks," Trans. Am. Soc. Civ. Engrs., vol. III, 1946, pp. 895-958.

14. Fitch, E. B.,"The Significance of Detention in Sedimentation," Sewage and Industrial Wastes, vol. 29, no. 10, October 1957, pp. 1123-1133.

15. Rouse, Hunter, "Experiments on the Mechanics of Sediment Suspension," Proc. 5th International Cong. for Applied Mechanics, 1938, pp. 550-554.

16. Camp, Thomas R., Discussion to "Effect of Turbulence on Sedimentation," Trans. Am. Soc. Civ. Engrs., vol. 103, 1944, pp. 660-667.